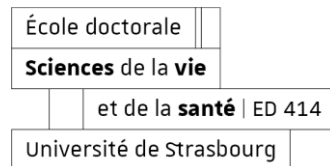




UNIVERSITÉ DE  
STRASBOURG



*Science de la vie e de la santé*

**Biopathologie de la myéline, neuroprotection et stratégies thérapeutiques -  
INSERM U1119**

**THÈSE** présentée par / **DISSERTATION** presented by :

**Chiara TREMOLANTI**

soutenue le /defended on : 29 Juin 2022

pour obtenir le grade de / **to obtain the grade of :**

**Docteur de l'Université de Strasbourg / Strasbourg University Doctor**

Discipline/Spécialité / Discipline/specialty : Neuroscience

**Neuroprotection against myelin disorders:**

***in vitro* and *in vivo* studies to explore the protective roles of  
TSPO ligands and genome editing-based strategies**

**THÈSE dirigée par / DISSERTATION supervisor :**

**MENSAH-NYAGAN Ayikoé-Guy**

Professeur, Université de Strasbourg

**COSTA Barbara**

Professeur, Università di Pisa

**RAPPORTEURS :**

**AZCOITIA ELIAS Iñigo**

Professeur, Universidad Complutense de Madrid

**KASSIOU Michael**

Professeur, University of Sydney

**AUTRES MEMBRES DU JURY / OTHER MEMBERS OF THE JURY :**

**TRINCAVELLI Letizia**

Professeur, Università di Pisa

**KEYSER Christine**

Professeur, Université de Strasbourg

## Avertissement au lecteur / Warning to the reader

Ce document est le fruit d'un long travail approuvé par le jury de soutenance et mis à disposition des membres de la communauté universitaire. Il est soumis à la propriété intellectuelle de l'auteur. Cela implique une obligation de citation et de référencement lors de l'utilisation de ce document. D'autre part, toute contrefaçon, plagiat, reproduction ou représentation illicite encourt une poursuite pénale. This document is the result of a long process approved by the jury and made available to members of the university community. It is subject to the intellectual property rights of its author. This implies an obligation to quote and reference when using this document. Furthermore, any infringement, plagiarism, unlawful reproduction or representation will be prosecuted.

### Code de la Propriété Intellectuelle

Article L122-4 : Toute représentation ou reproduction intégrale ou partielle faite sans le consentement de l'auteur ou de ses ayants droit ou ayants cause est illicite. Il en est de même pour la traduction, l'adaptation ou la transformation, l'arrangement ou la reproduction par un art ou un procédé quelconque.

Any representation or reproduction in whole or in part without the consent of the author or his successors in title or assigns is unlawful. The same applies to translation, adaptation or transformation, arrangement or reproduction by any art or process whatsoever.

Articles L335-1 à L335-9 : Dispositions pénales / Penal provisions.

## Licence attribuée par l'auteur / Licence attributed by the author

[Veillez à ne conserver que la licence qui vous convient / Make sure you only keep the licence that suits you best]



<https://creativecommons.org/licenses/?lang=fr-FR>

# Chiara TREMOLANTI

## Neuroprotection against myelin disorders: *in vitro* and *in vivo* studies to explore the protective roles of TSPO ligands and genome editing based strategies

### Abstract

In the CNS, the oligodendrocytes (OLs) produce myelin, the lipophilic structure which allows for the proper conduction of nerve impulses. Abnormal formation or damages of myelin or OLs underlie myelin pathologies, which are characterized by severe neurological deficits. Accumulating evidence are showing anti-inflammatory and neuroprotective effects in several *in vitro* and *in vivo* models of neuroinflammation and neurodegeneration exerted by translocator protein (TSPO) ligands. In the present thesis, we attempted to investigate several aspects of myelin diseases in order to find innovative therapeutic approaches. Our first results showed that TSPO negatively modulates microglia activation towards the classical inflammatory phenotype. After, we demonstrated the beneficial effect of the administration of two TSPO ligands in a murine model of MS by the evaluation of pathological markers. Finally, we proved that TSPO may possess also an important role during OLs differentiation, thus proposing TSPO as a promising target to promote remyelination.

Key-words: Myelin pathologies, multiple sclerosis, PMD, TSPO, microglia, neuroinflammation.

### Résumé

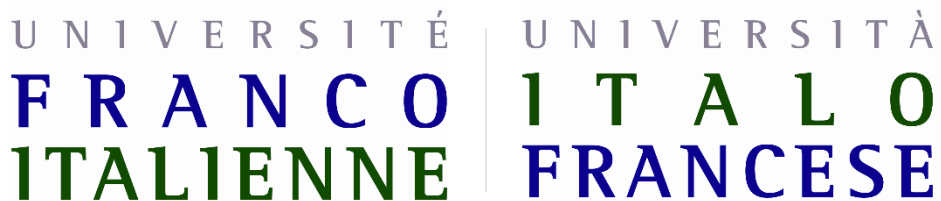
Dans le SNC, les oligodendrocytes (OLs) produisent de la myéline, la structure lipophile qui permet la bonne conduction de l'influx nerveux. La formation anormale ou les dommages de la myéline ou des OLs sous-tendent les pathologies de la myéline, caractérisées par de graves déficits neurologiques.

Diverses données de la littérature suggèrent des effets anti-inflammatoires et neuroprotecteurs des ligands de la protéine translocatrice (TSPO) dans plusieurs modèles de neuroinflammation et de neurodégénérescence *in vitro* et *in vivo*. Dans la présente thèse, nous avons vérifié spécifiquement cette hypothèse en étudiant divers aspects des pathologies de la myéline afin d'identifier de nouvelles approches thérapeutiques. Nos résultats montrent que TSPO module négativement l'activation de la microglie vers le phénotype inflammatoire classique. Ensuite, nous avons démontré l'effet bénéfique de l'administration de deux ligands TSPO dans un modèle murin de SEP par l'évaluation de marqueurs pathologiques. Enfin, nous avons prouvé que TSPO peut également jouer un rôle important lors de la différenciation des OLs, ce qui fait de la protéine TSPO une cible prometteuse pour favoriser la remyélinisation.

Mots-clés : Pathologies de la myéline, sclérose en plaques, PMD, TSPO, microglie, neuroinflammation.

Questo lavoro di Dottorato è stato supportato dall'Università Italo-Francese (UFI) mediante il finanziamento VINCI 2020, che ha coperto le spese di mobilità tra l'ateneo Italiano e l'ateneo Francese nel contesto della co-tutela di dottorato.

Ce travail de Doctorat a été soutenu par l'Université Franco-Italienne (UFI) à travers le financement VINCI 2020, qui a couvert les coûts de mobilité entre l'université Italienne et l'université Français dans le cadre de la cotutelle du doctorat.





*Dedicated to my parents and my sister*

<b>INDEX</b> .....	<b>6</b>
<b>PREFACE</b> .....	<b>10</b>
<b>SUMMARY</b> .....	<b>11</b>
<b>ABBREVIATIONS</b> .....	<b>16</b>
<b>INTRODUCTION</b> .....	<b>18</b>
<b>1.1 OVERVIEW OF THE CENTRAL NERVOUS SYSTEM</b> .....	<b>19</b>
1.1.1 NEURONS.....	19
1.1.2 ASTROCYTES.....	20
1.1.3 MICROGLIA.....	20
<i>Function during homeostasis</i> .....	21
<i>Function during stress</i> .....	22
1.1.4 OLIGODENDROCYTES.....	24
<i>Myelin composition and structure</i> .....	26
<i>The development of oligodendrocytes</i> .....	30
<b>1.2 MYELIN PATHOLOGIES</b> .....	<b>32</b>
1.2.1 DYSMYELINATING PATHOLOGIES: PELIZAEUS-MERZBACHER DISEASE.....	32
<i>Clinical forms and physiopathology</i> .....	33
<i>Experimental models of the severe PMD form: Jimpy mouse and 158JP OLS cell line</i> .....	34
<i>Current therapies and innovative therapeutic approaches</i> .....	35
<i>CRISPR/Cas9 technology: overview and principle</i> .....	36
1.2.2 DEMYELINATING PATHOLOGIES: MULTIPLE SCLEROSIS.....	38
<i>Epidemiology and risk factors</i> .....	40
<i>Physiopathology</i> .....	43
<i>In vivo model of MS: the experimental autoimmune encephalomyelitis (EAE)</i> .....	49
<i>Current treatments</i> .....	51
<i>New therapeutic approaches</i> .....	52
<b>1.3 TRANSLOCATOR PROTEIN 18 KDA (TSPO)</b> .....	<b>53</b>
1.3.1 LOCALIZATION AND STRUCTURE.....	53
1.3.2 CHOLESTEROL TRANSPORT AND STEROIDOGENESIS.....	54
1.3.3 OTHER TSPO FUNCTIONS.....	58
1.3.4 TSPO LIGANDS IN NEUROINFLAMMATION: <i>IN VITRO</i> STUDIES ON GLIAL CELL MODELS.....	61
1.3.5 TSPO AS A TARGET IN MULTIPLE SCLEROSIS: <i>IN VIVO</i> STUDIES.....	63

<b>AIMS OF THE THESIS</b> .....	<b>66</b>
<b>MATERIALS AND METHODS</b> .....	<b>68</b>
2.1 CELL CULTURE .....	69
2.2 CRISPR/CAS9 TECHNOLOGY: EXPERIMENTAL PROCEDURE.....	70
<i>In silico design of the gRNA and ssODN</i> .....	70
<i>Obtaining of the plasmid vectors encoding for the gRNA and the Cas9:</i> .....	71
<i>Cloning of oligonucleotides encoding crRNAs in the plasmids:</i> .....	71
<i>Bacterial transformation and isolation of colonies:</i> .....	72
<i>Analysis of clones</i> .....	72
<i>Production of plasmid vectors:</i> .....	72
<i>158JP Transfection</i> .....	73
<i>Selection of transfected cells, clonal isolation, and expansion:</i> .....	73
<i>DNA extraction from the clones and PCR amplification</i> .....	74
<i>DdeI digestion</i> .....	74
2.3 <i>IN VITRO TREATMENTS</i> .....	74
<i>C20 Cells Pharmacological Treatments</i> .....	74
<i>Treatments for WB protein analysis</i> .....	74
<i>Treatments for MTS viability assay</i> .....	75
<i>Treatments for the evaluation of cytokine release following TSPO ligands administration</i> .....	75
<i>HOG cells Differentiation</i> .....	75
<i>HOG Transfection for TSPO KD</i> .....	75
<i>Cell Viability Assay</i> .....	76
2.4 GENE AND PROTEIN EXPRESSION ANALYSIS .....	76
<i>Relative mRNA expression: Real-Time RT-PCR</i> .....	76
<i>ELISA-based Quantification of Cytokine Release</i> .....	77
<i>Western Blotting Analysis</i> .....	78
<i>Immunofluorescence Analysis</i> .....	78
2.5 CELL-BASED FUNCTIONAL ASSAYS .....	79
<i>ROS Production Evaluation</i> .....	79
<i>Pregnenolone Production Quantification</i> .....	79
<i>Intracellular Cholesterol Content Evaluation</i> .....	80
2.6 <i>EX VIVO EXPERIMENTS</i> .....	80
<i>Immunohistochemical Analysis</i> .....	80
<i>ELISA-based IL-10 Quantification in Serum</i> .....	81
<i>LC/HR-MS Quantification of Allopregnanolone in spinal cord tissues</i> .....	82
2.7 STATISTICAL ANALYSIS .....	82

<b>RESULTS AND DISCUSSION</b> .....	<b>84</b>
<b>CHAPTER 3.1</b> .....	<b>85</b>
3.1.1 RESULTS.....	85
<b>DISCUSSION</b> .....	<b>90</b>
<b>CHAPTER 3.2</b> .....	<b>93</b>
<b>RESULTS</b> .....	<b>93</b>
3.2.1 HUMAN MICROGLIAL ACTIVATION: <i>IN VITRO</i> MODEL SETTING .....	93
3.2.2 EFFECT OF TSPO PHARMACOLOGICAL STIMULATION ON THE PRO-INFLAMMATORY ACTIVATION OF C20 CELLS .....	96
3.2.3 EFFECT OF TSPO SILENCING ON C20 CELLS RESPONSIVENESS TO THE INFLAMMATORY STIMULUS .....	98
3.2.4 REGULATION OF TSPO TRANSCRIPTION FOLLOWING INFLAMMATORY STIMULI .....	100
3.2.5 EFFECT OF DEXAMETHASONE TREATMENT ON TSPO EXPRESSION FOLLOWING INFLAMMATORY STIMULI IN C20 CELLS .....	100
<b>DISCUSSION</b> .....	<b>102</b>
<b>CHAPTER 3.3</b> .....	<b>108</b>
PRELIMINARY REMARKS .....	108
<b>RESULTS</b> .....	<b>108</b>
3.3.1 EFFECT OF PIGA1138 AND PIGA839 ON MBP EXPRESSION IN SPINAL CORD AND BRAIN STRUCTURES .....	108
3.3.2 EFFECT OF PIGA1138 AND PIGA839 ON NF200 EXPRESSION IN SPINAL CORD AND <i>CEREBELLUM</i> .....	113
3.3.3 EFFECT OF PIGA1138 AND PIGA839 ON IMMUNE CELLS INFILTRATION IN SPINAL CORD .....	115
3.3.4 EFFECT OF PIGA1138 AND PIGA839 ON IL-10 CONCENTRATION IN SERUM.....	118
3.3.5 EFFECT OF PIGA1138 AND PIGA839 ON ALLO CONCENTRATION IN SPINAL CORD.....	118
<b>DISCUSSION</b> .....	<b>120</b>
<b>CHAPTER 3.4</b> .....	<b>124</b>
<b>RESULTS</b> .....	<b>124</b>
3.4.1 HOG CELL DIFFERENTIATION PROTOCOL SET UP .....	124
3.4.2 INVESTIGATION OF TSPO EXPRESSION AND STEROIDOGENIC MACHINERY COMPONENTS DURING HOG DIFFERENTIATION .....	128
3.4.3 EFFECT OF NEUROSTEROIDOGENESIS INHIBITION ON HOG DIFFERENTIATION .....	130
3.4.4 EFFECT OF TSPO SILENCING ON HOG DIFFERENTIATION .....	133
<b>DISCUSSION</b> .....	<b>135</b>
<b>CONCLUDING REMARKS AND FUTURE PERSPECTIVES</b> .....	<b>140</b>
<b>LIST OF PUBLICATIONS</b> .....	<b>142</b>
<b>DECLARATIONS</b> .....	<b>143</b>
<b>RESUMÉ DE THÈSE</b> .....	<b>144</b>
<b>RIASSUNTO DELLA TESI</b> .....	<b>148</b>
<b>RINGRAZIAMENTI</b> .....	<b>152</b>



## Preface

---

The present PhD thesis is the results of a co-supervision of PhD project, which has been established between the University of Pisa (Italy) and the University of Strasbourg (France). I started my PhD in the Laboratory of Cellular and Molecular Biology at the Department of Pharmacy of the University of Pisa. Then, I had the opportunity to spend 18 months of my PhD program at the University of Strasbourg, and join the INSERM Research Unit 1119 - Biopathology of Myelin, Neuroprotection and Therapeutic Strategies.

This research project has involved numerous and multidisciplinary approaches, as a result of the collaboration between the two Laboratories. The extensive expertise on the pathophysiological mechanisms of neurodegeneration, neuroinflammation, and brain aging of the Laboratory of Biochemistry and Molecular Biology at the University of Pisa was fitting perfectly with the main interest of the Research Unit U1119 in Strasbourg, which is the development of new therapeutic strategies against neurodegenerative diseases and in particular myelin pathologies.

Therefore, on one hand, I was focused on understanding the molecular and cellular mechanisms involved in myelin diseases and in particular in neuroinflammation. Besides, the development and the preclinical evaluation of new possible treatments for multiple sclerosis, the most known demyelinating disease, was another important goal of my thesis.

The complementarity of the expertise of the two laboratories has been extremely advantageous and beneficial to the project and my studies, allowing me to gain knowledge on different aspects of myelin pathologies by the means of different techniques, and to shed some light on new possible pharmacological approaches.

## Summary

---

### Background

The myelin of the central nervous system (CNS) is produced by glial cells called oligodendrocytes (OLs). OLs membrane wraps around axons forming the myelin sheath, a lipoprotein structure that insulates axons thereby facilitating rapid transmission of nervous impulses. Damages of the myelin sheath and/or OLs death impact the velocity of nervous impulses conduction, leading to neurological symptoms, including motor and cognitive impairments typical of myelin diseases. Dysmyelinating diseases, such as the genetic Pelizaeus-Merzbacher Disease (PMD) are caused by abnormalities in the formation or maintenance of the myelin sheath. Conversely, demyelinating diseases such as Multiple Sclerosis (MS) are caused by internal and/or external factors which induce myelin and OLs damage. As part of the first group, the clinical spectrum of PMD is caused by genetic mutations of the X-linked *PLP1* gene which encodes for the proteolipid myelin protein (PLP), leading to critical neurological problems due to abnormalities in myelin formation and maintenance. The spontaneous *jimpy* mouse, a model of severe PMD, carries a single point mutation in the *Plp1* gene, which determines the production of misfolded PLP responsible for premature OLs death through molecular mechanisms which have not been elucidated yet.

On the other hand, MS is an autoimmune disease characterized by an immune system abnormal response directed against myelin and OLs, leading to the formation of demyelinated lesions, neuroinflammation, axonal damage, and neurodegeneration. Moreover, the chronic neuroinflammation occurring in MS over time impairs the endogenous remyelination, a process whereby OLs precursor cells (OPCs) are recruited at the lesion site and differentiate into mature OLs to form new myelin.

Despite a large number of *in vitro* and *in vivo* models of myelin diseases, and the numerous efforts that have been made over the years, the development of effective treatments for those pathologies remains extremely challenging, and no cure exists for PMD and MS. Therefore, there is an urgent need to identify novel therapeutic compounds and/or find new therapeutic approaches to prevent myelin loss, axonal degeneration and to support OLs functions and OPCs differentiation.

For genetic diseases such as PMD, innovative genome editing methods such as the CRISPR/Cas9 technologies appear to be appealing. In particular, the possibility an *in vitro* correction of the mutation responsible for PMD to restore the WT genotype would allow the uncovering of the molecular

mechanisms responsible for OLs death, thus exploring the possibility of innovative therapeutic approaches against such pathology.

Conversely, the pharmacological approach seems to give important results against MS clinical signs. Among the therapeutic strategies to cope with MS, acting on persistent neuroinflammation is the most classical approach and represents a common strategy. Besides, the stimulation of Oligodendrocytes precursor cells (OPCs) differentiation represents an interesting innovative approach for MS treatment, to promote endogenous remyelination.

Several compounds are under consideration for MS, including selective ligands of the mitochondrial Translocator Protein (TSPO), which have been shown to have beneficial effects in both *in vitro* and *in vivo* models of neuroinflammatory and neurodegenerative disorders, including myelin diseases. Their beneficial effects have often been attributed to the production of neurosteroids, widely-known neuroprotective and anti-inflammatory molecules able to positively modulate glial and neuronal function acting through several mechanisms. However, TSPO has been proposed to be implicated in several other cellular processes, such as mitochondrial respiration, apoptosis, ATP production, and redox balance. Despite a key role in neuroinflammation that has been recently proposed for TSPO, little is known about TSPO-activated pathways underlying the modulation of reactive microglia, the resident immune cells of the CNS. In addition, TSPO has recently emerged as a putative regulator of the differentiation of neural cells, although the precise TSPO function in such context has not been clarified yet.

## **Aims**

In the present PhD project, in order to find new therapeutic strategies against myelin disease, different approaches have been chosen, facing different aspects of myelin diseases. At first, *in vitro* studies were performed on the jimpy-derived 158JP murine OLs cell line, exploiting the CRISPR/Cas9 genome editing technology to uncover the pathological mechanism of PMD which is responsible for OLs death. To tackle MS, *in vitro* studies were first carried out on human microglia to dissect the role of TSPO in the modulation of neuroinflammation and to explore its potential as a target against microglia activation. Then, the assessment of the therapeutic potential of two novel TSPO ligands was performed in the experimental autoimmune encephalomyelitis (EAE) murine model of progressive MS. Lastly, an *in vitro* model of OPCs differentiation into mature OLs was characterized by the means of a human oligodendrocyte cell line. Herein, the role of TSPO and neurosteroids in the differentiation

process of OLs were investigated to explore the possibility to promote OPCs differentiation and thus remyelination by the use of selective TSPO ligands.

### **Results Part I**

Concerning PMD, the CRISPR/Cas9 genome editing technology was chosen to correct PLP1 missense mutation in 158JP OLs in order to determine the possible benefits of this approach in the 158JP OL cell model and to dissect the pathological mechanisms underlying OLs death. Unfortunately, no corrected clone has been obtained from the experiments and we were not able to reverse the *PLP1* pathological mutation in 158JP OLs. However, several DNA rearrangements were observed at the break points, suggesting a possible delivery of the genome editing system. Our explanation for the difficulty to obtain edited clones is related both to intrinsic issues of the technology and to peculiar experimental conditions. In the context of finding new therapeutical strategies to tackle MS, different strategies have been used.

### **Results Part II**

First, an *in vitro* model of activated microglia was set up and characterized by the evaluation of pro-inflammatory markers. Distinct experimental approaches were used to investigate the immunomodulatory role of TSPO in microglia: the pharmacological amplification of TSPO activity or the silencing of TSPO expression. Our main results showed that TSPO stimulation by the administration of selective ligands negatively modulates microglia pro-inflammatory activation, and such effects were shown to be mediated by neurosteroidogenesis induction. Moreover, the TSPO silencing increased microglia susceptibility to the immunogenic stimulus, indicating that TSPO may have a homeostatic role in the context of the dynamic balance between anti-inflammatory and proinflammatory mediators.

### **Results Part III**

In second instance, two TSPO ligands, PIGA1138 and PIGA839 were tested in the EAE mice model of progressive MS. Preliminary results obtained *in vivo* regarding the clinical scoring and motor performance showed that the pre-treatment with both ligands at the dose of 15 mg/kg was able to reduce the severity of the pathology at the peak of the disease, and PIGA1138 was also able to delay the onset of the clinical symptoms in EAE mice. The experimental work performed herein involved the assessment of different neuropathological markers such as demyelination level, axonal damage,

immune cell infiltration, and systemic levels of cytokines. Our immunohistochemical results showed that PIGA1138 was effective in protecting mice against EAE-evoked demyelination and axonal damage in the spinal cord and brain areas. Moreover, PIGA1138-treated EAE mice evidenced a reduced number of infiltrated immune cells in the spinal cord and an increased serum level of the anti-inflammatory cytokine IL-10 when compared to vehicle-treated, suggesting an anti-inflammatory action of the ligand. Interestingly, the treatment with PIGA1138 caused an increase in allopregnanolone level in the spinal cord of EAE mice compared to vehicle, suggesting that neurosteroidogenesis induction may participate in the mechanism of action of the TSPO ligand. Altogether, these results suggest that PIGA1138 TSPO ligands exert a protective effect against demyelination, axonal suffering, and inflammation in EAE-MOG mice, reinforcing TSPO as a promising target for pharmacological treatment in MS.

#### **Results Part IV**

Finally, after setting up an *in vitro* model of human OLs differentiation by the use of an oligodendrocytic cell line (HOG cells), we explored the role of TSPO during OPCs differentiation towards mature OLs. Interestingly, TSPO expression level was found notably increased upon HOG maturation, together with the other two main steroidogenic machinery components, the Steroid Acute Regulatory protein (StAR) and the cholesterol side-cleavage enzyme CYP11A1. Moreover, differentiated HOG produced a higher amount of pregnenolone, the precursor of all neurosteroids, and the treatment with the steroidogenesis inhibitor aminoglutethimide (AMG) reduced HOG differentiation. These findings suggested a role for TSPO in the differentiation process, therefore we evaluated the differentiation capacity of HOG cells following TSPO silencing. Interestingly, TSPO knockdown (KD) HOG showed impaired differentiation, indicating that TSPO is required for the correct maturation process of OPCs, thus making TSPO an appealing target to promote remyelination.

#### **Conclusions**

In conclusion, thanks to the combination of various *in vitro* and *in vivo* models, the present PhD research project has made it possible to achieve critical results that may contribute to the elaboration of promising therapeutic options against myelin disorders. The obtained findings strongly support the amount of evidence that proposes TSPO as a promising target against neuroinflammation and neurodegeneration, pointing out new potential implications for TSPO in the treatment of different myelin pathologies due to its possible role during the oligodendrocytic lineage differentiation.



## Abbreviations

---

<b>AD</b>	Alzheimer's Disease
<b>ALLO</b>	Allopregnanolone
<b>AMG</b>	Aminoglutethimide
<b>APC</b>	Antigen Presenting Cell
<b>BBB</b>	Blood Brain Barrier
<b>BDNF</b>	Brain Derived Neurotrophic Factor
<b>CNPase</b>	2', 3'-Cyclic Nucleotide 3'-Phosphodiesterase
<b>CNS</b>	Central Nervous System
<b>CRISPR/Cas</b>	Clustered Regularly Interspaced Short Palindromic Repeats/Cas
<b>crRNA</b>	CrisprRNA
<b>CSF</b>	Cerebrospinal Fluid
<b>DAMPs</b>	Damage Associated Molecular Patterns
<b>DEXA</b>	Dexamethasone
<b>DMTs</b>	Disease-Modifying Therapies
<b>DSB</b>	Double Strand Break
<b>EBV</b>	Epstein-Barr Virus
<b>ER</b>	Endoplasmic Reticulum
<b>Fdft-1</b>	Farnesyl-Diphosphate Farnesyltransferase 1
<b>GABA<sub>A</sub>-R</b>	$\gamma$ -aminobutyric acid type A receptor
<b>GalC</b>	Galactosylceramidase
<b>GC/MS</b>	Gas Chromatography / Mass Spectrometry
<b>HDR</b>	Homology-Directed Repair
<b>HMGCR</b>	3-Hydroxy-3-Methylglutaryl-CoA Reductase
<b>IL</b>	Interleukin
<b>INF-<math>\gamma</math></b>	Interferon-gamma
<b>iPSc</b>	Induced-Pluripotent Stem Cells
<b>LPS</b>	Lipopolysaccharide
<b>MBP</b>	Myelin Basic Protein
<b>MHC</b>	Major Histocompatibility Complex
<b>MMP</b>	Mitochondrial Membrane Potential
<b>m-OL</b>	Myelinating Oligodendrocyte
<b>mPTP</b>	Mitochondrial Permeability Transition Pore

<b>MRI</b>	Magnetic Resonance Imaging
<b>MS</b>	Multiple Sclerosis
<b>nCas9</b>	Nickase Cas9
<b>NF-<math>\kappa</math>B</b>	Nuclear Factor Kappa Light-Chain-Enhancer of Activated B cells
<b>NHEJ</b>	Non-Homologous End Joining
<b>OLs</b>	Oligodendrocytes
<b>OPCs</b>	Oligodendrocytes Precursor Cells
<b>PAM</b>	Protospacer Adjacent Motif
<b>PBR</b>	Peripheral Benzodiazepine Receptor
<b>PDGF</b>	Platelet-Derived Growth Factor
<b>PET</b>	Positron Emission Tomography
<b>PIGA</b>	2-Phenylindolylglyoxylamides
<b>PLP/DM20</b>	Proteolipid Protein
<b>PMD</b>	Pelizaeus-Merzbacher Disease
<b>PPMS</b>	Primary Progressive Multiple Sclerosis
<b>PREG</b>	Pregnenolone
<b>pre-OL</b>	Pre-myelinating Oligodendrocyte
<b>RE</b>	Restriction enzyme
<b>RNAtracr</b>	Transactivating CRISPR RNA
<b>ROS</b>	Reactive Oxygen Species
<b>RRMS</b>	Relapsing–Remitting Multiple Sclerosis
<b>RT</b>	Residence Time
<b>SDS-PAGE</b>	Sodium Dodecyl Sulphate-Polyacrylamide Gel Electrophoresis
<b>SPMS</b>	Secondary Progressive Multiple Sclerosis
<b>ssODN</b>	Single-Stranded Oligodeoxynucleotides
<b>StAR</b>	Steroidogenic Acute Regulatory Protein
<b>TGF-<math>\beta</math></b>	Transforming Growth Factor-beta
<b>TLRs</b>	Toll-like receptor ligands
<b>TNF-<math>\alpha</math></b>	Tumor-Necrosis Factor-alpha
<b>UPR</b>	Unfolded Protein Response
<b>VDAC</b>	Voltage-Dependent Anion Channel
<b>WT</b>	Wild-Type

# Chapter 1

## INTRODUCTION

## 1.1 Overview of the Central Nervous System

---

The central nervous system (CNS) is in charge of the regulation, the organization, and the control of all the functions of the whole body. It is composed of white and gray matter, which can be seen macroscopically on brain tissue. The white matter comprises myelinated axons bundles, whereas the gray matter consists mainly of neuronal bodies, dendrites, and unmyelinated fibers. Despite more abundant in the white matter, both include a number of glial cells, which are often referred to as supporting cells of the CNS. Glial cells fulfill precise functions, and the interactions between them are complex and highly specialized. In particular, the constant interplay between neurons and glia has been recognized as essential for the homeostasis of the CNS. The dysregulation of their communication and signaling is observed in almost every pathology of the CNS.

### 1.1.1 Neurons

The neuron has been considered for years the star of the CNS, and responsible for the largest part of events in the brain. Indeed, the neuronal cell receives, integrates, and transmits nerve impulses as an electrochemical signal, which is transmitted in the form of an action potential. The neuron has three functionally distinct compartments: the cell body or soma, the dendrites, and the axon. Dendrites are short, branched cytoplasmic extensions that receive afferences from other neurons at the synapses, areas of chemical contact between different neurons. Dendrites conduct electrochemical currents generated at the synaptic level to the cell body. Herein, the nucleus integrates the nerve impulses, processes them, and transmits the information along the axon, the main cytoplasmic extension of the neuron. The main function of the axon in the CNS physiological activity is to reach the dendrites of other neurons and delivers the signal in form of a synaptic potential.

A requirement for the correct axonal impulse conduction, synaptic transmission, and information processing, is the neuron to glia cross-talk. Glial cells support and nourish neurons throughout life, being essential for the homeostasis of the entire CNS. The most abundant types of glial cells taking part to the neuronal environment are astrocytes, microglia, and OLs [1].

### 1.1.2 Astrocytes

Astrocytes are star-shaped glial cells that perform a variety of functions in the CNS. Herein, they provide them physical and metabolic support, monitoring also the chemical composition of the fluid surrounding neurons. Astrocytes are in charge of the maintenance of the blood-brain barrier (BBB), and participate in the immune response [1]. In fact, they assume the activated phenotype following certain stimuli, acquiring the ability to remove toxic cellular debris within the brain [2]. In order to provide physical support for neurons, astrocytes form a matrix that keeps them in place and serves to isolate synapses from one another. Thus, such a matrix limits the dispersion of transmitter substances released by neuronal terminal buttons, aiding in the fluent transmission of neural impulses. Astrocytes provide nourishment to neurons by 1) receiving glucose from capillaries 2) breaking the glucose down into lactate 3) releasing the lactate into the extra cellular fluid surrounding the neurons. In this process, astrocytes store a small amount of glycogen, which stays stored until the metabolic rate of neurons is especially high.

### 1.1.3 Microglia

Microglia represent the resident innate immune cells of the CNS. They constitute about 5-10% of all CNS cells [3] and form a distinct population from circulating blood monocytes and hematopoietic macrophages [4]. As members of the innate immune system, microglia constantly survey the brain microenvironment thanks to their highly motile processes [5], in search of signals of damage (damage-associated molecular patterns, DAMPs) or infection (pathogen-associated molecular patterns, PAMPs) via their pattern-recognition receptors, in order to maintain the CNS homeostasis. They are highly sensitive and subjected to several signals from their microenvironment, which induce a plethora of activation responses [6]. Differently from what the scientific community was used to recognize until some years ago, microglia activation has been associated not only with damaging responses, but also with regenerative ones. Indeed, despite microglia activation being traditionally classified either as pro-inflammatory or anti-inflammatory, it is nowadays evident that activated microglia can mediate in parallel both types of responses, and rapidly shift between different phenotypes, depending on the nature of the stimuli [7]. The idea of “M1” and “M2” polarization was initially introduced to describe the ability of macrophages to change their phenotype *in vitro* in response to cytokines, such as interferon- $\gamma$  (INF-  $\gamma$ ) or interleukin (IL)-4. Such nomenclature was then extended to microglia

polarization, referred as classically activated (M1) or alternatively activated (M2) [8]. However, more recent *in vivo* analyses in patients and experimental models revealed that microglia responses are more heterogeneous, and that microglial polarization is multidimensional, with an extensive overlap in gene expression between pro- and anti-inflammatory states, in contrast to the M1/M2 dichotomic oversimplification [9]. In addition, although microglia depletion has been shown to reduce the severity of the pathology in some experimental models of Alzheimer's Disease (AD) [10] and Multiple Sclerosis (MS) [11], recent findings support the evidence that microglia have regenerative properties by supporting neurogenesis [12], recovery from stroke [13], and remyelination [14]. Therefore, it is more correct to indicate microglial activation as a pro- or anti-inflammatory phenotype based on the molecular signature that is observed following exposure to certain stimuli [15]. However, microglia activation, regardless of their particular polarized state, is considered the main hallmark of neuroinflammation, a phenomenon occurring in almost every pathology of the CNS [16]. It is important also to point out that, despite being polarized onto a certain phenotype, microglia retain their plasticity to switch between pro- and anti-inflammatory phenotypes and can display a spectrum of intermediate phenotypes [17], [18].

### Function during homeostasis

In physiological condition, microglia exhibit the so-called “resting” ramified phenotype, which continuously inspects the CNS microenvironment by extending and retracting their processes [19].

It is well known that anti-inflammatory cytokines such as transforming growth factor- $\beta$  (TGF- $\beta$ ) constitutively present within the CNS in a homeostatic context, prevent microglia from activation [20]. In addition, cell-to-cell interactions between microglia and neurons represent inhibitory signals for microglia, and studies demonstrated that loss of constitutive inhibitory signaling causes the loss of resting-state of microglia [21], which increase the expression of activation markers such as CD11b and CD45 in healthy CNS.

Microglia are a source of neurotrophic and growth factors within the CNS, such as brain-derived neurotrophic factor (BDNF), insulin-like growth factor 1 (IGF-1), nerve growth factor (NGF), and TGF- $\beta$  [22]–[24], which regulate the proliferation of neuronal progenitors, survival of neurons and OL, axonal growth, synapse formation and OL differentiation [25], [26]. In addition to neurotrophic function, microglia contribute to normal CNS development since they have a first-line role in the clearance of dispensable neurons during CNS development and adult neurogenesis [27], [28]. In fact,

microglia express different types of receptors recognizing specific signals from apoptotic cells, which mediate phagocytosis of cellular debris [29], preventing also collateral inflammation-induced damage [30], [31].

Furthermore, microglia are involved in synapse elimination or synaptic pruning, which is required to establish efficient neuronal networks. Inappropriate synaptic connections are recognized by microglia through specific patterns, which enables phagocytosis of tagged synaptic material, thus rendering microglia important in the restructuring of neuronal connections [32].

### Function during stress

Microglia represent the first line of defense against pathogens and tissue injury within the CNS. Infectious CNS diseases, neurodegenerative diseases, traumatic brain injury (TBI) and ischemia, neuropsychiatric disorders, and autoimmune diseases have been widely associated with microglia activation [33]–[35].

Upon detecting disturbances to CNS homeostasis, and activating signals are encountered, resting microglia go through polarization, switching from scouting the CNS to shielding the injured site. Microglia undergo morphological changes by moving towards the affected site, creating a physical barrier between healthy and injured tissue, and preventing further spreading of cellular stress within the CNS [19], [36]. Morphological changes, such as the acquisition of amoeboid shape, are associated with specific molecular signatures involving the release of cytokines, chemokines, and/or trophic factors. Microglia activation subsequently initiates an immune response, which involves the recruitment of peripheral immune cells to the site of inflammation in the brain parenchyma by the secretion of different chemokines, such as CCL2, -3, -4, -22, or IL-8 and -10, macrophage inflammatory protein (MIP)-1 $\alpha$  and -1 $\beta$  [37]. In addition, microglia acts as antigen-presenting cells (APCs) to the adaptive immune system, therefore facilitating phagocytosis of pathogens and cellular debris that have been tagged by antibodies or complement proteins [38]. Microglial antigen presentation may go accompanied by the increased expression of major histocompatibility complex (MHC) molecules and co-stimulatory molecules, such as CD40, CD80, and CD86 [39]. Activated microglia secrete a plethora of inflammatory mediators including reactive species, growth factors, pro- and anti-inflammatory cytokines, and chemokines. Pro-inflammatory cytokines produced by microglia include IL-1 $\beta$ , IFN- $\gamma$ , tumor-necrosis factor (TNF- $\alpha$ ), IL-6, and IL-12, which can induce, amplify and/or alter pro-inflammatory responses [40]. For example, IL-1 $\beta$  is known to specifically

induce and amplify T helper (Th) 17 cells responses [41], whereas IL-23 is known to promote Th1 responses [42]. Anti-inflammatory cytokines produced by microglia include IL-1-receptor antagonist (IL-1RA), TGF- $\beta$ , and IL-10, which dampen pro-inflammatory responses and induce regulatory responses [8], [18]. In particular, IL-1RA prevents IL-1 $\beta$ -mediated signaling by binding to the IL-1 receptor without subsequent activation, while IL-10 induces regulatory T cells (Treg) activation [39]. Thereby, anti-inflammatory cytokines can prevent the continuous activation of the immune cells and/or contribute to the resolution of an inflammatory response.

In summary, microglia efficiently aid in the removal of pathogens and other potentially detrimental substances from the CNS and can help to induce an efficient, appropriate immune response under pathological conditions. However, persistent activation of microglia is well known to contribute to tissue damage and neurodegeneration. For example, the accumulation of amyloid- $\beta$  plaques in AD, or the production of autoantibodies in MS have been reported to cause overactivation or dysregulation of microglia [43] [44]. Microglia chronic activation is associated with OL death, demyelination, and increased neuronal vulnerability. Furthermore, the production of neurotoxic factors by microglia, such as reactive oxygen species (ROS), nitric oxide, IL-1 $\beta$ , and TNF- $\alpha$ , directly lead to neurodegeneration.

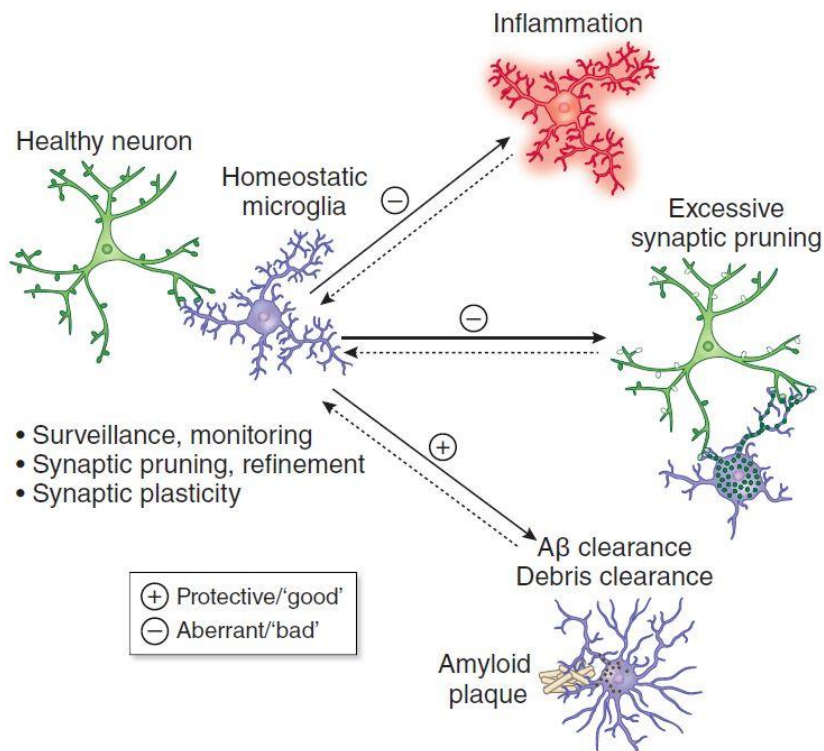


**Figure 1. Microglia states in health and disease.** *Microglia possess a complex role in the CNS, as they carry out functions that are both beneficial and detrimental. For example, beneficial functions include the engulfment or degradation of toxic proteins (i.e., amyloid plaques), and cell debris. However, dysregulation in microglia's normal homeostatic functions such as surveillance, synaptic pruning, and neuronal plasticity induce neurotoxicity through excessive inflammatory cytokine release and contribute to chronic neuroinflammation leading to excessive synapse loss and neurodegeneration. Adapted from Salter MW. Et al., Microglia emerge as central players in brain disease. Nat Med. 2017 [16]*

#### 1.1.4 Oligodendrocytes

The OLs are extremely specialized glial cells in the CNS responsible for the production of the axonal ensheathment called myelin. OLs and myelin provide functional and metabolic support to axons, ensuring also their physical protection in addition to the efficient transmission of nerve impulses [45]. For one OL it is possible to myelinate multiple axons by ensheathing their structure, in a process called myelination. The interaction between OLs and axons is known to be determined by the diameter of axons. Large diameter fibres myelinate before than small diameter one, and the optic nerve myelinates later than the spinal cord. The finely regulated myelination process, presented in a simplified manner, occurs as follows: in the early stages of myelination, the OLs extend highly ramified plasma membrane processes that contact nude axons and trigger myelination [46]. OL processes expand upon axonal contact, wrap around the axon in concentric layers of membrane, and then compact themselves to produce a specialized insulating spiral lipo-protein structure [47]. As the membrane wraps, squeezing out all the cytoplasm, two different membrane appositions are formed: the intracellular or major dense line (MDL) and the extracellular or intraperiod line (IPL) [48], in a way that little or no cytoplasm remains between adjacent wraps (**Figure 3**). As the process of myelination continues, the link between the OL cell body and the compacted membrane becomes less apparent and is less visible by electron microscopy [49] (**Figure 2**).

The physiological function of the myelin is to ensure the high-speed impulse transmission along the axon. This is possible as the myelin sheath, having insulating properties, is not continuous along the axon but is organized in a segmental manner, which defines several distinct zones. The individually myelinated axon segments (insulating internodes) are interspersed by unmyelinated axon regions,

called nodes of Ranvier [50]. At this level, sodium channels allow the nerve impulse to propagate rapidly from node to node, enabling the so-called saltatory conduction (**Figure 2**). Therefore, OLs and myelin are essential for the proper functioning of the CNS, and myelin disruption or alteration leads to very disabling conditions.

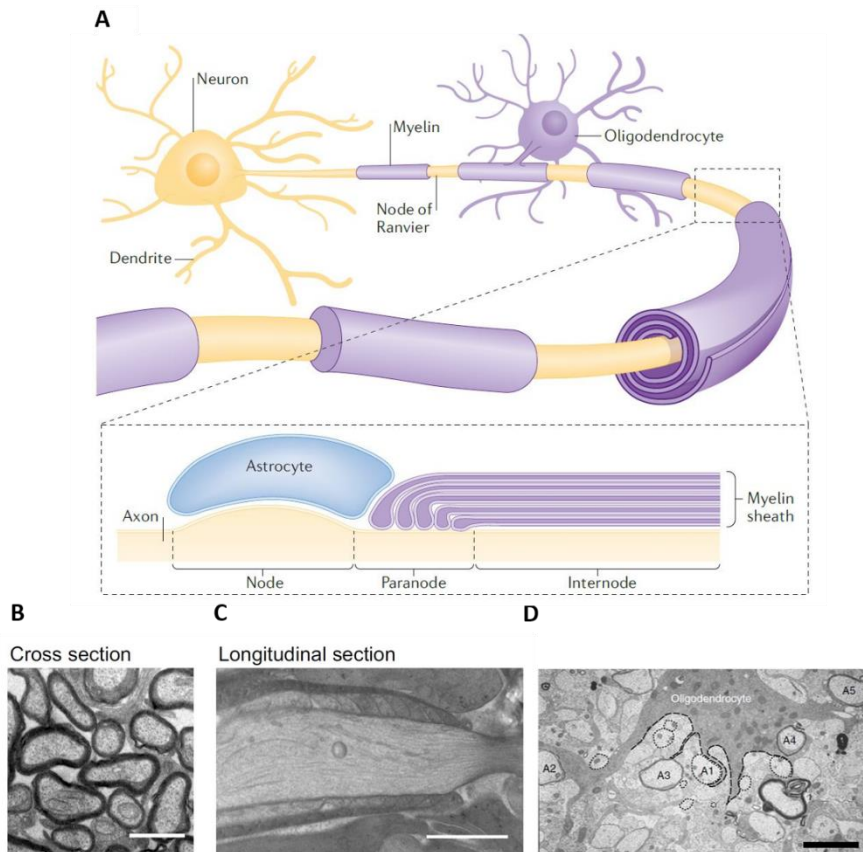


**Figure 2. Myelin and the node of Ranvier.** (A): OLs myelinate axons to increase the velocity of conduction of nerve impulses via saltatory conduction. (B): Action potentials are generated at nodes of Ranvier which are dispersed periodically along the axon between internodal segments of axons insulated by myelin. Perinodal astrocytes are in contact with the axon at nodal regions. (C): Transmission electron micrograph (TEM) of mouse optic nerve axons in a cross and longitudinal sections. (D): Electronmicrograph from a postnatal day 3 mouse brain, in which is evident that a single OL can myelinate several axons by extending many processes that wraps around a segment of a single axon. Scale bar: 2  $\mu\text{m}$ .

A, B: Adapted from Fields RD. A new mechanism of nervous system plasticity: activity-dependent myelination. *Nat Rev Neurosci.* 2015 [51]. C: Adapted from Stadelmann C. et al., Myelin in the

*Central Nervous System: Structure, Function, and Pathology. Physiol Rev. 2019 [45]. D: Adapted from Edgar J and Griffiths R., White Matter Structure: A Microscopist's View, Chapter 5 of Diffusion MRI for quantitative measurement, 2009.*

## Myelin composition and structure

Myelin is a compact, multi-lamellar, high-specialized membrane, composed of 70% of lipids and 30% of protein [52]. Its particular composition where the lipids/protein ratio is inverted if compared to the plasma membrane of other cell types confers to myelin an insulating capacity, able to accelerate the conduction of the action potential along the axon. Once produced by the OLs to ensheath axons, myelin is not a stable static membrane, but its components are constantly renewed and replaced by the cell during its life span. However, this process occurs more slowly than for components of other membranes in the CNS, as the half-life of the lipids and proteins in myelin can be as long as several months [53].

### *Lipids*

Three main families of lipids make up myelin: cholesterol (40%), phospholipids (40%) and glycosphingolipids (20%) [54], [55]. Cholesterol is one of the major constituents of myelin and more generally of all the cell membranes in mammals [56]. Cerebral cholesterol is synthesized *de novo* in the brain and OLs are responsible for a peak in cerebral cholesterol during the active period of myelination [57]. Indeed, a significant production of cholesterol within OLs is essential for the proper formation of the myelin sheath, and cholesterol synthesis is considered the rate-limiting step of the myelin assembly. The main function of cholesterol in myelin is the regulation of its fluidity and permeability [54], together with the aid in the stabilization of compact myelin by its association with myelin proteins. Phospholipids are necessary for the stability and maintenance of the structural integrity of the myelin sheath over time. The most representative one is plasma phosphatidylethanolamine, which has been proposed to have a protective role against oxidative stress and in preventing lipid peroxidation [58]. Among the glycosphingolipids, the two main galactocerebroside (GalC) and sulfatide are known to facilitate myelin compaction [59]. GalCs are accumulated on the external face of OL membranes and are known to be involved in maintaining the stability of the myelin sheath by contributing to the adhesion of the membrane layers one to each other [60], [61]. During active myelination, the concentration of GalC in the brain is directly proportional

to the degree of myelination, making it a reliable indicator of the amount of myelin present in the CNS. In addition, inhibition of GalC using antibodies is capable of abolishing myelination *in vivo* [62].

### *Proteins*

Recent advances in the field of proteomics have evidenced that the quantity of proteins present in myelin has been greatly underestimated over the years [63]. About a third of the myelin sheath is made up of proteins, and the largest part of them is specific to this structure, thus can be exploited as a myelin marker. The most abundant proteins in CNS myelin are the Proteolipid protein (PLP/DM20) and the Myelin Basic Protein (MBP), which co-operate in the formation of a stabilizing junction between the different layers of myelin, allowing for the compaction of the structure [64].

PLP/DM20 constitute the 50% of all myelin proteins in the CNS. PLP is 30 kDa, while DM20 represents the smaller isoform of 26 kDa [65]. These two proteins have identical amino acid sequences, except for 35 amino acids encoded by exon 3B of the *PLP1* gene, which are absent from the DM20 isoform. During myelination, the DM20 is expressed earlier and is selectively excluded from the compacted myelin, and enriched on the external surface of OLs [66]. On the contrary, PLP is expressed later and it is associated predominantly within the myelin sheath after its compaction and has been demonstrated to be required for myelin maintenance and its integrity [67]. PLP is synthesized on the surface of the ER, then exported via Golgi apparatus and vesicular transport to the OL membrane. During its transport, PLP binds cholesterol and has been showed to have a role in the incorporation of cholesterol into myelin membranes [68]. Mutations of the *PLP1* gene in human and mouse are responsible for leukodystrophies (pathologies affecting the white matter), in line with its role of structural protein of myelin.

After PLP, MBP is the second abundant protein in myelin. It interacts with glycosphingolipids to allow the compaction of the internal layers of the myelin [45]. Several isoforms of the protein produced by different splice variant are present, forming the family of MBP proteins [69]. The predominantly expressed forms are those of 18.5 kDa in humans and 18.5 kDa and 14 kDa in mice. MBP plays a fundamental role in the myelination process as evidenced by the mouse mutant *shiverer*, which possesses a partial deletion of the MBP gene which prevents protein synthesis [70]. *Shiverer* mice have a lifespan of approximately 90-150 days and exhibit various symptoms such as tremors and seizures. Analysis of the CNS of these animals shows an almost non-existent myelin sheath [71].

The study of the MBP protein has generated great interest because it is a candidate autoantigen in MS disease. In fact, MBP-specific T lymphocytes have been found in the lesions of MS patients [72], [73]. Myelin has been for long considered to be an inert structure. However, the discovery of proteins having an enzymatic function in the myelin sheath revealed a metabolically active membrane in the synthesis and renewal of its constituents. The 2',3'-cyclic nucleotide 3'-phosphodiesterase (CNPase) is another functionally important protein that is present only in the non-compacted regions of myelin, and it has been shown to have enzymatic activity [74]. CNPase enzyme is encoded by the *CNPI* gene, and has two different isoforms which are differentially expressed between the different stages of OLs maturation (see below): OLs precursors seem to express only the larger isoform of 55 kDa, whereas mature OLs were shown to express both isoforms of 55 and 46-48 kDa [75]. Although discovered many years ago, its biological function is still unclear. Studies demonstrated its ability to interact with the actin cytoskeleton, and to facilitate the wrapping of the OL membrane around axons during myelination, suggesting a role in the growth of oligodendrocytic extensions [76].

Other well-known although minor myelin proteins include the Myelin-Associated Glycoprotein (MAG) and the Myelin Oligodendrocytes Glycoprotein (MOG) [64]. MAG is detected before the other myelin proteins at the very earliest stages of myelination, suggesting a role in the initial axon-glial recognition events that occur before myelination, for example to indicate the path of myelin deposition [77]. MOG, owing to the immunoglobulin family, is a transmembrane protein predominantly expressed on the surface of the myelin sheath, and it has been found only weakly in the coils of the compact myelin sheath. Its expression is detected late, and it is expressed only in the myelinating OLs, thus being a marker for mature myelinating OLs [78].

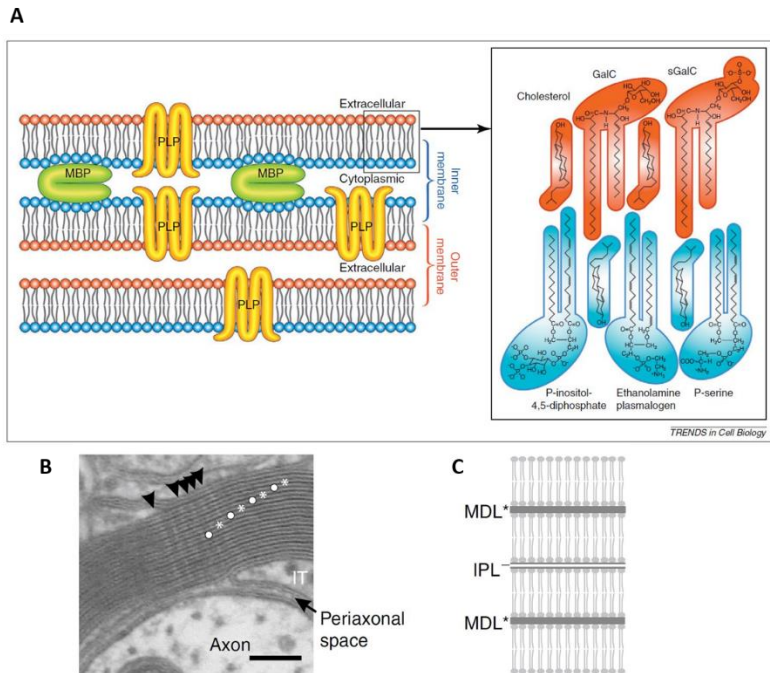


**Figure 3. The structure of the myelin.** (A) Compact myelin is formed due to the stacking of the external and internal surfaces of the myelin bilayer that constitute the intracellular and extracellular lines, respectively. PLP and MBP represent the main myelin proteins. The myelin bilayer possesses an asymmetric lipid composition. On the right panel, myelin major lipid classes are presented. (B) The spiral wrapping of the OLs process gives to the compact myelin its typical cross-sectional ultrastructure. Two distinct bands give the periodicity of compact myelin seen in this electronmicrograph. (C) The major dense line (MDL; asterisks) is due to the coalescence of the two surfaces of the plasma membranes of the OL process facing the cytoplasm, while the intraperiod line (IPL; circles) forms at the junction between the surfaces of the plasma membranes facing the extracellular space. In this case, the two membranes are separated by a small space, about 20 Å (2 nm) in width, which is filled with extracellular fluid. A: Adapted from Aggarwal S. et al.; Central nervous system myelin: structure, synthesis, and assembly. Trends Cell Biol. (2011) [79]. B, C: Adapted from Edgar J and Griffiths R., White Matter Structure: A Microscopist's View, Chapter 5 of Diffusion MRI for quantitative measurement (2009).

## The development of oligodendrocytes

The development of the oligodendrocytic lineage is a highly regulated process dependent on a multitude of intrinsic and extrinsic factors, such as transcription factors (Olig1 / 2, Sox10, Nkx2.2), growth factors, molecules of the extracellular matrix, morphogens (mainly Sonic Hedgehog) and several highly regulated epigenetic mechanisms, such as DNA methylation and histone modification [80], [81]. OLs arise from the neuroepithelial stem cells present in the ventricular area of the neural tube during early embryonic development. Then, they differentiate into radial glia cells, which are the last common precursors between neurons and glial cells. They subsequently divide to give rise to astrocytes precursors and then to the precursor cells of OLs [82]. During embryonic development, these precursor cells migrate to the subventricular zone where they mature to become oligodendrocyte progenitor cells or OLs precursor cells (OPCs) [83]. Subsequently, additional sources of OPCs emerge during development in the dorsal CNS, supporting the existence of different spatiotemporal waves of OLs production [84]. After their generation, OPCs migrate through the CNS attracted by the platelet-derived growth factor (PDGF) and repulsed by Netrin-1 signals [48]. Once in the subventricular zone, OPCs proliferate and then acquire their mature phenotype finalizing their differentiation when they identify axons to be myelinated [83].

The cells which are known as pre-myelinating oligodendrocytes (pre-OL) engage with a target axon and start to extend radially and symmetrically multiple myelin outgrowths. At this differentiation stage, pre-OL expresses three main myelin-associated markers such as DM20, MAG, and CNPase which are distributed through the cell, but also the cell surface markers O4 and O1 respectively expressed in late progenitors and pre-OL [85]. The differentiation from a pre-OL to a myelinating oligodendrocyte (mOL) is again characterized by morphological and molecular changes. The most important change is the cell polarization, whereby mOLs targets myelin proteins to specific membrane domains. In particular, PLP/DM20 is targeted to compact myelin as transmembrane protein [86] CNP to non-compact myelin of the internode [75], MAG to periaxonal membranes, and MBP mRNA along processes to be translated *in situ* for its location on the cytoplasmic surface of the plasma membrane [87]. mOL is characterized also by the production of MAG [88], the membrane marker galactocerebroside (GalC) [89] and surface marker MOG [90] (**Figure 4**).

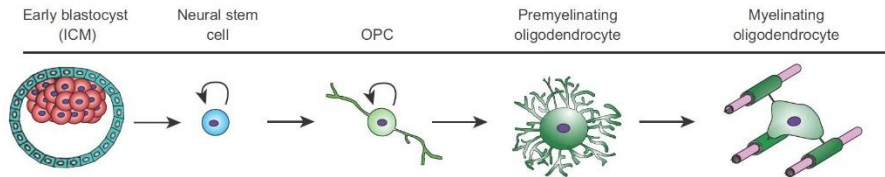


**Figure 4. Schematic representation of the developmental stages of the OL lineage.** *The morphological features of the oligodendrocytic lineage cells from the Neural stem cell, to OPC, pre-OL, and myelinating OL are shown. Adapted from Goldman SA and Kuypers NJ. How to make an oligodendrocyte. Development. 2015 [84].*

In summary, myelination of axons can be simplified in three steps: (1) recognition of target axons by OPCs and differentiation into immature OLs (pre-OL), (2) growth and coiling of the thin cell sheaths around axons, and (3) compaction of the myelin membrane to form the mature myelin sheath. At that point OLs are then said to be myelinating (mOL) (**Figure 4**) [45], [91], [92]. CNS myelination begins from the third trimester of pregnancy and continues throughout life although more slowly. OLs require specific factors produced by neurons which are essential for the formation and the maintenance of myelin in the CNS. To ensure the continuity of this process, a substantial number of OPCs persist in the brain during adulthood, and reside in the subventricular zone of the CNS accounting for 5-8% of the glial cell populations [83]. In the eventuality of damage to the myelin sheath, OPCs are recruited to the damaged area, proliferate, and then differentiate into mOLs which ensure myelin replacement, thus participating in brain plasticity [1].

## 1.2 Myelin Pathologies

---

Abnormal formation and/or disruption of the CNS myelin sheath leads to pathological consequences. Neuronal communication is impaired due to the decrease in the velocity of the nerve impulse transmission. In addition, depending on the severity of the damage, myelin-related problems may trigger neurodegenerative processes. Among the pathologies affecting myelin, two distinct categories are generally identified, which are easily recognized by specific myelination patterns observed by Magnetic Resonance Imaging (MRI) [93]. **Dysmyelinating diseases** are caused by abnormalities in the formation or maintenance of functional myelin sheath, and an example of such pathologies is represented by the genetic Pelizaeus-Merzbacher Disease (PMD). On the contrary, in **demyelinating diseases** myelin is correctly produced, however, it is damaged or disrupted by external factors, as it happens in MS. Moreover, myelin abnormalities are known to participate in the clinical picture of many neurological pathologies, including psychiatric disorders, AD, and all the disturbances involving aging [94], [95].

### 1.2.1 Dysmyelinating pathologies: Pelizaeus-Merzbacher Disease

Pelizaeus-Merzbacher disease (PMD) represents a Dysmyelinating pathology belonging to the leukodystrophies family, a term that groups together a set of genetic diseases affecting the myelin of the CNS. PMD is an X-linked recessive genetic disease, thus affecting mainly males. Its worldwide incidence (proportion of new cases) is estimated to be between 1,45 and 1,9 cases per 100.000 male births [96]. On clinical examination, PMD is characterized by a variable clinical spectrum with some frequent features: motor and cognitive developmental delay including from mild to severe intellectual disability, involuntary oscillatory movements of the eyes (nystagmus), tremors, ataxia, and hypotonia, which can progress to spastic paresis. A massive loss of myelin in white matter, evidenced by post-mortem analysis of the brain of PMD patients, impairs the transmission of nerve impulses, being the cause of neurological problems [97].

The etiology of PMD is represented by mutations in the proteolipid protein 1 (*PLP1*) gene which encodes the major myelin protein PLP, thus preventing the correct formation of the myelin sheath in the CNS. Indeed, the best-characterized function of PLP is structural, as it participates together with MBP in the formation of stabilizing junctions between myelin sheets [67]. The *PLP1* gene is located

on the X chromosome at position q22 in humans. It contains 7 exons, spread over 15 kb, and several splice isoforms have been described for this gene, including two main ones encoding PLP and DM20 [65]

### Clinical forms and physiopathology

PMD is characterized by a heterogeneous spectrum of clinical forms ranging from the most severe phenotype (neonatal form) to a more moderate phenotype (classical form) to the mildest phenotype. The PMD clinical forms classification is based on the observed clinical symptoms and severity, which are often associated to a specific type of genetic mutation.

Each clinical form of PMD is caused by a specific type of genetic mutation in the *PLP1* gene, which allowed to establish a correlation between the genotype and the phenotype. *PLP1* gene mutations comprise duplications, point mutations, as well as whole or partial deletions (**Figure 5**) [96]. The mildest form of PMD is referred to as the PLP1-null syndrome and is not clearly dissociable by objective criteria from type 2 spastic paraplegia (SPG-2). In this form, usually linked to nonsense point mutations or gene deletions leading to the absence of PLP protein, the deficits appear during adolescence or adulthood, involving developmental delay which may be accompanied by peripheral neuropathy. Patients are generally able to learn to walk independently and language develops normally, with a life expectancy not different from the rest of the population [98]. The classic form of PMD is the most common, representing between 60 and 70% of PMD cases [99]. This form involves duplications of the *PLP1* gene, which create additional copies of the genes leading to increased expression of the PLP / DM20 protein. The pathology evolves slowly throughout the life of patients, which begin to develop symptoms before the fifth year of life. The expected lifespan is on average forty years, although quite pronounced variability ( $\pm 11$  years) is observed [100].

The neonatal form is the rarest and most severe form, caused by missense point mutations. Point mutations alter PLP protein folding, leading to a gain of toxic function for OLs. This clinical form is characterized by total CNS dysmyelination [101]. Typical symptoms such as hypotonia, spasticity, nystagmus, and delayed development of motor and cognitive skills appear from birth and progress to the premature death of patients within the first decade of life [98]. For the purposes of the present thesis, this clinical form of PMD will be examined in detail.

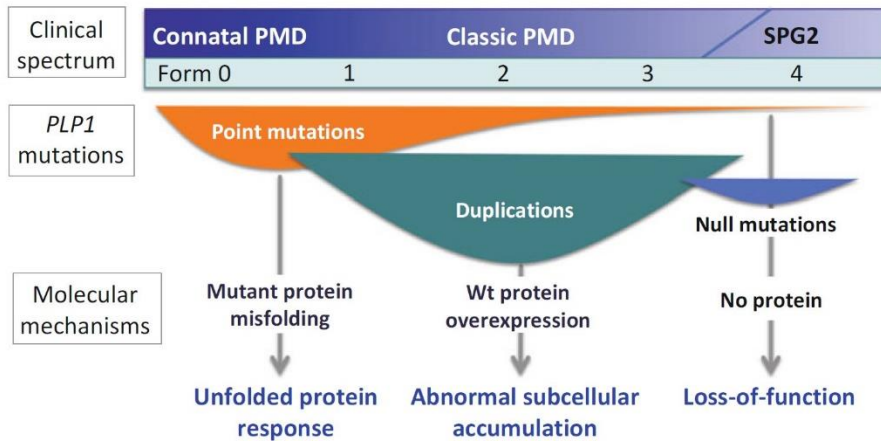


**Figure 5. Genotype-phenotype correlations and associated cellular and molecular mechanisms of PMD.** Different *PLP1* gene mutations (missense mutations, duplications, or deletions) result in distinct molecular events, leading to a wide variety of clinical phenotypes which vary from severe to mild. Adapted from Inoue K. Pelizaeus-Merzbacher Disease: Molecular and Cellular Pathologies and Associated Phenotypes. *Adv Exp Med Biol.* 2019 [96].

### Experimental models of the severe PMD form: *Jimpy* mouse and 158JP OLS cell line

The physiopathological mechanisms involved in the severe form of PMD have been demonstrated by means of different animal models. One of the most used models for the preclinical study of neonatal PMD is the spontaneous mutant *jimpy* (*jp*) mouse, which presents a significant dysmyelination of the CNS resulting in a severe clinical phenotype characterized by ataxia, tremors, seizures, and reduced life span to only four weeks [102]. Histological studies on *jimpy* mice revealed an almost complete absence of white matter in the CNS, and a few sheaths of uncompact myelin covering some axons [103]. *Jimpy* mice carry a single point mutation located at the splicing acceptor site between exon 4 and 5 of the *Plp1* gene (NM\_011123.4:c.623–2A>G) [104]. In detail, the 5'-AG-3' splicing acceptor site is abrogated in presence of the *jimpy* mutation (AG>GG) inducing a skipping of the exon 5 (74 base pairs loss) in the mRNA sequence, and a shift in the open reading frame, leading to the insertion of a premature stop codon and the production of a misfolded PLP truncated in its C-terminus [104]. Such conformational changes in PLP are responsible for its accumulation in the endoplasmic reticulum (ER), and the activation of apoptotic signals in OLs. Several studies have demonstrated that the dysmyelination observed in *jimpy* is due to the death of mature OLs by apoptosis [98], [105],

[106]. Briefly, misfolded/unfolded proteins in eukaryotic cells are removed from the ER to maintain cellular homeostasis, through the quality control process Unfolded Protein Response (UPR), which protects cells from the toxicity of accumulated proteins. When the ER stress is not tolerated by the cell, the pro-apoptotic signaling pathway of UPR is activated [107]. Therefore, the massive OLs death observed in severe PMD patients as well as in *jimpy* mice, is thought to be caused by misfolded PLP accumulation in the ER and UPR-induced apoptosis [96].

Of note, the very short lifespan of *jimpy* mice, and the chromosome X-linked transmission of the pathology render difficult the intensive study of the molecular mechanisms which clarify the correlation between PLP mutation, ER stress, and OLs death. Thus, to help the deciphering of the physiopathological mechanisms involved in severe PMD pathology, an immortalized cell line of *jimpy* OLs (158JP) has been generated and it is shown to possess markers of mature OLs such as MBP, PLP, and GalC [108]. Herein, PLP was demonstrated to be incorrectly inserted into the 158JP membrane, resulting in a defective cAMP signaling pathway [109]. Moreover, an increase in mitochondrial membrane potential (MMP) as well as higher production of ROS, together with an increased colocalization between PLP and mitochondria was evidenced in 158JP OLs compared to 158N wild-type OLs [110], suggesting that oxidative stress and mitochondrial dysfunctions could be also involved in OLs death together with ER stress.

### Current therapies and innovative therapeutic approaches

There is currently no cure for PMD; treatments involve management of symptoms and supportive therapies. Nevertheless, some therapeutic avenues are being explored. Several efforts have been carried out to cope with congenital PMD. Recently, *in vitro* studies performed 158JP OLs, a cellular model of the severe form of PMD, have shown promising results, against OLs death by the means of known ER stress modulators such as 4-phenyl-butyric acid (4-PBA) [111]. Concerning the classical form, involving *PLP1* gene duplication, a study demonstrated that the reduction of the expression of PLP1 with microRNAs made it possible in transgenic PLP1 mice to improve the survival of OLs and the clinical phenotypes observed [112]. Regarding the innovative therapeutic approaches, stem cell replacement therapy was shown encouraging for the treatment of severe PMD. A phase I clinical trial demonstrated small, but discernible increases in myelin after stem cell-based treatment to replace defective OLs [113]. In addition, a very recent study has found that PMD-associated *PLP1* mutations lead to iron toxicity in the OLs. Also, an iron-chelating FDA-approved drug was shown to reduce OLs

death and to boost myelin formation both in PMD patient IPs-derived OLs, and in *jimpy* mouse [114]. Among the genetic approaches, a very recent study showed that CRISPR/Cas9 mediated knock-out (KO) of mutated *PLP1* gene exerted beneficial effect in *jimpy* mice for what concern OLs viability, myelination, and recovery of neurological deficits [115]. The authors have based their *Plp1*-deletion strategy on the fact that PLP1-null genetic mutation is responsible for a milder phenotype if compared to missense PLP1 mutations, which cause the most severe PMD phenotype. These findings encourage the use of genome-editing tools such as CRISPR/Cas9 technology against genetic disorders including severe PMD, not only for a therapeutic approach, but also to elucidate the physiopathological mechanisms underlying the cytotoxic effects exerted by missense *PLP1* mutations.

### CRISPR/Cas9 technology: overview and principle

The Clustered Regularly Interspaced Short Palindromic Repeats/Cas (CRISPR/Cas) system has evolved in the Prokaryotes as an adaptive immune system against the infectious attacks of bacteriophages and eventual transfers of plasmids. The CRISPR/Cas9 system of type II was discovered for the first time in *Streptococcus Pyogenes* in 1987 and was shown capable of breaking DNA sequence in exact points. Only in 2012, it has started to be exploited by researchers as a possible genome editing tool, and such discovery awarded Jennifer Doudna and Emmanuelle Charpentier the Nobel Prize for Chemistry 2020 [116], [117].

The CRISPR/Cas9 system consists of two elements: the Cas9 protein and the guide RNA (gRNA) of 20 nucleotides (nt). The Cas9 is an endonuclease (a protein that cleaves phosphodiester bonds in DNA) having two nuclease domains. The gRNA is a hybrid molecule made up of two associated RNAs: the crRNA (CRISPR RNA) and the RNAtacr (transactivating CRISPR RNA). The RNAtacr recruits the Cas9 endonuclease, while the crRNA, composed of 20 nucleotides complementary to the target DNA, allows the targeting of a specific DNA sequence [118]. Inside the cell, Cas9 is bound to the gRNA forming a ribonucleoprotein that recognizes specific DNA sequences in the genome. For Cas9 to induce a double-stranded break (DSB), the target DNA sequence recognized by the gRNA must be immediately followed by a PAM (Protospacer Adjacent Motif) sequence [116]. The PAM sequence is variable depending on the employed Cas9. For *Streptococcus pyogenes* Cas9 (spCas9), the most widely used Cas9 for genome editing, the PAM sequence is 5'-NGG-3' [19,20]. Only after gRNA binding to the target sequence, and after PAM identification, Cas9 produce DBS on the DNA target sequence (**Figure 4**). The DBS is repaired by endogenous DSB repair systems, non-homologous

end joining (NHEJ), or homology-directed repair (HDR) systems. The repair by NHEJ takes place during all phases of the cell cycle, and is the most frequently occurring system. It quickly connects cut DNA strands [119] giving rise to short insertions or deletions (1-from dozens to several hundred nucleotides), which can cause a shift in the reading frame or the insertion of a stop codon. On the contrary, HDR is the less frequent repair mechanism, occurring only during the G2 and S phases of the cell cycle, when the DNA sister chromatid is available to serve as a template for homologous repair. To precisely edit the genome, *e.g.* to introduce a point mutation, a single-stranded deoxynucleotide (ssODN) which includes homology arms to both sides of the cleaved target sequence, and the DNA sequence that needs to be inserted, is provided to the cell. The ssODN will serve as a template for the HDR after Cas9-induced cut, thereby allowing the precise insertion of a mutation into the genome [119] (**Figure 6**).

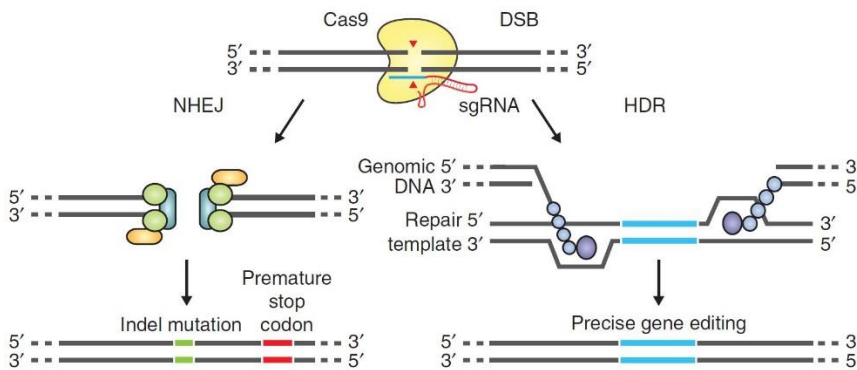


**Figure 6. CRISPR/Cas9 system representation: DSB promotes gene editing.** DSBs induced by the Cas9 enzyme can be repaired by two different repairing mechanisms. In the NHEJ pathway, the ends of a DSB are ligated by endogenous DNA repair machinery, which can result in random insertions/deletions (indel) at the site of the junction. Indel mutations that occur within coding regions can result in frameshifts and the creation of a premature stop codon, resulting in gene KO. Alternatively, in the presence of a homologous sequence, the HDR pathway can occur, allowing high fidelity and precise genome editing. Adapted from Ran FA. *Et al., Genome engineering using the CRISPR-Cas9 system. Nat Protoc. 2013* [120].

However, two important drawbacks need to be taken into account during the application of the CRISPR/Cas9 technology to introduce a single point mutation in the DNA: (i) the possibility of having off-target issues, and (ii) the reduced probability of HDR to occur compared to NHEJ.

In order to overcome these issues, Cas9 nickase (nCas9) has been generated by mutating one of the two nuclease domains of the WT Cas9. nCas9, instead of producing a DSB, induces a single-strand break (SSB) (also called nick) on the DNA strand, reducing the possibility of inducing the NHEJ repairing mechanism and promoting the homologous recombination, which represents the goal in order to achieve the point mutation [120]. In addition, the use of nCas9 limits the appearance of off-targets effects, as SSB is faithfully and quickly repaired by the cell. The introduction in the cell of nCas9, together with two different gRNAs which bind both sides of the target cleavage point, creates a nick on the two filaments (sense and antisense). If the SSB are close enough to each other, the result is the obtainment of a DSB, however, the HDR is more likely to occur. The present double nick strategy has been estimated to increase by around 1500x the specificity of the target site [121]. Despite several challenges in the design of CRISPR/Cas9 experiments, such technology is considered nowadays the gold standard in the genome editing approaches.

### 1.2.2 Demyelinating pathologies: Multiple Sclerosis

Multiple sclerosis (MS) is a chronic autoimmune and neurodegenerative pathology affecting the CNS, classified as an inflammatory disease because of the extensive infiltration and activation of peripheral immune cells in the CNS, which mediate the formations of focal lesions. MS hallmarks are represented by chronic demyelination, OLs death, and axonal loss in the brain and in the spinal cord, which determine motor, sensory and cognitive deficits [122].

MS affects around 2,3 million people worldwide and is considered the first cause of disability in young adults since its onset usually occurs between 20 and 40 years of age [123]. The clinical manifestations and the course of MS pathology are heterogeneous. In 85% of MS patients, the initial phase is characterized by reversible episodes of neurological deficits lasting usually for days or weeks, which are followed by so-called periods of remission. For this reason, such a clinical form is named relapsing-remitting MS (RRMS). The minority of patients (15%), have a progressive continuous disease course starting from the onset, which is referred to as primary progressive MS (PPMS). However, part of RRMS patients experience a reduction in the lasting of the remission phases over time, the progression of clinical disability become prominent and develop permanent neurological deficits. This form is known as secondary progressive MS (SPMS) [124] (**Figure 7**).

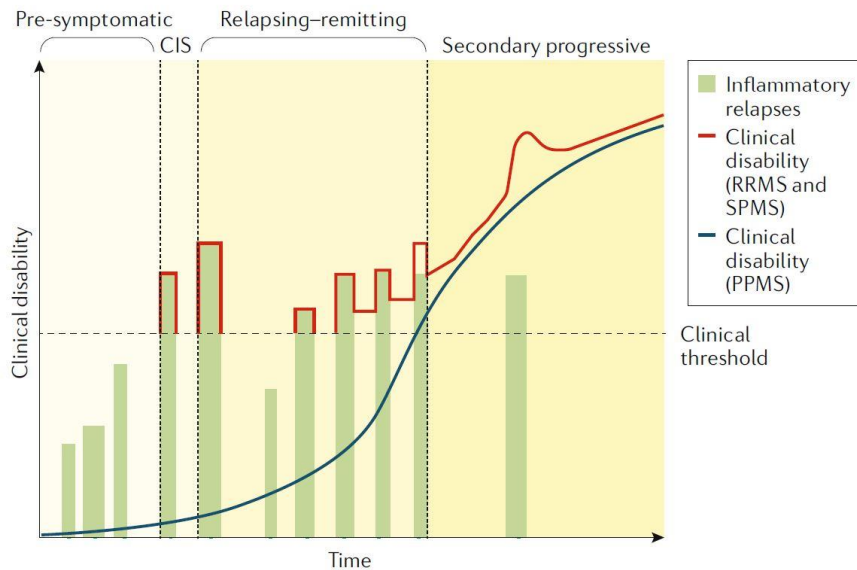


**Figure 7. The clinical course of MS.** Different clinical courses of MS are identified: relapsing–remitting MS (RRMS), primary progressive MS (PPMS), and secondary progressive MS (SPMS). RRMS accounts for ~85% of patients and is characterized by relapses occurring at irregular intervals with complete or incomplete recovery. A large part of patients with RRMS then develops SPMS, which is characterized by progressive, irreversible disability. Around 10–15% of patients present PPMS, which is characterized by progressive disease with acute relapses (with or without full clinical recovery) and periods of continuing progression between relapses. A revision of these phenotypes has been recently proposed and includes clinically isolated syndrome (CIS) for patients whose first clinical presentation has characteristics of inflammatory demyelination that could be MS but who do not fulfill all diagnostic criteria. Adapted from Filippi M, *Multiple Sclerosis, Nat Rev Dis Primers* 2018 [124].

MS has a wide range of clinical signs and symptoms, which may differ greatly from patient to patient and throughout the disease, depending on the location of affected nerve fibers. The most dramatic event that determines a motor syndrome is the development of acute myelitis which, by damaging the descending motor pathway, leads to weakness. Tremor, lack of coordination, and spasticity events are also frequently observed in MS patients and potentially disabling. The most common sensory symptoms are numbness, paresthesia in one or both legs, dysesthesia, and pain. Visual dysfunctions such as diplopia are also observed. Finally, cognitive impairments include difficulty to concentrate, learning and memory problems, sleep disorders and dizziness. The appearance of psychiatric diseases

symptoms such as depression is often reported [125]. MS symptoms are the main direct cause of death in >50% of patients with MS and the life expectancy of patients is reduced by 7–14 years, but recent estimates demonstrate no strong evidence in this regard [126].

To date, years of research on MS lead to the awareness that MS is a highly heterogeneous, multifactorial, immune-mediated disease that is caused by complex gene-environment interactions [127]. Unfortunately, much still escapes us concerning its etiology, pathogenesis, and progression, although recent advances have been done in this area of research thanks to the use of animal models which recapitulate quite accurately the pathophysiology of MS.

### Epidemiology and risk factors

Around 2,8 million people are estimated to live with MS worldwide in 2020. If compared to the latest global studies, MS prevalence is estimated 30% higher than in 2013, despite it is known to vary between countries (50-300 per 100.000 people) [128]. In particular, MS is mainly developed by Europeans and North Americans, while it is rare in African people, Asian, Native Americans, and Māori individuals. Prevalence studies estimate double values for individuals in Western countries (more than 100 per 100,000) compared to Asian (20-60 per 100,000), with peaks of 1 per 400 individuals in countries at high latitude, mainly in Europe and North America [129] (**Figure 8**). Migration studies indicate that environmental influence is higher than genetics, despite substantial racial discrepancies are observed in the development of the pathology. A systematic review estimated MS incidence of 2.1 per 100,000 persons/year, and data lead to think that someone in the world is diagnosed with MS every 5 minutes. Globally, females have a double possibility to have MS than males. However, the ratio of women to men reaches 4:1 in some countries, and in others, such a ratio has doubled since 2013 [128]. Several studies around the world suggest that after the 1950s, the incidence of MS has notably increased [130], and faster in women than in men, identifying a possible correlation between environmental and lifestyle changes in women in recent years.

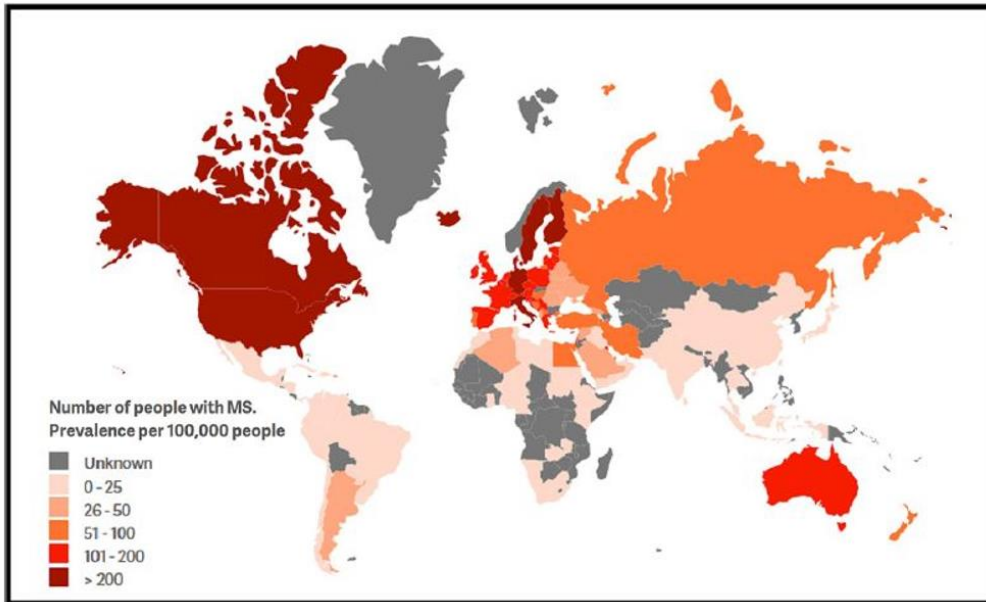


**Figure 8. The global prevalence of MS.** *This map shows geographic variation in MS prevalence (people with MS per 100,000 population) by country in shades of orange and red. The areas colored in dark red on the map correspond to geographic areas where we find the highest prevalence of the pathology (more than 200 per 100,000). Countries without prevalence data are shown in grey. Reported MS prevalence increased in every region between the 2013 and 2020 versions of the Atlas of MS. Data are taken from The MS International Federation's of Atlas, 3rd ed, September 2020, <https://www.atlasofms.org> [128].*

The exact causes of MS are to date still unknown. However, the largest part of the studies shares the common idea that the disease results from the interplay between genetic susceptibility and environmental risk factors [127] (**Figure 9**). The awareness about the immune-mediated pathogenesis of MS leads to suggest infectious diseases as possible triggers for the disease onset. Indeed, the most consistently and solidly risk factor associated so far is represented by the Epstein–Barr virus (EBV) infection in adolescence and early adulthood [127], [131]. However, a direct causal relationship between EVB and MS remains to date unestablished. In addition to viral infections, tobacco exposure through active or passive smoking, a lack of sun exposure, and obesity during adolescence have been proposed. Other, less-established risk factors include night work, excessive alcohol or caffeine consumption, and a history of infectious mononucleosis [127]. Sun exposure is the major determinant

of vitamin D levels, and tends to decrease in individuals living at higher latitudes. Thus, low vitamin D levels have been proposed to underlie the higher prevalence of MS in north countries [127]. Genetic risk factors have been also identified, although the prevalence of familial MS is only ~13% for all MS phenotypes, with a risk of recurrence within families which correlates to the percentage of genetic and environmental sharing [132]. The heritability of MS concerns polymorphisms in several genes, and more than 200 genetic variants have been identified by genome-wide association studies as predisposition factors to develop MS [133]. However, studies showed that different combinations of these variants, rather than single variants, contribute to increasing MS susceptibility in different patients [134]. The largest part of the identified variants encode molecules involved in the immune system and in particular in T cell activation and proliferation (such as the HLA, IL-2, and IL-7R and TNF polymorphisms) [135]. For example, an individual carrying the allele, HLA-DRB1 \* 1501 presents three more times the risk of developing MS compared to an individual who does not have it [136]. Moreover, a very recent study evidenced an epigenetic regulation of HLA expression as the mechanism which mediates this effect [137]. However, such a relationship can be not direct, because combinations of alleles of different genes are more or less involved in the development of the disease. In addition, as epidemiological studies show the higher prevalence of MS in women than in men, with sex ratios varying from 1.1 to 4 affected women per one man, the investigation about the involvement of X-chromosome in the development of MS has arisen between researchers. In fact, several genes related to the immune response are present on the X chromosome, such as TLR7 (Toll-like receptor), CD40L (cluster of differentiation), and FoxP3 (forkhead box), being proposed to be involved in MS [138] as their mutation was showed to lead to autoimmunity recognition problems [139].

Risk factor	Odds ratio	HLA gene interaction	Combined odds ratio <sup>a</sup>	Effect during adolescence	Immune system implied	Level of evidence
Smoking	~1.6	Yes	14	No	Yes	+++
EBV infection (seropositivity)	~3.6	Yes	~15	Yes	Yes	+++
Vitamin D level <50 mM	~1.4	No	NA	Probable	Yes	+++
Adolescent obesity <sup>b</sup>	~2.0	Yes	~15	Yes	Yes	+++
CMV infection (seropositivity)	0.7	No	NA	Unknown	Yes	++
Night work	~1.7	No	NA	Yes	Yes	++
Low sun exposure	~2.0	No	NA	Probable	Yes	++
Infectious mononucleosis	~2.0	Yes	7	Yes	Yes	++
Passive smoking	~1.3	Yes	6	No	Yes	+
Organic solvent exposure	~1.5	Unknown	Unknown	Unknown	Unknown	+
Oral tobacco or nicotine consumption	0.5	No	NA	Unknown	Yes	+
Alcohol	~0.6	No	NA	Unknown	Yes	+
Coffee	~0.7	No	NA	Unknown	Yes	+

+, non-replicated observations that require further study; ++, case-control observations that have been replicated and/or supported by independent methods; +++, high level of evidence from large prospective studies or a case-control observation that is supported by Mendelian randomization studies; CMV, cytomegalovirus; EBV, Epstein-Barr virus; HLA, human leukocyte antigen; MS, multiple sclerosis; NA, not applicable. <sup>a</sup>Combined odds ratio for the non-genetic factor and HLA allele. <sup>b</sup>Adolescent obesity defined as body mass index >27 at 20 years of age. Adapted from REF.<sup>17</sup>, Springer Nature Limited.

**Figure 9. Lifestyle and environmental risk factors for MS.** Adapted from Filippi M, *Multiple Sclerosis, Nat Rev Dis Primers*. 2018 [124].

## Physiopathology

The pathological hallmark common to all MS clinical forms is the presence of perivenular inflammatory lesions (or focal plaques), showing accumulation of activated immune cells which are responsible for the demyelination. Plaques occur in both white matter and gray matter and are typically found throughout the brain, spinal cord, and optic nerve [140]. The total volume of focal lesions is only moderately correlated with overall clinical disability and cognitive impairment, although the anatomical location of the lesions in the white matter is associated with specific clinical symptoms [141].

MS diagnosis is often made based on clinical criteria. However, MRI represents the exam of choice due to the sensitivity and specificity of this imaging modality in detecting macroscopic abnormalities, and in demonstrating the presence of demyelinating lesions. MRI is required to not only establish the basis of the diagnosis, but also to monitor disease activity, and to assess the prognosis and the pharmacological treatment [142]. In MRI, the disruption of the BBB is used as an indicator of disease activity. In parallel, emerging approaches exploit positron emission tomography (PET) imaging of activated microglia or macrophages to directly visualize the inflammatory state of the disease. In

particular, the user-specific markers of CNS immune cells activation to quantify microglial activation *in vivo*, and distinguish different functional states of microglia, provides a more direct approach to assess disease activity in MS. Moreover, PET imaging with radiotracers allows to assess of longitudinal changes, and determine how to monitor responses to DMTs [143]. Among the employed target for PET imaging, the Translocator Protein (TSPO) (see section 3) is widely recognized as a useful para clinical marker for monitoring disease activity not only in relapsing but also in progressive MS [144].

### *Neuroinflammation and demyelination*

The knowledge of the immunopathophysiology of MS, which underlies chronic neuroinflammation and neurodegeneration, has recently evolved. The traditional view of MS, a result of decades of research, is that relapses are principally caused by aberrantly activated and/or insufficiently regulated CNS-specific effector T cells, that from the periphery reach the CNS parenchyma and induce perivascular demyelination, glial cell activation, and axonal injury [122], [145]. The most widely implicated pro-inflammatory effector T cells are IL-17-expressing CD4 T cells, known as Th17 cells, and CD8 T cells, known as cytotoxic T cells. That these cells are believed to contribute to the direct injury of OLs and neurons, although the precise mechanism has not been identified yet [146]. The trigger of MS is thought to be represented by an initial degenerative event that brings myelin-related antigens or CNS-resident pathogens from the CNS, to lymph nodes and spleen in the periphery. Herein, the antigens would be processed and presented via MHC-I and II molecules from APCs such as B cells and myeloid cells (macrophages, dendritic cells, and microglia) to CD4+ and CD8 T lymphocytes, leading to lymphocyte clonal expansion and acquisition of effector functions [44], [147]. The activated lymphocytes would therefore migrate to the CNS, where they would recognize peptides presented by APCs in the brain. The MS responsible antigens have not been clearly identified [148]. Myelin-related antigens are strongly suspected to be involved, however, there is no consensus, and some studies have proposed the possible implication of neuronal or glial cell surface antigens. Once reactivated in the CNS, the lymphocytes begin to release cytokines, chemokines, and antibodies capable of recalling local microglia and macrophages. Recent studies have proposed to extend the range of immune cells involved in the onset and progression of MS, demonstrating that the interaction between T cells, B cells, and myeloid cells in the periphery [149], with the resident cells of the CNS such as microglia and astrocytes, is highly relevant in the pathophysiology of MS. Together with

peripheral immune cells, CNS-resident cells secrete a range of inflammatory mediators that can further recruit inflammatory cells into the CNS, leading to neuronal demyelination and inducing persistent neuroinflammation within the CNS parenchyma. In particular, CNS-resident cells that sense homeostatic disturbances, mainly microglia, and astrocytes, can also produce neurotoxic inflammatory mediators (such as cytokines, chemokines, and ROS) that can promote and sustain neuro-axonal damage and neurodegeneration in MS [150]. Importantly, the infiltration of inflammatory cells in the CNS is facilitated by the increase of the permeability of the BBB, due to direct effects of pro-inflammatory cytokines and chemokines (such as TNF, IL-1 $\beta$ , and IL-6) produced by resident immune cells and endothelial cells, as well as indirect cytokine-dependent leukocyte-mediated injury. The dysregulation of the BBB increases the trans-endothelial migration of activated macrophages, T cells, and B cells, from the periphery into the CNS, leading to further inflammation and reactive gliosis, demyelination, and axonal damage [151]. The modalities by which autoreactive T cells interact with APCs in the CNS and reactivate, and if such reactivation is crucial for the disease evolution, represents an unanswered question in the immuno-etiology of MS. Microglia, activated by pattern recognition receptors, are rapidly recruited to sites of the lesion, where they upregulate the expression of major histocompatibility complex class II molecules (MHCII) and the costimulatory molecules CD40, CD80, and CD86 [152], suggesting that possess the capacity of presenting antigens to T cells (**Figure 10**).

The earliest phases of MS are typically characterized by active demyelinating lesions, presenting massive lymphocyte infiltration (mainly CD8<sup>+</sup> T cells and CD20<sup>+</sup> B cells, with fewer CD4<sup>+</sup> T cells), activated microglia and macrophages (containing myelin debris), and reactive astrocytes [153]. Recent studies exploiting the microglia-specific marker TMEM19 showed that the initial pool of phagocytic cells in an early MS lesion is comprised of roughly 40% microglia derived from the original resident pool, while peripheral macrophages are increasingly recruited as the lesion progresses [152]. Active demyelinated lesions are usually associated with a proinflammatory microglia phenotype, which dominantly expresses markers associated with cytotoxicity, oxidative injury, and antigen presentation or co-stimulation, while anti-inflammatory markers (CD206, CD163) have been shown to be increased in the inactive lesion center. Not surprisingly, other studies report the presence of macrophage- and microglia-like cells in active MS lesions expressing, at the same time, markers that the traditional nomenclature would have identified as M1 and M2 [17], [18], supporting the evidence that in reality microglia possess a broad spectrum of activation phenotypes. Moreover, postmortem analyses of MS lesions have identified microglia having both the capacity for

detrimental antigen presentation, as well as for the beneficial myelin debris phagocytosis (described as having a “foamy” appearance) [154]. Interestingly, alternative M2 polarization of microglia/macrophages has been reported to normally follow myelin debris phagocytosis and it has been recently demonstrated to be a key event in remyelination [155] (see remyelination section).

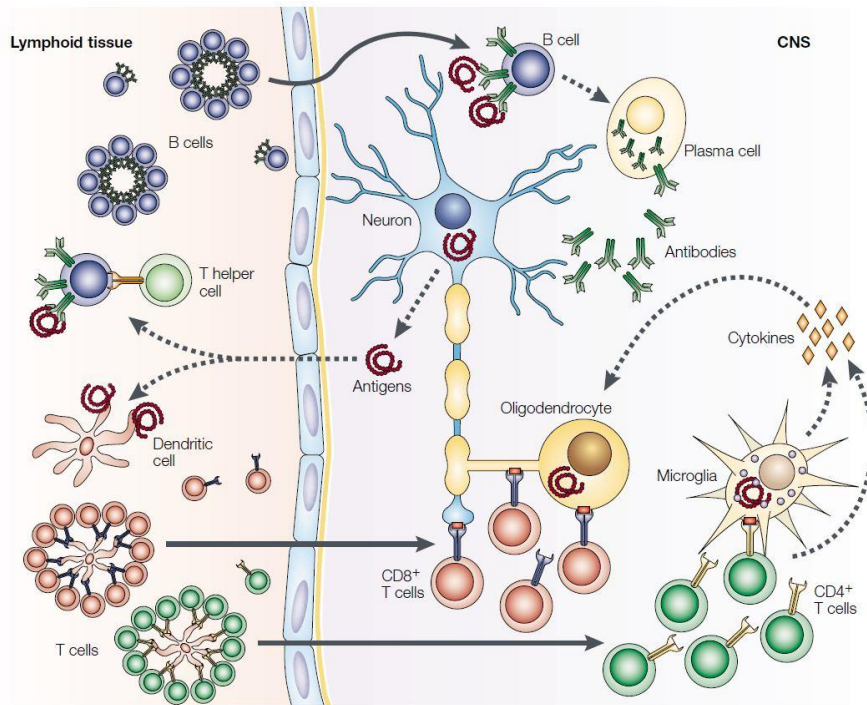


**Figure 10. Hypothetical view of immune responses in acute MS lesions.** *In MS, a pro-inflammatory milieu in the CNS, leading to upregulation of MHC molecules, co-stimulatory receptors, and inflammatory cytokines is accompanied by an antigen-driven acquired immune response. T- and B-cell responses arise in the periphery following the interaction with CNS-derived antigens or cross-reactive foreign antigens such as viruses. Dendritic cells present neural antigens and strongly stimulate T-cell activation. After clonal expansion, T and B cells infiltrate the CNS, where they re-activate, mature, and release large amounts of immunoglobulin- $\gamma$  (IgG) antibodies. These antibodies bind soluble or membrane-bound antigens on expressing cells. Effector CD8<sup>+</sup> T cells also could encounter their specific antigen, presented by glial or neuronal cells on MHC class I molecules, causing direct damage to expressing cells. Effector CD4<sup>+</sup> T cells migrate into the CNS and encounter antigens that are presented by microglial cells on MHC class II molecules. Their reactivation leads to an increase in the production of inflammatory cytokines, which attract other immune cells, such as*

macrophages. Peripheral and central immune cells contribute to inflammation by the release of damaging mediators and the direct phagocytic attack on the myelin sheath and OLs. Adapted from Hemmer B. et al., *New concepts in the immunopathogenesis of multiple sclerosis. Nat Rev Neurosci.* 2002 [156].

### Axonal degeneration

Axonal damage and loss are key features of MS and are the most important predictor of permanent clinical deficits and persistent disability in patients [157], [158]. Although occurring early in the pathology, axonal degeneration is commonly observed in progressive disease. The mechanisms underlying axonal damage include neuronal apoptosis induced by immune cells activation. In particular, a pro-inflammatory environment, characterized by cytotoxic mediators, is responsible for oxidative stress, mitochondrial ion channel dysfunctions, extracellular free iron accumulation, hypoxia, and altered glutamate homeostasis, factors that have been proven to have a detrimental impact on neurons [159] (**Figure 11**). Moreover, the direct correlation between loss of axonal integrity and demyelination has been determined by imaging and neuropathological studies from MS postmortem tissue [160], [161], which detected extensive grey matter pathology in MS, often presenting demyelinated cortical plaques and transected axons, apoptotic neurons, and reduced neuronal density with brain atrophy [162]. Indeed myelin, besides representing a physical protective layer to axons, provides trophic support and accounts for their energetic balance.

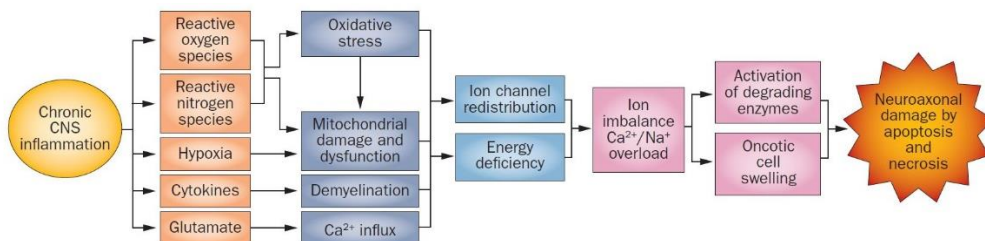


**Figure 11. Cascade of events leading to inflammation-induced neuroaxonal damage.** The scheme illustrates the hypothetical sequence of events leading to neuroaxonal degeneration in MS. Chronic CNS inflammation stands at the base of the dysregulation of neuronal metabolism. Adapted from Friese MA. et al., *Mechanisms of neurodegeneration and axonal dysfunction in multiple sclerosis. Nat Rev Neurol.* 2014 [163].

## Remyelination

The remyelination process consists of the events by the means of which OPCs are called to replace the death/damaged OLs after the demyelinating damage. It is highly complex and depends on several factors. In particular, OPCs proliferate, migrate towards the site of the injury, and then differentiate into mature OLs that remyelinate axons. Successful remyelination restores the conduction of nerve impulses and exerts a protective role on the axons by preventing their degeneration, although the newly formed myelin sheath is thinner, and the internodes shorter. Among the factors which favor OPCs recruitment and differentiation, there is the intervention of Tregs lymphocytes which directly stimulate remyelination regardless of immunomodulation [164]. Moreover, as anticipated before, the phenotypic change in microglia/macrophage represents a major event for successful remyelination. In fact, once that the target antigens have been removed from the focal inflammation site by phagocytic cells such as macrophages and microglia, these cells are required to undergo apoptosis or assume a deactivated/alternative phenotype, which would be followed by the establishment of repair mechanisms, *i.e.* remyelination [165]. Gene expression profile analyses of microglia during experimental remyelination indicate that the regenerative profile of microglia is characterized by the expression of several genes related to phagocytosis and breakdown of myelin debris, secretion of regenerative factors, and tissue remodeling [14], [166]. In particular, an initial pro-inflammatory microglia activation (identified by the expression of iNOS, CD16/32, TNF- $\alpha$ ) has been observed early in remyelination, when OPCs are called to proliferate. Then, a shift in microglia activation towards a different phenotype (identified by expression of TREM2, Arg1, IGF-1, and mannose receptor CD206) has been detected later during the subsequent OPCs differentiation process [167], [168]. Interestingly, the density of CD206+ microglia was found increased only in postmortem MS lesions that were actively remyelinating, and not in lesions considered to have impaired remyelination (chronic inactive lesions), providing, therefore, a positive correlation between this microglia phenotype with remyelination efficiency [155], [169].

MS patients can experience either entire or, more frequently, partial remyelination of the plaques, which is reflected by the complete or partial functional recovery after a relapse. Indeed, in the absence of remyelination, axons undergo irreversible degeneration and neurological deficits become permanent. Although quite efficient in the early stages of the disease, the remyelination process becomes less efficient over time, due to not only to the chronic inflammation which is established at the focal lesions in consequence of the persistent activation of microglia towards the classical pro-

inflammatory phenotype, but also due to the progressive depletion of the OPCs pool. These events lead to the impaired replacement of damaged OLs with the consequent progression of MS pathology. Therefore, the stimulation of OPCs differentiation represents a promising approach in the treatment of MS, and pre-clinical studies involving the study of the factor promoting OPCs differentiation are recently emerging [170].

### *In vivo* model of MS: the experimental autoimmune encephalomyelitis (EAE)

The use of animal models has been unavoidable to understand the etiopathogenic mechanisms of MS and to perform pre-clinical studies whereby investigate the effectiveness of potential therapies.

It should be noted that no animal model can mimic all the characteristics of human disease, and include all of them in an identical context. In addition, MS is a heterogeneous pathology characterized by multiple aspects, which are difficult to be entirely recapitulated in one experimental model [171]. So far, different animal models of MS have been established, according to the agent used to induce the pathology. Demyelination can be either induced by CNS-targeting viral infection, or by toxic agents such as cuprizone, being the latter the one employed to create models to study remyelination processes [171]–[173]. Also, transgenic models are often employed to shed light on immunopathological aspects of MS, as well as immunological models such as the experimental autoimmune encephalomyelitis (EAE) [174]. EAE is the most commonly used animal model to study inflammation and autoimmune-mediated diseases in the CNS, and it is widely recognized as a standard model of MS as it is capable of reproducing the main neuroimmunological and histopathological features of the disease. Indeed, the destruction of the myelin sheath of nerve fibers and CNS lesions, more pronounced in the cerebral trunk and the spinal cord, appear at the same stage of the MS pathology [175], [176]. Likewise, the temporal evolution of the lesions, from acute inflammation to demyelination, and then to partial remyelination, together with the presence of IgG in the CNS and the CSF, is similar between MS and EAE [177].

EAE is initiated by animal immunization using CNS-related antigens which are presented to CD4<sup>+</sup> Th cells, thus triggering the autoimmune response [175], [178], making it possible to study the development of Th cells activation, effector functions, and T cell signaling *in vivo*. One of the interests of EAE models is to study the cellular pathogenic mechanisms of injury and autoimmunity which are difficult to observe in humans, such as the investigations aimed at unrevealing the antigens recognized by T cells as non-self [179]. Rodent EAE represents to date the preferential autoimmune model of

MS, and different animal strains and numerous immunization protocols have been established. Depending on the animal strain and the method of induction, encephalomyelitis presents variable clinical development, demyelination, and axonal damage [180]. For the present purpose, we are going to focus on the induction of EAE pathology in mice. EAE can be induced by active or passive immunization. The administration of CNS homogenate of the spinal cord or small peptides derived from purified myelin proteins (*i.e.* MOG, MBP, or PLP) in emulsion with a strong adjuvant, usually complete Freund's adjuvant (CFA), enable active immunization [178]. In order to induce an immunological boost, some murine strains require the injection of inactivated *Mycobacterium tuberculosis* toxin. Alternatively, passive EAE is induced by the transfer of isolated CD4+ T lymphocytes obtained from secondary lymphoid organs of actively immunized animals. These lymphocytes are first reactivated *in vitro* against the encephalitogenic antigen used to induce EAE in the donor, and subsequently re-infused into a healthy animal [181].

Following immunization, the CNS antigens are phagocytized by local APCs, which reach via the lymphatic route peripheral lymph nodes or the spleen, where interact with lymphocytes and trigger the activation and clonal expansion of encephalitogenic Th1 and Th17 cells. The activated T cells leave the peripheral lymphoid organs and reach the brain via the BBB or the blood–CSF barrier. Herein, they recognize myelin antigens as non-self, thus inducing the onset of the EAE pathology [180], which comprises inflammation and demyelination in the spinal cord and the brain including the cerebellum, the cortex, the corpus callosum, and the optic nerve [182], [183].

Depending on the chosen antigen and the mouse strain employed to induce EAE, distinct clinical forms of EAE can arise: the chronic EAE, resembling the human progressive MS, and the acute EAE, resembling the RRMS form [179]. The progressive disease can be achieved by immunization of C57BL/6J mice with the MOG<sub>35-55</sub> peptide. The clinical condition of the animals gradually worsens through a monophasic chronic disease after the first signs of the pathology, without possible improvement [175]. On the contrary, the acute model of EAE is usually obtained in SJL/J RJ mice immunized with the PLP<sub>139-151</sub> peptide [184]. Here, the disease reaches a maximum point of severity, and then undergoes complete remission of the neurological symptoms (remyelination phase).

Regardless of the form of EAE considered, the clinical symptoms are similar and usually classified on a scale from 0 (no pathology) to 10 (death). Briefly, no visible symptoms are present at stage 0; the first signs of paralysis are observed in the tail (stage 2), and then the grade increases as the paralysis progresses and motor functions decline. At stage 5, both the hind limbs are fully paralyzed and weakness in the forelimbs is observed; at stage 8 all limbs are affected, and stage 9 corresponds to the

moribund state of the mouse [175]. In the research of treatment for MS, the EAE model has clear limitations, since some molecules which were promising in counteract EAE pathology had no beneficial clinical impact or even deleterious effects when tested in MS patients [179], [185]. Indeed, the exact contributions of different cytokines may vary between human pathology and EAE, and therefore the potential molecules tested in the EAE models which play a role in reducing inflammatory response may be effective in the animal model and not in human patients. However, the EAE model is an interesting and widely used exploratory model for pre-clinical studies. In fact, it has revealed drugs that are now used in the clinic, such as  $\beta$ -interferon or natalizumab [176], [179], [186]. This animal model is relatively easy to employ and highly adaptable, as it makes it possible to mimic the different forms of the pathology depending on the chosen antigen and the employed mouse strain. In addition, all the clinical symptoms observed in humans are mimicked, and both the inflammatory and the neurodegenerative components have been observed in EAE animals [187], [188] Therefore, EAE is considered to be highly representative of the immunopathophysiology of MS, and it is well recognized as a model of choice for testing new potential therapeutic molecules.

### Current treatments

To date, there is no cure for MS. The available treatments for MS patients typically focus on speeding the recovery from attacks, slowing the progression of the disease, and managing MS acute symptoms. Disease-modifying therapies (DMTs) are used to reduce the inflammatory part of the pathology and slow down its clinical evolution, while symptomatic treatments are used for short-term amelioration of MS symptoms such as fatigue, pain, and spasticity.

The largest part of the immune response associated with MS occurs in the early stages of the disease. The treatment with aggressive DMTs as early as possible was demonstrated to lower the relapse rate, slow the formation of new lesions, and potentially reduce the risk of brain atrophy and disability accumulation. However, many of the DMTs used to treat MS carry significant health risks, and doctors are often forced to find a balance between beneficial and detrimental effects.

For primary-progressive MS, ocrelizumab (Ocrevus<sup>®</sup>) is the only FDA-approved DMT. Those who receive this treatment are slightly less likely to progress than those who are untreated. On the contrary, several DMTs are available for RRMS patients [189]. Most of them are immunomodulators and immunosuppressors, targeting the proliferation of immune cells or their migration towards the CNS [124], [190]. Therefore, their administration is often limited due to the many side effects of these

drugs and the high risk of developing cancer possibly due to immunodeficiency [191]. In addition, they have no effect either on neurodegeneration or on the handicap which sets in over time. The symptomatic treatment prescribed to cope with relapses is mainly anti-inflammatory drugs such as corticosteroids. Corticosteroids work primarily through genomic effects (nuclear receptor glucocorticoids) to suppress the synthesis of pro-inflammatory cytokines and stimulate those of anti-inflammatory cytokines. These treatments are recommended to improve the quality of life of patients, for example, to relieve pain or to remedy chronic fatigue that may set in from the onset of the disease [192]. Additional DMTs are now in clinical trials for RRMS, PPMS, and SPMS, and intense efforts are being made to identify novel therapeutic targets. In particular, progress has also been made in repurposing older drugs used in other contexts, identifying therapeutic agents with potential neuroprotective or remyelinating effects [189], [193].

### New therapeutic approaches

There is great interest in implanting stem cells (SCs) to treat MS, and several scientific publications show encouraging results [194], [195] in this sense. SCs therapy involves either transplanting stem cells or targeting the dysfunctional cells strains present in the body. Different kinds of SCs have shown a beneficial effect in animal models of EAE, but also in MS patients during clinical trials [196].

For example, autologous hematopoietic stem cell (HSCs) transplantation, already used to treat blood malignancies, is currently employed in the very severe forms of MS. Despite this therapeutic perspective is still at the experimental stage, is considered the most powerful therapeutic intervention for MS so far. In difference to conventional DMTs, it represents a one-time procedure that can arrest and sometimes reverse disability in MS patients. In fact, HSCs could prevent the degradation of myelin by modulating specific functions of the immune system [194]. Moreover, mesenchymal stem cells (MSCs) which exhibit antiproliferative effects, anti-inflammatory and anti-apoptotic on neurons, have been successfully tested in the EAE model. Promisingly, MSCs treatment has been shown to inhibit the functions of autoreactive T cells and this immunomodulation is neuroprotective [197]. Neural stem cells (NSCs) are also currently under investigation for their regenerative, trophic, immunomodulatory, and neuroprotective properties. However, the difficulty to obtain them slows down the process and no NSCs implantation therapy is available for MS patients so far [198].

One of the new frontiers in MS therapy seems to be represented by mRNA vaccines. As recently published, Krienke *et al.*, have shown that the systemic administration of a synthetic mRNA coding

for disease-related autoantigens resulted in antigen presentation on splenic CD11c<sup>+</sup> APCs in the absence of costimulatory signals, suppressing the pathology in different *in vivo* models of MS [199]. Most importantly, they also found a reduction effector T cells activation and a development of Treg cell populations, indicating the great potential of their approach which needs to be further implemented.

## 1.3 Translocator Protein 18 kDa (TSPO)

---

### 1.3.1 Localization and structure

The mitochondrial 18 kDa translocator protein (TSPO) was originally discovered in 1977 in the kidney as a protein able to bind the benzodiazepine diazepam, and it was called for this reason Peripheral Benzodiazepine Receptor (PBR) [200]. After the discovery of its presence in the CNS, and the awareness about its involvement in the translocation of molecules across mitochondria membranes, the name of the protein was changed in the one which is known nowadays, Translocator Protein or TSPO [201]. Since the beginning, the pharmacological approach has always been the one of choice in the study of TSPO expression and function. Indeed, TSPO was early discovered as able to bind with specificity and high-affinity various classes of chemicals, but also endogenous ligands including porphyrins, cholesterol, and the endozepine diazepam binding inhibitor (DBI) [200], [202], [203]. The 5-chloro derivative of diazepam Ro5-4864 and the imidazoquinoline PK11195 were the first selective TSPO ligands synthesized, thus named classical TSPO ligands [204]. They have been widely used as radiolabeled probes (<sup>3</sup>H]Ro5-4864 and <sup>3</sup>H]PK11195) to determine TSPO distribution in the tissues, as well as pharmacological tools to understand TSPO function. Radiolabeled binding experiments demonstrated a ubiquitous although variable TSPO expression in mammal tissues. Interestingly, TSPO expression was found enriched in tissues with a steroidogenic ability such as the adipose tissue, the adrenal cortex, the gonads, and the CNS [201]. In the brain, TSPO basal expression is low and mainly restricted to glial cells. However, during neuropathological conditions involving neuroinflammation, TSPO expression has been shown to notably increase [205], [206]. For this reason, [<sup>3</sup>H]PK11195 has been traditionally used as a biomarker in PET imaging to visualize microglia activation in pre-clinical and clinical studies involving neuroinflammatory conditions [207].

At the subcellular level, TSPO is located in the outer mitochondrial membrane (OMM), and it has been found as a monomer, dimer, or polymer, in association with other mitochondrial proteins (see following sections) [208]. It is encoded by the nuclear genome and known to be evolutionarily conserved. Sequence and structure analysis evidenced that TSPO is composed of 169 amino acids organized into 5 transmembrane (TM) helices, with the C-terminal and the N-terminal pointing towards the cytoplasm and the intermembrane space, respectively [209]. Recently, Jaremko and colleagues succeed to reconstitute by NMR spectroscopy the 3D high-resolution structure of mammalian monomeric TSPO in complex with its high-affinity ligand PK11195 [210] embedded in detergent micelles. The complex structure is characterized by tight packing of the  $\alpha$ -helical transmembrane region (**Figure 12**).

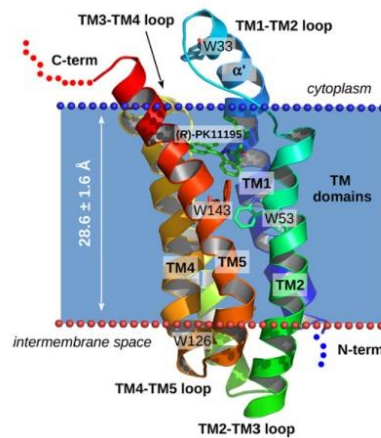


**Figure 12.** 3D structure of mouse TSPO in complex with (R)-PK11195. Adapted from Jaremko M. et al., *Structure of the mammalian TSPO/PBR protein*. *Biochem Soc Trans.* 2015 [211].

### 1.3.2 Cholesterol transport and steroidogenesis

Consistent with the enrichment of its expression in steroidogenic tissues, TSPO was proposed to be a key regulator in steroid synthesis, supported by accumulating experimental evidence [212].

The consequence of PK11195 and Ro5-4864 binding to TSPO included the stimulation of steroidogenesis and neurosteroidogenesis both *in vitro* and *in vivo* [213]. In particular, the translocation of cholesterol across the mitochondria is essential for the initiation of the steroidogenic process, and TSPO was suggested to have a critical role in this step [214], [215]. In support, TSPO

sequence analyses have allowed for the identification of a cholesterol-recognition amino acid consensus (CRAC: (L/V) - X(1-5) - (Y/F) - X(1-5) - (R/K)) [216], in the C-terminus of the TM5 helix as cholesterol-binding site, because site-specific mutations of the CRAC domain were shown to abolish TSPO ability to bind cholesterol [217]. In addition, the human functional single nucleotide polymorphism (SNP) rs6971, which lead to the Ala147Thr substitution near the CRAC domain, has been shown to affect cholesterol binding and to impair steroid synthesis [218].

For years it was proposed that TSPO main function was to shuttle cholesterol from the OMM to the IMM to supply the first steroidogenic enzyme, the cytochrome P450 side-chain cleavage enzyme (P450<sub>scc</sub>) CYP11A1 [215], [219] located in the inner mitochondrial membrane (IMM), which converts cholesterol into pregnenolone in a reaction which is considered the rate-limiting step of steroidogenesis [94]. Accordingly, the induction of steroid synthesis [213], [215], [220], or the increase in the expression of the steroidogenic enzymes in peripheral and CNS steroidogenic models [221] was observed after TSPO stimulation in several experimental models. Moreover, the *in vivo* administration of TSPO ligands has been shown to stimulate the production of neurosteroids in the brain of rats deprived of their peripheral steroidogenic sources [222], [223].

Noteworthy, TSPO ligand's ability to induce steroid formation was recently recognized to be positively correlated to a parameter called Residence Time (RT), indicating the time spent by the ligand at the binding site, rather than to the ligand-binding affinity [224], [225]. Studies carried out in astrocytic cell lines have shown that synthetic TSPO ligands, owing to phenylindolylglyoxylamides (PIGA) class of compound, which have been assessed to have long RT, were able to increase pregnenolone production [226] to higher levels when compared to ligands having short RT [204], [225], [226]. In support of its implication in steroidogenesis, TSPO has been recently proposed to be part of the transduceosome multiprotein complex of the OMM that, together with the metabolon, represents the steroidogenic machinery of the cell [208], [227].

For what concern the functional biological consequences, TSPO stimulation has been widely shown to exert neuroprotective and anti-inflammatory effects in various *in vitro* and *in vivo* models of neuroinflammation and neurodegeneration [228], [229]. The observed effects after the administration of TSPO ligands have been generally attributed to the neurosteroidogenesis induction. In fact, neurosteroids are well-known endogenous molecules synthesized by neurons and glial cells able to modulate inflammatory-related gene expression by the nuclear translocation of hormone-related receptors [230], [231]. Furthermore, neurosteroids can act in an autocrine and paracrine manner as potent positive allosteric modulators of synaptic and extra-synaptic neurotransmitter receptors such

as GABA<sub>A</sub>-R ( $\gamma$ -aminobutyric acid type A receptors) 202, which owe for the main inhibitory pathway of CNS signals [232] (**Figure 13**).

However, the recent establishment of global TSPO KO mouse models has raised an intriguing scientific debate due to the generation of conflicting data regarding the involvement of TSPO in the steroidogenic process [233]–[235]. In particular, studies from Tu and Selvaraj questioned the widely proven TSPO function in steroidogenesis, since in their experimental conditions TSPO KO mice displayed normal steroids levels [236], [237]. On the contrary, different phenotypes such as embryonic lethality [235], [238], and defective steroidogenic ability were found by other research groups in theoretically equivalent TSPO KO models [239]. To date, the encountered discrepancies in such findings could be attributed either to technical differences in the experimental strategy either to the genetic background of the animals, suggesting that *in vivo* genetic manipulation required more standardized methodologies, and additional controls in order to provide reliable and consistent results.

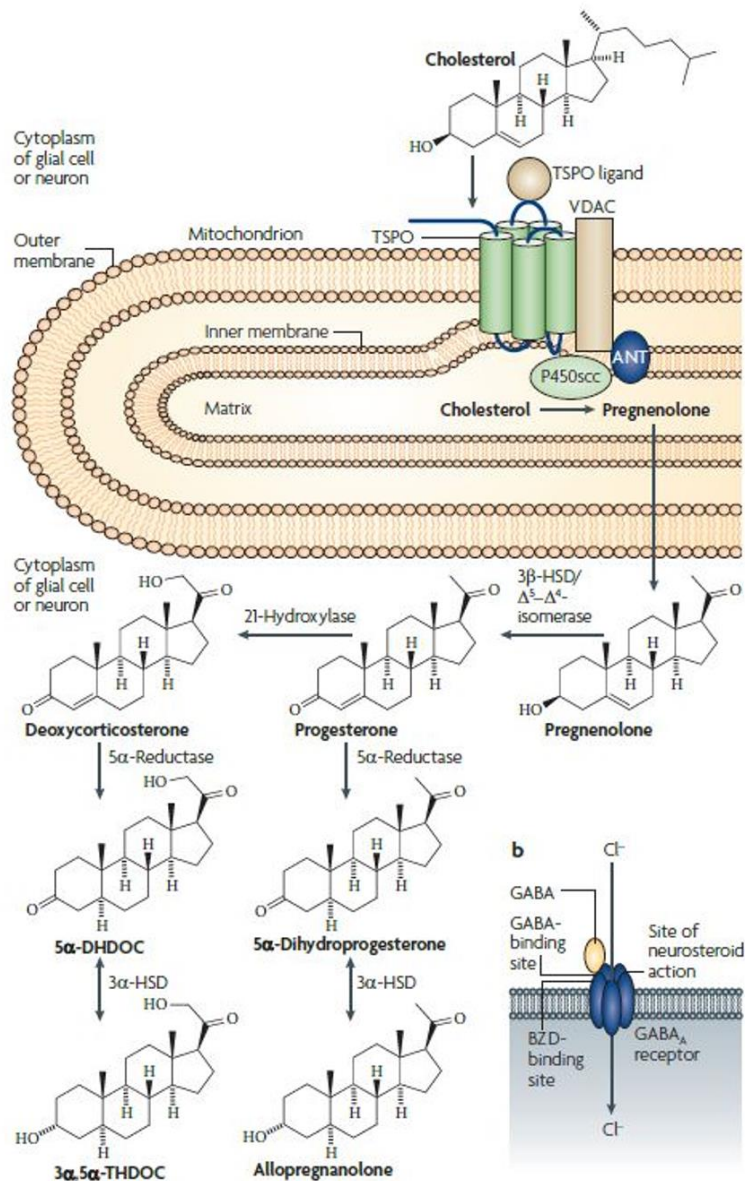


**Figure 13. Neurosteroidogenesis and neurosteroid signaling induced by TSPO Ligands.** *The binding of a TSPO ligand promotes the transport of cholesterol to the IMM, where the CYP11A1 enzyme converts cholesterol to pregnenolone, which is the first neurosteroid of the cascade. Presumably by diffusion through the cell membrane, all neurosteroids act in an autocrine and paracrine manner through a long-term genomic activity or a direct shot-term allosteric modulation activity of neurotransmitter receptors such as GABA<sub>A</sub>-R. Adapted from Rupprecht R et al.,*

*Translocator protein (18 kDa) (TSPO) as a therapeutic target for neurological and psychiatric disorders. Nat Rev Drug Discov. 2010 [240].*

### 1.3.3 Other TSPO functions

Despite accumulating literature data exploring the biological consequence of TSPO stimulation by selective ligands, as well as investigating TSPO functions in several experimental models, the exact mechanisms of action responsible for the observed effects were often elusive. Indeed, a plethora of effects was observed following TSPO stimulation, rendering the interpretation of the underlying molecular mechanism difficult and mainly speculative [241].

TSPO main physiological function has been under investigation for decades, and besides its involvement in the steroidogenic process, several implications in different fundamental biological processes have been proposed so far, supported by both *in vitro* and *in vivo* studies.

Most of the proposed functions of TSPO are related to mitochondrial activities, *i.e.* the involvement in heme biosynthesis, the modulation of the mitochondrial permeability transition pore (mPTP), mitochondrial respiration and ATP production, apoptosis, ROS metabolism, and regulation of redox balance/oxidative stress [228], [241], [242] (**Figure 14**).

A recent hypothesis has proposed TSPO as part of the mitochondrial transduceosome protein complex, suggesting that the complexity of the TSPO-mediated responses could be explained by the dynamic interactions of TSPO with different mitochondrial proteins [208]. In particular, TSPO has been recently recognized as located at the contact site between OMM and IMM interacting with the other components of the transduceosome such as the steroidogenic acute regulatory protein (StAR), the voltage-dependent anion channel (VDAC), the ATP synthase, and the AAA domain-containing protein-3 (ATAD-3). The demonstrated direct interaction between TSPO with VDAC is known to contribute to mitochondrial quality control and the regulation of mitochondrial structure and function [243]. Moreover, VDAC, together with the adenine nucleotide transporter (ANT) is part of the mPTP, a multiprotein complex responsible for the permeability of the mitochondrial membrane by water, ions, and small molecules [244]. TSPO has also been proposed to modulate mPTP opening, allowing for the release of substances from mitochondria to the cytoplasm. Among them, are the pro-apoptotic cytochrome c, ROS species, ATP, and protons. The mPTP opening induces MMP increase, with subsequent impairment of mitochondrial function, including ATP production. For example, the

interaction between TSPO and VDAC appears to play a critical role in apoptotic cell death [245] through TSPO-mediated ROS generation.

Additional evidence suggested that TSPO is a key participant in the regulation of mitochondrial ROS levels [246], although conflicting data have been generated. An increased TSPO expression [247] or TSPO treatment with ligands [248], [249] was often associated with resistance against excessive ROS production and hydrogen peroxide cytotoxicity, while TSPO silencing enhanced ROS production [250], [251], suggesting that TSPO may participate in an antioxidant response pathway.

Interestingly, recent studies have also reported that genetic deletion of TSPO results in an increase in mitochondrial fatty acid oxidation in steroidogenic cells [250] and a decrease in oxygen consumption rate and ATP production in microglia [236], [252], suggesting a positive regulation by TSPO on cellular respiration. Accordingly, TSPO ligand administration has been often linked to increased ATP production, oxygen consumption, and MMP preservation in cellular models of murine and human microglia. On these lines, a recent work from Fu and colleagues evidenced a strong impairment on global mitochondrial function *i.e.* MMP collapse, reduced ATP production, mitochondrial fragmentation, in CRISPR/Cas9-mediated TSPO KO astrogloma [253]. However, the underlying molecular mechanisms of these findings and their relevance to the overall mitochondrial function require further investigation.

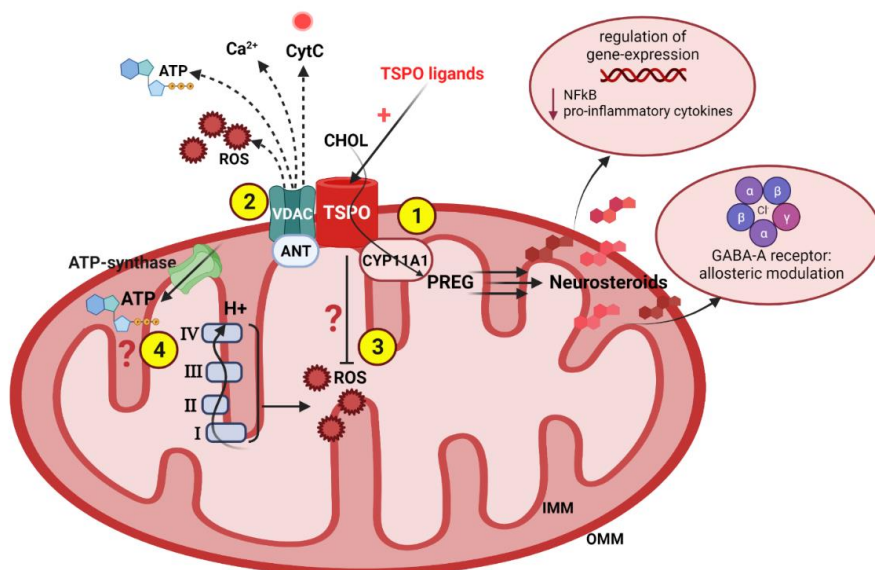


**Figure 14. Overview of the main biological functions of TSPO.** (1) *TSPO* localizes in the OMM, binds cholesterol (*CHOL*) in the cytosol, and allows for its translocation to the IMM. Here, the *CYP11A1* enzyme synthesizes pregnenolone (*PREG*), the precursor of all neurosteroids. Neurosteroids can exert genomic-mediated anti-inflammatory effects by *NFκB* pathway modulation. In addition, neurosteroids exert positive allosteric modulation of *GABA<sub>A</sub>-R*. *TSPO* ligands increase neurosteroidogenesis. (2) *TSPO* is associated with *VDAC* and close to *ANT*, the main components of the *mPTP*. *TSPO* is proposed to modulate *mPTP* opening, affecting *ROS*,  $\text{Ca}^{2+}$ , and *ATP* release. *TSPO* ligands have been proved to counteract the *mPTP* opening. (3) Monomeric *TSPO* is hypothesized to participate in *ROS* metabolism. Studies demonstrated that *TSPO* ligands counteract mitochondrial respiration-related *ROS* production, despite the precise mechanism is not yet clarified. (4) *TSPO* has been proposed to be associated with the *ATP* synthase function and therefore to modulate *ATP* production. *TSPO* ligands were proved to restore *ATP* levels after *mPTP* opening-induced cellular intoxication. Cartoon created with *BioRender.com*. Adapted from *Tremolanti et al., Translocator Protein 18-kDa: a promising target to treat neuroinflammation-related degenerative diseases, Current Medicinal Chemistry 2022 [229]*.

Among the attractive biological functions in which *TSPO* is known to be implicated, there is the regulation of differentiation processes [254]. Indeed, specific tricyclic quinazoline derivatives were shown able to regulate apoptosis and stimulate extensive neuronal differentiation of PC-12 neuronal progenitor cells [255], [256]. In addition, PK11195 classical *TSPO* ligand was shown to induce itself

PC-12 neuronal differentiation, including the development of neurites and increased expression of  $\beta$ III-tubulin neuronal marker [257]. Herein, Yasin and colleagues also pointed out a relevant function of TSPO in the regulation of nuclear gene expression, proposing that the regulation by TSPO of gene expression occurs via mitochondria-to-nucleus signaling pathway and that such nuclear gene expression regulation by TSPO could explain TSPO's numerous functional effects. Interestingly, TSPO has been described to be expressed at a significant level in neuronal and glial progenitor stem cells within regions of neurogenesis such as the hippocampus and the sub-ventricular zone in the healthy brain [258]. Accordingly, Varga and colleagues indicate that non-differentiated neuroectodermal cells and neuronal precursors express TSPO, whereas during neuronal maturation this capacity is lost [259]. In parallel, the authors proposed an inverse trend occurring in glial precursor cells, where TSPO expression positively correlates with the differentiation of glial cells.

Besides the largest part of the studies on TSPO implication in the differentiation process, which have been conducted on neuronal cells, it was recently reported that TSPO stimulation with a cholesterol-like selective ligand was able to induce primary rat OPCs differentiation [260], *i.e.* morphological changes and MBP expression. However, the paucity of data in the literature makes it difficult to unravel the precise function of TSPO in the regulation of differentiation processes both in neuronal and glial precursors.

#### 1.3.4 TSPO ligands in neuroinflammation: *in vitro* studies on glial cell models

Nowadays, TSPO is considered a multifaced protein, known to regulate different cellular processes. Based on the evidence that TSPO expression is finely regulated during inflammatory processes [258], a large body of literature has dissected the functional effect of TSPO stimulation in different cellular models of CNS pathologies, to explore its potential as a target against neuroinflammation. However, the functional consequences of the fluctuations of TSPO expression have not been clarified yet. It was supposed that TSPO induces the production of neurosteroids locally in the damaged area, which modulates glia and/or neuron activities and promotes neuronal survival [261].

In order to characterize the role of TSPO both during physiological and pathological conditions, most of the *in vitro* studies were performed on glial models challenged by different types of stimuli. One of the most employed *in vitro* models to recapitulate microglia activation is represented by lipopolysaccharide (LPS) administration to murine BV-2 microglial cells, promoting the polarization

towards the classical pro-inflammatory phenotype [262], [263], characterized by the production of pro-inflammatory cytokines (TNF- $\alpha$ , IL-6, and NO). The pre-treatment with classical TSPO ligands PK11195 or Ro5-4864 was shown able to counteract microglia activation towards the neurotoxic state and to promote the alternative form of microglial activation [8]. Interestingly, the nuclear translocation of NF- $\kappa$ B, as well as the NLRP3 inflammasome activation [264], which are both known to play a crucial role in the activation of neuroinflammatory response in LPS-treated BV-2 cells, were found to be reduced in TSPO-treated microglia. Despite the majority of the studies usually ascribe the observed TSPO ligands' anti-inflammatory effects to the induction of the neurosteroidogenesis, the precise cellular and molecular mechanisms underlying TSPO ligand-mediated neuroprotection in neuropathological conditions are not well defined. In fact, the treatment with TSPO ligands has been proven to affect several processes such as steroidogenesis, mitochondrial respiration, and ATP production, oxidative stress balance, and calcium homeostasis maintenance, in line with the idea that TSPO establishes dynamic interactions with different mitochondrial proteins and therefore can control several mitochondrial functions [208], [265].

For example, the involvement of other mechanisms including mPTP opening, the release of ROS, and the regulation of mitochondrial respiration cannot be excluded from TSPO immunomodulatory activity. Interestingly, PK11195 and Ro5-4864 administration in microglial BV-2 cells evidenced greater effect in promoting basal and ATP-related respiration, whereas only a slight increase in steroidogenesis was observed [266]. On the contrary, in the same experimental conditions, the treatment with a highly steroidogenic TSPO ligand, XBD-173, stimulated *de novo* neurosteroidogenesis in microglia through the enhancement of pregnenolone production, but it did not affect mitochondrial respiration in basal conditions. Following microglia activation, XBD-173 administration was proven to reduce the pro-inflammatory state of LPS-treated BV-2 cells and to increase their regenerative-associated phagocytic activity. On this line, XBD-173 effect in enhancing phagocytosis was also proven in human microglia derived from induced-pluripotent stem cells (iPSc) [267]. Furthermore, Da Pozzo and colleagues have found that novel TSPO selective ligands, called PIGA, prevented lipid peroxidation and counteracted glial pro-inflammatory state after IFN- $\gamma$ /LPS treatment of the murine C6 astrocytic cell line [226]. Notably, such effects were abolished in presence of aminoglutethimide (AMG), a selective inhibitor of the first enzyme of the steroidogenesis cascade CYP11A1, proving the correlation of the observed effect with the induction of neurosteroidogenesis. To summarize, accumulating evidence implicates that synthetic TSPO ligands reduce glial activation

in various CNS disorders [263], [264], [266], and thereby, TSPO can be regarded as a therapeutic target for neurological disorders involving neuroinflammation [209], [228].

Nevertheless, the largest part of the studies have been performed in rodents, and heterogeneous data have emerged, suggesting that the most employed pharmacological approach requires more precise molecular investigations before proposing a reliable mechanistic model, and clarifying TSPO immunomodulatory function [241]. In addition, only a few recent works better investigate the specificity of TSPO ligand effects employing TSPO knockdown (KD) models [252], [266], therefore, the possibility of the occurrence of non-specific effects induced by different TSPO ligands, especially when employed at high concentration, should be taken into account.

### 1.3.5 TSPO as a target in Multiple Sclerosis: *in vivo* studies

TSPO ligands represent an emerging class of chemicals in pre-clinical studies for the treatment of neuroinflammatory and neurodegenerative disorders, including MS. In fact, several TSPO chemical compounds have demonstrated beneficial effects in the EAE *in vivo* models of MS [187], [268], [269].

Behind the employment of TSPO ligands in the treatment of MS, there is evidence that MS patients show an impairment in the neurosteroidogenesis and a consequent drop in neurosteroids level [270], [271]. Furthermore, the administration of neurosteroids such as progesterone and allopregnanolone (ALLO) has been demonstrated not only to reduce inflammation, myelin injury, and axonal damage, but also to improve neurobehavioral symptoms in chronic EAE models [272]–[274]. For these reasons, due to the widely accepted involvement of TSPO in neurosteroidogenesis induction, TSPO ligand-based therapy appears as a promising strategy to be explored for the development of innovative treatments against MS.

In addition, high TSPO expression levels have been observed during neuroinflammation in MS [275], especially during recovery and remyelination [276], in support of the idea of targeting TSPO to reduce chronic inflammation in MS. In particular, pharmacological stimulation of TSPO has been shown to counteract typical pathological events of MS such as the inhibition of lymphoid cell proliferation, the release of cytokine by macrophages, and the regulation of inflammatory processes related to neurodegenerative diseases. Altogether, these data suggest that TSPO ligands may offer interesting

options to be investigated for the development of protective strategies against neurodegenerative disease, including PPMS.

The *in vivo* administration (50 mg/kg) of Etifoxine, a benzoxazine derivative TSPO ligand which is approved for the treatment of anxiety since 1979 (Stresam Biocodex®, Gentilly, France) [277], has been demonstrated to reduce microglial activation, decrease peripheral immune cell infiltration in the spinal cord, and promote OLs regeneration after demyelination in chronic EAE model [187]. Another work [269] provided further characterization of the effects of Etifoxine treatment on EAE animals, by the means of gas chromatography/mass spectrometry (GC/MS)-based measurement of neurosteroid levels in the brain after the ligand administration. Interestingly, despite Etifoxine administration being able to reduce the severity of clinical symptoms at the peak of the pathology, the authors found no alteration in the levels of neurosteroids in Etifoxine-treated animals compared to vehicles, proposing instead a direct immunomodulatory effect of the TSPO ligand [269]. In parallel, they demonstrated that the administration of XBD-173 (30 mg/kg) TSPO ligand increased the brain level of several neurosteroids, although it was not able to reduce clinical symptoms in the same pathological model. Notably, XBD-173 is TSPO selective, whereas Etifoxine also binds to GABA<sub>A</sub>-R, suggesting the possibility for Etifoxine to promote anti-inflammatory and neuroprotective activities apart of neurosteroidogenesis induction.

Intriguingly, XBD-173 was recently shown to delay the onset of the pathology and reduce the severity of clinical and behavioral symptoms in EAE mice mimicking the RRMS [268]. XBD-173 treated-EAE mice evidenced a reduction in pro-inflammatory cytokines in serum and increased ALLO levels in the spinal cord and brain compared to vehicle-treated EAE mice. Noteworthy, no correlation between dose-effect was observed, evidencing the fine regulation mechanisms that could be affected following TSPO stimulation. In another work, Daugherty and colleagues observed a beneficial effect against EAE pathology when the treatment with Etifoxine was started before the onset of clinical symptoms or at the peak of the pathology [187]. Conversely, the administration of XBD-173 at the peak of the clinical symptoms could not rescue EAE-mice from the pathology, whereas its administration as pre-treatment and at lower dosage evidenced a positive outcome in the progressive EAE murine model of MS [269].

However, in contrast to the neuroprotective role of ligand-mediated TSPO signaling as outlined above, the hGFAP-driven-conditional TSPO KO mice exhibited reduced astrogliosis and clinical scoring in the EAE mouse model of MS [278] and such discrepancies between the genetic and pharmacological studies require further investigations. In particular, it is becoming necessary to

reassess the neuroprotective efficacy of TSPO ligands employing transgenic TSPO KO animal models, to validate the functional role of TSPO as a therapeutic target in various neuropathological conditions.

## AIMS OF THE THESIS

---

The development of effective treatments for myelin pathologies remains challenging, and to date no effective cures are available. Therefore, it is crucial to identify novel therapeutical approaches to prevent myelin loss, axonal degeneration and to support OLs functions and OPCs differentiation. To shed light on pathophysiological mechanisms of myelin diseases and find new possible therapeutic targets, different approaches were explored in the present PhD thesis.

In order to get insights on both dysmyelinating and demyelinating diseases, and to cover many issues related to myelin pathologies, we focused our attention on PMD and MS as representative pathologies for the first and the second group, respectively. A genetic approach was chosen against PMD, whereas three pharmacological approaches *in vitro* and *in vivo* were chosen against MS, dealing with different features of the disease such as chronic neuroinflammation and remyelination. In particular, to cope with neuroinflammation, we first dissected the role of TSPO during microglia activation. Then, we explored the potential protective of two TSPO ligands on a murine model of MS, and finally, we investigated the potential of TSPO as a possible target to promote remyelination.

The first section of the results describes the genetic approach to tackle PMD. The neonatal form of PMD leukodystrophy is caused by *PLP1* point mutations responsible for misfolded PLP production, OLs death, and dysmyelination, along with neurological disorders. The pathophysiological mechanisms involved in PMD are poorly understood, and further clarifications of the abnormal PLP-induced OLs degeneration are necessary in order to identify relevant mechanisms to be targeted for efficient protection of OLs. Herein, we investigated the potential benefit of CRISPR/Cas9-mediated genome editing correction of *Plp1* mutation in a murine oligodendroglial cell line (158JP). The expression profile of key factors such as cell survival, ER stress, and mitochondrial markers in 158JP OLs after PLP mutation correction thus the restoration of the wild-type genotype, would allow us to better clarify the molecular mechanisms underlying the relationship between PLP mutation and OLs degeneration, representing a crucial step for the development of effective therapeutic strategies against myelin disorders.

Starting from the second section on, we investigated possible therapeutic approaches against MS. Neuroinflammation has a critical role in the pathogenesis and progression of demyelinating disorders such as MS. Abnormal activation of microglia, the resident macrophages of the CNS, is known to

sustain the neuroinflammatory process and progressively lead to neurodegeneration. Therefore, particular attention has been paid to understanding the mechanisms underlying microglial activation, for the identification of new possible therapeutic targets. The mitochondrial TSPO has been demonstrated to be highly expressed in activated microglia and is emerging as an interesting target for neuroprotection. Therefore, we sought to deeply investigate the role of TSPO in the neuroinflammatory response by studying its function in the modulation of microglial reactivity. The effects observed following TSPO stimulation or depletion were investigated by setting up an *in vitro* model of activated pro-inflammatory human microglia cells, which allowed us to shed some light on the negative modulation of microglia activation by TSPO.

Afterward, we explored the therapeutic potential of two novel TSPO ligands (PIGA1138 and PIGA839) in the EAE murine *in vivo* model of MS. Preliminary results indicated that PIGA-treated EAE mice showed slower symptom appearance and disease progression. Particularly, PIGA1138 was able to delay the onset of the symptoms of EAE mice and reduce the severity of the pathology at the peak of the disease, and PIGA839 reduced the severity of the clinical symptoms at the peak. Therefore, to corroborate their potential protective effect, herein we analyzed critical parameters of disease progression such as demyelination and axonal damage, CNS infiltration of immune cells, and serum levels of the anti-inflammatory cytokine IL-10.

Finally, in the fourth and last section, we dissected the role of TSPO during *in vitro* OPC differentiation into mature OLs, showing that TSPO might be an appealing target in favoring the remyelination process.

# Chapter 2

## MATERIALS AND METHODS

## 2.1 Cell culture

- The murine oligodendrocytic 158JP cell line was obtained by immortalization of *jimpy* mouse-derived primary OLs [108]. 158JP cells were grown at 37 °C and 5% CO<sub>2</sub> and cultured in Dubelcco's modified eagle medium (DMEM + GlutaMax; Gibco®) with 4.5 g/L of glucose, supplemented with 1 mM sodium pyruvate, 5% fetal calf serum (Sigma #F7524), and 0,5% penicillin / streptomycin antibiotics.
- The C20 human microglial cell line has been generated by David Alvarez-Carbonell, Ph.D. (Case Western Reserve University) as previously described [76]. C20 cells were grown at 37 °C and 5% CO<sub>2</sub>, and cultured in DMEM-F12 medium supplemented with 10% fetal bovine serum (FBS) and 1% of pen/strep. The medium was supplemented with neomycin (600 µg/mL) to select immortalized cells expressing constitutively active telomerase. KD-TSPO and scramble (SCR) C20 cells were cultured in the same medium of C20 cells with the addition of blasticidin (2,5 µg/mL) acting as a selection marker for KD cells. The TSPO KD in C20 cells was performed by the use of a lentiviral expression vector (pLKO-shTSPO), which was generously gifted by David Root (Addgene plasmid #10878). The design of the human TSPO shRNA was taken from the RNAi Consortium [77] (Cambridge, UK) with the clone ID (TRCN0000060433). The scramble shRNA was a gift from David Sabatini (Addgene plasmid #1864). For cell maintenance in culture, WT C20, TSPO-KD C20, and SCR C20 cells were detached by incubation with Trypsin/EDTA for 5 min at 37 °C. After proper growth medium addition, cells were centrifuged at 1200 rpm for 5 min, resuspended in fresh medium and plated in T75 flasks. Cells were used until passage 15.
- The human oligodendroglioma cell line (HOG) was established from a surgically removed oligodendroglioma, as described previously (Post and Dawson, 1991). HOG cells were grown at 37 °C and 5% CO<sub>2</sub> and cultured in DMEM (#10-017-CV Corning, New York, USA) with 4.5 g/L of glucose, supplemented with 1 mM sodium pyruvate, 10% heat-inactivated FBS (#35-089-CV, Corning), and 1% pen/strep antibiotics (#30-002-CI, Corning). For cell culture maintenance, cells were detached by incubation with Trypsin/EDTA for 5 min at 37 °C, then centrifuged at 1200 rpm for 5 min, resuspended in fresh medium, and plated in T25 or T75 flasks. Cells were used until passage 12.

## 2.2 CRISPR/Cas9 technology: experimental procedure

The main steps of a CRISPR/Cas9 genome-editing experiment are: 1) *in silico* design of the gRNA and the ssODN 2) cloning of the gRNA into the plasmid encoding Cas9 expression; 3) cellular transfection with the vector encoding the Cas9 and the gRNA, plus the naked ssODN; 4) clonal selection, isolation, and expansion; 5) genotyping of the clones.

### *In silico* design of the gRNA and ssODN

The gRNAs were designed by the means of CRISPOR website (<http://crispor.tefor.net/crispor.py>) [279].

- Strategy A: the gRNA was designed to allow the DSB by WT Cas9 as close as possible to the point mutation. Sequence of the selected gRNA1 (10 nt upstream of the mutation):

5' -TAGCCTTATGAAGTTTACTCTGG-3'

- Strategy B: two different gRNAs were designed to bind sense and antisense strands on the target DNA sequence, and to cut one upstream and one downstream to the mutation. Thus, being the two nicks performed by nCas9 close enough to each other, a DSB is obtained. The two gRNAs were chosen with a PAM-out orientation, meaning that the PAM sequences of the gRNAs were oriented outside the point of insertion of the mutation [120]. Sequences of the selected gRNAs:

gRNA1 (cut 10 nt upstream to the mutation): 5' -TAGCCTTATGAAGTTTACTCTGG-3'

gRNA2 (cut 15 nt downstream to the mutation): 5' -TGCCAGGGAAAGCATTCCATGGG-3'  
(reverse)

A 174 nt long ssODN serving as a template for the HDR repair mechanism was designed. The ssODN carries the *Plp1* WT sequence and possesses 80-90 nt long homology arms on either side of the mutation. The PAM sequences present on the ssODN sequence were intentionally mutated to prevent the DNA corrected sequence from being re-cleaved by Cas9.

## Obtaining of the plasmid vectors encoding for the gRNA and the Cas9:

### *Plasmids*

The plasmid pSpCas9 sgRNA-2A-Puro (pX459) (Addgene plasmid #62988) encoding for WT Cas9 was used for strategy A. The plasmid pSpCas9n sgRNA-2A-Puro (pX462) (Addgene plasmid #62987) encoding for nCas9 was used for strategy B. The plasmid pSpCas9 sgRNA-2A-GFP (pX458) (Addgene plasmid #48138) was used for transfection optimization experiments. All Cas9 sequences are under the control of the promoter Chicken Beta Actin. The vectors encode also genes for puromycin and ampicillin resistance, as well as the coding sequence for RNAttract controlled by the U6 promoter. Between the U6 promoter sequence and the RNAttract coding sequences, two restriction sites for the *BbsI* enzyme are present, allowing for the introduction of the oligonucleotide encoding for the crRNA in frame with the RNAttract.

### Cloning of oligonucleotides encoding crRNAs in the plasmids:

\* *Digestion of plasmids* Vectors pX459 and pX462 were digested by restriction enzyme (RE) *BbsI* to introduce the oligonucleotides encoding the respective gRNAs. The reaction mix comprised: 1 µg of plasmid, and 0.2 U/µL of RE *BbsI* (#R0539, New England BioLabs, NEB, Massachusetts, USA). Digestion reaction has taken place for 15 min at 37 °C, then the enzyme was inactivated for 20 min at 65 °C.

\* *Hybridization* of sense and antisense oligonucleotides encoding gRNAs. The oligonucleotides have four nucleotides at their ends (5'-CAAA-3' for sense and 5'-CACC-3' for antisense) to generate cohesive ends with those generated by *BbsI* on the vector. The ends of the oligonucleotides were phosphorylated as follows: 100 ng of sense and antisense oligonucleotide (Sigma-Aldrich), and 1 U/µL of T4 Polynucleotide Kinase (NEB #M0201). The mix was placed in a T100 thermal cycler (Bio-Rad, Hercules, CA, USA) with the following cycling protocol: 1) 30 min at 37 °C (phosphorylation), 2) 5 min at 95 °C (dehybridization), and 3) gradual cooling of 5 °C / min up to 25 °C (hybridization).

\* *Ligation of oligonucleotides into plasmids*. The different gRNAs were cloned in the two different vectors. The ligation reaction mix was composed of 100 ng of plasmid, 5 nM of hybridized

oligonucleotides, and 2 U/ $\mu$ L of T4 DNA ligase (NEB #M0202). Ligation has taken place at 25 °C for 15 min, then the enzyme was inactivated for 15 min at 65 °C.

### Bacterial transformation and isolation of colonies:

Competent bacteria (Escherichia Coli; One Shot® TOP10; Thermo-Fisher #C404010) were transformed with the ligation mix containing either the plasmid pX459 + gRNA1 (strategy A), or pX462 + gRNA1, or pX462 + gRNA2 (strategy B). Bacterial cells were transformed by heat shock according to the manufacturer's instructions. Transformed cells were grown in Luria-Bertani (LB) agar plates containing 100  $\mu$ g/mL ampicillin and grown overnight at 37 °C.

### Analysis of clones

\* *Extraction of plasmid DNAs.* Six colonies isolated by a Petri dish from each cloning were amplified by inoculation in 5 mL of LB medium with ampicillin (100  $\mu$ g/mL) and grown overnight at 37 °C while shaking. Plasmid DNA was extracted with the NucleoSpin® Plasmid Kit (#1190242, Macherey-Nagel, Allentown, PA, USA) following the manufacturer's instructions.

\* *BbsI digestion.* The extracted plasmid DNA was digested with the RE *BbsI* to prove the insertion of oligonucleotides encoding the gRNA in the vector. The reaction mix was composed of 500 ng of pDNA, 0.5 U/ $\mu$ L of BbsI (NEB #R0539), and 1X digestion buffer (NEBuffer CutSmart® # B7204). Digestion has taken place for 30 min at 37 °C.

\* *Agarose gel electrophoresis of the digestion products.* To distinguish the digested and therefore linearized pDNA from the intact plasmids, samples were migrated on a 1% agarose gel. Migration has taken place for 30 min at a constant voltage of 130 V. The DNAs were visualized by ethidium bromide gel staining (0.8  $\mu$ g/mL; Bio-Rad #1610433) with the ChemiDoc™ Imaging system (Bio-Rad).

\* *Sanger sequencing of selected clones.* All constructs were checked by sequencing (Eurofins Genomics - GATC Services; [www.eurofinsgenomics.eu](http://www.eurofinsgenomics.eu)).

### Production of plasmid vectors:

The pX459-gRNA1 clone #5, pX462-gRNA1 clone #2, and pX462-gRNA2 clone #4 were selected based on sequencing results, amplified by inoculating 500  $\mu$ L of the previous pDNA mini-preparation

in 5 mL of starter culture containing LB medium with ampicillin (100 µg/mL), and incubated for 5 h at 37 °C while shaking. Then, the starter culture was inoculated in 250 mL of LB medium with ampicillin (100 µg/mL) and incubated overnight at 37 °C while shaking. The pDNA of each clone was extracted by the means of the NucleoBond® Xtra Midi kit (Macherey-Nagel #12752653) according to the manufacturer's instructions.

### 158JP Transfection

158JP cells were seeded in a 24-well plate at a density of 75.000 cells/well and incubated in medium w/o antibiotics at 37 °C under 5% CO<sub>2</sub>. After reaching 80% of confluency, transfection of cells was carried out with Lipofectamine 3000 (Lipo3000; Thermo Fisher #L3000-01) transfection reagent. The transfection mix consisted of (strategy A) 1 µg of plasmids pX459-gRNA1, and (strategy B) 1 µg of pX462-gRNA1 + 1 µg of pX462-gRNA2 diluted in 25 µL of Opti-MEM (Gibco® #31985) and mixed with 0,75 µL or 1,5 µL of Lipo3000 diluted in 25 µL of Opti-MEM. 2 µL of the ssODN repairing template (10 µM) was added. The transfection medium was replaced the day after transfection. For the optimization of transfection efficiency, cells were transfected with 1 µg of plasmids pX458-GFP and imaged after 48 h with an inverted fluorescence microscope (Olympus IX73, ex/em filters 488/510 nm).

### Selection of transfected cells, clonal isolation, and expansion:

48 hours post-transfection, the culture medium was replaced by a medium containing the selection antibiotic puromycin (2 µg/mL; Sigma-Aldrich #P9620). 4 hours after puromycin treatment, cells were detached and serial dilutions were performed to obtain a final concentration of 0,5 cells / 100 µL, and plated in a 96-well plate dispensing 100 µL per well to obtain no more than one single cell per well. Single clones were monitored each day during growth. When confluency was reached, each clone was separately split in a 6-well plate for amplification and monitored during growth. When confluence was reached, cells were detached and cryo-preserved at -80 °C. One aliquot of cells from each clone was collected for genomic analysis.

## DNA extraction from the clones and PCR amplification

Genomic DNA was extracted from each clone by the use of the NucleoSpin® Tissue kit (Macherey-Nagel #740952) according to the manufacturer's instructions and quantified using the  $\mu$ Drop system (Thermo-Fisher). A polymerase chain reaction (PCR) with primers designed with the Primer3 site (<http://primer3.ut.ee/>; forward primer: 5'-ACAACGCAAAGCAGCACATT-3'; reverse primer: 5'-TCCTCCATGTCTAGCCAATCT-3') targeting the *Plp1* gene region across the mutation (PCR amplicon 345 bp) was performed. The reaction mix comprised: 75 ng of genomic DNA, 200 nM of each primer, and 1X of Red Taq Master Mix (Sigma-Aldrich #R2523). The PCR reactions were placed in a T100 thermal cycler (Bio-Rad) with the following protocol: 95 °C for 2 min, then 35 cycles of 95 °C 30 sec, 61 °C 30 sec, 72 °C 80 sec and a final step at 72 °C for 5 min.

## DdeI digestion

The screening was performed by creating restriction maps using the DdeI RE. The reaction mix comprised: 25  $\mu$ L of PCR product, 0.2 U/ $\mu$ L of DdeI (NEB #R0175), and 1X digestion buffer (NEBuffer CutSmart® #B7204). The digestion reaction has taken place for 15 min at 37 °C, then the enzyme was inactivated for 20 min at 65 °C. The digestion products were analyzed on a 2% agarose gel stained with ethidium bromide. The gel was imaged with the ChemiDoc™ Imaging system (Bio-Rad).

## 2.3 In vitro treatments

### C20 Cells Pharmacological Treatments

Cells were seeded in a 6-well plate (at a density of 300,000 cells/well) for relative mRNA quantification and in a 24-well plate (at a density of 75,000 cells/well) for cytokine release evaluation and maintained in complete culture media. The following day, cells were exposed to mild (IL-1 $\beta$  20 ng/mL) or strong (IL-1 $\beta$  100 ng/mL + INF- $\gamma$  50 ng/mL) inflammatory stimulus in serum-free medium and incubated for 24 h.

Treatments for WB protein analysis were carried out as follows: cells were seeded in P60 Petri dishes at a density of 300,000 cells/plate and maintained in their complete culture media for 24 h.

After, cells were treated with both mild inflammatory stimulus (IL-1 $\beta$  20 ng/mL) and strong stimulus (IL-1 $\beta$  100 ng/mL + INF- $\gamma$  50 ng/mL) in the presence or absence of 1  $\mu$ M DEXA for 24 h.

**Treatments for MTS viability assay** were carried out as follows: cells were seeded in a 96-well plate (10,000 cells/well) and maintained in their complete culture media for 24 h. Then, cells were treated with three different concentrations (10 nM, 100 nM, and 1  $\mu$ M) of TSPO ligands PK11195, Ro5-4864, Etifoxine, and XBD-173 for 24 h.

**Treatments for the evaluation of cytokine release following TSPO ligands administration** were carried out as follows: cells were seeded in a 24-well plate (100,000 cells/well) and maintained in their complete culture media for 24 h. Then, cells were pre-treated with 100 nM of TSPO ligands (PK11195, Ro5-4864, Etifoxine, and XBD-173) in a serum-free medium for 2 h. Subsequently, the medium was replaced and cells were subjected to the administration of mild inflammatory stimulus IL-1 $\beta$  (20 ng/mL) or a strong inflammatory stimulus (IL-1 $\beta$  100 ng/mL plus INF- $\gamma$  50 ng/mL) and incubated for 22 h. In the experiments performed to evaluate the specific contribution of XBD-173-induced steroids production, cells were pre-treated (1 h before the addition of XBD-173) with 50  $\mu$ M AMG.

### HOG cells Differentiation

HOG cells were seeded in their growth medium on multi-well plates or Petri dishes (day 0). After 24 h (day 1) the growth medium was replaced by the differentiation medium (DM) which was composed as follows: DMEM 4,5 g/L glucose, 1 mM sodium pyruvate, N2 supplement (Life Technologies, Eugene, OR, USA), 30 nM triiodothyronine (3,3',5'-Triiodo-L-thyronine, Sigma-Aldrich) and 0.05% FBS. Cells were cultured until day 9, during which DM was replaced at day 4 and 7.

### HOG Transfection for TSPO KD

HOG cells were seeded in a 6-well plate or 24-well (at a density of 100,000 cells/well or 10,000 cells/well) and maintained in complete culture media for 24 h. On day 4, DM was replaced and cells were transfected by the use of HiPerfect<sup>®</sup> Transfection Reagent (QIAGEN, Hilden, Germany) following manufacturer's instructions. GeneSolution siRNA for hTSPO (Cat. No. 1027416, Gene ID: 706) were employed. Hs\_BZRP\_4 (#SI00314566) and Hs\_BZRP\_3 (#SI00314559) were chosen among the four siRNA for their better silencing efficiency. 5 nM final concentration) of siRNA were

used for each transfection reaction. A SCR siRNA (#1022076) was employed as a negative control in preliminary experiments and no changes in TSPO expression were observed when compared with non-transfected cells.

### Cell Viability Assay

Cells were seeded in 96-well plates and treated accordingly to the experimental setup. Cell viability was determined using the [3-(4,5-dimethylthiazol-2-yl)-5-(3-carboxymethoxyphenol)-2-(4-sulfophenyl)-2H-tetrazolium, inner salt] (MTS) assay according to the manufacturer's instructions (Promega, Milano, Italy). This yellow tetrazolium dye can be reduced by cellular reducing agents NADH and NADPH to a water-soluble dark brown formazan salt. The amount of formazan produced is considered a marker of cell viability as it reflects cellular metabolic activity. On the day of the assay, 20  $\mu$ L of MTS reagent was added to 100  $\mu$ L of cell medium, and the colorimetric MTS conversion was quantified after 1 h by measuring the absorbance at 490 nm using the EnSight<sup>TM</sup> multimode plate reader, equipped with Kaleido Data Acquisition and Analysis Software.

## 2.4 Gene and protein expression analysis

### Relative mRNA expression: Real-Time RT-PCR

The relative mRNA quantification of genes of interest was performed by real-time RT-PCR. Total RNA from each sample was isolated using the RNeasy Mini Kit (QIAGEN, Hilden, Germany). The RNA purity was determined by measuring the 260/280 nm ratio, using the NanoDrop Instrument (Thermo Fischer Scientific). The cDNA synthesis was performed with 1  $\mu$ g of RNA using the iScript cDNA Synthesis Kit (Bio-Rad). The primers used for the real-time RT-PCR were designed to span intron/exon boundaries to avoid non-specific PCR amplification of genomic DNA (**Table 1**).

For the experiments on C20 cells, the real-time RT-PCR reaction was performed in 50  $\mu$ L as follows: 200 nM final concentration of forward and reverse primers, 50 ng cDNA, SYBR Green Master Mix (SsoAdvanced Master Mix, Bio-Rad) to a final concentration of 1X. The reactions were run for 40 cycles using the following temperature profiles: 98  $^{\circ}$ C for 30 s (initial denaturation), 55  $^{\circ}$ C for 30 s (annealing), and 72 $^{\circ}$ C for 3 s (extension).

For the experiments on HOG cells, the real-time RT-PCR reaction was performed in 20  $\mu$ L as follows: 300 nM final concentration of forward and reverse primers, 20 ng cDNA, SYBR Green Master Mix (SsoAdvanced Master Mix, Bio-Rad) to a final concentration of 1X. The reactions were run using the following temperature profiles: 98 °C for 2 min (initial denaturation), then 98 °C for 10 sec, and 60 °C for 30 s (annealing) for 40 cycles.

The amplification efficiency of each primer was preliminarily determined by the means of a cDNA standard curve, and values between 90% and 110% were considered acceptable. PCR specificity was determined using both a melting curve analysis post-amplification (65,0°C to 95,0°C: increment 0,5°C 0:05) and agarose gel electrophoresis. The housekeeping gene  $\beta$ -actin was used as a reference for relative quantification. The mRNA expression of the genes of interest was calculated by the means of the  $\Delta\Delta$ Ct method.

Gene	Primers	PCR product	Annealing Temp
IL-6	for: 5'-TCCTCGACGGCATCTCA-3'	165 bp	55 °C
	rev: 5'-TTTTACCAGGCAAGTCTCT-3'		
IL-8	for: 5'-AAGAGAGCTCTGTCTGGACC-3'	408 bp	56 °C
	rev: 5'-GATATTCTCTTGGCCCTTGG-3'		
IL-4	for: 5'-ACTTTGAACAGCCTCACAGAG-3'	74 bp	56 °C
	rev: 5'-TTGGAGGCAGCAAAGATGC-3'		
IL-10	for: 5'-CAAGCTGAGAACCAAGACCC-3'	141 bp	55 °C
	rev: 5'-AAGATGTCAAACCTCACTCATGGC-3'		
MBP	for: 5'-CATCCTTGACTCCATCGGGC-3'	184 bp	60 °C
	rev: 5'-GGAGCCGTAGTGAGCAGTTC-3'		
CNPase	for: 5'-TTGTGACTACGGGAAGGCTC-3'	122 bp	60 °C
	rev: 5'-CAGTCGTCTGGGTGTACA-3'		
TSPO	for: 5'-CTTTGGTGCCCGACAAATGG-3'	51 bp	60 °C
	rev: 5'-CTGACCAGCAGGAGATCCAC-3'		
CYP11A1	for: 5'-GTCTCGGGACTTCGTAGT-3'	168 bp	60 °C
	rev: 5'-GCCTCGGGTTCACTACTTC-3'		
HMGR	for: 5'-CAGCCATTTGCCCGAGTTT-3'	254 bp	60 °C
	rev: 5'-TCTGCTGACTGTTTTGAGGAGA-3'		
Fdft-1	for: 5'-GAAGGTCCCCTGTTACACA-3'	242 bp	60 °C
	rev: 5'-GGCAGTACTGTCCCACTCC-3'		
$\beta$ -actin	for: 5'-GCACTCTCCAGCCTTCTTCC-3'	254 bp	55 °C- 60 °C
	rev: 5'-GAGCCCGATCCACAGC-3'		

**Table 1.** Nucleotide sequences, product size, and annealing temperature of the primers employed in real-time RT-PCR experiments.

## ELISA-based Quantification of Cytokine Release

The conditioned medium from each well was collected and centrifuged for 5 min at 20,000 g (4 °C) before quantification of pro- and anti-inflammatory markers by the use of a commercial enzyme-linked immunosorbent assay (ELISA). The most highly sensitive ELISAs were chosen to measure the concentrations of IL-8 (Cloud Clone Corp., detection range: 15.6–1000 pg/mL, sensitivity < 6.7 pg/mL), and IL-4 (Cloud Clone Corp., detection range: 15.6–1000 pg/mL, sensitivity < 5.6 pg/mL).

## Western Blotting Analysis

Cells plated in P60 or P100 Petri Dishes. At the end of the experiment, cells were extensively washed with PBS, collected by scraping on ice, and centrifuged at 1200 rpm for 5 min at 4 °C. Protein extracts were obtained as follows: RIPA buffer (0.5% sodium deoxycholate PBS, pH 7.4, 1% Igepal, 0.1% SDS, and protease inhibitors: 4 µg/mL aprotinin, 1 µM orthovanadate, and 0.1 mg/mL PMSF) was used to resuspend and lyse cells. Protein quantification of cell lysates was performed by a Bio-Rad DC Protein Assay by following the manufacturer's protocol. Cell protein extracts (20-40 µg) were diluted in Laemmli solution, resolved by SDS-PAGE (4–20%), transferred to PVDF membranes, and incubated overnight at 4 °C with primary antibodies in 5% skim milk or 5% BSA in TBS 0,05% Tween. Primary antibodies: rabbit anti-TSPO 1:7500 (ab40390, Abcam), rabbit anti-MBP 1:500 (BK78896S Cell Signaling Technology CST, Danvers, Massachusetts, USA), rabbit anti-CNPase 1:500 (BK5664S CST), rabbit anti-CYP11A1 1:600 (BK14217S CST), rabbit anti-StAR 1:1000 (BK8449S CST), mouse anti-β-actin 1:10,000 (#A2228 Sigma-Aldrich-Merck KGaA). Then, membranes were washed 3 times with TBS-Tween and incubated with proper peroxidase-conjugated secondary antibody diluted 1:10,000 (#A6154 Sigma-Aldrich). After extensive washes, the peroxidase was detected by a chemo-luminescent substrate (ECL max reagent, Bio-Rad), using the ChemiDoc™ XRS+ instrument. Densitometric analysis of bands and their relative quantification versus the reference gene β-actin was performed using ImageJ software [Rueden et al., 2017].

## Immunofluorescence Analysis

Cells were fixed with 4% of PFA for 15 min followed by three washes with PBS, then permeabilized with a PBS solution containing 2.5% BSA and 0.1% Triton X100 for 10 min, blocked with 2.5% BSA PBS (blocking solution) for 1 h at room temperature, and then incubated 2 h room temperature with rabbit anti-TSPO 1:1000 (ab109497, Abcam) primary antibody diluted in blocking solution. After, cells were washed with PBS and incubated for 1 h with an anti-rabbit goat IgG conjugated with an Alexa Fluor® 488 dye (#A32723 Invitrogen, 1:500). After washes with PBS, coverslips were mounted with Fluoroshield Mounting Medium with DAPI (ab104139, Abcam) on microscope support and imaged with an epifluorescence microscope (Nikon E-Ri) using a 60X/1.4 oil objective. Sequential images in the blue and green channel were acquired for the detection of DAPI and TSPO signal,

respectively. Exposition time and acquisition parameters were kept constant for the imaging of different conditions. Images were analyzed using the ImageJ program (nih.gov) [280].

## 2.5 Cell-based functional assays

### ROS Production Evaluation

The ROS production by C20 cells was determined using the fluorogenic probe DCFH<sub>2</sub>-DA (Molecular Probes, Thermo Fischer Scientific). C20 WT cells were seeded in a 96-well plate at a density of 10,000 cells/well and maintained in complete culture media for 24 h. Then, cells were incubated in PBS/glucose containing 25 μM DCFH<sub>2</sub>-DA for 30 min in the dark (37 °C). Then the medium was removed and replaced with PBS/glucose. In the presence of ROS species, DCFH<sub>2</sub>-DA is oxidized to fluorescent 2',7'-dichlorofluorescein (DCF). The fluorescence intensity of DCF was examined by the use of the EnSight<sup>TM</sup> multimode plate reader (Perkin Elmer, Waltham, Massachusetts, USA) using 485/520 nm ex/em wavelengths. For data normalization, cells were fixed with 4% paraformaldehyde (PFA) for 15 min, washed with PBS, and with crystal violet staining solution for 30 min at room temperature. After extensive washing, cells were incubated for 1 h under shaking with 200 μL of PBS 1% SDS. The solution was transferred to another cell plate and the absorbance at 595 nm was read. The DCF fluorescence intensity values were normalized to the cell content of each well, which is known to be proportional to the crystal violet absorbance value.

### Pregnenolone Production Quantification

Pregnenolone production evaluation in HOG cells was performed by ELISA, as previously reported [281]. Briefly, 6,000 cells/well were seeded in 96-well plates, and differentiated as described above or used for the experiment on day 1 (non-differentiated control). On the day of the experiment (day 1 and day 9) the culture medium was replaced at time zero with saline medium (140 mM NaCl, 5 mM KCl, 1.8 mM CaCl<sub>2</sub>, 1 mM MgSO<sub>4</sub>, 10 mM glucose, 10 mM (HEPES)-NaOH, pH 7.4, and 0.1% bovine serum albumin (BSA) in the presence or absence of 25 μM trilostane and 10 μM SU1060, inhibitors of PREG metabolism. For the evaluation of the effect of TSPO stimulation on PREG release, 40 μM of PIGA1138 were used to treat the cells. After 2 h incubation, the conditioned medium was collected and dosed by competitive ELISA (DB52031, IBL International, Hamburg, Germany)

following the manufacturer's instructions. Absorbance at 450 nm from each well was read with the Ensign Multimode Plate Reader instrument (PerkinElmer) and the ng/mL values were interpolated from a standard curve. PREG concentrations were normalized to the cell content of each well by crystal violet staining. Briefly, after the experiment, cells were fixed with 4% PFA in H<sub>2</sub>O for 15 min. After washes, 50 µM of a methanolic solution of crystal violet were added to each well and incubated for 30 min. Then, cells were extensively washed with PBS and lysed by adding 1% SDS solution. The absorbance at 595 nm was read with the Ensign Multimode Plate Reader instrument.

### Intracellular Cholesterol Content Evaluation

HOG cells were seeded on round glass coverslips in a 24-well plate with a density of 10,000 cells/well and differentiated. For the evaluation of intracellular free cholesterol content, the Cholesterol Assay Kit (ab133116, Abcam, Cambridge, UK) was employed following the manufacturer's protocol. Briefly, cells were fixed, washed, and stained with Filipin III solution for 30 min at room temperature. After, the excess was removed and coverslips were mounted with Vectashield (Vector Labs, Burlingame, California, USA) on microscope support and imaged with an epifluorescence microscope (Nikon E-Ri) using a 60X/1.4 oil objective using 380/405 ex/em wavelengths. Intracellular cholesterol level quantification was obtained by measuring the mean fluorescence intensity per cell and normalized by the area of interest.

## 2.6 *Ex vivo* experiments

### Immunohistochemical Analysis

Lumbar spinal cord transversal and brain sagittal sections (15 µm-thick) from healthy controls, vehicle, PIGA1138 (15 mg/kg)- and PIGA839 (15 mg/kg)- treated EAE mice were obtained by the use of a Cryostat CM1950 (Leica, Wetzlar, Germany), mounted on Superfrost Plus glass slides (Thermo Fisher Scientific) and stored at -20 °C. For immunofluorescence analysis, sections were dried at 40 °C for 1 h, rehydrated in PBS for 5 min, and then fixed in 4% PFA for 15 min at room temperature. After washes, sections were permeabilized for 5 min using absolute ethanol. Non-specific binding sites were blocked with a PBS solution containing 5% FBS and 1% BSA for 30 min at room temperature. The sections were incubated overnight at 4 °C with the proper primary antibodies

diluted in PBS containing 0.5% BSA. The following primary antibodies were employed: rabbit polyclonal antibody anti-MBP (ab40390, Abcam) diluted 1:250; goat polyclonal anti-CD45 (AF114 from R&D System, Minneapolis, USA) diluted 1:40; rabbit polyclonal anti-NF200 (#N4142, Merck KGaA) diluted 1:250. Then, the slides were washed in PBS and incubated in the dark for 1 h at room temperature with the appropriate secondary antibody diluted in PBS containing 0.5% BSA. The following secondary antibodies were employed: Alexa Fluor® 488-conjugated donkey anti-rabbit (#A-21206, Thermo Fischer Scientific) diluted 1:500; Alexa Fluor® 555-conjugated donkey anti-goat (ab150130, Abcam) diluted 1:500. Finally, the sections were rinsed in PBS and mounted by the use of a glycerol mounting medium (ab188804, Abcam) containing DAPI for nuclear staining. Images were acquired with a multichannel epifluorescence microscope (Olympus DP73, Hamburg, Germany), processed using the Olympus cellSens software equipped with a digital camera, and analyzed using ImageJ Software. In the spinal cord, MBP immunofluorescence quantification was obtained by analyzing the white matter. The mean fluorescence intensity (Fluorescence intensity/Area) was obtained by calculating the mean of four regions of interest (ROIs): left lateral, left medial, right lateral, right medial of the spinal cord section, as indicated in Figure 3 (part III). In the brain, MBP quantification was performed in the white matter of three different regions (cerebellum, corpus callosum, and cortex). For the spinal cord and the cerebellum, NF200 quantification was obtained by calculating the mean of three different ROIs. Results are indicated as fluorescence intensity signal normalized over the area of interest and expressed in Arbitrary Unit (A.U.). The number of CD45 positive (CD45+) cells in the spinal cord was assessed by manually counting the nuclei. Results are plotted as the number of CD45+ cells over the ROI area.

### ELISA-based IL-10 Quantification in Serum

To evaluate the systemic levels of the anti-inflammatory IL-10 in mice, sera from healthy controls, vehicle-treated, PIGA1138 (15 mg/kg) and PIGA839 (15 mg/kg)- treated EAE mice were collected at the end of the experiments. The quantification of IL-10 was performed using an enzyme-linked immunosorbent assay (ELISA). Concentrations of IL-10 were measured using an ELISA commercial kit (Cloud Clone Corporation, Houston, USA) having a detection range between 15.6–500 pg/mL and a sensitivity < 2.3 pg/mL, according to the manufacturer's instructions. IL-10 concentration was determined by comparison with a standard curve and presented as pg/mL serum.

## LC/HR-MS Quantification of Allopregnanolone in spinal cord tissues

Spinal cords of control, vehicle-, PIGA1138 (15 mg/kg)-, PIGA839 (15 mg/kg)- treated EAE mice were collected at the end of the experiment, and LC/HR-MS analysis of ALLO was performed according to the protocol described by Giatti *et al.*, [272] with minor modifications. Briefly, frozen tissues (50-70 mg wet weight), spiked with deuterated ALLO, were homogenized in 2 mL of MeOH/AcOH (99:1 v/v) by the use of a tissue homogenizer (T 25 digital ULTRA-TURRAX® from IKA®-Werke GmbH & Co. KG, Germany), and left overnight at 4 °C under agitation for optimal tissue extraction. Then, samples were centrifuged at 12,000 g for 15 min at 4 °C and the pellet was further extracted with 1 mL of MeOH/AcOH (99:1 v/v). The supernatants from the extractions were collected, combined, and dried under a nitrogen stream. After a purification step by liquid-liquid extraction with methyl tertiary-butyl ether (MTBE), the organic phase was transferred to a clean vial, evaporated to dryness, and derivatized with 100 µL of hydroxylamine 100 mM in 50% water/methanol for 1 h at 60 °C as previously reported [2], then centrifuged and analyzed by LC/HR-MS. The UHPLC-HR-MS system was composed of a Vanquish Flex Binary pump LC and a Q Exactive Plus MS equipped with heated electrospray ionization (H-ESI) source, Orbitrap-based FT-MS system (Thermo Fischer Scientific). The chromatography was performed on a C18-EVO column (100 × 2.1 mm, 2.6 µm particle size) provided of a SecurityGuard™ Ultra Cartridges (Phenomenex, Bologna, Italy), eluting with formic acid in methanol 0.1% v/v (solvent A) and formic acid in H<sub>2</sub>O 0.1% v/v (solvent B) with a linear solvent gradient (20 to 90% A within 18 min). MS parameters were: positive polarity, spray voltage 3.4 kV, capillary temperature 290 °C, S-lens RF level 50, sheath and auxiliary gas respectively 24 and 5 (arbitrary unit). Quantitative analysis of ALLO was performed based on calibration curves prepared and analyzed using a deuterated internal standard. The obtained data were normalized on the wet weight of the extracted tissue and expressed in pg/g.

## 2.7 Statistical analysis

Statistical analysis was performed using GraphPad Prism Software version 8.0.2 for Windows (GraphPad Software Inc., San Diego, CA, USA) and all data are presented as the mean of the values from the different experiments ± SEM. Statistical analyses were performed as precisely indicated in each figure legend. A p-value < 0.1 was considered statistically significant.



# Chapter 3

## RESULTS AND DISCUSSION

## Chapter 3.1

---

### 158JP cell line genome editing using CRISPR Cas/9 technology

#### 3.1.1 Results

---

In the present thesis, CRISPR/Cas9 genome editing technology was applied on murine 158JP OLs *in vitro* model of severe PMD, to correct the point mutation (A>G) located at the splicing acceptor site between exon 4 and 5 of the *Plp1* gene leading to the insertion the production of a misfolded PLP which exerts a toxic effect on OLs. In particular, we aimed at inserting a point mutation (G>A) which would restore the WT genotype in 158JP OLs. Based on the evidence in the literature, two different experimental strategies were chosen for this aim: A) 158JP cells were transfected with the pX459-gRNA1 plasmid encoding for WT Cas9 and the gRNA; B) 158JP cells were transfected with the pX462-gRNA1 and pX462-gRNA2 plasmids, encoding for nCas9 plus and the two gRNAs. In both strategies, a naked ssODN repairing template was provided to cells at the moment of the transfection. The first step of our CRISPR/Cas9 experiment concern the *in silico* design of the gRNA, which has been made by the use of CRISPOR website (<http://crispor.tefor.net/>) [282].

The CRISPOR site creates a ranking of the potentially suitable gRNA according to two criteria: 1) the specificity 2) the predicted efficiency score (probability of the target sequence to be cleaved by Cas9, and 3) the number of off-target for each number of mismatches in the gRNA. Based on the proposed ranking, the gRNA which cleaved the closest to the mutation was selected. Unfortunately, due to the limited availability of PAM sequences in the proximity of the mutation, our choice was limited. However, two gRNA having high efficiency and good enough selectivity were selected. The successful cloning of the two gRNA inside the selected vectors was confirmed by sequencing.

In order to find the optimal conditions of transfection, the pX458-GFP plasmid encoding for GFP was employed. By the use of 0,75 and 1,5  $\mu$ L of Lipofectamine 3000, a transfection efficiency of 30-40% was achieved by manual counting of positively transfected cells visualized under an epifluorescent microscope. Afterward, the CRISPR/Cas9 experiment was performed as described in detail in the

methods section. The nomenclature of the different obtained clones followed the scheme of each well of the 96-well plate where clonal isolation was performed (letter-number codification).

The CRISPR/Cas9 transfection experiments have allowed to obtain 255 clones for strategy A and 98 clones for strategy B. To perform a preliminary screening of the clones, genomic DNA was extracted, and a 345 bp region across the *jimpy* mutation of the *Plp1* gene was amplified by PCR. The PCR product from each clone was digested by DdeI RE, and restriction maps were obtained (**Figure 1**). The selected PCR sequence (345 bp) presents one restriction site for DdeI (5' C|TNAG 3') downstream to the site of *jimpy* mutation. The WT sequence of *Plp1* gene presents a second DdeI restriction site at the level of the mutation (5' C|TTAG 3'), which is suppressed by the A>G *jimpy* mutation in *Plp1* gene (5'CTTGG 3') (**1B**). The DdeI digestion of WT *Plp1* PCR amplicon would generate 3 different fragments due to two DdeI restriction sites (205, 74, 58 bp). On the contrary, the DdeI digestion of *jimpy* mutated *Plp1* PCR amplicon would generate 2 different fragments due to only one restriction site for DdeI (279, 58 bp), as the presence of A>G *jimpy* mutation destroys the upstream restriction site. As a reference for our screening, we employed DdeI restriction maps of the PCR product of *Plp1* gene obtained by *jimpy* and WT mice, which is shown in **Figure 1A**.

## A

Gene: proteolipid protein (myelin) 1

Location: Chromosome X: 135,723,420-135,740,482 forward strand.

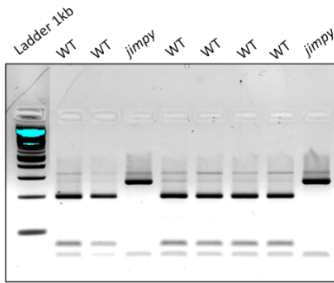
Ref transcript sequence: ENSMUST00000033800.12

The sequence showed corresponds to the PCR amplicon of 354 bp: part of intron 4,

Exon 5 (ENSMUSE00000209384; start: 135,734,904\_end: 135,734,977), part of intron 5.

```
>>
60 bp CTCAC TTTTCTCCGATTGACTGATATTAACAACGCAAAGCAGCACATTTCAATAATATA
60 bp AACTTCACAATTAGTCAATAGCACCTTTGTTCTATGTAAC TTTTAGAAAAAAGATGA
60 bp TGCATACTGTCAATATCAGGTTTACAGCCAGGATAGAGAAGGTAGAAAAGCTATGTAGAAC
60 bp GTCTCCGCATGGCCTCTAGCCTTATGAAGTTTACTCTGGCTGCTTTTATGTATCTTAGGT
60 bp GTTCTCCCATGGAATGCTTTCCCTGGCAAGGTTTGTGGCTCCAACCTTCTGTCCATCTGC
60 bp AAAACAGCTGAGGTAAGTGAATGAGAAGAGTGCTTTTAAAAAATAGATTGGCTAGACAT
6 bp GGAGGA
```

## B



**PCR Primers:**

Forward: 5'-**TGATATTAACAACGCAAAGCAGC**-3'

Reverse: 5'-**TCCTCCATGTCTAGCCAATCT**-3'

**PCR product: 345 bp**

Digestion with **DdeI**

DdeI restriction site: 5' C/TNAG 3'

3' GANT/C 5'

**C**

**WT sequence**

```
>>
60 bp CTCAC TTTTCTCCGATTGAC TGATATTAACAACGCAAAGCAGCACATTTCAATAATATA
60 bp AAAC TTCACAATTAGTCAATAGCACCTTTGTTCTATGTAAC TTTTAGAAAAAAGATGA
60 bp TGCATACTGTCAATATCAGGTTTACAGCCAGGATAGAGAAGGTAGAAAAGCTATGTAGAAC
60 bp GTCTCCGCATGGCCTCTAGCCTTATGAAGTTTACTCTGGCTGCTTTTATGTAT C/TTAGGT
60 bp GTTCTCCCATGGAATGCTTTCCTGGCAAGGTTTGTGGCTCCAACCTTCTGTCCATCTGC
60 bp AAAACAG C/TGAGGTAAGTGAATGAGAAGAGTGCTTTTAAAAAATAGATTGGCTAGACAT
6 bp GGAGGA
```

Two DdeI sites are present:

Site 1) = C/TTAG

Site 2) = C/TGAG

**Generation of 3 fragments**

Fragment 1 : 205 bp

Fragment 2 : 74 bp

Fragment 3 : 58 bp

**Jimpy sequence (point mutation A>G)**

```
>>
60 bp CTCAC TTTTCTCCGATTGAC TGATATTAACAACGCAAAGCAGCACATTTCAATAATATA
60 bp AAAC TTCACAATTAGTCAATAGCACCTTTGTTCTATGTAAC TTTTAGAAAAAAGATGA
60 bp TGCATACTGTCAATATCAGGTTTACAGCCAGGATAGAGAAGGTAGAAAAGCTATGTAGAAC
60 bp GTCTCCGCATGGCCTCTAGCCTTATGAAGTTTACTCTGGCTGCTTTTATGTAT CTTGGGT
60 bp GTTCTCCCATGGAATGCTTTCCTGGCAAGGTTTGTGGCTCCAACCTTCTGTCCATCTGC
60 bp AAAACAG C/TGAGGTAAGTGAATGAGAAGAGTGCTTTTAAAAAATAGATTGGCTAGACAT
6 bp GGAGGA
```

One DdeI site is present:

Site 2) = C/TGAG

**Generation of 2 fragments**

Fragment 1 : 279 bp

Fragment 2 : 58 bp

**Figure 1. The rationale of the preliminary screening of CRISPR/Cas9 clones. (A) Selected PCR product sequence (345 bp) across the jimpy mutation and its location in the genome. The number of bp at the beginning of each line in the sequence is mentioned to help the reader for the counting of**

the length of the fragment. Exon 5 sequence (74 bp) is in green. **(B)** Genotyping analysis of *jimpy* and WT mice (restriction maps are used as a reference for the preliminary screening of CRISPR/Cas9 clones). Gel electrophoresis of *DdeI* digestion products after PCR amplification of the region across the *jimpy* mutation (345 bp). Two bands are obtained from *DdeI* digestion of *jimpy*-derived DNA, three bands are obtained from *DdeI* digestion of WT-derived DNA. **(C)** Schematic representation of the rationale of the preliminary screening of clones by *DdeI* digestion. Forward and reverse primers for PCR amplification are highlighted in grey. ER sites for *DdeI* are in bold underlined (**CTNAG**) and the cleavage point is represented by the slash.

Unfortunately, electrophoresis of the PCR products digested by *DdeI* RE showed that no *jimpy* reverted thus WT sequence clone was obtained from the different experiments. **Figure 2** shows a representative part of the electrophoresis of the digestion products of clones obtained by the means of strategy A, which were assigned by letter-number codification. All the clones except a few number (e.g. C2, C10) evidenced a restriction map identical between them and corresponding to the *jimpy* mutated sequence (1B). **Figure 3** shows the digestion products of a representative part of the high number of clones obtained with strategy B. Unfortunately, the results did not change and no corrected clone having WT *Plp1* sequence was found.

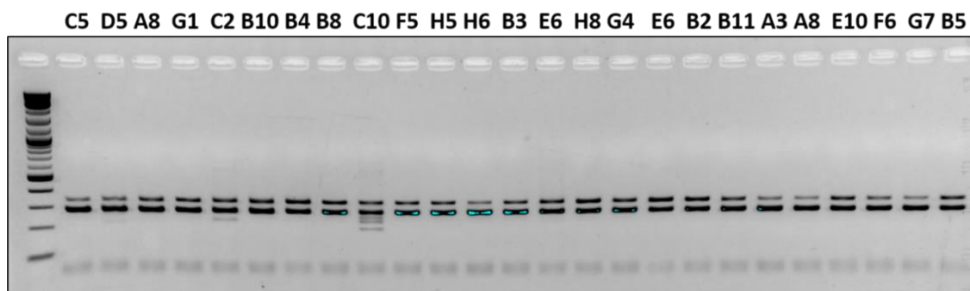


**Figure 2.** Example of electrophoresis profile of *DdeI* digestion products after PCR amplification of the region across the *jimpy* mutation from 25 clones obtained with the strategy A (WT Cas9 + gRNA1).

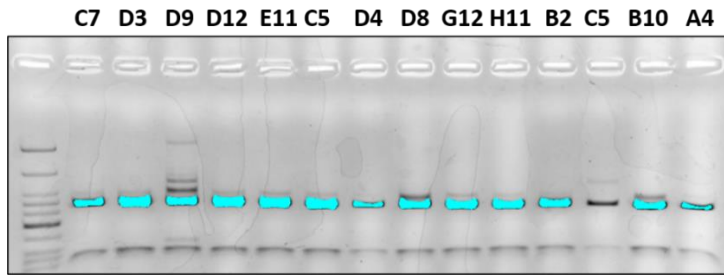


**Figure 3.** Example of electrophoresis profile of *DdeI* digestion products after PCR amplification of the region across the jimpy mutation from 14 clones obtained with the strategy B (nCas9 + gRNA1 + gRNA2).

## Discussion

---

One of the objectives of the present PhD thesis was the editing of the *jimpy* A>G mutation on *Plp1* gene (NM\_011123.4:c.623–2A>G) responsible for 158JP OLs death, by the replacement of the pathological mutation to restore the WT genotype. The CRISPR/Cas9 technology was chosen because it represents a highly adaptable genome editing tool, allowing for a precise and permanent modification of genomic DNA sequences.

Indeed, studies have demonstrated its efficacy and applicability in several experimental models of genetic diseases, such as PMD. In particular, a very recent work published by Elitt and colleagues demonstrated that *Plp1* suppression mediated by CRISPR/Cas9 in *jimpy* mouse either in the germline or postnatally was able to partially recover of jimpy mice from the pathology [115]. Indeed, CRISPR-modified jimpy (*CR-jimpy*) mice lacking PLP expression, evidenced increased myelination and restored nerve conduction velocity, motor function, and lifespan of the mice to WT levels, indicating that absence of PLP is better tolerated than the presence of misfolded PLP being toxic to OLs. However, the authors did not shed light on the mechanisms by which *Plp1* suppression rescues *jimpy* mice from the pathology especially in the first weeks of life. Therefore, our approach of editing *jimpy* pathological mutation in 158JP by CRISPR/Cas9 technology could further increase the understanding of the pathological mechanisms underlying PLP jimpy mutation, as well as clarify the relationship between misfolded PLP production and OLs dysfunctions, including mitochondrial impairments and reduced viability.

Despite we were not able to correct the *Plp1* mutation in 158JP OLs, due to peculiarly unfavorable experimental conditions (detailed below), together with the intrinsic limitations of the employed technology, DNA rearrangements such as insertion or deletion were observed in several CRISPR/Cas9 transfected clones (*i.e.* C10 from strategy A and D9 from strategy B), indicating that the gRNAs correctly bound to the target genomic DNA and that the Cas9 efficiently cleaved the DNA in both our transfection approaches.

The design of the gRNAs is crucial for successful genome editing with CRISPR/Cas9 technology, and its efficiency is a determinant parameter for the outcome of a CRISPR/Cas9 genome editing experiment. The efficiency of a gRNA depends on the nucleotides by which it is composed, as gRNAs having a too rich (>80%) or too poor (<20%) GC content have lower efficiency, being the ideal GC content around 60-70% [279]. As our aim was the insertion of a single point mutation, the possibilities in the choice of the gRNAs were limited, because the gRNA needs to bind a specific region on the

target sequence to allow the Cas9 cleavage to be as close as possible to the site of the mutation. In addition, the PAM availability in the target sequence further restricts the choice of the gRNA. Therefore, the selected gRNAs for our purpose could not be optimal, as the region for the design was quite restricted.

Optimal cellular transfection is the other crucial step in genome editing with the CRISPR/Cas9 technology. Therefore, we optimized transfection conditions by the use of a GFP-encoding plasmid, exploiting also different transfection reagents such as Lipofectamine and JetPEI. Unfortunately, 158JP cells, representing a pathological model with several cellular dysfunctions, were shown difficult to transfect, as different reagents presented low efficiency and induced massive cell death. The best result in terms of efficiency and less toxicity was obtained by the use of Lipofectamine 3000, which was therefore chosen for our CRISPR/Cas9 experiments. However, the transfection efficiency was not above 30%, representing a determinant factor for the outcome of our experiment. In fact, a reduced number of positively transfected cells further reduces the possibility to have clones carrying successful recombination.

A method to overcome the problems of transfection efficiency could be the employment of viral vectors. The main advantage of viral-mediated gene transfer is represented by the delivery of the cargo in a highly efficient manner, which is currently unachievable by non-viral methods. In particular, lentiviral transduction is one of the most high-efficiency delivery methods for introducing exogenous DNA constructs into almost any cell type, representing therefore the optimal option for delivering CRISPR-Cas9 system [283], as they also display low cytotoxicity and immunogenicity. However, lentiviruses are integrative, thus this limitation needs to be considered. To reduce the risk of insertional mutagenesis inherent in integrating delivery platforms, novel integrase-deficient lentiviral vectors, adenoviruses, or adeno-associated vectors have recently achieved significant interest for precise *in vivo* genome editing.

One of our approaches (strategy B) consisted of the use of two nCas9 with two gRNAs. Among the several possible explanations for the difficulty to replace the jimpy mutation, and to obtaining clones carrying the wild-type *Plp1* sequence, is the difficulty of promoting the HDR repair mechanism in the cells. In fact, homology recombination is known to occur rarely in the cells, being esteemed at a rate of 5%, and is cell-type dependent [120]. The use of two nCas9 instead of WT Cas9 has been suggested to increase the HDR frequency [121]. Indeed, two nCas9 with two gRNAs binding either upstream or downstream the mutation and on opposite DNA strand can realize the double nick. In this way, being the nicks close enough to each other, a DSB is obtained, however homologous recombination instead

of NHEJ repair is promoted. nCas9 strategy is usually chosen also to reduce the possibility of off-target cuts. On this line, an innovative method to increase the precision and flexibility of the CRISPR/Cas9 system, called prime editing, has been recently developed by the research group of David Liu [284]. Briefly, this new approach includes a nCas9 fused with reverse transcriptase enzyme, together with an engineered prime editing guide RNA (pegRNA) serving as a template for the reverse transcriptase to synthesize the desired modification. Such an innovative approach renders CRISPR/Cas9 genome editing more versatile and less constrained by PAM availability in the proximity of the site of editing. Indeed, the site editable by prime editing can be either near or even 30 base pairs far from PAM sites. In addition, prime editing was shown to induce HDR in 20-50% of the cases compared to the 5% of the classic approach [285]. For these reasons, prime editing CRISPR/Cas9 could represent the approach of election in inserting point mutations, such as the correction of 158JP mutated OLs. However, despite prime editing represents the new frontier in the avenue of single-point mutation insertion, as it has been demonstrated to be more precise and efficient than the classical CRISPR/cas9 approach, researchers pointed out the need to investigate off-targets of the system in a genome-wide manner, identify any accidental consequences the prime editors could have on the cells, and assess *in vitro* and *in vivo* delivery strategies of the system [285].

To conclude, CRISPR/Cas9 represents a promising tool for genome editing. However, some drawbacks reduce its applicability, especially for what concerns point mutation insertion. Although our idea of creating a model of *Plp1*-corrected 158JP is appealing and potentially applicable, several technical issues were encountered, thus further optimizations are required.

# Microglial Pro-Inflammatory and Anti-Inflammatory Phenotypes Are Modulated by TSPO Activation

## Results

---

### 3.2.1 Human microglial activation: *in vitro* model setting

Herein, the C20 human microglial cell line, which has been demonstrated to respond similarly to primary human microglia [286], was employed to set up our *in vitro* model of activated microglia. Two different *in vitro* settings of inflammatory activation were applied to C20 cells. In the first, we exposed C20 cells to IL-1 $\beta$  (20 ng/mL), while the second was obtained by the simultaneous exposure of C20 cells to IL-1 $\beta$  at higher dosage (100 ng/mL) and INF- $\gamma$  (50 ng/mL) to mimic a stronger inflammatory response by microglia. Both stimuli were administered in a serum-free medium for 24 h. mRNA levels of cytokines, migration ability, and ROS production were assessed following IL-1 $\beta$  or IL-1 $\beta$ /INF- $\gamma$  exposure (**Figure 1**). For both immunogenic stimuli, the results showed a significant increase in the transcripts of the pro-inflammatory cytokine IL-6 (**1A**) and IL-8 (**1B**). Interestingly, both stimuli promoted a higher transcription of IL-8 compared to IL-6.

Challenging C20 cells with the single or combined inflammatory stimulus produced different responses for the transcription of the anti-inflammatory interleukin IL-4. A significant increase in IL-4 (**1C**) was shown following exposure to IL-1 $\beta$ /INF- $\gamma$ . Conversely, an increase in IL-10 (**1D**) was observed following exposure to IL-1 $\beta$ .

As the activation of microglia involves the production of ROS [287], we measured ROS level after both activation stimuli (**Figure 2**). Only the combined stimulus produced a statistically significant increase in ROS production ( $116.5 \pm 3.9$  % vs. CTRL) compared to the control cells. To assess the effect of IL-1 $\beta$  or IL-1 $\beta$ /INF- $\gamma$  on microglial motility, which is generally increased in activated microglia, we performed a scratch assay. In **Figure 2B**, representative images illustrate that the activated-C20 cells possess an increased migratory potential when compared to the control. In

particular, both IL-1 $\beta$  alone and the combined stimulus significantly enhance gap closure when compared to the untreated microglia.

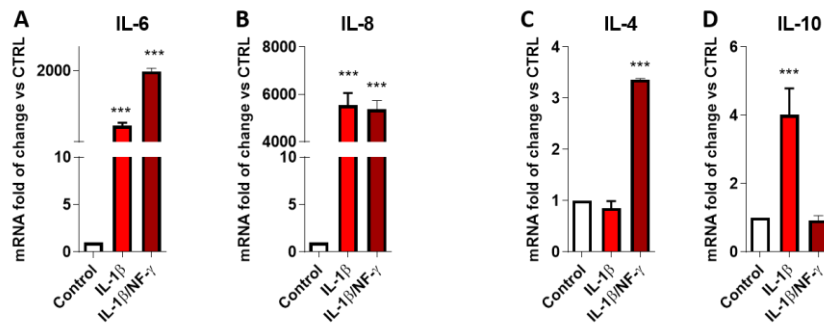


**Figure 1. Effects of inflammatory stimuli on mRNA levels of cytokines in C20 cells.** The mRNA levels of the pro-inflammatory cytokines IL-6 and IL-8 (A, B) and the anti-inflammatory cytokines IL-4 and IL-10 (C, D) were monitored in C20 cells following IL-1 $\beta$  (20 ng/mL) and IL-1 $\beta$ /INF- $\gamma$  (100 ng/mL/50 ng/mL) treatment for 24 h. Data are expressed as fold of change versus the control (CTRL) set to 1, and each bar represents the mean  $\pm$  SEM of two independent experiments performed in duplicate. \*\*\* $p \leq 0.001$  vs. to the control, calculated using one-way ANOVA followed by Bonferroni's post-test. Adapted from Da Pozzo E, Tremolanti C et al., Microglial Pro-Inflammatory and Anti-Inflammatory Phenotypes Are Modulated by Translocator Protein Activation, IJMS 2019 [288].

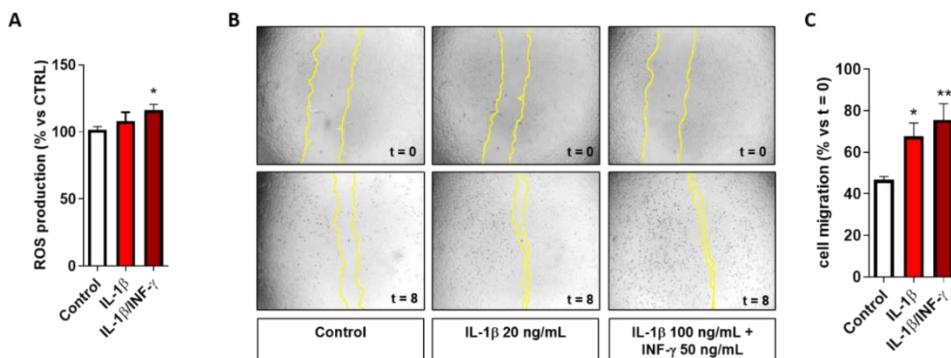


**Figure 2. Effects of inflammatory stimuli on cell migration and ROS production by C20 cells.** C20 cells were exposed to the inflammatory stimuli for 24 h. (A) ROS generation after treatment with IL-1 $\beta$  (20 ng/mL) or IL-1 $\beta$ /INF- $\gamma$  (100 ng/mL/50 ng/mL), was quantified and presented as a

percentage versus the control (CTRL). Each bar represents the mean values  $\pm$  SEM of three replicates from two independent experiments. **(B)** Representative images (4x magnification) of the scratch wounds at  $t = 0$  h and  $t = 8$  h are shown. The percentage of gap closure is reported with respect to the gap measured at  $t = 0$  h **(C)**. Data are presented as the mean values  $\pm$  SEM of two independent experiments performed in duplicate. \*  $p \leq 0.05$ , \*\*  $p \leq 0.01$  vs. control, calculated by one-way ANOVA, followed by Bonferroni's post-test. Adapted from Da Pozzo E, Tremolanti C et al., *Microglial Pro-Inflammatory and Anti-Inflammatory Phenotypes Are Modulated by Translocator Protein Activation*, *IJMS* 2019 [288].

Previous data indicated a critical role of IL-8 in the human reactive microglia, therefore this molecule was chosen as an example of pro-inflammatory cytokine and monitored in the following experiments. In parallel, IL-4 was chosen as a representative anti-inflammatory interleukin, as it is a key pleiotropic cytokine regulating brain homeostasis [289] **(Figure 3)**.

Following exposure with IL-1 $\beta$  or IL-1 $\beta$ /INF- $\gamma$ , C20 cells significantly increased the release of IL-8 **(3A)**, in line with the observed increase of its mRNA levels **(1B)**. Moreover, a significant decrease of IL-4 release was shown **(3B)**, even if the above results **(1C)** showed a simultaneous increase of IL-4 mRNA for the IL-1 $\beta$ /INF- $\gamma$  sample

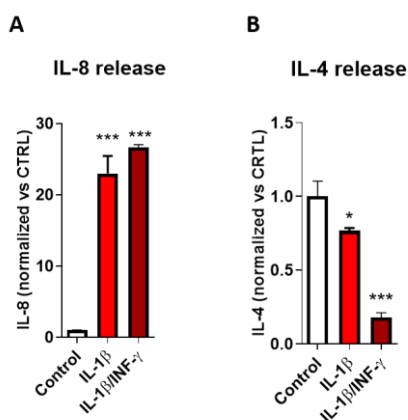


**Figure 3. Effects of inflammatory stimuli on IL-8 and IL-4 release by C20 cells.** **(A)** The proinflammatory IL-8 and **(B)** anti-inflammatory IL-4 levels were evaluated by ELISA in the conditioned medium of C20 cells treated with IL-1 $\beta$  (20 ng/mL) or IL-1 $\beta$ /INF- $\gamma$  (100 ng/mL/50 ng/mL) for 24 h. The concentration of cytokines was normalized to the number of cells and expressed as fg/mL/#cells. Each bar represents the mean  $\pm$  SEM of two different experiments performed in

triplicate. \*\*  $p \leq 0.01$ , \*\*\*  $p \leq 0.001$ , vs. control, calculated by one-way ANOVA, followed by Bonferroni's post-test. Adapted from Da Pozzo E, Tremolanti C et al., *Microglial Pro-Inflammatory and Anti-Inflammatory Phenotypes Are Modulated by Translocator Protein Activation*, *IJMS* 2019 [288].

### 3.2.2 Effect of TSPO pharmacological stimulation on the pro-inflammatory activation of C20 cells

The effect of several TSPO ligands on C20 cells viability was investigated (**Figure 4A**) for the first time.

Increasing concentrations (10 nM, 100 nM, and 1  $\mu$ M) of TSPO ligands did not induce significant differences in the viability between TSPO ligand-treated and control C20 cells. Herein, the commonly employed [226], [266] concentration of 100 nM was chosen as explorative treatment in IL-8 and IL-4 release experiments.

To assess the effect of pharmacological stimulation of TSPO on microglial activation, C20 cells were treated with TSPO ligands (100 nM) for 2 h, before the administration of the inflammatory stimulus (IL-1 $\beta$  or IL-1 $\beta$ /INF- $\gamma$ ) for 24 h in a serum-free medium. We investigated the effect of TPSP ligand pre-treatment on ROS production by activated microglia. All the TSPO ligands were able to significantly counteract the production of ROS mediated by the combined stimulus (**4B**).

C20 pre-treatment with classical TSPO ligands PK11195 and Ro5-4864 did not give statistically significant results concerning IL-8 release, despite a trend toward a decrease in the IL-8 release being observed. Conversely, the pre-treatment with the highly steroidogenic compounds Etifoxine and XBD-173 (**4C**, **4D**) was able to significantly counteract the IL-1 $\beta$  and IL-1 $\beta$ /INF- $\gamma$ -induced IL-8 release. The classical TSPO ligands were able to increase the IL-4 release differently in the two inflammatory models. In particular, Ro5-4864 increased the IL-4 production upon both the inflammatory stimuli (statistically significant following IL-1 $\beta$  treatment and near significance under IL-1 $\beta$ /INF- $\gamma$  activation). Conversely, PK11195 induced IL-4 release only after IL-1 $\beta$ /INF- $\gamma$  stimulus. Interestingly, a significant increase of IL-4 levels was observed following the pre-treatment with Etifoxine and XBD-173 (**4E**, **4F**).

As TSPO ligands are known to induce neurosteroids production, we exploited an inhibitor of the steroidogenesis, AMG, to assess whether the observed effects on cytokines release were mediated by neurosteroid release by microglia (**Figure 5**). Despite similar effects were obtained by XBD-173 and

Etifoxine in the previous experiments, the present experiment was performed only for XBD-173 pre-treatment because of its TSPO selectivity, differently from Etifoxine. C20 cells were pre-treated with 50  $\mu$ M AMG for 1 h before the treatment with XBD-173 100 nM and the administration of IL-1 $\beta$  or IL-1 $\beta$ /INF- $\gamma$  stimulus for 24 h. Our results demonstrated that the pre-treatment with AMG abolished the reduction of IL-8 release following microglial activation exerted by XBD-173 (**5A**, **5B**). Also, the XBD-173-induced increase in IL-4 production was significantly counteracted in presence of AMG pre-treatment during the IL-1 $\beta$ /INF- $\gamma$  combined stimulus (**5D**). These data suggest that XBD-173 observed effects may be mediated by neurosteroids production.

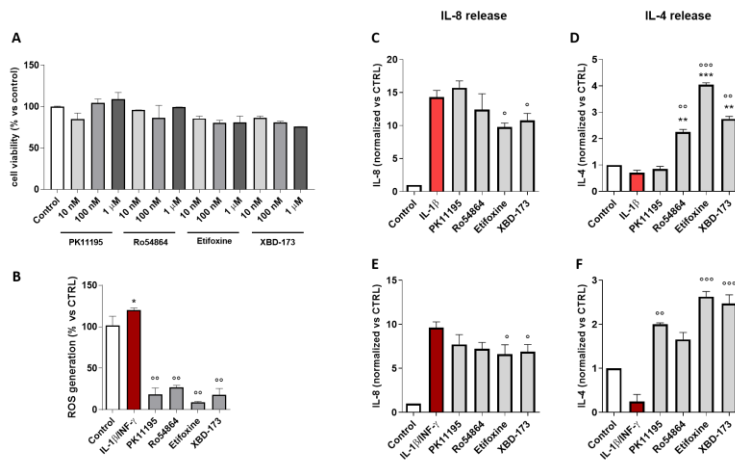


**Figure 4. Effects of TSPO stimulation on cell viability and cytokines release by activated C20 cells.** (A) C20 microglial cells were exposed to three different concentrations of PK11195, Ro5-4864, XBD-173, or Etifoxine (10 nM, 100 nM, and 1  $\mu$ M) in a serum-free medium. The MTS assay was performed after 24 h of treatment. Data are expressed as a percentage of cell viability compared to the control, which was set to 100%. No significant differences between groups were observed. (B) ROS generation after C20 treatment as described above was quantified and presented as a percentage versus the control (CTRL), set to 100%. Each bar represents the mean  $\pm$  SEM of three replicates from two independent experiments. (C-F) C20 cells were pre-treated with TSPO ligands (100 nM) for 2 h in a serum-free medium before the administration of IL-1 $\beta$  (20 ng/mL) or IL-1 $\beta$ /INF- $\gamma$  (100 ng/mL/50 ng/mL) for 24 h. After microglia activation by the inflammatory stimuli, IL-8 and IL-4 release were quantified by ELISA in IL-1 $\beta$ -treated C20 (C, E) and IL-1 $\beta$ /INF- $\gamma$ -treated C20 (D, F). The concentration of ILs was normalized to the amount of cytokine in untreated cells, set to 1. Each bar represents the mean values  $\pm$  SEM of three duplicates from three different experiments \*  $p \leq 0.05$ , \*\*  $p \leq 0.01$ , \*\*\*  $p \leq 0.001$ , vs. control,  $^{\circ}$   $p \leq 0.05$ ,  $^{\circ\circ}$   $p \leq 0.01$ ,  $^{\circ\circ\circ}$   $p \leq 0.001$ , vs. IL-1 $\beta$  or IL-1 $\beta$ /INF- $\gamma$ , #

$p \leq 0.05$ , and ####  $p \leq 0.001$  vs. XBD-173, determined by one-way ANOVA, followed by Bonferroni's post-test or student t-test. Adapted from Da Pozzo E, Tremolanti C et al., Microglial Pro-Inflammatory and Anti-Inflammatory Phenotypes Are Modulated by Translocator Protein Activation, IJMS 2019 [288].

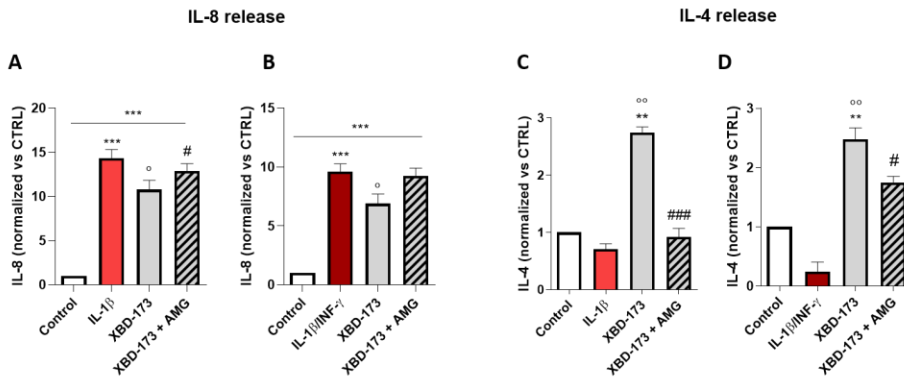


**Figure 5. Effects of AMG administration on cytokine release by XBD-173 pre-treated activated C20 cells.** C20 cells were in a serum-free medium. C20 microglial cells were exposed to 100 nM XBD-173 TSPO ligand for 2 h in a serum-free medium before the administration of the inflammatory stimuli for 24 h. For the XBD-173+AMG group, C20 were in parallel pre-treated with AMG (50 μM) 1 h before the addition of the TSPO ligand. IL-8 and IL-4 release were quantified after microglia activation by IL-1β- (A, C) or IL-1β/INF-γ (B, D). The concentration of ILs was normalized to the amount of cytokine in untreated cells, set to 1. Each bar represents the mean ± SEM of three replicates from two independent experiments. \*  $p \leq 0.05$ , \*\*  $p \leq 0.01$ , \*\*\*  $p \leq 0.001$ , vs. control, °  $p \leq 0.05$ , °°  $p \leq 0.01$ , °°°  $p \leq 0.001$ , vs. IL-1β or IL1-β/INF-γ, #  $p \leq 0.05$ , and ####  $p \leq 0.001$  vs. XBD-173, determined by one-way ANOVA, followed by Bonferroni's post-test or student t-test. Adapted from Da Pozzo E, Tremolanti C et al., Microglial Pro-Inflammatory and Anti-Inflammatory Phenotypes Are Modulated by Translocator Protein Activation, IJMS 2019 [288].

### 3.2.3 Effect of TSPO silencing on C20 cells responsiveness to the inflammatory stimulus

In order to investigate the effect of TSPO silencing in microglial activation *in vitro*, the stably transfected knockdown (KD) TSPO C20 cell line was employed. Herein, the reduction of TSPO expression was first confirmed by western blot analysis (**Figure 6A**). Upon both inflammatory stimuli,

TSPO KD C20 showed an increase in the release of the pro-inflammatory cytokine IL-8 compared to scramble (SCR) C20 (**6B**). In parallel, TSPO KD C20 presented a reduction in the release of the anti-inflammatory cytokine IL-4 (**6C**). These results suggest that TSPO has a negative modulatory effect on the pro-inflammatory activation of microglia. Interestingly, in the absence of inflammatory stimulus, TSPO KD cells evidenced a higher basal release of IL-8 and a lower basal release of IL-4 when compared to SCR cells (**6B**, **6C**), suggesting that TSPO has a critical role in maintaining the balance in the regulation of the release of pro-inflammatory and anti-inflammatory cytokines in controlled condition.

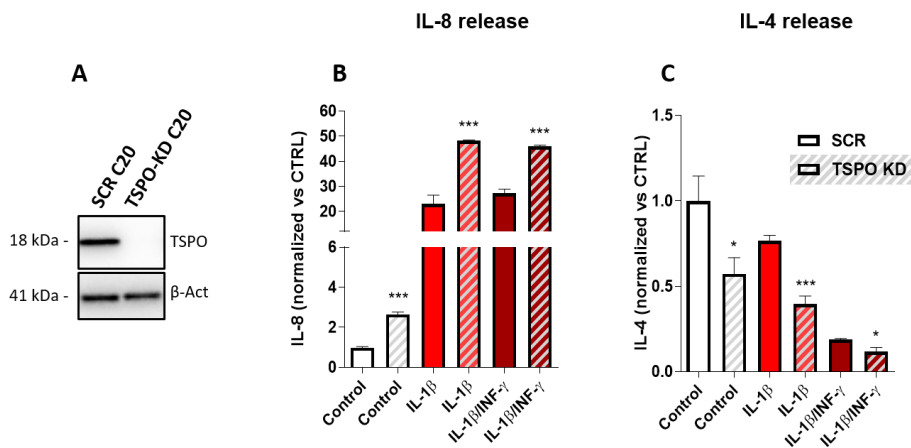


**Figure 6. Effects of TSPO KD on cytokine release by C20 cells.** (A) Representative images of TSPO and  $\beta$ -actin expression in SCR and TSPO KD C20 cells by western blot analysis. SCR and TSPO KD C20 cells were treated with IL-1 $\beta$  (20 ng/mL) or IL1- $\beta$ /INF- $\gamma$  (100 ng/mL/50 ng/mL) for 24 h in a serum-free medium, and pro-inflammatory IL-8 (B) and anti-inflammatory IL-4 release (C) were evaluated. The concentration of the released cytokines was normalized to the number of cells and expressed as fg/mL/#cells. Each bar represents the mean values  $\pm$  SEM of two different experiments performed in triplicate. \*  $p \leq 0.05$ , \*\*  $p \leq 0.01$ , \*\*\*  $p \leq 0.001$ , vs. SCR C20, determined by one-way ANOVA, followed by Bonferroni's post-test. Adapted from Da Pozzo E, Tremolanti C et al., Microglial Pro-Inflammatory and Anti-Inflammatory Phenotypes Are Modulated by Translocator Protein Activation, *IJMS* 2019 [288]

### 3.2.4 Regulation of TSPO transcription following inflammatory stimuli

Based on previous data demonstrating that the IL-1 $\beta$ -induced inflammatory signaling activates NF- $\kappa$ B signaling in C20 cells [31], the presence of the consensus sequence for this transcription factor (TF) was explored in the TSPO proximal promoter (**Figure 7A**). By Transcription Factor Affinity Prediction (TRAP) analysis (<http://trap.molgen.mpg.de>) [290], which shows the affinity-based ranking of TFs binding to the sequence of interest, NF- $\kappa$ B (position 1 in the ranking, **7B**) showed the highest binding affinity (p = 0.0068). The predicted binding sequence for NF- $\kappa$ B was located in the position -312/-325 of the TSPO promoter (numbering accordingly to the TSS of the NCBI site, *TSPO* reference NM\_714.6). Afterward, the PROMO analysis showed that 12 of the 14 nucleotides in the NF- $\kappa$ B sequence correspond to the most probable consensus sequence generated for this TF (dissimilarity 8.39%).

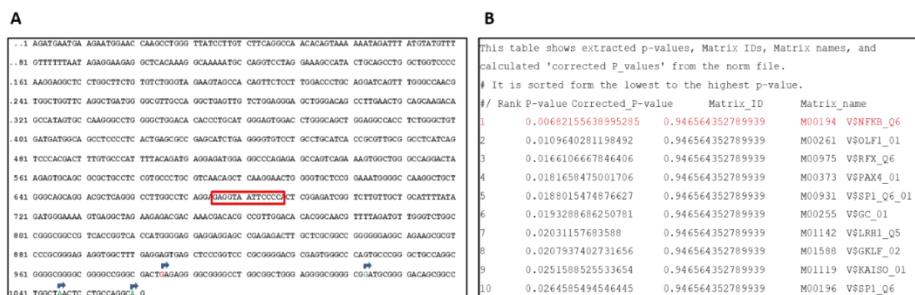


**Figure 7. Human *TSPO* proximal promoter.** The nucleotide sequence for NF- $\kappa$ B is labeled. The first arrow indicates the TSS reported on the NCBI site.

### 3.2.5 Effect of Dexamethasone treatment on TSPO expression following inflammatory stimuli in C20 cells

TSPO expression is reported to increase during microglia activation in several experimental models. Herein, the level of TSPO mRNA was evaluated after treatment with both the pro-inflammatory stimuli (**Figure 8**). The results showed that the treatment with both IL-1 $\beta$  or IL-1 $\beta$ /INF- $\gamma$  significantly increased the TSPO transcript levels (**8A**,  $2.2 \pm 0.4$ -fold of change for IL-1 $\beta$ ,  $2.9 \pm 0.2$ -fold of change for IL-1 $\beta$ /INF- $\gamma$ ). To better investigate the correlation between NF- $\kappa$ B activation and TSPO increased expression during microglial activation, we employed dexamethasone (DEXA), a synthetic glucocorticoid known to inhibit the NF- $\kappa$ B activation in different cellular models [291], thus exerting

anti-inflammatory and immunosuppressive activities. We treated C20 cells with 50  $\mu$ M DEXA in parallel to the administration of the inflammatory stimuli. Interestingly, DEXA significantly counteracted the IL-1 $\beta$ -induced TSPO transcript increase (**8A**). Accordingly, the same effect exerted by DEXA was observed for TSPO protein expression (**8B**). Unexpectedly, despite the treatment with IL-1 $\beta$ /INF- $\gamma$  increased TSPO mRNA, only a slight increase in the protein level was observed.

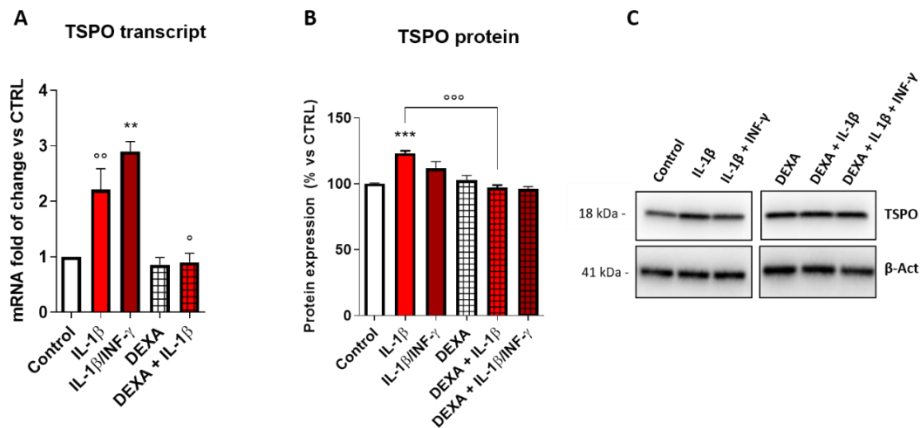


**Figure 8. Effect of DEXA treatment on TSPO expression in activated C20 cells.** (A) *TSPO* mRNA expression following inflammatory stimuli in C20 cells. Cells were treated with IL-1 $\beta$  (20 ng/mL) or IL1- $\beta$ /INF- $\gamma$  (100 ng/mL/ 50 ng/mL) for 24 h in serum-free medium. Cells were treated with IL-1 $\beta$  (20 ng/mL) or IL1- $\beta$ /INF- $\gamma$  (100 ng/mL/50 ng/mL) for 24 h in serum-free medium with or without (CTRL) 50  $\mu$ M DEXA. *TSPO* mRNA transcript levels were quantified and expressed as fold of change versus the control, set to 1. Data are presented as the mean values  $\pm$  SEM of two independent experiments performed in duplicate. C20 cells were treated as above and *TSPO* protein expression was determined by western blot analysis. Densitometric analysis of the bands (B) and representative images (C) are shown. Data are expressed as the percentage of protein expression versus control set to 100%. Each bar represents the mean values  $\pm$  SEM of three different experiments. \*\*  $p \leq 0.01$ , \*\*\*  $p \leq 0.001$  vs. control. <sup>o</sup>  $p \leq 0.05$ , <sup>oo</sup>  $p \leq 0.001$  vs. IL-1 $\beta$ , determined by one-way ANOVA, followed by Bonferroni's post-test. Adapted from Da Pozzo E, Tremolanti C et al., *Microglial Pro-Inflammatory and Anti-Inflammatory Phenotypes Are Modulated by Translocator Protein Activation*, *IJMS* 2019 [288].

## Discussion

---

Microglia participate in the establishment and regulation of the inflammatory response in the CNS. The acquisition of complex functional phenotypes upon activation allows microglia to determine beneficial effects as well as detrimental consequences, being the latter responsible for chronic neuroinflammation [292]. However, the mechanisms underlying the dynamic changes of microglia phenotypes have not been elucidated yet, especially what controls the secretion of pro-inflammatory or anti-inflammatory cytokines. In the present thesis, we first reported the characterization of an *in vitro* model of activated human microglia, which was then employed to explore the immunomodulatory function of TSPO, a mitochondrial protein proposed as a target to counteract neuroinflammation [293]. The obtained results support the hypothesis that TSPO possesses a homeostatic role in the context of the dynamic balance between anti-inflammatory and pro-inflammatory mediators secreted by human microglia during the inflammatory response. In particular, our results suggest a negative modulation of microglia activation by TSPO, which operates through several mitochondrial mechanisms including neurosteroids production.

The largest part of the information on microglia responsiveness to inflammatory stimuli is derived from studies conducted on rodent-derived microglia cells. However, it was reported that human microglia respond to different stimuli compared to rodents, which is well-known to respond to LPS [40], [294]. Conversely, only human microglia are susceptible to IL-1 $\beta$  [295] which is considered one of the major regulators of neuroinflammation, released by microglia and astrocytes as the main source [296]. Therefore, IL-1 $\beta$  was chosen herein as a mild activation stimulus on microglia cells. Then, another soluble cytokine exerting an important role in the human microgliosis, INF- $\gamma$ , was used at high concentration in combination with IL-1 $\beta$  to mimic an exaggerated inflammatory response by microglia [297]. The choice of these immunogenic stimuli has been also supported by previous data demonstrating that activated C20 cells upregulate the transcription of genes related to the INF- $\gamma$  response, along with NF- $\kappa$ B signaling, which is considered the main pathway activated by IL-1 $\beta$  [286].

In our hands, to challenge of C20 cells with both inflammatory stimuli resulted in increased cell migration ability, according to the reported ability of activated microglia to increase cell motility [298]. Furthermore, a considerable albeit low enhanced ROS production was observed, in agreement with literature data suggesting that human inflamed microglia, unlike those of the rodents, do not secrete large quantities of ROS [294]. Regarding inflammatory mediators, after IL-1 $\beta$  and IL-1 $\beta$ /INF-

$\gamma$  challenging of microglia, we detected increased mRNA transcripts not only for IL-6 and IL-8 pro-inflammatory cytokines but also for IL-4 and IL-10 anti-inflammatory cytokines. Of note, the increase in anti-inflammatory molecules was much lower than the one observed for the pro-inflammatory interleukins. In addition, only the IL-1 $\beta$ /INF- $\gamma$  stimulus significantly increased IL-4, and only IL-1 $\beta$  alone increased IL-10 transcript level. It should be taken into account that the microglia cytokine secretion profile is regulated by complex control machinery which aims at maintaining a proper balance among pro-inflammatory and anti-inflammatory mediators. Interestingly, we observed a marked increase in pro-inflammatory cytokine IL-8 release and a significant reduction in IL-4 anti-inflammatory cytokine release by C20 cells upon both activation stimuli compared to controls. Noteworthy, the discrepancy between released proteins and their mRNA level is frequently observed, being ascribed to the different mechanisms that regulate transcription, translation, and the release of the protein from the intracellular pools [299].

Herein, to investigate TSPO function during the activation of human microglia, the level of IL-8 and IL-4 release, selected as examples of pro- and anti-inflammatory cytokines respectively, were monitored under pharmacological amplification of TSPO activity or TSPO silencing. The chosen concentration of 100 nM is in line with previous reports showing pro-life effects exerted by TSPO ligands on several experimental models, including C20 [226], [266], [266]. The reported TSPO ligands were divided into two groups, based on previous evaluation of their RT at TSPO: poorly steroidogenic ligands (PK11195 and Ro5-4864) and highly steroidogenic ligands (XBD-173 and Etifoxine) [224], [225]. All of them are selective for TSPO, except for Etifoxine, which also binds with low affinity the GABA<sub>A</sub>-R [300]. Interestingly, highly steroidogenic ligands (XBD-173 and Etifoxine) were able to attenuate microglial pro-inflammatory activation more effectively compared to poorly steroidogenic ones (PK11195 and Ro5-4864), suggesting that the modulation of the cytokine release may be influenced by the quantity of produced neurosteroids. In particular, the pre-treatment of activated C20 cells with XBD-173 and Etifoxine counteracted the increased secretion of IL-8 following inflammatory stimuli, and besides stimulated the release of the IL-4, shifting the dynamic equilibrium of cytokine secretion by microglia toward an anti-inflammatory profile. Similar data have been previously obtained in murine microglia, where XBD-173 was reported to counteract microglia activation, by reducing the mRNA level of the pro-inflammatory IL-6, whereas PK11195 and Ro5-4864 did not affect the level of pro-inflammatory cytokines, such as TNF- $\alpha$  and IL-1 $\beta$  [267], [293], [301].

In our hands, the XBD-173-induced effects were abolished when the steroidogenic pathway was enzymatically inhibited by the use of AMG. In support, neurosteroids are widely known as the most potent endogenous molecules capable of modulating the inflammatory process exerting effects on different cell populations, including microglia [302]. Of note, it has been reported that some steroids are pro-inflammatory molecules, however, the majority of them exert anti-inflammatory effects [303]. In this complex mechanism, our results support that TSPO stimulation upregulates the whole biosynthetic pathway, leading to an overall anti-inflammatory effect. Intriguingly, the stimulation of the anti-inflammatory cytokine IL-4 release was induced by both highly and poorly steroidogenic ligands, even though with a stronger effect for the formers.

It is necessary to point that AMG pre-treatment did not completely abolish the effect induced by XBD-173 when C20 were challenged with IL-1 $\beta$ /INF- $\gamma$  stimulus, suggesting that the release of IL-8 and IL-4 may be in part influenced by additional TSPO activities. In agreement, it has been recently shown that XBD-173 treatment can modulate other mitochondrial functions, such as oxidative phosphorylation, MMP, and calcium homeostasis in murine and human microglia [252], [266]. In addition to the known ability of steroids to suppress the multiple inflammation-related genes [302], some of the effects induced by steroidogenic TSPO ligands could be explained by the neurosteroid-mediated activation of the GABA<sub>A</sub>-R. Indeed, recent works have reported that GABA<sub>A</sub>-R stimulation attenuates the release of pro-inflammatory cytokines from activated microglia [304], [305].

Moreover, in our experimental conditions, all the TSPO ligands negatively modulated another pro-inflammatory signaling parameter such as the production of ROS in activated C20 cells, in agreement with the previous data obtained in several experimental models including human macrophages [306] and murine microglia [307], reporting a protective role of TSPO against ROS-induced damage [248], [308]. Despite little is known about the mechanism by which TSPO could exert this modulatory activity on ROS production in microglia, our results suggest that this TSPO function is not related to steroidogenesis stimulation. Indeed, all TSPO ligands effectively counteracted the increased production of ROS to a similar extent, regardless of their steroidogenic capacity. The observed effect is likely due to the modulation of other mitochondrial activities in which TSPO has been proposed to be involved, such as mitochondrial respiration and calcium signaling [309]. In addition, TSPO is known to be involved in the transport of the precursor of heme (protoporphyrinogen IX), which is also an important cofactor for molecules involved in the ROS production, such as the cytochromes of the electron transport chain) and for antioxidant enzymes [310]. Recently, it has been revealed an interaction between TSPO and NOX 2 (NADPH oxidase 2) in primary murine microglia, and the

authors found that an acute burst of ROS increased TSPO levels on the surface of microglia, suggesting that ROS production may alter the subcellular distribution of TSPO [311]. To further dissect the role of TSPO during microglia activation, the release of IL-8 and IL-4 following C20 cells activation was evaluated after silencing TSPO expression. When TSPO KD C20 cells were subjected to the immunogenic stimulation, they evidenced pronounced responsiveness, showing a more marked IL-8 increase and IL-4 decrease when compared to SCR C20, in agreement with previous data documented in murine microglia [263] reporting increased susceptibility of microglia to pro-inflammatory activation if TSPO expression was reduced. Interestingly, in the absence of the insult, TSPO KD C20 evidenced a higher basal level of pro-inflammatory cytokine IL-8, and a lower basal level of IL-4 release compared to SCR cells, appearing unable to maintain the basal controlled release of pro-inflammatory and anti-inflammatory cytokines. These results suggest that TSPO may be required for the negative modulation of pro-inflammatory signaling in active microglia, supporting the hypothesis that TSPO could have a homeostatic role in maintaining the physiological balance between the release of pro- and anti-inflammatory mediators.

The TSPO function in modulating microglial activation is corroborated by the increase in TSPO level that we detected in C20 cells following IL-1 $\beta$  administration, in agreement with literature data showing an increase in TSPO expression level upon activation of microglia as well as during neuroinflammatory conditions *in vivo* [258], [312], [313]. Possibly, microglia might increase TSPO expression to ensure a controlled release of pro-inflammatory and anti-inflammatory cytokines following an activation stimulus.

Based on previous data demonstrating that the IL-1 $\beta$ -induced inflammatory pathway leads to the activation of the NF- $\kappa$ B pathway in C20 cells, we investigated the presence of this TF binding sequence in the proximal promoter of *TSPO* gene. The human *TSPO* (NCBI gene ID\_706) is located from the nucleotide position 43151514 to 43163242 on chromosome 22. Here, the analyzed sequence (1061 nucleotides) includes both the transcription starting site (TSS) reported in the NCBI site and additional TSS recently reported in various cell lines (located in a window of 40 to 50 bases downstream from the NCBI TSS) [205]. By TRAP analysis, performed by selecting “vertebrate matrices” and the “human promoter” as a background model, the affinity-based ranking of TFs showed that 30 sequences presented significantly higher binding affinity if compared with random sequences in the chosen background set. Interestingly, NF- $\kappa$ B gave the most significant result in terms of predicted binding affinity and binding sequence homology. The predicted binding sequence for NF- $\kappa$ B was localized in the promoter region that has been proposed to be involved in epigenetic

regulation of TSPO [314]. Although our *in silico* results offer a theoretical indication, further experiments to ascertain the role of NF- $\kappa$ B in the TSPO transcription regulation, are certainly encouraged. Herein, we demonstrated that the treatment with DEXA, an inhibitor of the NF- $\kappa$ B pathway, counteracted the increase in TSPO expression level in activated C20, providing the first experimental evidence in support of the hypothesis of NF- $\kappa$ B implication within TSPO expression regulation. Such effect was evident for both TSO mRNA and protein following C20 activation with IL-1 $\beta$ , whereas the administration of the IL-1 $\beta$ /INF- $\gamma$  did not induce a significant increase in TSPO levels. Even though the TSPO transcript level increased following the combined stimulus, the lack of a significant increase in TSPO protein expression could be likely related to the activation of unknown degradative and/or compensative mechanisms occurring after a pronounced microglia stimulation. In summary, based on our results, we can propose an important role for TSPO in modulating different cellular activities addressed to counteract the establishment of the pro-inflammatory phenotype of human microglia, as depicted in **Figure 9**.

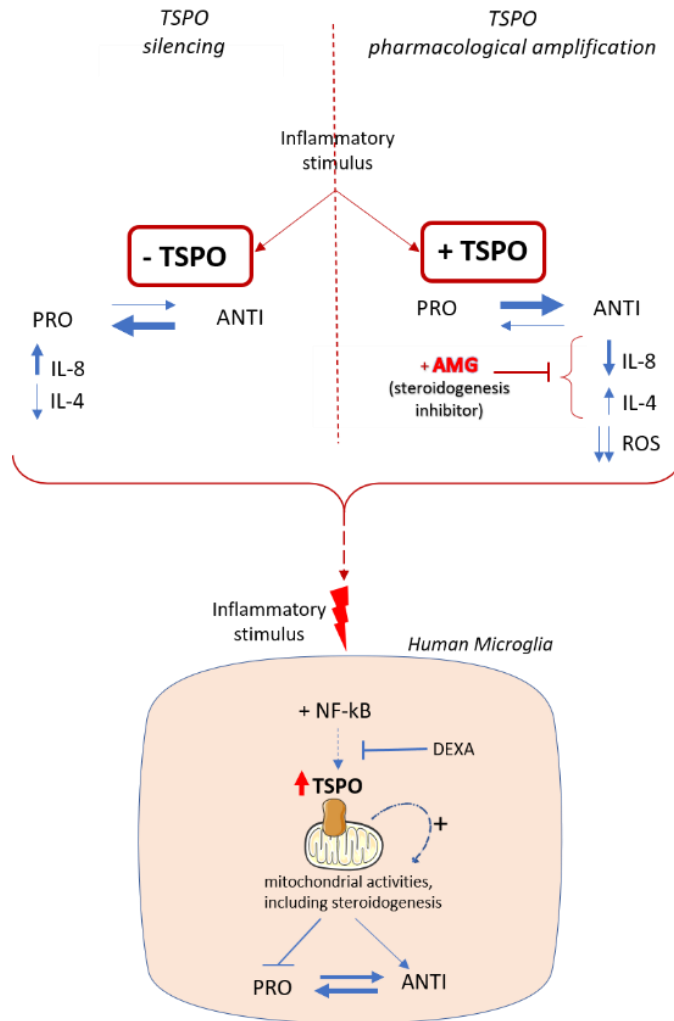


**Figure 9.** The proposed role of TSPO in orchestrating different cellular activities during activation of human microglia. Adapted from Da Pozzo E, Tremolanti C et al., *Microglial Pro-Inflammatory and Anti-Inflammatory Phenotypes Are Modulated by Translocator Protein Activation*, *IJMS* 2019 [288].

# Beneficial effects of PIGA1138 TSPO ligand against disease symptoms and severity in EAE model of primary progressive MS

### Preliminary remarks

The EAE-mice treatment with TSPO ligands PIGA1138 and PIGA839 at the dose of 15 mg/kg had the best outcome if compared with the different concentrations (from 5 to 30 mg/kg) used for the experiments. In particular, *in vivo* data previously collected demonstrated that the treatment with PIGAs (15 mg/kg) lead to the amelioration of motor performance, reduction of clinical symptoms, and body weight loss in EAE mice (**Tremolanti et al., *Molecular Biology* 2022**) [315].

## Results

---

### 3.3.1 Effect of PIGA1138 and PIGA839 on MBP expression in spinal cord and brain structures

As MBP is considered a primary target of auto-reactive T cells in MS and EAE [73], [124], its expression level is a major marker to assess the degree of myelination [316]. Therefore, in order to explore the effect of PIGA1138 and PIGA839 against EAE-induced demyelination, we explored the level of MBP by immunofluorescence in the white matter of the lumbar spinal cord (**Figure 1**) and the brain (**Figure 2**). In particular, we analyzed the *cerebellum* (Cer), the *corpus callosum* (CC), and the *cortex* (CTX), three brain structures known to be strongly myelinated in normal brain. The evaluation of the immunofluorescent signal evidenced dense and deeply stained MBP in both the spinal cord white matter (**1A, 1E**), and in Cer, CC and CTX (**2A-C**) of non-immunized healthy animals. By contrast, MBP immunofluorescent labeling was strongly reduced in the spinal cord (**1B, 1F**) and in the brain (**2D-F**) of vehicle-treated EAE mice. Interestingly, representative images of PIGA1138 (15 mg/kg) -treated EAE mice showed that the treatment counteracted the EAE-induced MBP labeling reduction both in the spinal cord (**1C, 1G**) and in the brain (**2G-I**). In particular, we detected a robust effect in the Cer, where the reduction in MBP immunolabeling in vehicle-treated EAE mice was particularly marked. On the other hand, PIGA839 (15 mg/kg) treatment did not show

any significant result in the restoration of MBP immunofluorescent signal in the spinal cord (**1D, 6H**) and in the brain (**2J-L**) compared to vehicle-treated. Qualitative observations were confirmed by quantitative analysis of the MBP immunofluorescent signal, in the spinal cord white matter (**1I**) and in brain structures (**2M-O**). Noteworthy, no significant differences were observed between healthy control and PIGA1138-treated EAE mice groups, indicating that PIGA1138 (15 mg/kg) treatment was effective in preventing demyelination in EAE-evoked MBP loss.

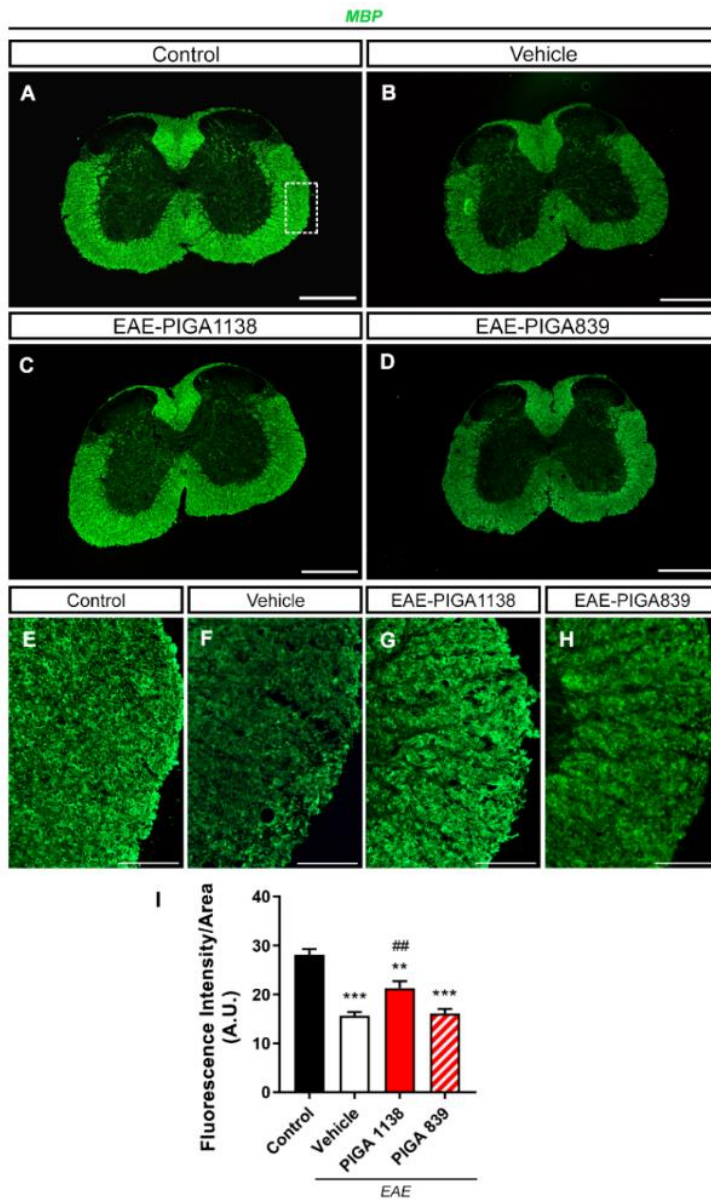


**Figure 1. MBP expression in the lumbar spinal cord.** Distribution of MBP-immunostaining in the spinal cord of non-immunized control animals (**A**) or EAE mice treated with the vehicle (**B**), PIGA1138 at 15 mg/kg (**C**) or PIGA839 at 15 mg/kg (**D**). Scale bar = 500  $\mu$ m. Distribution of MBP immunostaining in the right lateral zone (white rectangle) of the spinal cord of non-immunized control animals (**E**) or EAE mice treated with the vehicle (**F**), PIGA1138 at 15 mg/kg (**G**), or PIGA839 at 15 mg/kg (**H**). The sections were labeled with a rabbit anti-MBP revealed with an Alexa Fluor® 488-conjugated donkey anti-rabbit. Scale bar = 100  $\mu$ m. **I**: MBP immunostaining quantification. Each bar

*represents the mean fluorescence intensity (+ SEM) normalized over the region of interest and expressed in Arbitrary Unit (A.U.). The sections were dissected from non-immunized control animals (n=3) and from EAE mice treated with the vehicle, PIGA1138 (15mg/kg) or PIGA839 (15 mg/kg) (n=4/group). \*\*\*p < 0.001, \*\*p < 0.01 compared to the control; ##p < 0.01 compared to the EAE-vehicle calculated using one-way ANOVA followed by Tukey's post-test. Taken from Tremolanti C et al., Translocator Protein Ligand PIGA1138 Reduces Disease Symptoms and Severity in Experimental Autoimmune Encephalomyelitis Model of Primary Progressive Multiple Sclerosis, Mol Neurobiol 2022 [315].*

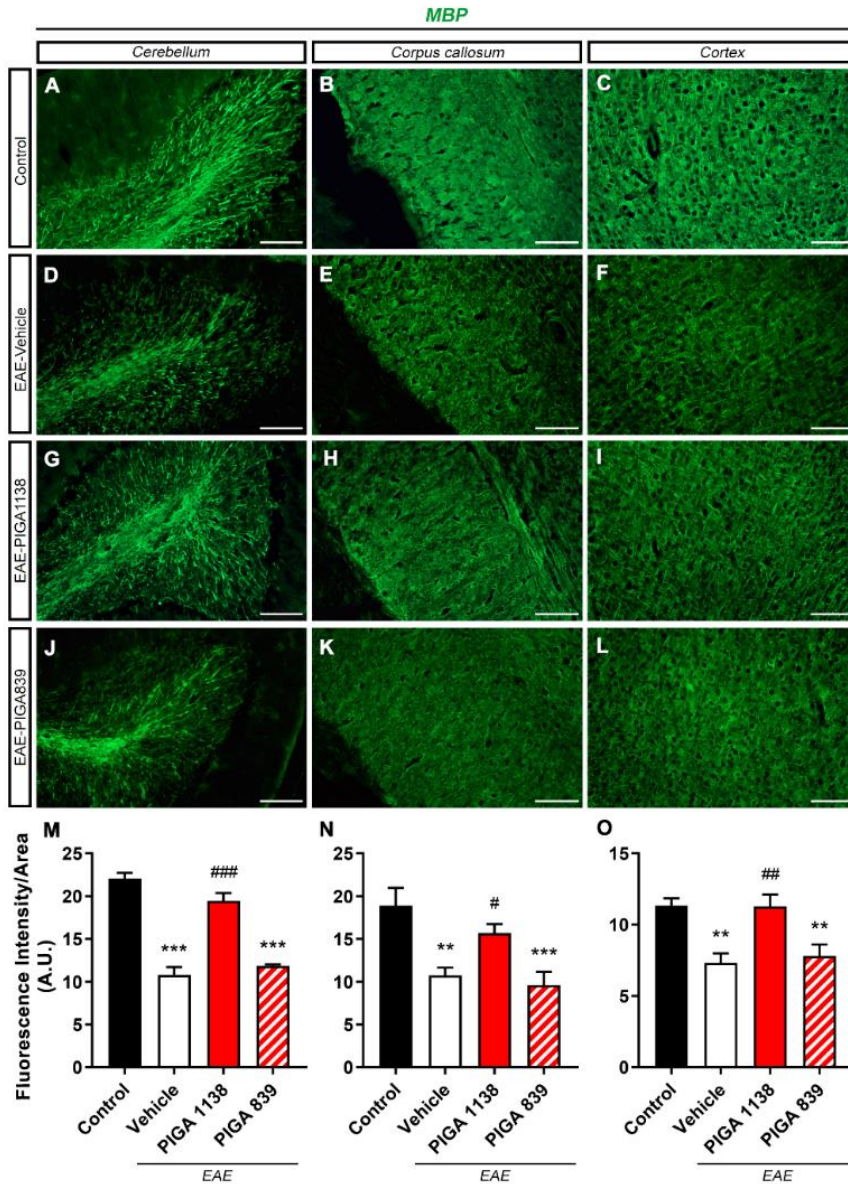


**Figure 2. MBP expression in brain structures.** Distribution of MBP-immunostaining in the cerebellum, CC, and CTX of non-immunized control animals (A-C), and EAE mice treated with the vehicle (D-F), PIGA1138 at 15 mg/kg (G-I) or PIGA839 at 15 mg/kg (J-L). The sections were labeled with a polyclonal rabbit anti-MBP revealed with an Alexa Fluor® 488-conjugated donkey anti-rabbit. Scale bar = 100  $\mu$ m. MBP immunostaining quantification in the cerebellum (M), CC (N), and CTX (O). Each bar represents the mean fluorescence intensity signal (+ SEM) normalized over the area of interest and expressed in Arbitrary Unit (A.U.). The sections were dissected from non-immunized control animals (n=3) and from EAE mice treated with the vehicle, PIGA1138 (15 mg/kg) or PIGA839

(15 mg/kg) (n=4/group). \*\*\* $p < 0.001$ , \*\* $p < 0.01$  compared to the control; ### $p < 0.001$ , ## $p < 0.01$ , # $p < 0.05$  compared to the EAE-vehicle calculated using one-way ANOVA followed by Tukey's post-test. Taken from Tremolanti C et al., *Translocator Protein Ligand PIGA1138 Reduces Disease Symptoms and Severity in Experimental Autoimmune Encephalomyelitis Model of Primary Progressive Multiple Sclerosis*, *Mol Neurobiol* 2022 [315].

### 3.3.2 Effect of PIGA1138 and PIGA839 on NF200 expression in spinal cord and cerebellum

Together with demyelination, axonal suffering is another hallmark of MS, in particular for the PPMS [317]. Neurofilaments (NFs) are part of the mature neuronal cytoskeleton, providing regulating axonal diameter and providing structural support for the axons [318]. Since axonal injury can be detected by NF200-loss, we explored the effect of PIGAs TSPO ligands against axonal damage in EAE mice analyzing NF200 levels by immunofluorescence staining in the ventral horn of the lumbar spinal cord (**Figure 3**) to assess the status of motor neurons. In addition, we investigated NF200 expression level in the Cer (**3F-J**), which regulates motor functions including coordination and equilibrium that are usually impaired in EAE pathology [319]. Immunolabeling studies showed a considerable reduction in NF200 signal density both in the spinal cord (**3B**) and in the Cer (**3G**) of vehicle-treated EAE mice, compared to healthy controls (**3A, 3F**). In the spinal cord, NF200 reduction was significantly prevented by both PIGA1138 and PIGA839 treatment (**3C, 3D**), as evidenced by the quantitative analysis of NF200 immunofluorescence signal (**3E**). However, in the Cer, only the PIGA1138 showed a protective effect against EAE-induced axonal loss (**3H**). Interestingly, no statistically significant differences were observed between the control mice and PIGA1138 (15 mg/kg) -treated EAE mice, suggesting that PIGA1138 TSPO ligand prevented NF200 loss and therefore axonal damage.

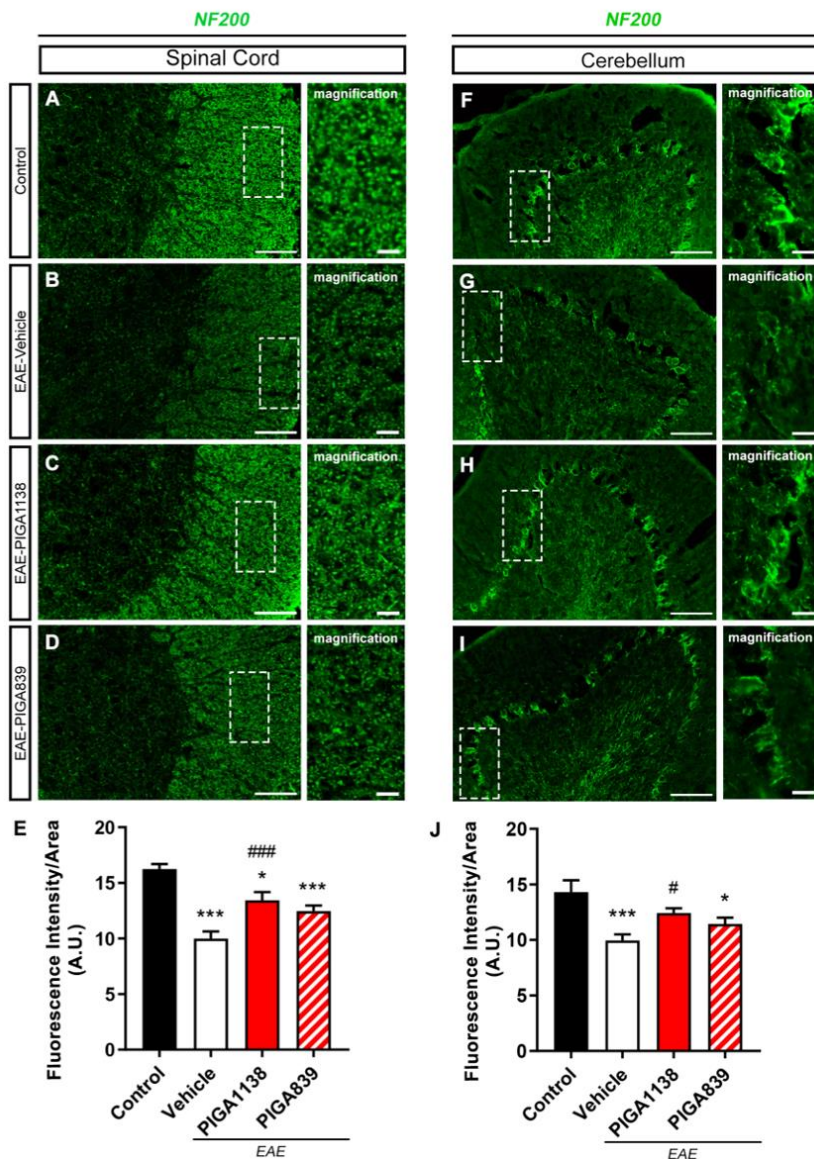


**Figure 3.** NF200 expression in lumbar spinal cord and cerebellum. Distribution of NF200-immunostaining in the spinal cord and the cerebellum of non-immunized control animals (3A, 3F) or EAE mice treated with the vehicle (3B, 3G), PIGA1138 at 15 mg/kg (3C, 3H) or PIGA839 at 15 mg/kg (3D, 3I). Scale bar = 100  $\mu\text{m}$ ; magnification scale bar = 20  $\mu\text{m}$ . The sections were labeled with a rabbit anti-NF200 revealed with an Alexa Fluor® 488-conjugated donkey anti-rabbit. 3E, 3J: NF200 immunostaining quantification in the spinal cord and the cerebellum. Each bar represents the mean fluorescence intensity signal (+SEM) normalized over the area of interest and expressed in Arbitrary Unit (A.U.). The sections were dissected from non-immunized control animals (n=3) and from EAE

mice treated with the vehicle, PIGA1138 (15 mg/kg) or PIGA839 (15 mg/kg) (n=4/group). \*\*\* $p < 0.001$ , \* $p < 0.05$  compared to the control; # $p < 0.05$ , ### $p < 0.001$  compared to the EAE vehicle calculated using one-way ANOVA followed by Tukey's post-test. Taken from Tremolanti C et al., *Translocator Protein Ligand PIGA1138 Reduces Disease Symptoms and Severity in Experimental Autoimmune Encephalomyelitis Model of Primary Progressive Multiple Sclerosis*, *Mol Neurobiol* 2022 [315]

### 3.3.3 Effect of PIGA1138 and PIGA839 on immune cells infiltration in spinal cord

A major contribution in the development and progression of MS and EAE is given by the infiltration of peripheral immune cells into the CNS [124], [320]. Inflammatory lesions in the brain and the spinal cord are characterized by the infiltration of lymphocytes, granulocytes, monocytes, and macrophages, which express the leukocyte's common antigen CD45 [321]. Therefore, we employed a specific antibody anti-CD45 to identify their presence in the spinal cord of EAE mice (**Figure 4**). No significant immunofluorescent signal was detected in non-immunized control mice (**4A**), whereas a substantially higher number of CD45-positive (CD45+) cells was found in vehicle-treated EAE mice (**4B**). Interestingly, the number of CD45+ cells in the spinal cord of PIGA1138- (**4C**) and PIGA839-treated (**4D**) EAE mice was reduced by 50% or 25% respectively, compared to vehicle-treated.

These observations prompted us to investigate the possible correlation between the immune cell infiltration and the demyelinated lesions that we observed in the spinal cord by the use of MBP immunostaining. To this aim, we performed a double-staining of MBP (green) and CD45 (red) in mice spinal cords (**Figure 5**). Interestingly, our study demonstrated that the majority of infiltrated CD45+ immune cells were precisely localized in the areas of the spinal cord that exhibited also a strong MBP expression reduction, particularly in vehicle-treated EAE mice (**5C**). CD45+ cell infiltrates in the demyelinated areas of PIGA1138- and PIGA839-treated EAE mice (**5F**, **5H**) were reduced when compared to vehicle-treated EAE mice, accordingly to the higher preservation of MBP immunolabeling in the same areas.

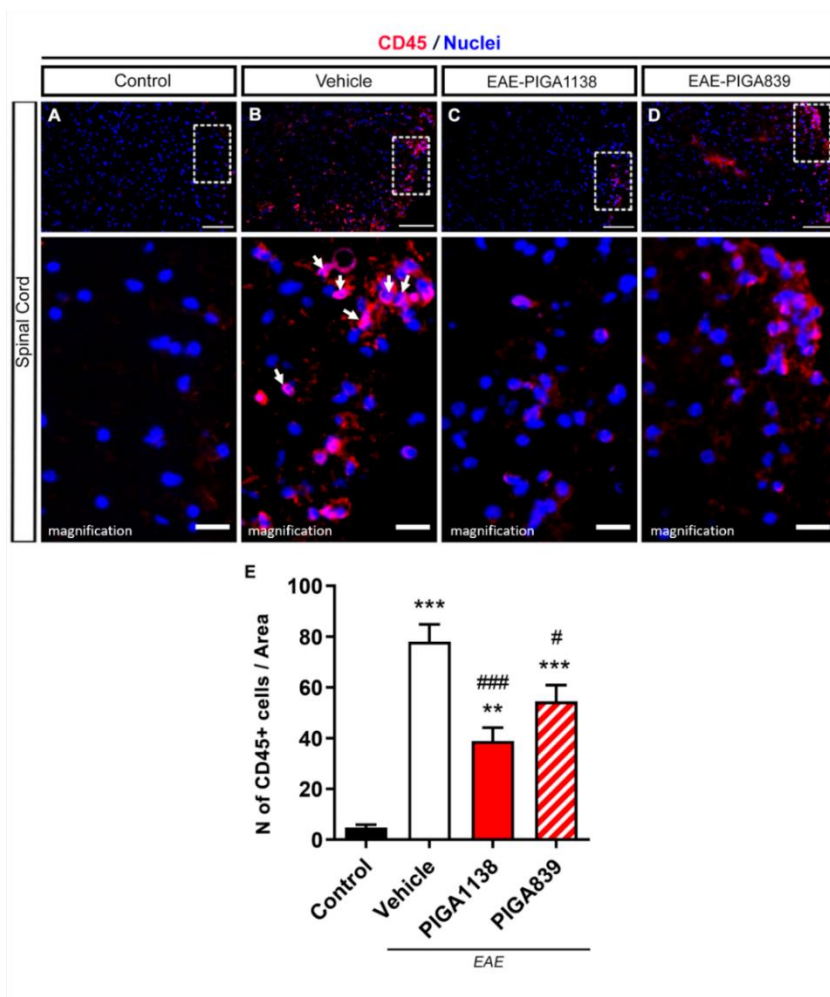


**Figure 4. CD45+ cells quantification in the lumbar spinal cord.** Localization of CD45 (red) and nuclei (blue) fluorescent staining in the spinal cord of non-immunized control animals (A) or EAE mice treated with the vehicle (B), PIGA1138 at 15 mg/kg (C), or PIGA839 at 15 mg/kg (D). Scale bar = 100  $\mu$ m; magnification scale bar = 30  $\mu$ m. Arrowheads in B magnification picture indicate part of the total number of CD45+ cells. The sections were labeled with a goat anti-CD45 and revealed with an Alexa Fluor® 555-conjugated donkey anti-goat. Nuclei were stained with DAPI. **E:** CD45+ cell quantification. Each bar represents the number of CD45+ cells (+ SEM) counted in the region of interest (n=4/group). \*\*\* $p$  < 0.001, \*\* $p$  < 0.01 compared to the control; ### $p$  < 0.001, # $p$  < 0.05 compared to the EAE-vehicle calculated using one-way ANOVA followed by Tukey's post-test. Taken from Tremolanti C et al., Translocator Protein Ligand PIGA1138 Reduces Disease Symptoms and Severity in Experimental Autoimmune Encephalomyelitis Model of Primary Progressive Multiple Sclerosis, *Mol Neurobiol* 2022 [315].

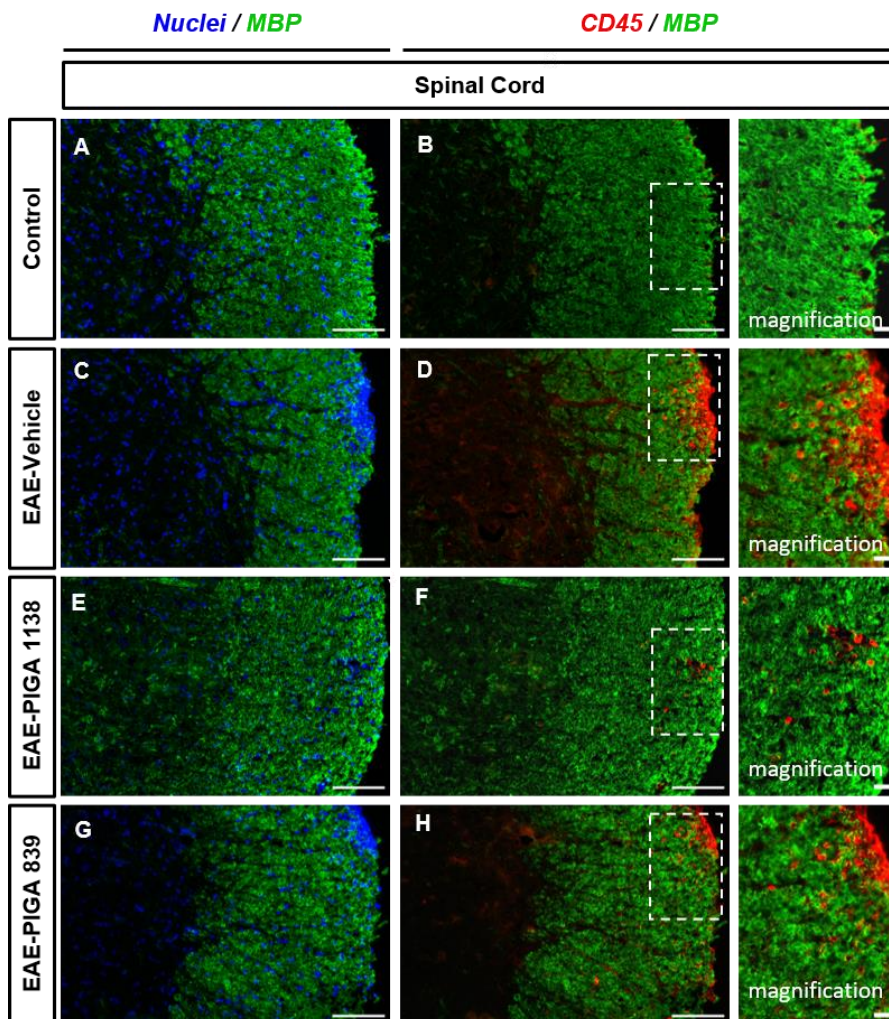


**Figure 5. MBP and CD45 localization in the lumbar spinal cord.** On the left panel, localization of MBP (green) and nuclei (blue) staining in the spinal cord of non-immunized control animals (A) or EAE mice treated with the vehicle (C), PIGA1138 at 15 mg/kg (E) or PIGA839 at 15 mg/kg (G). Scale bar = 100  $\mu$ m. On the right panel, localization of MBP (green) and CD45 (red) in the spinal cord of non-immunized control animals (B) or EAE mice treated with the vehicle (D), PIGA1138 at 15 mg/kg (F), or PIGA839 at 15 mg/kg (H). Scale bar = 100  $\mu$ m, magnification scale bar = 20  $\mu$ m. Nuclei were stained with DAPI. The sections were co-stained with a rabbit anti-MBP revealed with an Alexa Fluor® 488-conjugated donkey anti-rabbit, together with a goat anti-CD45 revealed with an Alexa Fluor® 555-conjugated donkey anti-goat. Taken from Tremolanti C et al., Translocator Protein

### 3.3.4 Effect of PIGA1138 and PIGA839 on IL-10 concentration in serum

As IL-10 represents a critical anti-inflammatory cytokine secreted by Th2 lymphocytes, and it has been demonstrated to be involved in the attenuation of the EAE-induced immune responses [322] we quantified the level of IL-10 in the serum of mice by flow-cytometry. Our results showed that PIGA1138-treated EAE mice presented an increased level of IL-10 in the serum compared to vehicle-treated EAE mice (mean values  $918,8 \text{ pg/mL} \pm 244,2$  vs  $147,1 \text{ pg/mL} \pm 38,75$ ;  $p = 0,0056$ ).

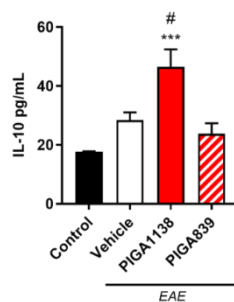


**Figure 6. IL-10 quantification in serum.** ELISA-based quantification of IL-10 level in serum of non-immunized control animals, vehicle-, PIGA1138- (15 mg/kg) and PIGA839- (15 mg/kg) - treated EAE mice. Each bar represents the mean (+ SEM) of IL-10 level expressed in pg/mL ( $n=4$ /group). \*\*\* $p < 0.001$  compared to the control; # $p < 0.05$  compared to the EAE-vehicle calculated using Klustall-Wallis test followed by Mann-Whitney U test. Taken from Tremolanti C et al., *Translocator Protein Ligand PIGA1138 Reduces Disease Symptoms and Severity in Experimental Autoimmune Encephalomyelitis Model of Primary Progressive Multiple Sclerosis, Mol Neurobiol 2022 [315].*

### 3.3.5 Effect of PIGA1138 and PIGA839 on ALLO concentration in spinal cord

It has been demonstrated that PIGA1138 and PIGA839 possess high neurosteroidogenic capacity in a series of *in vitro* experimental models [226], [323] and we supposed that this capacity could be involved in the beneficial effects exerted by PIGAs in treated EAE mice. To explore the potential mechanism underlying the effects observed in EAE mice treated with PIGAs, we measured the

concentration of ALLO in the spinal cord of healthy controls, and EAE mice treated with the vehicle or the PIGAs (**Figure 7**), as ALLO has shown neuroprotective effects in experimental models of MS [274], [324]. The results of Liquid Chromatography/High-Resolution Mass Spectrometry (LC/HR-MS) analysis evidenced an important reduction in ALLO level in the spinal cord of vehicle-treated EAE mice compared to controls. Interestingly, PIGA1138 treatment (15 mg/kg) was able to significantly restore ALLO levels in the spinal cord of EAE-mice. On the contrary, PIGA839 treatment showed no restoration in the neurosteroid production.

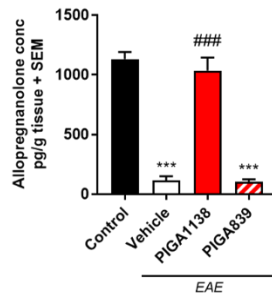


**Figure 7. Allopregnanolone quantification in the spinal cord.** LC/HR-MS-based quantification of ALLO concentration in the spinal cord of non-immunized control animals, vehicle-, PIGA1138- (15 mg/kg) and PIGA839- (15 mg/kg)-treated EAE mice. Each bar represents the mean (+ SEM) of ALLO concentration expressed in pg/g tissue ( $n=3/\text{group}$ ). \*\*\* $p < 0.001$  compared to the control; ### $p < 0.001$  compared to the EAE-vehicle, calculated using ANOVA followed by Tukey's multiple comparisons test. Taken from Tremolanti C et al., Translocator Protein Ligand PIGA1138 Reduces Disease Symptoms and Severity in Experimental Autoimmune Encephalomyelitis Model of Primary Progressive Multiple Sclerosis, *Mol Neurobiol* 2022 [315]

## Discussion

---

The development of new neuroprotective and anti-inflammatory treatments against MS is challenging. In particular, no cure exists to date for the progressive form of MS (PPMS), characterized by axonal damage and chronic neuroinflammation leading to irreversible neurological deficits [159].

Previous *in vivo* results obtained by our Laboratory showed that the pre-treatment with the TSPO ligand PIGA839 (15 mg/kg) on the EAE mice model of PPMS was able to delay the onset of the pathology, whereas the pre-treatment of PIGA1138 (15 mg/kg) was able to reduce the severity of clinical symptoms as well to delay the onset of the pathology. Importantly, PIGA1138 was also capable of reducing the weight lost on EAE mice and ameliorating the normal value of the maximum contact area parameter (Catwalk index) whose decrease lead to severe motor dysfunctions.

In the present thesis, we investigated *ex vivo* the effect of PIGA839 and PIGA1138 on several markers of the PPMS pathology such as demyelination, axonal damage, immune cells infiltration, and systemic cytokine levels. Moreover, as TSPO ligands are widely known to promote neurosteroidogenesis, the level of the neurosteroid ALLO was determined in the spinal cord, to shed light on the mechanism of action of the compound.

Our results demonstrated that PIGA1138 (15 mg/kg) administration counteracted the EAE-induced demyelination by preserving the expression of MBP in the spinal cord and brain of EAE-mice. Indeed, as MBP represents a primary target of auto-reactive T cells in MS and EAE, the reduction of its level is accepted to reflect the degree of demyelination [316]. Interestingly, a strong expression of MBP was found in the Cer of PIGA1138-treated EAE mice compared to vehicle-treated, which were characterized by severe demyelination, suggesting that the beneficial effect exerted by the compound may be proportional to the severity of EAE attacks. In addition, PIGA1138 also exerted a considerable effect against EAE-induced axonal damage, as no significant differences in the expression level of the axonal marker NF200 were detected in spinal and cerebellar axons between the healthy controls and PIGA1138-treated EAE mice. Because NF200 is a crucial protein for neuronal cytoskeleton organization and determines the proper axonal structure and functions [318], [325] our results indicate that PIGA1138 may possess neuroprotective properties.

In our study, we also demonstrated that PIGA1138 treatment significantly reduced immune cells (CD45 positive) infiltration in the spinal cord of EAE mice compared to vehicle, in line with our results regarding the reduction in other signs of the pathology. Indeed, immune cells are known to be primarily responsible for the establishment of chronic neuroinflammation, white matter lesions, and

thus disease progression [156]. Our results suggest that PIGA1138 may attenuate inflammatory mechanisms involved in the pathogenesis of myelin disorders, and might possess an anti-inflammatory action, in agreement with previous works reporting the beneficial effect of the administration of several TSPO ligands on several *in vitro* and *in vivo* experimental models of neuroinflammation and neurodegeneration [122], [321], [326]. In support, our data evidenced that PIGA1138 treatment markedly induced the production of the anti-inflammatory cytokine IL-10, which has been shown to have a strong inhibitory effect against EAE-evoked immune response [322]. In particular, IL-10-KO mice were demonstrated to develop a more severe form of EAE pathology if compared to WT [327].

In our experimental conditions, the effect of two different PIGA TSPO ligands was explored. Although PIGA1138 was shown able to promote beneficial effects against EAE disease in mice, PIGA839 exerted only partial effect if compared to vehicle-treated EAE mice. Such differences between the two PIGAs effects are not immediately explainable because the precise mechanisms of TSPO ligand action underlying their proven beneficial effects are not fully clarified yet, due to the functional complexity of this protein. However, our experiment using the LC/HR-MS method for the quantification of neuroactive steroids in tissue demonstrated that PIGA1138 treatment induced a significant increase in the ALLO production in the spinal cord of EAE mice, while PIGA839 did not enhance neurosteroidogenesis *in vivo*. Previous studies demonstrate that both ligands have long RT at TSPO, thus possess a high steroidogenic capacity *in vitro*, the RT of PIGA1138 is  $144 \pm 4$  minutes, while the RT of PIGA839 is  $109 \pm 4$  min [224]. Despite the difference in their RT and steroidogenic efficacy *in vitro* is not meaningfully pronounced, it appears sufficient to determine significant differences in their ability to maintain an effective neurosteroidogenic activity *in vivo* during chronic administration. Noteworthy, PIGA839 exhibited a substantial steroidogenic activity in glioma C6 cells *in vitro* [226], and exerted anxiolytic effects on rodents [328]. In our conditions, the lower steroidogenic efficacy of PIGA839 may fail to achieve the required levels of specific neurosteroids to exert a protective effect against EAE pathology.

Despite our result regarding the increase in the ALLO level in the spinal cord shed some light on the mechanism by which PIGA1138 ameliorates clinical and pathological parameters in the EAE model of PPMS, it is not sufficient to state that the induction of neurosteroidogenesis represents the major mechanism involved in the observed beneficial effect. In support of the positive effect of high ALLO level in the spinal cord, it has been demonstrated that the intrathecal injection of an inhibitor of  $3\alpha$ -hydroxysteroid oxidoreductase ( $3\alpha$ -HSOR), converting  $3\alpha,5\alpha$ -reduced neurosteroids to ALLO

(3 $\alpha$ ,5 $\alpha$ -THP) decreased thermal and mechanical nociceptive thresholds in naive rats, whereas direct ALLO administration increased pain sensitivity thresholds [329]. On this line, to corroborate our idea that local stimulation of ALLO production is fundamental in the PIGA1138 effect of recovery EAE mice from pathology, additional experiments would be helpful to provide confirmations. In particular, the administration of PIGA1138 together with direct injection of an inhibitor of ALLO synthesis in the spinal cord might provide crucial information to reveal if the induction of ALLO synthesis in the spinal cord is a major determinant in the beneficial effect exerted by PIGA1138. We support the hypothesis that an enhanced production of ALLO induced by PIGA1138 in glial and/or neuronal cells may regulate the expression of various genes involved in myelin formation and axonal repair to contribute to the beneficial/protective effects observed in MOG-EAE mice. Concordantly, it has been demonstrated that ALLO can interact with GABAA-R to stimulate MBP expression and CNS myelination [330].

Moreover, in agreement with this idea, previous reports have shown that the long RT TSPO ligand XBD-173 enhanced the production of the neuroprotective neurosteroid ALLO to ameliorate the clinical symptoms and neuropathological markers of PLP-EAE mice that mimic the human RRMS [268], whereas it failed in rescuing MOG-EAE mice mimicking human PPMS from the pathology [269], although inducing neurosteroidogenesis.

However, TSPO is known to modulate different cellular functions also through its dynamic interaction with different mitochondrial proteins. In particular, besides steroidogenesis/neurosteroidogenesis, it is involved in the regulation of mPTP activity, intracellular calcium levels, oxidative stress balance, and ATP production. Therefore, the overall beneficial effect triggered by TSPO ligands probably depends not only on one function. No one can rule out the possibility that PIGA1138 may also affect the modulatory activity of TSPO on other mitochondrial processes such as the balance of oxidative stress whose dysregulation has often been associated with neurodegenerative and neurological diseases, including MS [240]. In support, oxidative stress is known to play a critical role in the pathogenesis and development of MS [331], and several reports have shown the ability of TSPO ligands to reduce ROS production of and counteract oxidative stress in cellular models of neuroinflammation and neurodegeneration [288], [332].

For these reasons, it cannot be excluded that the global protective effect observed for PIGA1138-treated EAE mice may be the result of the modulation of various mitochondrial mechanisms. Future cellular investigations will certainly help to decipher all intracellular events underlying specific

cellular responses following the interaction of PIGA1138 with TSPO to improve the neurological symptoms and neuropathological parameters in EAE mice.

In conclusion, the diverse and complementary approaches combined in this work allowed us to affirm that PIGA1138 may represent an effective compound to prevent or tackle MOG-EAE disease in mice. Moreover, our results allowed us to draw attention to the fact that the exploration of PIGA compound-based treatments may offer promising opportunities for the development of effective therapeutic strategies against PPMS.

### Investigation of TSPO function during OLs differentiation

#### Results

---

##### 3.4.1 HOG Cell Differentiation protocol set up

In order to study the differentiation of OPCs in mature OLs, we first set up an *in vitro* differentiation (DIV) protocol of the HOG oligodendroglial cell line, adapted from what was previously reported [333] (**Figure 1A**). HOG morphology was observed after culturing cells with a differentiation medium (DM) for 9 days. The F-actin immunofluorescence staining evidenced little but visible differences between undifferentiated cells at day 1 and differentiated HOG (dHOG) at day 9, such as a higher number of branches and short membrane extensions in dHOG (**1B**). In addition, the expression of differentiation markers was monitored over time by evaluating mRNA and protein levels at day 4, 7, and 9 (**Figure 2**). In particular, we investigated the expression of MBP and CNPase, well-known myelination markers, expressed in pre-myelinating OLs and in myelinating OLs. We found both mRNA (**2A**) and protein levels (**2C, 2D**) strongly increased over time, presenting at day 9 the highest level of expression.

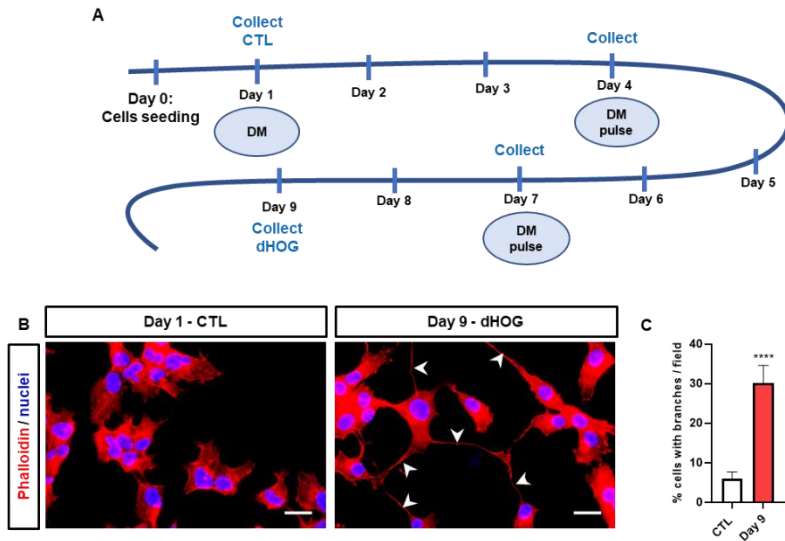


**Figure 1. Differentiation protocol set up.** (A) Schematic representation of the experimental steps of HOG cells DIV. HOG were incubated with DM starting from day 1 and cultured for 9 days. DM was replaced at day 4 and at day 7. Undifferentiated control cells (CTL) were collected at day 1. (B) Representative microscopy images of CTL and dHOG following phalloidin (red) and nuclei staining (blue). White arrowheads indicate cellular branches. Scale bar = 20  $\mu$ m. (C) Quantification of the number of cells that extended branches, calculated by manual counting. Cellular membrane extensions longer than 10  $\mu$ m were considered as branches.

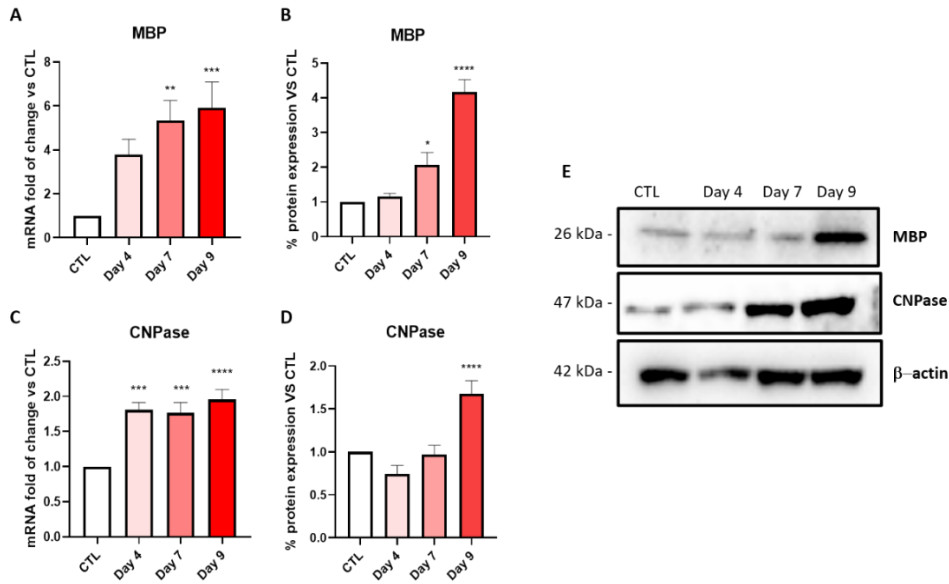


**Figure 2. Differentiation markers evaluation in dHOG.** mRNA levels of MBP (A) and CNPase (C) differentiation markers at day 4, 7, and 9 of DIV. Each bar represents the mean  $\pm$  SEM of four independent experiments performed in duplicate. (E) Protein expression of MBP and CNPase compared to the reference gene  $\beta$ -actin at day 4, 7, and 9 of DIV, and densitometric analysis of bands (B, D). Each bar represents the mean  $\pm$  SEM of three independent experiments performed in duplicate. \* $p \leq 0.1$ ; \*\* $p \leq 0.01$ ; \*\*\* $p \leq 0.001$  compared to the undifferentiated control (CTL), calculated using one-way ANOVA followed by Dunnett's multiple comparisons test.

It is well known that *de novo* cholesterol synthesis by OLS represents one of the major requirements for myelin synthesis [334]. In line with this, we investigated during HOG differentiation the changes in the expression of two enzymes involved in the cholesterol synthesis pathway. The mRNA levels of the 3-hydroxy-3-methylglutaryl-CoA reductase (HMGCR) and the farnesyl-diphosphate farnesyltransferase-1 (Fdft-1) genes were evaluated at day 4, 7, and 9, and compared to undifferentiated cells. We found both HMGCR and Fdft-1 mRNA transcript levels significantly increased during differentiation, especially at day 9 (Figure 3B, 3C). Next, we quantified the intracellular cholesterol in dHOG by Filipin III staining, and we detected a strong increase in cholesterol levels in dHOG. In addition, cholesterol distribution was different compared to undifferentiated cells (3A).

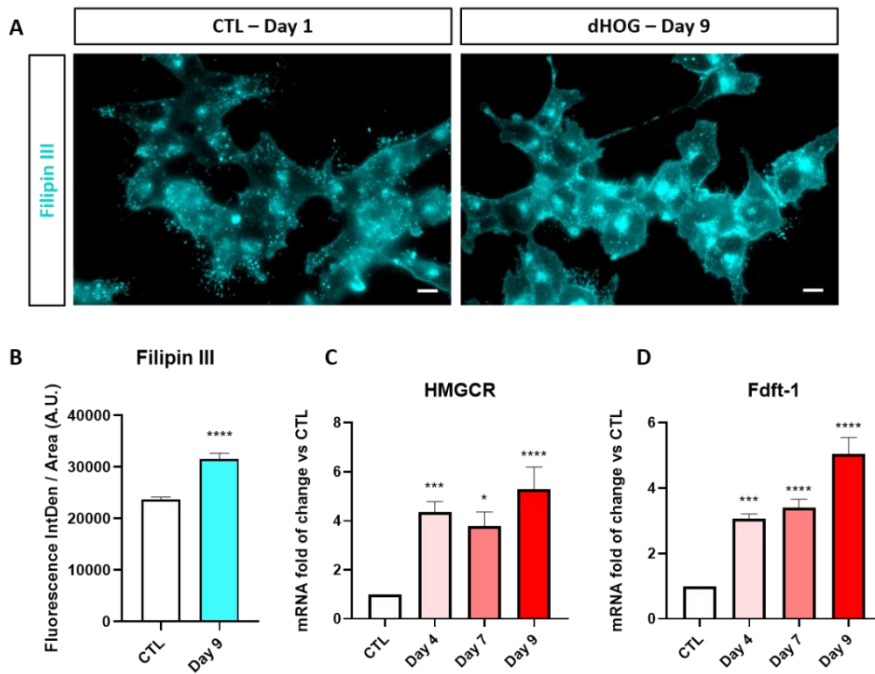


**Figure 3. Cholesterol intracellular level and expression of cholesterol synthesis enzymes during HOG differentiation.**

(A) Representative microscopy images of Filipin III staining (cyan) distribution in HOG cells at day 9 of DIV compared to control cells (CTL). Scale bar: 10  $\mu$ m. (B) Fluorescence intensity quantification. Each bar represents the mean fluorescence intensity signal ( $\pm$  SEM) normalized over the area of interest and expressed in Arbitrary Unit (A.U.) of two independent experiments performed in duplicate. mRNA levels of HMGR (C) and Fdft-1 (D) enzymes at day 4, 7, and 9 of DIV. Each bar represents the mean  $\pm$  SEM of three independent experiments performed in duplicate. \* $p \leq 0.1$ ; \*\*\* $p \leq 0.001$ ; \*\*\*\* $p \leq 0.0001$  compared to the control (CTL), calculated using one-way ANOVA followed by student *t*-test (B) or Dunnett's multiple comparisons test (B, C).

### 3.4.2 Investigation of TSPO expression and steroidogenic machinery components during HOG differentiation

TSPO has been recognized as a critical regulator of steroids synthesis, as is known to translocate cholesterol from the cytosol to the mitochondria [242]. Therefore, as we observed an increase in intracellular cholesterol level in dHOG, we investigated TSPO expression during HOG differentiation, by analyzing mRNA and protein levels at day 4, 7, and 9 of DIV. Interestingly, our results showed that TSPO mRNA and protein expression started to increase from day 7 of DIV, reaching the highest level of expression at day 9, in line with MBP and CNPase expression (**Figure 4A, 4B, 4C**). In addition, an immunofluorescence staining was performed for TSPO and nuclei, and TSPO expression was detected mainly in the perinuclear region (**4D**). The quantification of the fluorescent intensity signal further demonstrated the increase in TSPO expression level in dHOG compared to undifferentiated control cells (**4E**).

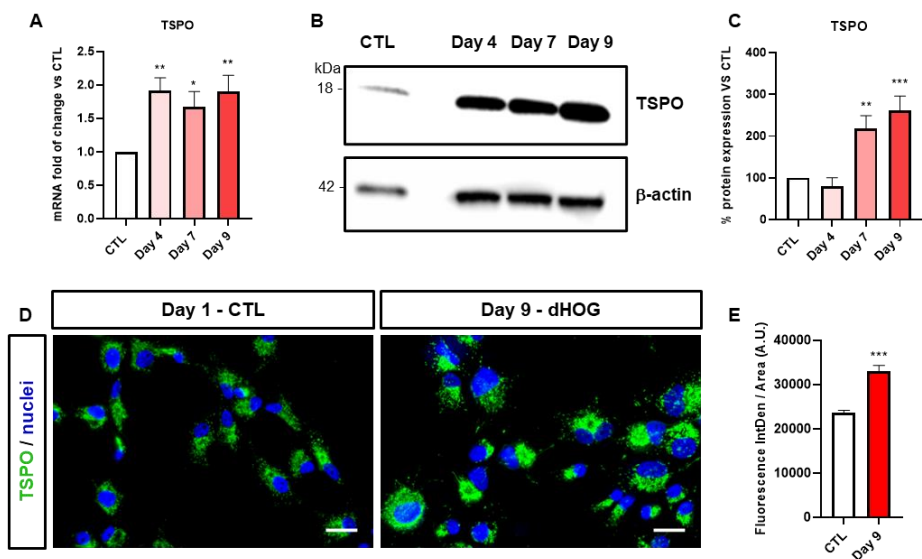


**Figure 4. TSPO expression in dHOG.** *TSPO mRNA (A) and protein (B) expression at quantification at day 4, 7, and 9 of DIV. (C) Protein expression level quantification of TSPO compared to the reference gene  $\beta$ -actin during differentiation. Each bar represents the mean  $\pm$  SEM of three independent experiments performed in duplicate. \* $p \leq 0.1$ ; \*\* $p \leq 0.01$ ; \*\*\* $p \leq 0.001$  compared to the control (CTL), calculated using one-way ANOVA followed by Tukey's multiple comparisons test. (D)*

*Representative microscopy images of TSPO immunostaining distribution (green) and nuclei (blue) in dHOG and CTL cells. Scale bar: 10  $\mu$ m. (E) Fluorescence intensity quantification. Each bar represents the mean fluorescence intensity signal ( $\pm$  SEM) normalized over the area of interest and expressed in Arbitrary Unit (A.U.) of two independent experiments performed in duplicate.*

Next, we sought to investigate other well-known components of the steroidogenic machinery such as the steroid acute regulatory protein (StAR), which aids in the translocation of cholesterol to the IMM, and the cholesterol-side cleavage enzyme CYP11A1, which converts cholesterol into pregnenolone (PREG), the first precursor of all steroids [208]. Interestingly, during HOG differentiation, CYP11A1 mRNA level was found notably increased starting from day 4 (**Figure 5C**). Moreover, both StAR and CYP11A1 protein expression significantly increased in dHOG (**5A, 5B, 5D**), suggesting a possible induction of neurosteroidogenesis in dHOG. Therefore, we use ELISA assay to investigate PREG production in HOG at day 9, by inhibiting PREG conversion to its metabolites using trilostane, which inhibits the 3-hydroxysteroid dehydrogenase ( $3\beta$ -HSD) enzyme, converting PREG to progesterone, and SU-10603, which inhibits the 17-hydroxylase (P450c17 or CYP17A1), converting PREG into DHEA (**5E**). Cells were treated for 2 h with the selective TSPO ligand PIGA1138 at the concentration of 40  $\mu$ M to stimulate PREG production. Interestingly, higher PREG concentrations in the medium of dHOG compared to undifferentiated controls were detected both in the presence or in absence of TSPO stimulation. As expected, when PREG metabolism was not blocked (w/o inhibitors), the detected concentrations were drastically reduced.

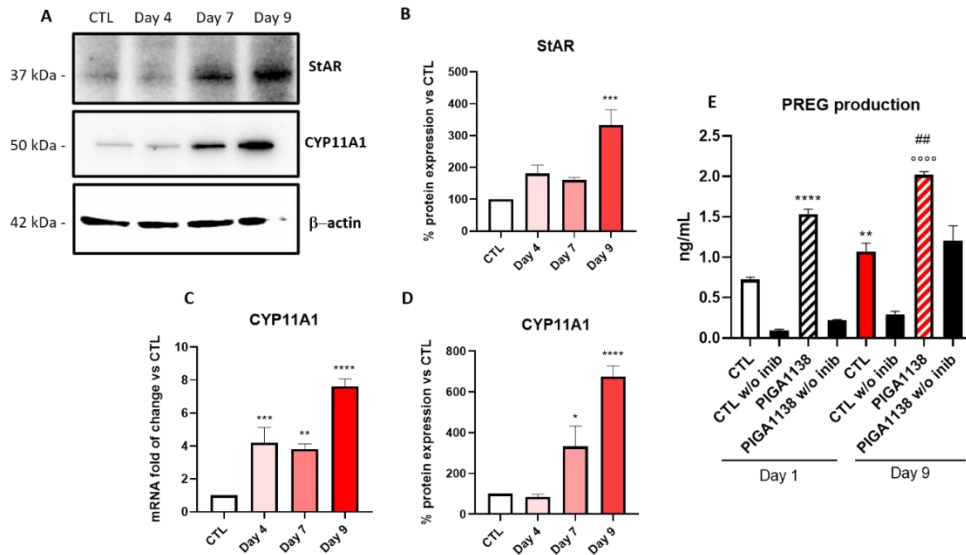


**Figure 5. Steroidogenic machinery components expression and PREG production evaluation in dHOG.**

(A) Protein expression level of CYP11A1 and StAR compared to the reference gene  $\beta$ -actin at day 4, 7, and 9 of DIV, and (B, D) densitometric analysis of bands. (C) mRNA levels of CYP11A1 at day 4, 7, and 9 of DIV. Each bar represents the mean  $\pm$  SEM of three independent experiments performed in duplicate. \* $p \leq 0.1$ ; \*\* $p \leq 0.01$ ; \*\*\* $p \leq 0.001$ ; \*\*\*\* $p \leq 0.001$  compared to the control (CTL), calculated using one-way ANOVA followed by Tukey's multiple comparisons test. (E) PREG production quantification in dHOG (day 9) and undifferentiated control cells (day 1). TSPO stimulation to achieve neurosteroidogenesis induction was performed by 2 h of treatment with 40  $\mu$ M PIGA1138 in presence of PREG metabolism inhibitors (w/o inhib: without PREG metabolism inhibitors). Each bar represents the mean  $\pm$  SEM of two independent experiments performed in quadruplicate. \*\*\*\* $p \leq 0.001$  \*\* $p \leq 0.01$  compared to the CTL day 1, °°° $p \leq 0.001$  compared to CTL day 9; ## $p \leq 0.01$  compared to PIGA1138 day 1, calculated using one-way ANOVA followed by Tukey's multiple comparisons test.

### 3.4.3 Effect of neurosteroidogenesis inhibition on HOG differentiation

In order to explore whether neurosteroids are required for HOG differentiation, we exploited a widely used inhibitor of steroidogenesis, aminoglutethimide (AMG). Starting from day 1 of DIV, we exposed

HOG cells to AMG at a dosage of 50  $\mu$ M to target the steroidogenesis cascade both upstream (CYP11A1) and downstream (aromatase), and we evaluated the expression of differentiation markers at day 9. To exclude possible toxic effects of AMG, we performed an MTS viability assay, and we observed no toxicity in AMG-treated dHOG (**Figure 6C**). Interestingly, we observed a significant reduction in the mRNA levels of HMGCR, and a trend in the reduction of Fdft-1 cholesterol synthesis genes, indicating the HOG downregulates cholesterol synthesis when it can be not metabolized to produce neurosteroids (**6D**, **6E**). To corroborate this result, we explored the effect of AMG on intracellular cholesterol by Filipin III staining, and we detected decreased cholesterol levels in AMG-treated HOG cells (**6A**, **6B**).

Importantly, also a significant reduction in CNPase mRNA and protein level was found in AMG-treated dHOG, suggesting that the differentiation process may be affected by the reduction of neurosteroids production (**Figure 7**). On the contrary, no significant differences were observed in MBP mRNA and protein expression in AMG-treated dHOG, despite a trend was observed.

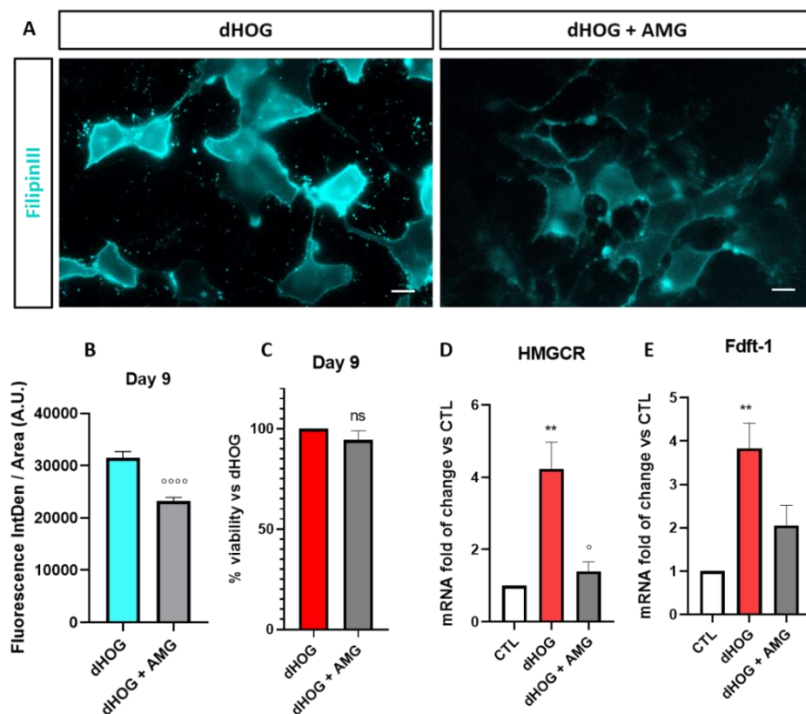


**Figure 6. Cholesterol intracellular level and expression of cholesterol synthesis enzymes in dHOG following AMG treatment. (A) Representative microscopy images of Filipin III staining**

(cyan) distribution in dHOG compared to control cells (CTL). Scale bar: 10  $\mu$ m. (B) Fluorescence intensity quantification. Each bar represents the mean fluorescence intensity signal ( $\pm$  SEM) normalized over the area of interest and expressed in Arbitrary Unit (A.U.) of two independent experiments performed in duplicate. (C) MTS cell viability evaluation of AMG-treated dHOG compared to control dHOG. mRNA levels of HMGCR (D) and Fdft-1 (E) enzymes in AMG-treated dHOG. Each bar represents the mean  $\pm$  SEM of two independent experiments performed in triplicate.  $**p \leq 0.01$ ; compared to CTL,  $^{\circ}p \leq 0.1$  compared to dHOG,  $^{\circ\circ\circ}p \leq 0.0001$  compared to dHOG, ns = non-significant, calculated using one-way ANOVA followed by Student *t*-test (C) or Dunnett's multiple comparisons test (D, E).

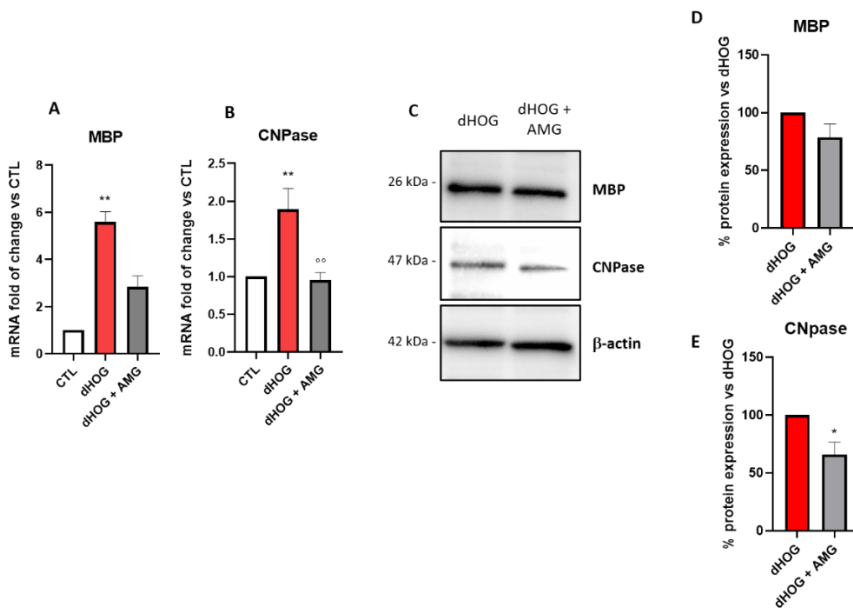


**Figure 7. Differentiation markers evaluation in dHOG during AMG treatment.** (A, B) mRNA levels of MBP, and CNPase in AMG-treated dHOG. (C) Protein expression of MBP, and CNPase differentiation markers compared to the reference gene  $\beta$ -actin in AMG-treated dHOG and densitometric analysis of bands (D, E). Each bar represents the mean  $\pm$  SEM of two independent experiments performed in duplicate.  $**p \leq 0.01$  compared to CTL,  $^{\circ}p \leq 0.01$  compared dHOG, calculated using one-way ANOVA followed by Dunnett's multiple comparisons test.

### 3.4.4 Effect of TSPO silencing on HOG differentiation

As TSPO has been proposed to be involved in the neurosteroids production in several cell types [235], [242], and TSPO expression was found to increase in mature HOG, we wondered if TSPO could play a critical role in HOG differentiation. To explore this possibility, we silenced TSPO expression by the use of RNA interference technology, employing two different siRNAs.

siRNA #3 and siRNA #4 were chosen for their better silencing efficiency compared to scramble-transfected (SCR), among four different TSPO-targeting siRNA based on preliminary experiments, which achieved a strong reduction in TSPO protein expression both after 72 h (silencing efficiency with respect to SCR: 77% for siRNA #3; 86% for siRNA #4) and after 96 h (silencing efficiency with respect to SCR: 69% for siRNA #3; 81% for siRNA #4) (**Figure 8**).

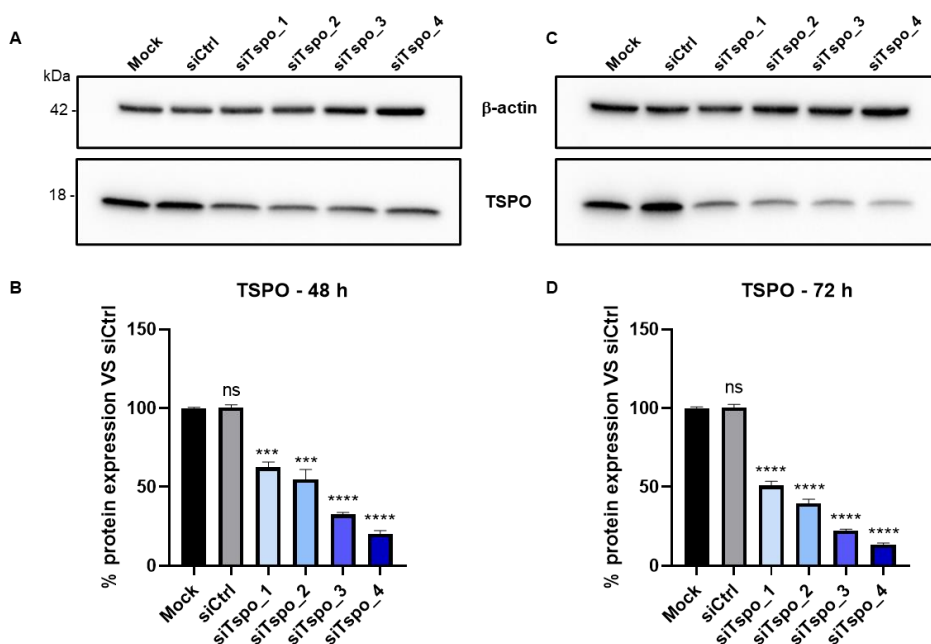


**Figure 1S. Silencing of TSPO expression in HOG.** Western blotting analysis of TSPO protein expression level and densitometric analysis of bands after 48 h (A, B) or 72 h (C, D) of no transfection (Mock) or transfection using 5 nM of four different TSPO-targeting siRNAs (siTspo) or 5 nM SCR-siRNA (siCtrl). Each bar represents the mean  $\pm$  SEM of two independent experiments performed in duplicate. \*\*\* $p \leq 0.001$ ; \*\*\*\* $p \leq 0.0001$  calculated using one-way ANOVA followed by Dunnett's post-test. (ns: not significant).

HOG cells were transfected starting from day 4 of DIV by the use of siRNA #3, siRNA #4, or SCR negative control. Our results evidenced that the transfection with both siRNAs significantly reduced TSPO protein expression in dHOG when compared to SCR-transfected dHOG. (**Figure 9A, 9B, 9C**). Then, we evaluated if the reduction of TSPO levels could affect the expression of a differentiation marker such as MBP and CNPase. Interestingly, MBP and CNPase protein expression was significantly decreased in KD TSPO cells, indicating that silencing of TSPO may impair proper OLGs differentiation (**9A, 9D**). In addition, we investigated if TSPO silencing leads to a reduction in neurosteroidogenesis in dHOG by measuring PREG production in control conditions and upon TSPO stimulation by the use of PIGA1138 TSPO ligand. Not surprisingly, TSPO KD dHOG showed a significant reduction in PREG release either unstimulated or after TSPO stimulation.

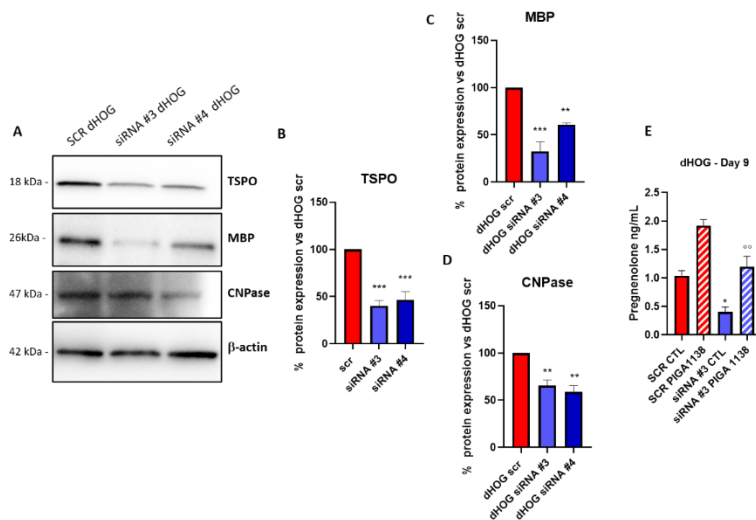


**Figure 9. Effects of TSPO silencing in dHOG.** (A) Protein expression of TSPO, MBP, and CNPase in dHOG following siRNA #3 and siRNA #4 transfection compared to the reference gene  $\beta$ -actin and (B, C, D) densitometric analysis of bands. (E) PREG production quantification in dHOG (day 9) after siRNA transfection. TSPO stimulation to achieve neurosteroidogenesis induction was performed by 2 h of treatment with 40  $\mu$ M PIGA1138 in presence of PREG metabolism inhibitors.

## Discussion

---

The OLs are extremely specialized glial cells, in charge of producing the axonal ensheathment, called myelin, in the CNS [45]. Myelin, due to its lipophilic structure, insulates long portions of the axons allowing for saltatory conduction, which ensures adequate speed of transmission of nerve impulses between axons. The myelination process is the result of the differentiation of OPCs into mature OLs, in a complex process involving both intrinsic and extrinsic signals, occurring mainly during the development [84]. However, a pool of undifferentiated OPCs persists in adulthood in particular areas of the brain, available for the so-called remyelination process if required [165]. Indeed, different types of injury can damage or destroy the myelin, leading to demyelinated areas, which are responsible for the slowing down of the nervous transmission along the unsheathed axons. Normally, a series of signals coming from the microenvironment of the inflammatory lesion, and in particular from regenerative microglia, recruits the OPCs at the site of the injury, promotes their differentiation into mature OLs, and allows for the formation of new myelin [168], [170]. This is what happens in demyelinating pathology such as MS, where endogenous remyelination occurs at the beginning of the disease. However, because of the progressive depletion of the OPCs pool, and due to the chronic inflammation at the focal lesion, the remyelination process becomes less efficient over time in MS patients, leading to the progression of the pathology and irreversible neuronal deficits due to myelin disruption [170]. For these reasons, besides acting on reducing the neuroinflammatory component of MS, there is an urgent need to identify new targets to promote the differentiation of OPCs into OLs for the development of new therapeutic approaches focused on remyelination process.

Herein, we first set up an *in vitro* model to explore oligodendrocytic lineage maturation. Then, we investigated the role of TSPO in the differentiation, showing its involvement during the OLs differentiation process. Moreover, there is no consensus regarding documented TSPO expression in mature OLs [187], [240], [278], and to the best of our knowledge, no report has investigated how TSPO expression is regulated during OPCs differentiation.

For this purpose, a human oligodendroglioma-derived cell line (HOG) was selected and exploited to establish an *in vitro* oligodendrocytic lineage differentiation protocol [335]. HOG cells have been demonstrated to express specific oligodendrocytic lineage markers and to possess OPCs characteristics [336], [337], thus representing a reliable model for the study of the oligodendrocytic cells. Although primary cultures of human OLs have been exploited in some studies, this approach is hampered by the limited availability of human brain tissue. Therefore, the development of an *in vitro*

experimental model of human OLs differentiation makes it easier the study of OLs as permits an unlimited supply of cells having characteristics similar to those of human OLs.

Our differentiation protocol was adapted from previous reports showing the significant capacity of HOG to differentiate [333], [336]. After 9 days of culturing in DM, immunofluorescence analysis evidenced morphological changes in dHOG, as a higher percentage of cells was shown to extend branched processes and short membrane extensions (**Figure 1**). Furthermore, differentiation markers were monitored over time (day 4, day 7, and day 9) and dHOG evidenced a progressive increase in the expression of mature OLs markers such as the myelin protein MBP and the CNPase enzyme, in agreement with previous works [333], [337]. In contrast to our results, recent work has shown that the same cell line was unable to express mature OLs markers such as MBP upon culturing with DM [338]. However, the observed differences can be explained by the employed differentiation medium containing diverse factors and/or different concentrations.

In addition to this primary characterization, we aimed at investigating cholesterol levels during HOG differentiation. In fact, it is well known that the *de novo* synthesis of cholesterol by mature OLs represents the rate-limiting step of myelination/remyelination in the CNS, being cholesterol an important component of the myelin sheath [45], [56], [334]. Interestingly, dHOG evidenced a significant increase, particularly at day 9, in the transcript level of HMGCR and Fdft-1, two main enzymes deputed to cholesterol synthesis, indicating that dHOG presented an enhanced cholesterol synthesis. Moreover, the intracellular content of free cholesterol was significantly higher at day 9 of DIV compared to control cells, in agreement with the upregulation of cholesterol synthesis genes. In particular, a strong signal on the plasma membrane was identified in dHOG compared to control, suggesting the correct delivery of cholesterol towards the membrane to begin myelin production.

Afterward, as TSPO is recognized to translocate cholesterol from the cytosol to mitochondria to give rise to the neurosteroidogenesis cascade [208], [215], we sought to investigate its expression during HOG differentiation. Moreover, very few reports have studied TSPO function in the oligodendrocytic lineage.

Interestingly, we found a strong increase in TSPO mRNA and protein expression starting from day 7 of differentiation, suggesting that TSPO could be involved in the differentiation process. In particular, as the highest TSPO mRNA and protein levels were detected at day 9. We corroborated our result by performing immunostaining of TSPO in dHOG and undifferentiated controls. The quantification of the fluorescence intensity signal confirmed the marked increase in TSPO expression at day 9

compared to controls. In addition, the immunofluorescence experiment revealed the typical perinuclear distribution of TSPO, which is known to localize in mitochondria.

Worthy of consideration is the fact that during OLs differentiation there is an overall mitochondrial transcript and mtDNA amplification, also due to the high metabolic demand that requires mitochondrial ATP production of myelinating OLs. Therefore, it cannot be excluded the possibility that this mitochondrial function stimulation could contribute to the detected upregulation of TSPO.

TSPO is known to take part in the steroidogenic machinery of the cell together with other mitochondrial proteins and promote the production of neurosteroids starting from cholesterol [201]. Therefore, we investigated the expression level of two other major components of the steroidogenic machinery [208]. Interestingly, our results showed an increase in the expression of StAR and CYP11A1 protein during HOG differentiation, suggesting that HOG cells upregulate steroidogenesis upon maturation. The cytochrome P450 enzyme CYP11A1 is responsible for the conversion of cholesterol into PREG, the precursor of all neurosteroids, and this reaction is considered the rate-limiting step of steroidogenesis. Therefore, to support our findings, we quantified the production of PREG by dHOG and undifferentiated controls in presence of the compounds which inhibited PREG metabolism, to ensure its accumulation in the cellular medium. Interestingly, we observed that the amount of the released PREG was higher in dHOG compared to undifferentiated control cells, both in unstimulated conditions and following TSPO stimulation by the selective ligand PIGA1138. Firstly, to the best of our knowledge, our results demonstrate for the first time that PIGA1138 TSPO ligand administration induces PREG production thus *de novo* neurosteroidogenesis in HOG cells. More importantly, we have shown that dHOG cells produce a discrete amount of PREG in control conditions and that TSPO stimulation further enhances steroidogenesis, in agreement with the increased expression level of the steroidogenic machinery proteins. Importantly, when its metabolism was not inhibited, PREG level was found to be reduced as expected, indicating that PREG is converted to its metabolites giving rise to all neurosteroids. However, when dHOG were stimulated by PIGA1138 in the absence of PREG metabolism inhibitors, PREG level was not drastically reduced. Our explanation for this result concerns the hypothesis that dHOG has markedly upregulated steroidogenic machinery components and thus neurosteroidogenesis, compared to undifferentiated control. Following the steroidogenesis induction due to TSPO pharmacological stimulation, the amount of PREG produced may be so high that, even if the enzymes in charge of its metabolism employ PREG to produce neurosteroids, PREG tends to accumulate anyway.

These findings prompted us to investigate whether neurosteroids were required by HOG cells to differentiate into mature OLs. Therefore, an inhibitor of the steroidogenesis (AMG) was diluted into DM during the differentiation of HOG cells. AMG was employed at 50  $\mu$ M concentration based on previous reports [226]. This concentration of AMG has been demonstrated to inhibit both the CYP11A1 and the aromatase enzymes leading to a general reduction of the level of neurosteroids [339]. Our results show that, at day 9, mRNA and protein level of the differentiation marker CNPase were significantly reduced in AMG-treated dHOG, while the levels of MBP were not strongly affected, suggesting that neurosteroids may in part regulate the expression of CNPase, while they are not directly related to the expression of MBP. Moreover, the synthesis of cholesterol was also reduced, as the mRNA level of HMGCR and Fdft-1 enzymes, as well as the intracellular cholesterol levels, were found decreased compared to untreated dHOG, suggesting that steroidogenesis inhibition may impair HOG differentiation.

In order to better investigate the role of TSPO and steroidogenesis during HOG differentiation and to explore whether TSPO was required for oligodendrocytic lineage maturation, we silenced TSPO expression during differentiation. By the use of two different siRNA (siRNA #3 and siRNA #4) to prove the specificity of the observed effect, a TSPO KD between 60-80% after 72 h and 96 was achieved. As TSPO expression was shown to increase at day 7 of differentiation, we silenced TSPO expression at day 4 and we repeated the transfection at day 7. The protein expression level of MBP and CNPase differentiation markers was determined at day 9, and interestingly was found to be decreased, suggesting that TSPO expression may be important to ensure the correct HOG maturation. However, further investigations are planned to confirm this result, such as the evaluation of the other important differentiation markers or phenotypic analyses in TSPO KD dHOG. To provide additional information regarding the events arising from TSPO expression silencing in HOG cells, we measured PREG production in KD TSPO dHOG, both in control conditions and upon PIGA1138 stimulation by a selective ligand. As expected, the release of PREG was significantly decreased in dHOG when TSPO was silenced, confirming that TSPO represents a crucial protein involved in neurosteroidogenic machinery of the cell. The reduction in PREG likely reflects in a global reduction in neurosteroids levels, with possible consequences on proper HOG differentiation. Moreover, this result draws our attention to the fact that PIGA1138, in agreement with previous reports demonstrating its high RT at TSPO, presents a potent steroidogenic capacity, being able to strongly promote neurosteroidogenesis *de novo* in HOG. Nevertheless, the possibility of off-target effects cannot be excluded, considering

that PIGA1138 is a high-affinity ligand and for the acute stimulus that is used in our experimental conditions, it is employed at a concentration far beyond its constant of affinity [323].

To summarize, these findings shed some light on the role of TSPO during oligodendrocytic lineage maturation, suggesting a novel implication for TSPO among the several biological functions already known. In particular, we demonstrated the importance of self-production of neurosteroids by HOG, which in our hands have been shown crucial for proper HOG differentiation. More importantly, as TSPO appears an important protein involved in OPCs differentiation, probably through the stimulation of neurosteroids production, its targeting with selective ligands could represent an interesting strategy to be applied in the context of promoting remyelination.

## CONCLUDING REMARKS AND FUTURE PERSPECTIVES

---

The present PhD work has made it possible to obtain significant results in the light of developing new therapeutic approaches to myelin diseases. Taken together, all data shed light on the role of TSPO as a possible target in neuroinflammatory and neurodegenerative diseases such as MS.

Our findings using the *in vitro* model of activated human microglia helped to uncover important mechanisms regulating TSPO expression upon microglia activation. A major result of the present work is the discovery of the involvement of NF- $\kappa$ B TF in TSPO expression regulation. Future investigations on the regulation of TSPO promoter, such as gene reporter assays, are certainly encouraged to confirm the binding of NF- $\kappa$ B to TSPO proximal promoter for transcriptional regulation. Moreover, our data demonstrated an important function for TSPO in orchestrating different microglial activities addressed to contrast the pro-inflammatory phenotype of human microglia. Interestingly, TSPO effects were abolished when steroidogenesis was inhibited, thus we propose that TSPO modulates microglia reactivity in part by promoting the production of neurosteroids which are going to act in an autocrine and/or paracrine manner on microglia function. However, microglia have been for years considered unable to produce neurosteroids *de novo*, as the expression of CYP11A1 was not detected. Undoubtedly, the imminent perspective of the present work involves the investigation of microglia capacity to synthesize neurosteroids starting from cholesterol, and initial data have been already published by our research group [281].

Novel TSPO selective ligands, synthesized by the Pharmaceutical Chemistry section of the Department of Pharmacy (University of Pisa) have been then assessed in the EAE murine model of progressive MS. Noteworthy, the INSERM research unit 1119 (University of Strasbourg) is strongly clinic-oriented, as many neurologists work together with researchers to develop new effective therapeutic strategies that may move forward to clinical studies. Such an environment strongly encourages the approach by which fundamental research is required to answer the demands of the clinics, and our pre-clinical study demonstrating beneficial effects of the PIGA1138 TSPO ligand provides important findings that might be exploited in the next future in the clinics. In particular, our work opens the possibility to consider how to set up a clinical trial for the use of PIGA1138 in PPMS patients. However, further pre-clinical evaluations are certainly necessary, and the toxicological profile of the ligands needs to be evaluated before advancing in this sense.

In addition, an important novelty of the present project is represented by the discovery of the important role of TSPO during oligodendrocytic cells development. Such findings enable the scientific

community which is studying TSPO as a possible therapeutic target, to draw attention to the involvement of TSPO in another cellular process that has been underestimated so far which is neural precursor differentiation.

To conclude, thanks to the combination of various *in vitro* and *in vivo* methods in a very well-integrated strategy, the present PhD research project has made it possible to achieve critical results that significantly contributed both to the elucidation of molecular mechanisms and to the elaboration of promising therapeutic options against myelin disorders. The obtained findings strongly support the amount of evidence that proposes TSPO as a promising target against neuroinflammation and neurodegeneration, pointing out new potential implications for TSPO in the treatment of different myelin pathologies due to its possible role during the oligodendrocytic lineage differentiation.

## List of publications

---

Translocator Protein Ligand PIGA1138 Reduces Disease Symptoms and Severity in Experimental Autoimmune Encephalomyelitis Model of Primary Progressive Multiple Sclerosis. **Tremolanti C\***, Cavallini C\*, Meyer L, Christian Klein C, Da Pozzo E, Costa B, Taliani S, Patte-Mensah C, Mensah-Nyagan AG. \*equal contribution *Molecular Neurobiology* 2022.

Microglial Pro-Inflammatory and Anti-Inflammatory Phenotypes Are Modulated by Translocator Protein Activation. Da Pozzo E\*, **Tremolanti C\***, Costa B, Giacomelli C, Milenkovic VM, Bader S, Wetzel CH, Rupprecht R, Taliani S, Da Settimo F. \*equal contribution. *Int J Mol Sci* 2019.

*De novo* Neurosteroidogenesis in Human Microglia: Involvement of the 18 kDa Translocator Protein. Germelli L, Da Pozzo E, Giacomelli C, **Tremolanti C**, Marchetti L, Wetzel et al. *Int J Mol Sci* 2021.

Discovery of pyrrole derivatives for the treatment of glioblastoma and chronic myeloid leukemia. Puxeddu M, Shen H, Bai R, Coluccia A, Bufano M, Nalli M, Sebastiani J, Brancaccio D, Da Pozzo E, **Tremolanti C**, Martini C, La Regina G. *Eur J Med Chem* 2021.

A Public Dataset of 24-h Multi-Levels Psycho-Physiological Responses in Young Healthy Adults. Rossi A, Da Pozzo E, Menicagli D, **Tremolanti C**, Priami C, Sîrbu A, Clifton DA, Martini C, Morelli D. *Data* 2020.

Review article: Translocator Protein 18-kDa: a promising target to treat neuroinflammation-related degenerative diseases. **Tremolanti C\***, Germelli L\*, Barresi E\*, Da Pozzo E, Taliani S, Da Settimo F, Costa B. \*equal contribution. *Current Medicinal Chemistry* 2022

Unpublished Manuscripts

Role of the Translocator Protein (TSPO) in the Differentiation of Oligodendrocyte-Like Cells.  
**Tremolanti C**, Angeloni E, Germelli L, Giacomelli C, Da Pozzo E, Costa B, Mensah-Nyagan AG,  
Martini C. (*In preparation*)

## Declarations

---

The figures included in the Results Chapter 3.2 and 3.3 have been adapted/taken by published articles. As declared by the Open Access Policy of the journals (International Journal of Molecular Science, MDPI; Molecular Neurobiology, Springer Nature), these published articles are under an open access Creative Common **CC BY license**, according to which any part of the article may be reused without permission provided that the original article is clearly cited.

## Resumé de thèse

---

La myéline du système nerveux central (SNC) est produite par des cellules gliales appelées oligodendrocytes (OLs). La membrane des OLs s'enroule autour des axones formant la gaine de myéline, une structure lipophile qui isole les axones facilitant ainsi la transmission rapide de l'influx nerveux. Les dommages de la gaine de myéline et / ou la mort des OLs ont un impact sur la vitesse de conduction de l'influx nerveux, entraînant des symptômes neurologiques, y compris des déficiences sensorielles, motrices et cognitives caractéristiques des pathologies de la myéline. Ces pathologies peuvent être dysmyélinisantes comme cela est observé dans les leucodystrophies, notamment dans la maladie génétique de Pelizaeus-Merzbacher (PMD), qui sont provoquées par des anomalies dans la formation ou le maintien de la gaine de myéline. Les maladies de la myéline peuvent aussi résulter d'une démyélinisation comme cela intervient dans le cas de la sclérose en plaques (SEP). La PMD est causée par des mutations génétiques du gène *PLP1* lié à l'X qui code pour la protéine protéolipide (PLP) de la myéline, entraînant des problèmes neurologiques critiques dus à des anomalies dans la formation et le maintien de la gaine de myéline. La souris *jimpy*, un modèle de PMD sévère, porte spontanément une mutation ponctuelle dans le gène *Plp1*, qui détermine la production de PLP mal replié responsable de la mort prématurée des OLs par des mécanismes moléculaires qui n'ont pas encore été élucidés.

La SEP est une maladie auto-immune caractérisée par une réponse anormale du système immunitaire dirigée contre la myéline centrale et les OLs, conduisant à une neuroinflammation, à des lésions démyélinisantes, à une souffrance axonale et à la neurodégénérescence. De plus, la neuroinflammation chronique qui est observée dans la SEP au cours du temps altère la remyélinisation endogène, un processus par lequel les cellules précurseurs des OLs (OPC) sont recrutées au site de la lésion et se différencient en OLs matures pour former une nouvelle myéline. On distingue la SEP par poussées (forme récurrente rémittente ou SEP-RR) de celle évoluant progressivement sans poussées (SEP progressive primaire ou SEP-PP). Certains patients ayant une forme rémittente évoluent secondairement vers une forme progressive.

Des progrès ont été réalisés dans la lutte contre la composante inflammatoire de la SEP mais à ce jour, il n'y a pas de médicaments neuroprotecteurs efficaces pour lutter contre la souffrance axonale et les dommages neuronaux faisant suite à la démyélinisation alors que ces dommages sont responsables du handicap et des symptômes neurologiques graves.

Concernant la PMD, la situation est encore plus grave car il n'existe aucun traitement efficace contre cette maladie et les mécanismes physiopathologiques sont encore mal connus. Compte tenu du caractère fortement génétique de cette maladie, les méthodes innovantes d'édition du génome telles que les technologies CRISPR / Cas9 semblent attrayantes pour élaborer des stratégies de thérapie génique. En particulier, la possibilité d'une correction *in vitro* de la mutation responsable de la PMD pour restaurer le génotype WT permettrait de décrypter les mécanismes moléculaires responsables de la mort des OLs, et d'explorer ainsi des pistes thérapeutiques innovantes contre cette pathologie.

Le but du projet de thèse a donc été d'utiliser divers modèles expérimentaux avec des approches méthodologiques pertinentes pour explorer (i) le potentiel d'agents pharmacologiques à protéger efficacement contre les symptômes de la SEP (maladie démyélinisante) et (ii) la capacité de la technologie d'édition du génome à corriger les anomalies cellulaires causées par la mutation du gène responsable de la PMD (maladie dysmyélinisante).

Tout d'abord, des études *in vitro* ont été réalisées sur la lignée cellulaire oligodendrocytaire 158JP dérivée de la souris *jimpy*, exploitant la technologie d'édition du génome CRISPR / Cas9 pour décrypter le mécanisme physiopathologique de la PMD responsable de la mort des OL.

Dans le cas de la SEP, des études *in vitro* ont d'abord été menées sur la microglie humaine afin de disséquer le rôle de la protéine translocatrice mitochondriale (TSPO) dans la modulation de la neuroinflammation et d'explorer son potentiel en tant que cible contre l'activation de la microglie. La protéine TSPO a retenu notre attention compte tenu des nombreuses données de la bibliographie qui ont démontré son implication dans la régulation de la biosynthèse des neurostéroïdes (neurostéroïdogenèse), des processus inflammatoires et neurophysiologiques. Ensuite, l'évaluation du potentiel thérapeutique de deux nouveaux ligands TSPO a été réalisée dans un modèle murin de SEP progressive. Enfin, un modèle *in vitro* de différenciation des OPC en OL matures a été caractérisé au moyen d'une lignée cellulaire d'oligodendrocytes humains. Ici, le rôle du TSPO et des neurostéroïdes dans le processus de différenciation des OL a été étudié pour explorer la possibilité de promouvoir la différenciation des OPC et donc la remyélinisation par l'utilisation de ligands TSPO sélectifs.

En ce qui concerne les PMD, la technologie d'édition du génome CRISPR/Cas9 a été choisie pour corriger la mutation faux-sens PLP1 dans les OL 158JP afin de déterminer les avantages possibles de cette approche dans le modèle cellulaire OL 158JP et de disséquer les mécanismes pathologiques sous-jacents la mort des OL. Malheureusement, aucun clone corrigé n'a été obtenu à partir des expériences et nous n'avons pas été en mesure d'inverser la mutation pathologique *PLP1* dans les OLs 158JP. Cependant, plusieurs réarrangements de l'ADN ont été observés aux points de rupture,

suggérant une livraison possible du système d'édition du génome. Notre explication de la difficulté à obtenir des clones édités est liée à la fois aux problèmes intrinsèques de la technologie et à des conditions expérimentales particulières.

Dans le contexte de la recherche de nouvelles stratégies thérapeutiques pour lutter contre la SEP, différentes stratégies ont été utilisées :

(i) Tout d'abord, un modèle *in vitro* de microglie activée a été mis en place et caractérisé par l'évaluation de marqueurs pro-inflammatoires. Des approches expérimentales distinctes ont été utilisées pour étudier le rôle immunomodulateur de TSPO dans la microglie : l'amplification pharmacologique de l'activité de TSPO ou l'inactivation de l'expression de TSPO avec des siRNA.

Nos principaux résultats ont montré que la stimulation de TSPO par l'administration de ligands sélectifs module négativement l'activation pro-inflammatoire de la microglie, et ces effets se sont avérés être médiés par l'induction de neurostéroïdogenèse. De plus, la susceptibilité microgliale au stimulus immunogène est augmentée, suggérant que TSPO peut avoir un rôle homéostatique dans le contexte de l'équilibre dynamique entre les médiateurs anti-inflammatoires et pro-inflammatoires.

(ii) Deux ligands TSPO, PIGA1138 et PIGA839 ont été testés dans le modèle de souris MOG-EAE (souris immunisées par injection de la *myelin oligodendrocyte glycoprotein* ou MOG<sub>35-55</sub>) mimant la SEP progressive primaire (SEP-PP). Plusieurs méthodes ont été combinées pour évaluer les effets des ligands TSPO PIGAs sur les symptômes cliniques et neurologiques des souris MOG-EAE de même que sur l'infiltration du SNC par les cellules immunitaires, la démyélinisation et les dommages axonaux. Le PIGA1138 (15 mg/kg) a considérablement réduit les scores cliniques des souris MOG-EAE, amélioré les dysfonctionnements moteurs évalués avec le dispositif Catwalk et neutralisé la démyélinisation induite par l'immunisation par injection MOG<sub>35-55</sub>, en préservant l'expression de la protéine basique de la myéline (MBP) dans le SNC. De plus, le traitement par PIGA1138 a empêché la diminution de l'expression du neurofilament 200 dans les axones spinaux et cérébelleux des souris MOG-EAE. Par ailleurs, le ligand PIGA1138 a inhibé l'infiltration périphérique des cellules immunitaires CD45+ dans le SNC, suggérant qu'il pourrait contrôler les mécanismes inflammatoires impliqués dans la SEP-PP. De manière concordante, PIGA1138 a aussi amélioré le taux sérique d'interleukine-10 anti-inflammatoire chez les souris MOG-EAE. Le traitement utilisant le composé PIGA1138, qui a stimulé la production du neurostéroïde allop régénolone dans le SNC, a amélioré tous les biomarqueurs neuropathologiques dans le modèle de souris MOG-EAE. En revanche, le ligand PIGA839, incapable d'activer la production d'allop régénolone dans le SNC *in vivo*, n'a exercé que des effets modérés/partiels chez les souris MOG-EAE. Dans l'ensemble, nos résultats suggèrent

que le traitement à base de PIGA1138 peut représenter une possibilité intéressante à explorer pour l'innovation de thérapies efficaces contre la SEP-PP.

Enfin, après avoir mis en place un modèle de différenciation d'OLs *in vitro* grâce à l'utilisation d'une lignée cellulaire oligodendrocytaire humaine (cellules HOG), nous avons exploré le rôle de TSPO lors de la différenciation des OPC vers les OL matures. Nos résultats révèlent que lors de la maturation des HOG, le niveau d'expression de TSPO augmente dans ces cellules oligodendrocytaires de façon concomitante avec deux autres composantes majeures de la voie de production endogène des stéroïdes. De façon intéressante, nous avons observé que les HOG différenciés produisent une quantité plus importante de prégnénolone, le précurseur commun de la majorité des neurostéroïdes. Mieux encore, nos résultats montrent que l'utilisation d'un inhibiteur pharmacologique de la neurostéroïdogénèse réduit significativement la différenciation des HOG. Ces données suggèrent un rôle déterminant de TSPO dans la régulation de la différenciation oligodendrocytaire. Pour vérifier cette hypothèse, nous avons alors évalué la capacité de différenciation des cellules HOG après inactivation ou knockdown de TSPO par des siRNA. Les résultats montrent que l'inactivation de l'expression de TSPO altère significativement la différenciation des HOG, suggérant que TSPO est un acteur indispensable dans le processus de maturation OPC. Cette observation confirme l'intérêt de la cible TSPO pour stimuler la remyélinisation.

En conclusion, le présent travail de thèse, qui a utilisé divers modèles expérimentaux (*in vitro* et *in vivo*) et combiné plusieurs approches méthodologiques et techniques, apporte de nombreuses données précliniques pertinentes pour contribuer à l'élaboration de stratégies thérapeutiques contre les pathologies de la myéline qui constituent un problème majeur de santé. Grâce aux diverses preuves expérimentales fournies, nos résultats suggèrent en particulier que TSPO pourrait constituer une protéine d'intérêt à cibler pour le développement de composés à visée thérapeutique pouvant permettre de réguler la différenciation oligodendrocytaire, de stimuler la remyélinisation et de lutter efficacement contre la neuroinflammation, la démyélinisation et la dégénérescence axonale ou neuronale.

## Riassunto della tesi

---

La mielina del sistema nervoso centrale (SNC) è prodotta da cellule gliali chiamate oligodendrociti (OL). La membrana plasmatica degli OL avvolge gli assoni formando la guaina mielinica, una struttura lipofila che isola gli assoni facilitando così la rapida trasmissione degli impulsi nervosi. Il danno alla guaina mielinica e / o la morte degli OL impattano negativamente sulla velocità di conduzione degli impulsi nervosi portando a sintomi neurologici, tra cui disturbi sensoriali, motori e cognitivi caratteristici delle patologie della mielina. Queste patologie possono essere demielinizzanti, come osservato nelle leucodistrofie, specialmente nella malattia genetica di Pelizaeus-Merzbacher (PMD), che sono causate da anomalie nella formazione o nel mantenimento della guaina mielinica. D'altro canto, le malattie mieliniche possono anche derivare dalla demielinizzazione come nel caso della sclerosi multipla (SM).

La PMD è causata da mutazioni genetiche nel gene legato al cromosoma X *PLP1*, che codifica per la proteina proteolipidica della mielina (PLP), portando a problemi neurologici critici dovuti ad anomalie nella formazione e nel mantenimento della guaina mielinica. Il topo *jimpy*, un modello di PMD severa, è portatore di una mutazione spontanea puntiforme nel gene *Plp1*, che determina la produzione di PLP tronca e mal ripiegata, responsabile della morte prematura degli OL per mezzo di meccanismi molecolari che non sono ancora stati chiariti.

La SM è una malattia autoimmune caratterizzata da una risposta anomala del sistema immunitario diretta contro la mielina del SNC e gli OL, che porta a neuroinfiammazione, lesioni demielinizzanti, sofferenza assonale e neurodegenerazione. Inoltre, la neuroinfiammazione cronica che si instaura nel tempo nella SM, altera la remielinizzazione endogena, un processo mediante il quale le cellule precursori degli OL (OPC) vengono reclutate al sito della lesione demielinizzante e si differenziano in OL maturi per formare nuova mielina. Viene fatta una distinzione tra SM recidivante (forma recidivante remittente) e SM progressiva senza recidive (SM progressiva primaria). Alcuni pazienti con una forma recidivante-remittente evolvono secondariamente in una forma progressiva.

Recentemente, sono stati fatti molti progressi nella lotta contro la componente infiammatoria della SM, ma ad oggi non esistono farmaci neuroprotettivi efficaci per combattere la sofferenza assonale e i danni neuronali a seguito della demielinizzazione, eventi responsabili di disabilità e gravi sintomi neurologici.

Per quanto riguarda la PMD, la situazione è ancora più grave in quanto non esiste un trattamento efficace per questa malattia e i meccanismi fisiopatologici sono ancora poco conosciuti. Data la natura

genetica di questa malattia, metodi innovativi di editing genomico come la tecnologia CRISPR / Cas9 possono offrire una proof-of-concept per lo sviluppo di strategie di terapia genica. In particolare, la possibilità di correggere *in vitro* la mutazione responsabile della PMD per ripristinare il genotipo wild-type (WT) consentirebbe di decifrare i meccanismi molecolari responsabili della morte delle OL, e quindi di esplorare vie terapeutiche innovative contro questa patologia.

Lo scopo del presente progetto di tesi è stato quindi quello di utilizzare vari modelli sperimentali con differenti approcci metodologici per esplorare (i) il potenziale di nuovi agenti farmacologici per proteggere efficacemente dai sintomi della SM (malattia demielinizzante) e (ii) la capacità della tecnologia di editing del genoma CRISPR / Cas9 di correggere le anomalie cellulari causate dalla mutazione del gene responsabile della PMD (malattia dismielinizzante).

In primo luogo, sono stati condotti studi *in vitro* sulla linea cellulare di oligodendrociti 158JP derivata dal topo *jimpy*, sfruttando la tecnologia CRISPR / Cas9 per decifrare il meccanismo fisiopatologico della PMD responsabile della morte degli OL.

Nel contesto della SM, sono stati in primis condotti studi *in vitro* su cellule di microglia umana per analizzare il ruolo della proteina traslocatrice mitocondriale (TSPO) nella modulazione della neuroinfiammazione e per esplorare il suo potenziale come target contro l'attivazione della microglia. Il TSPO ha attirato la nostra attenzione visti i numerosi dati in letteratura che hanno dimostrato il suo coinvolgimento nella regolazione della biosintesi dei neurosteroidi (neurosteroidogenesi), e dei processi neuroinfiammatori. Successivamente, la valutazione del potenziale terapeutico di due nuovi ligandi del TSPO è stata effettuata in un modello murino di SM progressiva. Infine, è stato caratterizzato un modello *in vitro* di differenziamento di OPC in OL maturi utilizzando una linea cellulare oligodendrocitaria umana. In questo studio, è stato studiato il ruolo del TSPO e dei neurosteroidi nel processo di differenziamento degli OL per esplorare la possibilità di promuovere il differenziamento degli OPC e quindi la remielinizzazione attraverso l'uso di ligandi TSPO selettivi.

Contro la PMD, la tecnologia di editing del genoma CRISPR / Cas9 è stata scelta per correggere la mutazione missenso del gene *PLP1* nella linea cellulare OL 158JP per determinare i possibili benefici di questo approccio e per esplorare i meccanismi patologici alla base della morte degli OL. Sfortunatamente, dai nostri esperimenti non sono stati ottenuti cloni WT e non siamo stati in grado di correggere la mutazione patologica *PLP1* negli OL 158JP. Tuttavia, diversi riarrangiamenti del DNA sono stati osservati nei pressi dei siti di taglio, che suggeriscono una corretta incorporazione cellulare del sistema di editing genomico. Le nostre spiegazioni alla difficoltà di ottenere cloni correttamente

modificati sono relative sia ai problemi intrinseci della tecnologia sia a peculiari condizioni sperimentali difficili da arginare.

Nel contesto della ricerca di nuove strategie terapeutiche per combattere la SM, sono state utilizzate diverse strategie:

(i) In primo luogo, è stato creato un modello *in vitro* di microglia attivata, e caratterizzato mediante la valutazione di marcatori pro-infiammatori. Sono stati utilizzati approcci sperimentali separati per studiare il ruolo immunomodulatore del TSPO nelle microglia: amplificazione farmacologica dell'attività del TSPO o inattivazione dell'espressione del TSPO mediante silenziamento con siRNA.

I nostri principali risultati hanno dimostrato che la stimolazione del TSPO mediante la somministrazione di ligandi selettivi è in grado di modulare negativamente l'attivazione pro-infiammatoria della microglia, e questi effetti sono risultati mediati dall'induzione dei neurosteroidogenesi. Inoltre, nelle cellule TSPO knockdown, la suscettibilità microgliale allo stimolo immunogenico era maggiore, suggerendo che il TSPO possa avere un ruolo omeostatico nel contesto dell'equilibrio dinamico tra il rilascio di mediatori antinfiammatori e pro-infiammatori.

(ii) Due nuovi ligandi TSPO, PIGA1138 e PIGA839 sono stati testati nel modello murino MOG-EAE (topi immunizzati mediante iniezione di un peptide derivato dalla proteina mielinica MOG<sub>35-55</sub>) in grado di mimare la SM progressiva. Sono stati combinati diverse metodologie per valutare gli effetti dei PIGA sui sintomi clinici e neurologici nei topi MOG-EAE, tra cui l'infiltrazione nel SNC da parte delle cellule immunitarie, la demielinizzazione e il danno assonale. Il ligando PIGA1138 (15 mg/kg) si è rivelato in grado di ridurre significativamente lo score clinico dei topi MOG-EAE, di migliorare le disfunzioni motorie valutate con il dispositivo Catwalk e di prevenire la demielinizzazione indotta dall'immunizzazione mediante iniezione di MOG<sub>35-55</sub>, preservando l'espressione della proteina basilica della mielina (MBP) nel SNC. Inoltre, il trattamento con PIGA1138 ha dimostrato di contrastare efficacemente la diminuzione dell'espressione del neurofilamento 200 negli assoni spinali e cerebellari dei topi MOG-EAE. Inoltre, il ligando PIGA1138 ha inibito l'infiltrazione periferica delle cellule immunitarie CD45<sup>+</sup> nel midollo spinale, dimostrandosi in grado di tenere sotto controllo i meccanismi infiammatori coinvolti nella SM progressiva. Coerentemente, il trattamento con PIGA1138 ha anche migliorato i livelli sierici dell'interleuchina-10 antinfiammatoria nei topi MOG-EAE e ha stimolato la produzione del neurosteroido allopregnanolone nel midollo spinale. Globalmente, tutti i biomarcatori neuropatologici nel modello murino di SM MOG-EAE sono stati migliorati in modo significativo dal ligando TSPO PIGA1138. Al contrario, il ligando PIGA839, incapace di attivare la produzione di allopregnanolone nel SNC *in vivo*, ha esercitato solamente effetti moderati/parziali nei

topi MOG-EAE. Nel complesso, i nostri risultati suggeriscono che il trattamento con PIGA1138 può rappresentare un'interessante possibilità da esplorare nell'ottica di trovare terapie efficaci contro la SM progressiva.

Infine, dopo aver caratterizzato un modello di differenziamento degli OL *in vitro* attraverso l'uso di una linea cellulare di oligodendrociti umani (cellule HOG), abbiamo esplorato il ruolo del TSPO durante il processo di maturazione degli OPC. I nostri risultati rivelano che durante la maturazione delle HOG, il livello di espressione di TSPO aumenta notevolmente in concomitanza con altri due componenti principali della via di produzione di steroidi endogeni. Abbiamo osservato che gli HOG differenziati producono una maggiore quantità di pregnenolone, il precursore comune della maggior parte dei neurosteroidi. Inoltre, i nostri risultati mostrano che l'uso di un inibitore farmacologico della neurosteroidogenesi riduce significativamente il differenziamento delle HOG. Questi dati suggeriscono per la prima volta un ruolo decisivo per il TSPO nella regolazione del differenziamento degli OL. Per testare questa ipotesi, abbiamo quindi valutato la capacità di differenziamento delle cellule HOG a seguito del silenziamento dell'espressione del TSPO da parte dei siRNA. I nostri risultati mostrano che il silenziamento del TSPO altera significativamente il differenziamento degli HOG, proponendo per il TSPO un ruolo chiave nel processo di maturazione degli OPC. Questa osservazione conferma l'idea di utilizzare il TSPO come target per stimolare la remielinizzazione nella SM.

In conclusione, il presente lavoro di tesi, che ha utilizzato vari modelli sperimentali (*in vitro* e *in vivo*) e combinato diversi approcci metodologici e tecnici, fornisce molti dati preclinici rilevanti per contribuire allo sviluppo di strategie terapeutiche contro le patologie della mielina. Grazie alle varie evidenze sperimentali fornite, i nostri risultati suggeriscono in particolare che il TSPO potrebbe essere una proteina di grande interesse per lo sviluppo di composti terapeutici in grado di regolare il differenziamento degli OL, stimolare la remielinizzazione e combattere efficacemente la neuroinfiammazione, la demielinizzazione e la degenerazione assonale o neuronale.

## Ringraziamenti

---

E adesso la pagina che spesso viene aperta per prima dalla maggior parte di voi. Giunta alla chiusura di questo importante capitolo della mia vita, è tempo di ringraziare tutte le persone che in un modo o nell'altro mi hanno aiutato a scriverlo.

Desidero ringraziare innanzitutto chi ha contribuito da vicino alla realizzazione di questo lavoro di Dottorato. In primis le mie due tutor **Barbara** ed **Eleonora**, e la **Professoressa Claudia Martini** per avermi accolto nel Martini Lab e per avermi reso parte della TSPO-family. Grazie Barbara per la tua infinita disponibilità e il tuo meticoloso contributo nelle fasi critiche del lavoro. Grazie Ele per aver avuto fiducia in me fin da subito, proponendomi il Dottorato nonostante mi conoscessi relativamente poco, e per aver sempre e profondamente creduto in me. Grazie per gli spunti di riflessione e i tuoi consigli scientifici e non. Grazie ad entrambe per aver sempre appoggiato le mie scelte, per avermi dato l'opportunità di stare lontana dal nostro lab per un po' e per avermi guidato quanto basta per poi darmi gli strumenti e l'indipendenza necessaria.

Grazie **Letizia**, per le tue parole di incoraggiamento e i tuoi consigli, per la tua simpatia e la tua disponibilità a presiedere la Commissione d'esame finale.

Grazie anche a **Chiara** e **Laura**, è stato bello sapere di poter contare sempre sulla vostra preziosa opinione e sulle vostre parole di incoraggiamento in ogni situazione. Grazie **Simo**, anche se purtroppo non abbiamo avuto modo di interfacciarci per troppo tempo, sei sempre stata per me un punto di riferimento prezioso. Tra le senior del Martini Lab, grazie anche a **Chiara C.** per avermi guidato all'inizio del mio Dottorato e per avermi dato la possibilità di portare a termine un progetto da cui è uscito un bellissimo lavoro.

I want to thank **Professor Mensah-Nyagan** for welcoming me into his Lab in Strasbourg, and for giving me the opportunity to live a fantastic professional and personal experience that I would never forget. Thank you for your constant support and for your strong effort to make me grow as a researcher. I will always remember with pleasure the scientific and professional discussions between us.

I really need to thank all the people from the Research Unit 1119 at the University of Strasbourg, first of all **Laurance** and **Christine**. Merci pour votre aide ne la réalisation de l'article, et pour votre encouragement. Je me suis amusée beaucoup pendant nos conversations en Français et nos plaisanteries.

**Cele**, I feel so lucky to had the possibility to share my days in Strasbourg with you. Without you, it would have never been so good. Thanks for your daily support, and for being always smiling and happy to me and everyone. Thanks for our lunch breaks, *meriendas*, beers, dancing, walks, picnic, chatting, and office days. Thank you, **Amandine**, for your care, kindness, and energy, and for making

us a wonderful trio. I miss so much our moments together and our infinite chatting inside and outside the lab. Thank you also to all my other Lab friends: **Benjamin, Gertrude, Jérémie, Clarisse, Dani, Rémi,** and **Chiara**. I am convinced that true friendship can last despite the distance. Hoping to see each other again either in Italy, Argentina, Nigeria, France, or Sweden. I wish you all the best.

Vorrei dire un grandissimo grazie ai miei compagni di lab di Pisa: **Rebecca, Deborah, Mimì, Marty, Lara, Cecca, Martina, Sofia**. Grazie per aver condiviso quotidianamente piccole gioie e routinari disagi, e per il fatto che siamo riusciti a creare un gruppo affiatato fin da subito. Grazie per il tempo condiviso in Lab e in stanza dottorandi, i nostri pranzi rigorosamente all'aperto con qualsiasi condizione climatica, e gli infiniti caffè (talvolta troppo lunghi, e di certo non nel senso di durata). Vi auguro che possiate realizzarvi al meglio delle vostre -grandi- possibilità. Vi voglio bene.

**Elisa**, grazie a te in modo particolare per aver condiviso così da vicino gli ultimi mesi del mio dottorato, e i primi del tuo, giorni intensi che porterò sempre nel cuore. Grazie per avermi aiutato e appoggiato sempre. Sei stata e continui ad essere anche a distanza estremamente preziosa. Un grazie speciale anche a **Lorenzo**: abbiamo affrontato insieme cinque anni di studio anche tre di dottorato, provando ad aggiungere di un piccolo tassellino di conoscenza sulla nostra mitica proteina. Grazie per la nostra amicizia *vera* e per le nostre discussioni scientifiche, anche a 1500 km di distanza. Hai visto che alla fine, un *Tremolanti and Germelli et al.*, esiste davvero.

Al di là della tesi di Dottorato, è la mia famiglia a cui devo dire il grazie più grande al termine di questo percorso. È impossibile rendere a parole quanto siate importanti per me. Grazie **Mamma e Babbo** per aver accolto e supportato le mie scelte in ogni contesto. Spero di continuare a rendervi orgogliosi almeno la metà di cui quanto lo sia io di avere voi come genitori. **Franci**, semplicemente grazie per essere la mia metà in tutto. Sai benissimo che la distanza fisica non è niente in confronto alla nostra vicinanza.

Grazie anche a tutta la mia grande famiglia: nonni, zii e cugini, per farmi realizzare quanto sia bello avere una famiglia numerosa e unita come la nostra. **Nonna Anna e Nonno Arnaldo**, grazie per il vostro affetto e i vostri pensieri che sento forte anche da lontano, vi voglio tanto bene.

Grazie **Sara e Giulia** per il vostro incoraggiamento e per continuare ad essere coloro con cui so di poter condividere tutto. Nonostante siano cambiate tantissime cose in questi ultimi anni, so che la nostra amicizia è qualcosa su cui potrò contare per la vita.

Grazie alle mie amiche storiche: **Camilla, Bianca, Susanna**. Siete speciali, grazie per aver accolto e abbracciato il cambiamento del nostro rapporto, che da una presenza quotidiana è diventato una vicinanza costante di spirito. Vi voglio un bene dell'anima e vi auguro tutto il meglio.

Manca solamente chi ha vissuto insieme a me questo Dottorato in modo più vicino di quanto si possa immaginare. Grazie **Stefano** per credere ogni giorno così tanto in me e per avermi sempre spronato a dare il meglio e spingermi oltre i miei limiti. Grazie per la pazienza, il tuo aiuto, per le nostre infinite

discussioni scientifiche, e soprattutto per aver reso più semplice da affrontare ogni aspetto di questi anni così intensi.

Mi sento una persona estremamente fortunata ad essere circondata da tanta stima, affetto e amore. Adesso, tutto questo mi dà una grande carica per andare avanti e affrontare sfide sempre nuove ...The best is yet to come!

Grazie di cuore,

Chiara

## BIBLIOGRAPHY

---

- [1] N. J. Allen e D. A. Lyons, «Glia as architects of central nervous system formation and function», *Science*, vol. 362, n. 6411, pagg. 181–185, ott. 2018, doi: 10.1126/science.aat0473.
- [2] P. J. Magistretti, «Neuron–glia metabolic coupling and plasticity», *Journal of Experimental Biology*, vol. 209, n. 12, pagg. 2304–2311, giu. 2006, doi: 10.1242/jeb.02208.
- [3] M.-E. Tremblay, B. Stevens, A. Sierra, H. Wake, A. Bessis, e A. Nimmerjahn, «The Role of Microglia in the Healthy Brain», *Journal of Neuroscience*, vol. 31, n. 45, pagg. 16064–16069, nov. 2011, doi: 10.1523/JNEUROSCI.4158-11.2011.
- [4] K. Kierdorf *et al.*, «Microglia emerge from erythromyeloid precursors via Pu.1- and Irf8-dependent pathways», *Nat Neurosci*, vol. 16, n. 3, pagg. 273–280, mar. 2013, doi: 10.1038/nn.3318.
- [5] D. Davalos *et al.*, «ATP mediates rapid microglial response to local brain injury in vivo», *Nat Neurosci*, vol. 8, n. 6, pagg. 752–758, giu. 2005, doi: 10.1038/nn1472.
- [6] O. Garaschuk e A. Verkhratsky, «Physiology of Microglia», in *Microglia*, vol. 2034, O. Garaschuk e A. Verkhratsky, A c. di New York, NY: Springer New York, 2019, pagg. 27–40. doi: 10.1007/978-1-4939-9658-2\_3.
- [7] T. R. Hammond *et al.*, «Single-Cell RNA Sequencing of Microglia throughout the Mouse Lifespan and in the Injured Brain Reveals Complex Cell-State Changes», *Immunity*, vol. 50, n. 1, pagg. 253-271.e6, gen. 2019, doi: 10.1016/j.immuni.2018.11.004.
- [8] R. Franco e D. Fernández-Suárez, «Alternatively activated microglia and macrophages in the central nervous system», *Progress in Neurobiology*, vol. 131, pagg. 65–86, ago. 2015, doi: 10.1016/j.pneurobio.2015.05.003.
- [9] R. M. Ransohoff, «A polarizing question: do M1 and M2 microglia exist?», *Nat Neurosci*, vol. 19, n. 8, pagg. 987–991, ago. 2016, doi: 10.1038/nn.4338.
- [10] J. D. Crapser, E. E. Spangenberg, R. A. Barahona, M. A. Arreola, L. A. Hohsfield, e K. N. Green, «Microglia facilitate loss of perineuronal nets in the Alzheimer’s disease brain», *EBioMedicine*, vol. 58, pag. 102919, ago. 2020, doi: 10.1016/j.ebiom.2020.102919.
- [11] J. C. Nissen, K. K. Thompson, B. L. West, e S. E. Tsirka, «Csf1R inhibition attenuates experimental autoimmune encephalomyelitis and promotes recovery», *Experimental Neurology*, vol. 307, pagg. 24–36, set. 2018, doi: 10.1016/j.expneurol.2018.05.021.

- [12] I. Diaz-Aparicio *et al.*, «Microglia Actively Remodel Adult Hippocampal Neurogenesis through the Phagocytosis Secretome», *J. Neurosci.*, vol. 40, n. 7, pagg. 1453–1482, feb. 2020, doi: 10.1523/JNEUROSCI.0993-19.2019.
- [13] M. Kanazawa *et al.*, «Microglia preconditioned by oxygen-glucose deprivation promote functional recovery in ischemic rats», *Sci Rep*, vol. 7, n. 1, pag. 42582, mar. 2017, doi: 10.1038/srep42582.
- [14] M. Olah *et al.*, «Identification of a microglia phenotype supportive of remyelination», *Glia*, vol. 60, n. 2, pagg. 306–321, feb. 2012, doi: 10.1002/glia.21266.
- [15] O. Butovsky e H. L. Weiner, «Microglial signatures and their role in health and disease», *Nat Rev Neurosci*, vol. 19, n. 10, pagg. 622–635, ott. 2018, doi: 10.1038/s41583-018-0057-5.
- [16] M. W. Salter e B. Stevens, «Microglia emerge as central players in brain disease», *Nat Med*, vol. 23, n. 9, pagg. 1018–1027, set. 2017, doi: 10.1038/nm.4397.
- [17] D. Y. Vogel *et al.*, «Macrophages in inflammatory multiple sclerosis lesions have an intermediate activation status», *J Neuroinflammation*, vol. 10, n. 1, pag. 809, dic. 2013, doi: 10.1186/1742-2094-10-35.
- [18] L. A. N. Peferoen *et al.*, «Activation Status of Human Microglia Is Dependent on Lesion Formation Stage and Remyelination in Multiple Sclerosis», *J Neuropathol Exp Neurol*, vol. 74, n. 1, pagg. 48–63, gen. 2015, doi: 10.1097/NEN.0000000000000149.
- [19] A. Nimmerjahn, F. Kirchhoff, e F. Helmchen, «Resting Microglial Cells Are Highly Dynamic Surveillants of Brain Parenchyma in Vivo», *Science*, vol. 308, n. 5726, pagg. 1314–1318, mag. 2005, doi: 10.1126/science.1110647.
- [20] T. C. Brionne, I. Tesseur, E. Masliah, e T. Wyss-Coray, «Loss of TGF- $\beta$ 1 Leads to Increased Neuronal Cell Death and Microgliosis in Mouse Brain», *Neuron*, vol. 40, n. 6, pagg. 1133–1145, dic. 2003, doi: 10.1016/S0896-6273(03)00766-9.
- [21] C. Liu, Y. Shen, Y. Tang, e Y. Gu, «The role of N-glycosylation of CD200-CD200R1 interaction in classical microglial activation», *J Inflamm*, vol. 15, n. 1, pag. 28, dic. 2018, doi: 10.1186/s12950-018-0205-8.
- [22] D. Battista, C. C. Ferrari, F. H. Gage, e F. J. Pitossi, «Neurogenic niche modulation by activated microglia: transforming growth factor  $\beta$  increases neurogenesis in the adult dentate gyrus», *European Journal of Neuroscience*, vol. 23, n. 1, pagg. 83–93, gen. 2006, doi: 10.1111/j.1460-9568.2005.04539.x.

- [23] C. Gomes *et al.*, «Activation of microglial cells triggers a release of brain-derived neurotrophic factor (BDNF) inducing their proliferation in an adenosine A2A receptor-dependent manner: A2A receptor blockade prevents BDNF release and proliferation of microglia», *J Neuroinflammation*, vol. 10, n. 1, pag. 780, dic. 2013, doi: 10.1186/1742-2094-10-16.
- [24] C. N. Parkhurst *et al.*, «Microglia Promote Learning-Dependent Synapse Formation through Brain-Derived Neurotrophic Factor», *Cell*, vol. 155, n. 7, pagg. 1596–1609, dic. 2013, doi: 10.1016/j.cell.2013.11.030.
- [25] E. J. Huang e L. F. Reichardt, «Neurotrophins: Roles in Neuronal Development and Function», *Annu. Rev. Neurosci.*, vol. 24, n. 1, pagg. 677–736, mar. 2001, doi: 10.1146/annurev.neuro.24.1.677.
- [26] N. M. Walton *et al.*, «Microglia instruct subventricular zone neurogenesis», *Glia*, vol. 54, n. 8, pagg. 815–825, dic. 2006, doi: 10.1002/glia.20419.
- [27] E. Bar e B. Barak, «Microglia roles in synaptic plasticity and myelination in homeostatic conditions and neurodevelopmental disorders», *Glia*, vol. 67, n. 11, pagg. 2125–2141, nov. 2019, doi: 10.1002/glia.23637.
- [28] A. Sierra *et al.*, «Microglia Shape Adult Hippocampal Neurogenesis through Apoptosis-Coupled Phagocytosis», *Cell Stem Cell*, vol. 7, n. 4, pagg. 483–495, ott. 2010, doi: 10.1016/j.stem.2010.08.014.
- [29] S. F. Yanuck, «Microglial Phagocytosis of Neurons: Diminishing Neuronal Loss in Traumatic, Infectious, Inflammatory, and Autoimmune CNS Disorders», *Front. Psychiatry*, vol. 10, pag. 712, ott. 2019, doi: 10.3389/fpsyt.2019.00712.
- [30] F. Mazaheri *et al.*, «Distinct roles for BAI1 and TIM-4 in the engulfment of dying neurons by microglia», *Nat Commun*, vol. 5, n. 1, pag. 4046, set. 2014, doi: 10.1038/ncomms5046.
- [31] K. Takahashi, C. D. P. Rochford, e H. Neumann, «Clearance of apoptotic neurons without inflammation by microglial triggering receptor expressed on myeloid cells-2», *Journal of Experimental Medicine*, vol. 201, n. 4, pagg. 647–657, feb. 2005, doi: 10.1084/jem.20041611.
- [32] D. P. Schafer *et al.*, «Microglia Sculpt Postnatal Neural Circuits in an Activity and Complement-Dependent Manner», *Neuron*, vol. 74, n. 4, pagg. 691–705, mag. 2012, doi: 10.1016/j.neuron.2012.03.026.
- [33] M. Dani *et al.*, «Microglial activation correlates in vivo with both tau and amyloid in Alzheimer's disease», *Brain*, lug. 2018, doi: 10.1093/brain/awy188.

- [34] C. K. Donat, G. Scott, S. M. Gentleman, e M. Sastre, «Microglial Activation in Traumatic Brain Injury», *Front. Aging Neurosci.*, vol. 9, pag. 208, giu. 2017, doi: 10.3389/fnagi.2017.00208.
- [35] O. W. Howell, J. L. Rundle, A. Garg, M. Komada, P. J. Brophy, e R. Reynolds, «Activated Microglia Mediate Axoglia Disruption That Contributes to Axonal Injury in Multiple Sclerosis», *J Neuropathol Exp Neurol*, vol. 69, n. 10, pagg. 1017–1033, ott. 2010, doi: 10.1097/NEN.0b013e3181f3a5b1.
- [36] M. del M. Fernández-Arjona, J. M. Grondona, P. Granados-Durán, P. Fernández-Llebrez, e M. D. López-Ávalos, «Microglia Morphological Categorization in a Rat Model of Neuroinflammation by Hierarchical Cluster and Principal Components Analysis», *Front. Cell. Neurosci.*, vol. 11, pag. 235, ago. 2017, doi: 10.3389/fncel.2017.00235.
- [37] D. Boche, V. H. Perry, e J. a. R. Nicoll, «Review: activation patterns of microglia and their identification in the human brain», *Neuropathol Appl Neurobiol*, vol. 39, n. 1, pagg. 3–18, feb. 2013, doi: 10.1111/nan.12011.
- [38] I. R. Holtman *et al.*, «Induction of a common microglia gene expression signature by aging and neurodegenerative conditions: a co-expression meta-analysis», *acta neuropathol commun*, vol. 3, n. 1, pag. 31, dic. 2015, doi: 10.1186/s40478-015-0203-5.
- [39] F. Ebner *et al.*, «Microglial activation milieu controls regulatory T cell responses», *J Immunol*, vol. 191, n. 11, pagg. 5594–5602, dic. 2013, doi: 10.4049/jimmunol.1203331.
- [40] S. Lively e L. C. Schlichter, «Microglia Responses to Pro-inflammatory Stimuli (LPS, IFN $\gamma$ +TNF $\alpha$ ) and Reprogramming by Resolving Cytokines (IL-4, IL-10)», *Front. Cell. Neurosci.*, vol. 12, pag. 215, lug. 2018, doi: 10.3389/fncel.2018.00215.
- [41] Y. Chung *et al.*, «Critical regulation of early Th17 cell differentiation by interleukin-1 signaling», *Immunity*, vol. 30, n. 4, pagg. 576–587, apr. 2009, doi: 10.1016/j.immuni.2009.02.007.
- [42] C. L. Langrish *et al.*, «IL-23 drives a pathogenic T cell population that induces autoimmune inflammation», *J Exp Med*, vol. 201, n. 2, pagg. 233–240, gen. 2005, doi: 10.1084/jem.20041257.
- [43] M. L. Block, L. Zecca, e J.-S. Hong, «Microglia-mediated neurotoxicity: uncovering the molecular mechanisms», *Nat Rev Neurosci*, vol. 8, n. 1, pagg. 57–69, gen. 2007, doi: 10.1038/nrn2038.
- [44] M. Sospedra e R. Martin, «Immunology of Multiple Sclerosis», *Semin Neurol*, vol. 36, n. 2, pagg. 115–127, apr. 2016, doi: 10.1055/s-0036-1579739.

- [45] C. Stadelmann, S. Timmler, A. Barrantes-Freer, e M. Simons, «Myelin in the Central Nervous System: Structure, Function, and Pathology», *Physiol Rev*, vol. 99, n. 3, pagg. 1381–1431, lug. 2019, doi: 10.1152/physrev.00031.2018.
- [46] S. Y. C. Chong *et al.*, «Neurite outgrowth inhibitor Nogo-A establishes spatial segregation and extent of oligodendrocyte myelination», *Proc Natl Acad Sci U S A*, vol. 109, n. 4, pagg. 1299–1304, gen. 2012, doi: 10.1073/pnas.1113540109.
- [47] N. Snaidero *et al.*, «Myelin membrane wrapping of CNS axons by PI(3,4,5)P3-dependent polarized growth at the inner tongue», *Cell*, vol. 156, n. 1–2, pagg. 277–290, gen. 2014, doi: 10.1016/j.cell.2013.11.044.
- [48] M. Simons e K.-A. Nave, «Oligodendrocytes: Myelination and Axonal Support», *Cold Spring Harb Perspect Biol*, vol. 8, n. 1, pag. a020479, giu. 2015, doi: 10.1101/cshperspect.a020479.
- [49] C. M. Deber e S. J. Reynolds, «Central nervous system myelin: structure, function, and pathology», *Clin Biochem*, vol. 24, n. 2, pagg. 113–134, apr. 1991, doi: 10.1016/0009-9120(91)90421-a.
- [50] S. Poliak e E. Peles, «The local differentiation of myelinated axons at nodes of Ranvier», *Nat Rev Neurosci*, vol. 4, n. 12, pagg. 968–980, dic. 2003, doi: 10.1038/nrn1253.
- [51] R. D. Fields, «A new mechanism of nervous system plasticity: activity-dependent myelination», *Nat Rev Neurosci*, vol. 16, n. 12, pagg. 756–767, dic. 2015, doi: 10.1038/nrn4023.
- [52] O. Jahn, S. Tenzer, e H. B. Werner, «Myelin proteomics: molecular anatomy of an insulating sheath», *Mol Neurobiol*, vol. 40, n. 1, pagg. 55–72, ago. 2009, doi: 10.1007/s12035-009-8071-2.
- [53] P. Morell e W. T. Norton, «Myelin», *Sci Am*, vol. 242, n. 5, pagg. 88–90, 92, 96 passim, mag. 1980, doi: 10.1038/scientificamerican0580-88.
- [54] S. Schmitt, L. C. Castelvetti, e M. Simons, «Metabolism and functions of lipids in myelin», *Biochim Biophys Acta*, vol. 1851, n. 8, pagg. 999–1005, ago. 2015, doi: 10.1016/j.bbaliip.2014.12.016.
- [55] Y. Poitelon, A. M. Kopec, e S. Belin, «Myelin Fat Facts: An Overview of Lipids and Fatty Acid Metabolism», *Cells*, vol. 9, n. 4, pag. E812, mar. 2020, doi: 10.3390/cells9040812.
- [56] J. Zhang e Q. Liu, «Cholesterol metabolism and homeostasis in the brain», *Protein Cell*, vol. 6, n. 4, pagg. 254–264, apr. 2015, doi: 10.1007/s13238-014-0131-3.
- [57] J. M. Dietschy e S. D. Turley, «Thematic review series: brain Lipids. Cholesterol metabolism in the central nervous system during early development and in the mature animal», *J Lipid Res*, vol. 45, n. 8, pagg. 1375–1397, ago. 2004, doi: 10.1194/jlr.R400004-JLR200.

- [58] J. Lessig e B. Fuchs, «Plasmalogens in biological systems: their role in oxidative processes in biological membranes, their contribution to pathological processes and aging and plasmalogen analysis», *Curr Med Chem*, vol. 16, n. 16, pagg. 2021–2041, 2009, doi: 10.2174/092986709788682164.
- [59] J. P. Palavicini *et al.*, «Novel molecular insights into the critical role of sulfatide in myelin maintenance/function», *J Neurochem*, vol. 139, n. 1, pagg. 40–54, ott. 2016, doi: 10.1111/jnc.13738.
- [60] J. L. Dupree, T. Coetzee, K. Suzuki, e B. Popko, «Myelin abnormalities in mice deficient in galactocerebroside and sulfatide», *J Neurocytol*, vol. 27, n. 9, pagg. 649–659, set. 1998, doi: 10.1023/a:1006908013972.
- [61] H. Ozgen, W. Baron, D. Hoekstra, e N. Kahya, «Oligodendroglial membrane dynamics in relation to myelin biogenesis», *Cell Mol Life Sci*, vol. 73, n. 17, pagg. 3291–3310, set. 2016, doi: 10.1007/s00018-016-2228-8.
- [62] J. Rosenbluth, Z. Liu, D. Guo, e R. Schiff, «Inhibition of CNS myelin development in vivo by implantation of anti-GalC hybridoma cells», *J Neurocytol*, vol. 23, n. 11, pagg. 699–707, nov. 1994, doi: 10.1007/BF01181644.
- [63] A. Ishii, D. Han, e R. Bansal, «Proteomics Analysis of Myelin Composition», *Methods Mol Biol*, vol. 1791, pagg. 67–77, 2018, doi: 10.1007/978-1-4939-7862-5\_6.
- [64] H. Han, M. Myllykoski, S. Ruskamo, C. Wang, e P. Kursula, «Myelin-specific proteins: a structurally diverse group of membrane-interacting molecules», *Biofactors*, vol. 39, n. 3, pagg. 233–241, giu. 2013, doi: 10.1002/biof.1076.
- [65] J. M. Greer e M. B. Lees, «Myelin proteolipid protein--the first 50 years», *Int J Biochem Cell Biol*, vol. 34, n. 3, pagg. 211–215, mar. 2002, doi: 10.1016/s1357-2725(01)00136-4.
- [66] P. A. Wight e A. Dobretsova, «Where, when and how much: regulation of myelin proteolipid protein gene expression», *Cell Mol Life Sci*, vol. 61, n. 7–8, pagg. 810–821, apr. 2004, doi: 10.1007/s00018-003-3309-z.
- [67] M. Klugmann *et al.*, «Assembly of CNS myelin in the absence of proteolipid protein», *Neuron*, vol. 18, n. 1, pagg. 59–70, gen. 1997, doi: 10.1016/s0896-6273(01)80046-5.
- [68] H. B. Werner *et al.*, «A critical role for the cholesterol-associated proteolipids PLP and M6B in myelination of the central nervous system», *Glia*, vol. 61, n. 4, pagg. 567–586, apr. 2013, doi: 10.1002/glia.22456.

- [69] G. Harauz e J. M. Boggs, «Myelin management by the 18.5-kDa and 21.5-kDa classic myelin basic protein isoforms», *J Neurochem*, vol. 125, n. 3, pagg. 334–361, mag. 2013, doi: 10.1111/jnc.12195.
- [70] M. Kimura *et al.*, «Molecular genetic analysis of myelin-deficient mice: shiverer mutant mice show deletion in gene(s) coding for myelin basic protein», *J Neurochem*, vol. 44, n. 3, pagg. 692–696, mar. 1985, doi: 10.1111/j.1471-4159.1985.tb12870.x.
- [71] A. Privat, C. Jacque, J. M. Bourre, P. Dupouey, e N. Baumann, «Absence of the major dense line in myelin of the mutant mouse “shiverer”», *Neurosci Lett*, vol. 12, n. 1, pagg. 107–112, apr. 1979, doi: 10.1016/0304-3940(79)91489-7.
- [72] N. A. Ponomarenko *et al.*, «Autoantibodies to myelin basic protein catalyze site-specific degradation of their antigen», *Proc Natl Acad Sci U S A*, vol. 103, n. 2, pagg. 281–286, gen. 2006, doi: 10.1073/pnas.0509849103.
- [73] M. Pette *et al.*, «Myelin basic protein-specific T lymphocyte lines from MS patients and healthy individuals», *Neurology*, vol. 40, n. 11, pagg. 1770–1776, nov. 1990, doi: 10.1212/wnl.40.11.1770.
- [74] A. Raasakka e P. Kursula, «The myelin membrane-associated enzyme 2',3'-cyclic nucleotide 3'-phosphodiesterase: on a highway to structure and function», *Neurosci Bull*, vol. 30, n. 6, pagg. 956–966, dic. 2014, doi: 10.1007/s12264-013-1437-5.
- [75] S. S. Scherer, P. E. Braun, J. Grinspan, E. Collarini, D. Y. Wang, e J. Kamholz, «Differential regulation of the 2',3'-cyclic nucleotide 3'-phosphodiesterase gene during oligodendrocyte development», *Neuron*, vol. 12, n. 6, pagg. 1363–1375, giu. 1994, doi: 10.1016/0896-6273(94)90451-0.
- [76] J. Lee, M. Gravel, R. Zhang, P. Thibault, e P. E. Braun, «Process outgrowth in oligodendrocytes is mediated by CNP, a novel microtubule assembly myelin protein», *J Cell Biol*, vol. 170, n. 4, pagg. 661–673, ago. 2005, doi: 10.1083/jcb.200411047.
- [77] Y. Chen, S. Aulia, e B. L. Tang, «Myelin-associated glycoprotein-mediated signaling in central nervous system pathophysiology», *Mol Neurobiol*, vol. 34, n. 2, pagg. 81–91, ott. 2006, doi: 10.1385/MN:34:2:81.
- [78] S. K. Solly *et al.*, «Myelin/oligodendrocyte glycoprotein (MOG) expression is associated with myelin deposition», *Glia*, vol. 18, n. 1, pagg. 39–48, set. 1996, doi: 10.1002/(SICI)1098-1136(199609)18:1<39::AID-GLIA4>3.0.CO;2-Z.

- [79] S. Aggarwal, L. Yurlova, e M. Simons, «Central nervous system myelin: structure, synthesis and assembly», *Trends Cell Biol*, vol. 21, n. 10, pagg. 585–593, ott. 2011, doi: 10.1016/j.tcb.2011.06.004.
- [80] B. Elbaz e B. Popko, «Molecular Control of Oligodendrocyte Development», *Trends Neurosci*, vol. 42, n. 4, pagg. 263–277, apr. 2019, doi: 10.1016/j.tins.2019.01.002.
- [81] A. Tiane *et al.*, «From OPC to Oligodendrocyte: An Epigenetic Journey», *Cells*, vol. 8, n. 10, pag. E1236, ott. 2019, doi: 10.3390/cells8101236.
- [82] B. Rogister, T. Ben-Hur, e M. Dubois-Dalcq, «From neural stem cells to myelinating oligodendrocytes», *Mol Cell Neurosci*, vol. 14, n. 4–5, pagg. 287–300, nov. 1999, doi: 10.1006/mcne.1999.0790.
- [83] S. Kuhn, L. Gritti, D. Crooks, e Y. Dombrowski, «Oligodendrocytes in Development, Myelin Generation and Beyond», *Cells*, vol. 8, n. 11, pag. E1424, nov. 2019, doi: 10.3390/cells8111424.
- [84] S. A. Goldman e N. J. Kuypers, «How to make an oligodendrocyte», *Development*, vol. 142, n. 23, pagg. 3983–3995, dic. 2015, doi: 10.1242/dev.126409.
- [85] I. Sommer e M. Schachner, «Monoclonal antibodies (O1 to O4) to oligodendrocyte cell surfaces: an immunocytological study in the central nervous system», *Dev Biol*, vol. 83, n. 2, pagg. 311–327, apr. 1981, doi: 10.1016/0012-1606(81)90477-2.
- [86] J.-P. Michalski, C. Anderson, A. Beauvais, Y. De Repentigny, e R. Kothary, «The proteolipid protein promoter drives expression outside of the oligodendrocyte lineage during embryonic and early postnatal development», *PLoS One*, vol. 6, n. 5, pag. e19772, mag. 2011, doi: 10.1371/journal.pone.0019772.
- [87] E. Barbarese *et al.*, «Expression and localization of myelin basic protein in oligodendrocytes and transfected fibroblasts», *J Neurochem*, vol. 51, n. 6, pagg. 1737–1745, dic. 1988, doi: 10.1111/j.1471-4159.1988.tb01153.x.
- [88] B. D. Trapp, «Myelin-associated glycoprotein. Location and potential functions», *Ann N Y Acad Sci*, vol. 605, pagg. 29–43, 1990, doi: 10.1111/j.1749-6632.1990.tb42378.x.
- [89] M. C. Raff *et al.*, «Galactocerebroside is a specific cell-surface antigenic marker for oligodendrocytes in culture», *Nature*, vol. 274, n. 5673, pagg. 813–816, ago. 1978.
- [90] C. Brunner, H. Lassmann, T. V. Waehneltd, J. M. Matthieu, e C. Linington, «Differential ultrastructural localization of myelin basic protein, myelin/oligodendroglial glycoprotein, and 2',3'-cyclic nucleotide 3'-phosphodiesterase in the CNS of adult rats», *J Neurochem*, vol. 52, n. 1, pagg. 296–304, gen. 1989, doi: 10.1111/j.1471-4159.1989.tb10930.x.

- [91] N. Kessaris, M. Fogarty, P. Iannarelli, M. Grist, M. Wegner, e W. D. Richardson, «Competing waves of oligodendrocytes in the forebrain and postnatal elimination of an embryonic lineage», *Nat Neurosci*, vol. 9, n. 2, pagg. 173–179, feb. 2006, doi: 10.1038/nn1620.
- [92] K.-A. Nave e H. B. Werner, «Myelination of the nervous system: mechanisms and functions», *Annu Rev Cell Dev Biol*, vol. 30, pagg. 503–533, 2014, doi: 10.1146/annurev-cellbio-100913-013101.
- [93] K. M. Welker e A. Patton, «Assessment of normal myelination with magnetic resonance imaging», *Semin Neurol*, vol. 32, n. 1, pagg. 15–28, feb. 2012, doi: 10.1055/s-0032-1306382.
- [94] S. E. Nasrabady, B. Rizvi, J. E. Goldman, e A. M. Brickman, «White matter changes in Alzheimer’s disease: a focus on myelin and oligodendrocytes», *Acta Neuropathol Commun*, vol. 6, n. 1, pag. 22, mar. 2018, doi: 10.1186/s40478-018-0515-3.
- [95] F. Wang *et al.*, «Myelin degeneration and diminished myelin renewal contribute to age-related deficits in memory», *Nat Neurosci*, vol. 23, n. 4, pagg. 481–486, apr. 2020, doi: 10.1038/s41593-020-0588-8.
- [96] K. Inoue, «Pelizaeus-Merzbacher Disease: Molecular and Cellular Pathologies and Associated Phenotypes», *Adv Exp Med Biol*, vol. 1190, pagg. 201–216, 2019, doi: 10.1007/978-981-32-9636-7\_13.
- [97] R. Singh e D. Samanta, «Pelizaeus-Merzbacher Disease», in *StatPearls*, Treasure Island (FL): StatPearls Publishing, 2021. Consultato: 24 dicembre 2021. [Online]. Disponibile su: <http://www.ncbi.nlm.nih.gov/books/NBK560522/>
- [98] K. Inoue, «PLP1-related inherited dysmyelinating disorders: Pelizaeus-Merzbacher disease and spastic paraplegia type 2», *Neurogenetics*, vol. 6, n. 1, pagg. 1–16, feb. 2005, doi: 10.1007/s10048-004-0207-y.
- [99] K. Inoue *et al.*, «Proteolipid protein gene duplications causing Pelizaeus-Merzbacher disease: molecular mechanism and phenotypic manifestations», *Ann Neurol*, vol. 45, n. 5, pagg. 624–632, mag. 1999.
- [100] G. M. Hobson e J. Y. Garbern, «Pelizaeus-Merzbacher disease, Pelizaeus-Merzbacher-like disease 1, and related hypomyelinating disorders», *Semin Neurol*, vol. 32, n. 1, pagg. 62–67, feb. 2012, doi: 10.1055/s-0032-1306388.
- [101] F. Cailloux *et al.*, «Genotype-phenotype correlation in inherited brain myelination defects due to proteolipid protein gene mutations. Clinical European Network on Brain Dysmyelinating Disease», *Eur J Hum Genet*, vol. 8, n. 11, pagg. 837–845, nov. 2000, doi: 10.1038/sj.ejhg.5200537.

- [102] R. L. Sidman, M. M. Dickie, e S. H. Appel, «MUTANT MICE (QUAKING AND JIMPY) WITH DEFICIENT MYELINATION IN THE CENTRAL NERVOUS SYSTEM», *Science*, vol. 144, n. 3616, pagg. 309–311, apr. 1964, doi: 10.1126/science.144.3616.309.
- [103] L. Harsan, W. Jalabi, D. Grucker, e M. S. Ghandour, «New insights on neuronal alterations in jimpy mutant brain», *Neurochem Res*, vol. 29, n. 5, pagg. 943–952, mag. 2004, doi: 10.1023/b:nere.0000021238.00299.93.
- [104] K. A. Nave, C. Lai, F. E. Bloom, e R. J. Milner, «Jimpy mutant mouse: a 74-base deletion in the mRNA for myelin proteolipid protein and evidence for a primary defect in RNA splicing», *Proc Natl Acad Sci U S A*, vol. 83, n. 23, pagg. 9264–9268, dic. 1986, doi: 10.1073/pnas.83.23.9264.
- [105] R. P. Skoff, I. Saluja, D. Bessert, e X. Yang, «Analyses of proteolipid protein mutants show levels of proteolipid protein regulate oligodendrocyte number and cell death in vitro and in vivo», *Neurochem Res*, vol. 29, n. 11, pagg. 2095–2103, nov. 2004, doi: 10.1007/s11064-004-6882-0.
- [106] C. M. Southwood, J. Garbern, W. Jiang, e A. Gow, «The unfolded protein response modulates disease severity in Pelizaeus-Merzbacher disease», *Neuron*, vol. 36, n. 4, pagg. 585–596, nov. 2002, doi: 10.1016/s0896-6273(02)01045-0.
- [107] C. Hetz, K. Zhang, e R. J. Kaufman, «Mechanisms, regulation and functions of the unfolded protein response», *Nat Rev Mol Cell Biol*, vol. 21, n. 8, pagg. 421–438, ago. 2020, doi: 10.1038/s41580-020-0250-z.
- [108] A. C. Feutz, D. Pham-Dinh, B. Allinquant, M. Mieke, e M. S. Ghandour, «An immortalized jimpy oligodendrocyte cell line: defects in cell cycle and cAMP pathway», *Glia*, vol. 34, n. 4, pagg. 241–252, giu. 2001, doi: 10.1002/glia.1058.
- [109] M. S. Ghandour *et al.*, «Trafficking of PLP/DM20 and cAMP signaling in immortalized jimpy oligodendrocytes», *Glia*, vol. 40, n. 3, pagg. 300–311, dic. 2002, doi: 10.1002/glia.10122.
- [110] M. Baarine *et al.*, «Peroxisomal and mitochondrial status of two murine oligodendrocytic cell lines (158N, 158JP): potential models for the study of peroxisomal disorders associated with dysmyelination processes», *J Neurochem*, vol. 111, n. 1, pagg. 119–131, ott. 2009, doi: 10.1111/j.1471-4159.2009.06311.x.
- [111] A.-S. Wilding, C. Patte-Mensah, O. Taleb, S. Brun, V. Kemmel, e A.-G. Mensah-Nyagan, «Protective effect of 4-Phenylbutyrate against proteolipid protein mutation-induced endoplasmic reticulum stress and oligodendroglial cell death», *Neurochem Int*, vol. 118, pagg. 185–194, set. 2018, doi: 10.1016/j.neuint.2018.06.008.

- [112] H. Li *et al.*, «Gene suppressing therapy for Pelizaeus-Merzbacher disease using artificial microRNA», *JCI Insight*, vol. 4, n. 10, pag. 125052, mag. 2019, doi: 10.1172/jci.insight.125052.
- [113] M. J. Osorio, D. H. Rowitch, P. Tesar, M. Wernig, M. S. Windrem, e S. A. Goldman, «Concise Review: Stem Cell-Based Treatment of Pelizaeus-Merzbacher Disease», *Stem Cells*, vol. 35, n. 2, pagg. 311–315, feb. 2017, doi: 10.1002/stem.2530.
- [114] H. Nobuta *et al.*, «Oligodendrocyte Death in Pelizaeus-Merzbacher Disease Is Rescued by Iron Chelation», *Cell Stem Cell*, vol. 25, n. 4, pagg. 531-541.e6, ott. 2019, doi: 10.1016/j.stem.2019.09.003.
- [115] M. S. Elitt *et al.*, «Suppression of proteolipid protein rescues Pelizaeus-Merzbacher disease», *Nature*, vol. 585, n. 7825, pagg. 397–403, set. 2020, doi: 10.1038/s41586-020-2494-3.
- [116] M. Jinek, K. Chylinski, I. Fonfara, M. Hauer, J. A. Doudna, e E. Charpentier, «A programmable dual-RNA-guided DNA endonuclease in adaptive bacterial immunity», *Science*, vol. 337, n. 6096, pagg. 816–821, ago. 2012, doi: 10.1126/science.1225829.
- [117] Y. Jiang, B. Chen, C. Duan, B. Sun, J. Yang, e S. Yang, «Multigene editing in the Escherichia coli genome via the CRISPR-Cas9 system», *Appl Environ Microbiol*, vol. 81, n. 7, pagg. 2506–2514, apr. 2015, doi: 10.1128/AEM.04023-14.
- [118] F. Zhang, Y. Wen, e X. Guo, «CRISPR/Cas9 for genome editing: progress, implications and challenges», *Hum Mol Genet*, vol. 23, n. R1, pagg. R40-46, set. 2014, doi: 10.1093/hmg/ddu125.
- [119] E. Danner, S. Bashir, S. Yumlu, W. Wurst, B. Wefers, e R. Kühn, «Control of gene editing by manipulation of DNA repair mechanisms», *Mamm Genome*, vol. 28, n. 7–8, pagg. 262–274, ago. 2017, doi: 10.1007/s00335-017-9688-5.
- [120] F. A. Ran *et al.*, «Double nicking by RNA-guided CRISPR Cas9 for enhanced genome editing specificity», *Cell*, vol. 154, n. 6, pagg. 1380–1389, set. 2013, doi: 10.1016/j.cell.2013.08.021.
- [121] S. W. Cho *et al.*, «Analysis of off-target effects of CRISPR/Cas-derived RNA-guided endonucleases and nickases», *Genome Res*, vol. 24, n. 1, pagg. 132–141, gen. 2014, doi: 10.1101/gr.162339.113.
- [122] C. A. Dendrou, L. Fugger, e M. A. Friese, «Immunopathology of multiple sclerosis», *Nat Rev Immunol*, vol. 15, n. 9, pagg. 545–558, set. 2015, doi: 10.1038/nri3871.
- [123] P. Browne *et al.*, «Atlas of Multiple Sclerosis 2013: A growing global problem with widespread inequity», *Neurology*, vol. 83, n. 11, pagg. 1022–1024, set. 2014, doi: 10.1212/WNL.0000000000000768.

- [124] M. Filippi *et al.*, «Author Correction: Multiple sclerosis», *Nat Rev Dis Primers*, vol. 4, n. 1, pag. 49, nov. 2018, doi: 10.1038/s41572-018-0050-3.
- [125] F. D. Lublin *et al.*, «Defining the clinical course of multiple sclerosis: the 2013 revisions», *Neurology*, vol. 83, n. 3, pagg. 278–286, lug. 2014, doi: 10.1212/WNL.0000000000000560.
- [126] A. Scalfari, V. Knappertz, G. Cutter, D. S. Goodin, R. Ashton, e G. C. Ebers, «Mortality in patients with multiple sclerosis», *Neurology*, vol. 81, n. 2, pagg. 184–192, lug. 2013, doi: 10.1212/WNL.0b013e31829a3388.
- [127] T. Olsson, L. F. Barcellos, e L. Alfredsson, «Interactions between genetic, lifestyle and environmental risk factors for multiple sclerosis», *Nat Rev Neurol*, vol. 13, n. 1, pagg. 25–36, gen. 2017, doi: 10.1038/nrneurol.2016.187.
- [128] C. Walton *et al.*, «Rising prevalence of multiple sclerosis worldwide: Insights from the Atlas of MS, third edition», *Mult Scler*, vol. 26, n. 14, pagg. 1816–1821, dic. 2020, doi: 10.1177/1352458520970841.
- [129] N. Koch-Henriksen e P. S. Sørensen, «The changing demographic pattern of multiple sclerosis epidemiology», *Lancet Neurol*, vol. 9, n. 5, pagg. 520–532, mag. 2010, doi: 10.1016/S1474-4422(10)70064-8.
- [130] M. H. Barnett, D. B. Williams, S. Day, P. Macaskill, e J. G. McLeod, «Progressive increase in incidence and prevalence of multiple sclerosis in Newcastle, Australia: a 35-year study», *J Neurol Sci*, vol. 213, n. 1–2, pagg. 1–6, set. 2003, doi: 10.1016/s0022-510x(03)00122-9.
- [131] L. I. Levin *et al.*, «Temporal relationship between elevation of epstein-barr virus antibody titers and initial onset of neurological symptoms in multiple sclerosis», *JAMA*, vol. 293, n. 20, pagg. 2496–2500, mag. 2005, doi: 10.1001/jama.293.20.2496.
- [132] M. H. Harirchian, F. Fatehi, P. Sarraf, N. M. Honarvar, e S. Bitarafan, «Worldwide prevalence of familial multiple sclerosis: A systematic review and meta-analysis», *Mult Scler Relat Disord*, vol. 20, pagg. 43–47, feb. 2018, doi: 10.1016/j.msard.2017.12.015.
- [133] C. Cotsapas e M. Mitrovic, «Genome-wide association studies of multiple sclerosis», *Clin Transl Immunology*, vol. 7, n. 6, pag. e1018, 2018, doi: 10.1002/cti2.1018.
- [134] S. E. Baranzini e J. R. Oksenberg, «The Genetics of Multiple Sclerosis: From 0 to 200 in 50 Years», *Trends Genet*, vol. 33, n. 12, pagg. 960–970, dic. 2017, doi: 10.1016/j.tig.2017.09.004.
- [135] N. A. Patsopoulos *et al.*, «Fine-mapping the genetic association of the major histocompatibility complex in multiple sclerosis: HLA and non-HLA effects», *PLoS Genet*, vol. 9, n. 11, pag. e1003926, nov. 2013, doi: 10.1371/journal.pgen.1003926.

- [136] International Multiple Sclerosis Genetics Consortium *et al.*, «Risk alleles for multiple sclerosis identified by a genomewide study», *N Engl J Med*, vol. 357, n. 9, pagg. 851–862, ago. 2007, doi: 10.1056/NEJMoa073493.
- [137] L. Kular *et al.*, «DNA methylation as a mediator of HLA-DRB1\*15:01 and a protective variant in multiple sclerosis», *Nat Commun*, vol. 9, n. 1, pag. 2397, giu. 2018, doi: 10.1038/s41467-018-04732-5.
- [138] M. Magyari, «Gender differences in multiple sclerosis epidemiology and treatment response», *Dan Med J*, vol. 63, n. 3, pag. B5212, mar. 2016.
- [139] C. Selmi, «The X in sex: how autoimmune diseases revolve around sex chromosomes», *Best Pract Res Clin Rheumatol*, vol. 22, n. 5, pagg. 913–922, ott. 2008, doi: 10.1016/j.berh.2008.09.002.
- [140] E. M. Frohman, M. K. Racke, e C. S. Raine, «Multiple sclerosis--the plaque and its pathogenesis», *N Engl J Med*, vol. 354, n. 9, pagg. 942–955, mar. 2006, doi: 10.1056/NEJMra052130.
- [141] M. A. Rocca *et al.*, «Clinical and imaging assessment of cognitive dysfunction in multiple sclerosis», *Lancet Neurol*, vol. 14, n. 3, pagg. 302–317, mar. 2015, doi: 10.1016/S1474-4422(14)70250-9.
- [142] M. Filippi *et al.*, «Assessment of lesions on magnetic resonance imaging in multiple sclerosis: practical guidelines», *Brain*, vol. 142, n. 7, pagg. 1858–1875, lug. 2019, doi: 10.1093/brain/awz144.
- [143] D. de P. Faria, S. Copray, C. Buchpiguel, R. Dierckx, e E. de Vries, «PET imaging in multiple sclerosis», *J Neuroimmune Pharmacol*, vol. 9, n. 4, pagg. 468–482, set. 2014, doi: 10.1007/s11481-014-9544-2.
- [144] L. Airas, E. Rissanen, e J. O. Rinne, «Imaging neuroinflammation in multiple sclerosis using TSPO-PET», *Clin Transl Imaging*, vol. 3, pagg. 461–473, 2015, doi: 10.1007/s40336-015-0147-6.
- [145] C. Baecher-Allan, B. J. Kaskow, e H. L. Weiner, «Multiple Sclerosis: Mechanisms and Immunotherapy», *Neuron*, vol. 97, n. 4, pagg. 742–768, feb. 2018, doi: 10.1016/j.neuron.2018.01.021.
- [146] H. Kebir *et al.*, «Human TH17 lymphocytes promote blood-brain barrier disruption and central nervous system inflammation», *Nat Med*, vol. 13, n. 10, pagg. 1173–1175, ott. 2007, doi: 10.1038/nm1651.
- [147] B. Hemmer, M. Kerschensteiner, e T. Korn, «Role of the innate and adaptive immune responses in the course of multiple sclerosis», *Lancet Neurol*, vol. 14, n. 4, pagg. 406–419, apr. 2015, doi: 10.1016/S1474-4422(14)70305-9.

- [148] L. Schirmer, R. Srivastava, e B. Hemmer, «To look for a needle in a haystack: the search for autoantibodies in multiple sclerosis», *Mult Scler*, vol. 20, n. 3, pagg. 271–279, mar. 2014, doi: 10.1177/1352458514522104.
- [149] R. Li, K. R. Patterson, e A. Bar-Or, «Reassessing B cell contributions in multiple sclerosis», *Nat Immunol*, vol. 19, n. 7, pagg. 696–707, lug. 2018, doi: 10.1038/s41590-018-0135-x.
- [150] J. van Horssen *et al.*, «Clusters of activated microglia in normal-appearing white matter show signs of innate immune activation», *J Neuroinflammation*, vol. 9, pag. 156, lug. 2012, doi: 10.1186/1742-2094-9-156.
- [151] G. G. Ortiz *et al.*, «Role of the blood-brain barrier in multiple sclerosis», *Arch Med Res*, vol. 45, n. 8, pagg. 687–697, nov. 2014, doi: 10.1016/j.arcmed.2014.11.013.
- [152] T. Zrzavy, S. Hametner, I. Wimmer, O. Butovsky, H. L. Weiner, e H. Lassmann, «Loss of “homeostatic” microglia and patterns of their activation in active multiple sclerosis», *Brain*, vol. 140, n. 7, pagg. 1900–1913, lug. 2017, doi: 10.1093/brain/awx113.
- [153] J. Machado-Santos *et al.*, «The compartmentalized inflammatory response in the multiple sclerosis brain is composed of tissue-resident CD8+ T lymphocytes and B cells», *Brain*, vol. 141, n. 7, pagg. 2066–2082, lug. 2018, doi: 10.1093/brain/awy151.
- [154] L. A. Boven *et al.*, «Myelin-laden macrophages are anti-inflammatory, consistent with foam cells in multiple sclerosis», *Brain*, vol. 129, n. Pt 2, pagg. 517–526, feb. 2006, doi: 10.1093/brain/awh707.
- [155] V. E. Miron *et al.*, «M2 microglia and macrophages drive oligodendrocyte differentiation during CNS remyelination», *Nat Neurosci*, vol. 16, n. 9, pagg. 1211–1218, set. 2013, doi: 10.1038/nn.3469.
- [156] B. Hemmer, J. J. Archelos, e H.-P. Hartung, «New concepts in the immunopathogenesis of multiple sclerosis», *Nat Rev Neurosci*, vol. 3, n. 4, pagg. 291–301, apr. 2002, doi: 10.1038/nrn784.
- [157] M. Filippi *et al.*, «Evidence for widespread axonal damage at the earliest clinical stage of multiple sclerosis», *Brain*, vol. 126, n. Pt 2, pagg. 433–437, feb. 2003, doi: 10.1093/brain/awg038.
- [158] N. De Stefano *et al.*, «Diffuse axonal and tissue injury in patients with multiple sclerosis with low cerebral lesion load and no disability», *Arch Neurol*, vol. 59, n. 10, pagg. 1565–1571, ott. 2002, doi: 10.1001/archneur.59.10.1565.
- [159] D. H. Mahad, B. D. Trapp, e H. Lassmann, «Pathological mechanisms in progressive multiple sclerosis», *Lancet Neurol*, vol. 14, n. 2, pagg. 183–193, feb. 2015, doi: 10.1016/S1474-4422(14)70256-X.

- [160] A. N. Bankston, M. D. Mandler, e Y. Feng, «Oligodendroglia and neurotrophic factors in neurodegeneration», *Neurosci Bull*, vol. 29, n. 2, pagg. 216–228, apr. 2013, doi: 10.1007/s12264-013-1321-3.
- [161] R. Dutta e B. D. Trapp, «Mechanisms of neuronal dysfunction and degeneration in multiple sclerosis», *Prog Neurobiol*, vol. 93, n. 1, pagg. 1–12, gen. 2011, doi: 10.1016/j.pneurobio.2010.09.005.
- [162] J. W. Peterson, L. Bö, S. Mörk, A. Chang, e B. D. Trapp, «Transected neurites, apoptotic neurons, and reduced inflammation in cortical multiple sclerosis lesions», *Ann Neurol*, vol. 50, n. 3, pagg. 389–400, set. 2001, doi: 10.1002/ana.1123.
- [163] M. A. Friese, B. Schattling, e L. Fugger, «Mechanisms of neurodegeneration and axonal dysfunction in multiple sclerosis», *Nat Rev Neurol*, vol. 10, n. 4, pagg. 225–238, apr. 2014, doi: 10.1038/nrneurol.2014.37.
- [164] Y. Dombrowski *et al.*, «Regulatory T cells promote myelin regeneration in the central nervous system», *Nat Neurosci*, vol. 20, n. 5, pagg. 674–680, mag. 2017, doi: 10.1038/nn.4528.
- [165] C. Lubetzki, B. Zalc, A. Williams, C. Stadelmann, e B. Stankoff, «Remyelination in multiple sclerosis: from basic science to clinical translation», *Lancet Neurol*, vol. 19, n. 8, pagg. 678–688, ago. 2020, doi: 10.1016/S1474-4422(20)30140-X.
- [166] E. V. Voss *et al.*, «Characterisation of microglia during de- and remyelination: can they create a repair promoting environment?», *Neurobiol Dis*, vol. 45, n. 1, pagg. 519–528, gen. 2012, doi: 10.1016/j.nbd.2011.09.008.
- [167] F. Cignarella *et al.*, «TREM2 activation on microglia promotes myelin debris clearance and remyelination in a model of multiple sclerosis», *Acta Neuropathol*, vol. 140, n. 4, pagg. 513–534, ott. 2020, doi: 10.1007/s00401-020-02193-z.
- [168] A. F. Lloyd e V. E. Miron, «The pro-remyelination properties of microglia in the central nervous system», *Nat Rev Neurol*, vol. 15, n. 8, pagg. 447–458, ago. 2019, doi: 10.1038/s41582-019-0184-2.
- [169] S. A. Berghoff *et al.*, «Microglia facilitate repair of demyelinated lesions via post-squalene sterol synthesis», *Nat Neurosci*, vol. 24, n. 1, pagg. 47–60, gen. 2021, doi: 10.1038/s41593-020-00757-6.
- [170] N. Cunniffe e A. Coles, «Promoting remyelination in multiple sclerosis», *J Neurol*, vol. 268, n. 1, pagg. 30–44, gen. 2021, doi: 10.1007/s00415-019-09421-x.

- [171] S. Palumbo e S. Pellegrini, «Experimental In Vivo Models of Multiple Sclerosis: State of the Art», in *Multiple Sclerosis: Perspectives in Treatment and Pathogenesis*, I. S. Zagon e P. J. McLaughlin, A c. di Brisbane (AU): Codon Publications, 2017. Consultato: 26 dicembre 2021. [Online]. Disponibile su: <http://www.ncbi.nlm.nih.gov/books/NBK470145/>
- [172] L. Torre-Fuentes, L. Moreno-Jiménez, V. Pytel, J. A. Matías-Guiu, U. Gómez-Pinedo, e J. Matías-Guiu, «Experimental models of demyelination and remyelination», *Neurologia (Engl Ed)*, vol. 35, n. 1, pagg. 32–39, feb. 2020, doi: 10.1016/j.nrl.2017.07.002.
- [173] E. Leitzen *et al.*, «Comparison of Reported Spinal Cord Lesions in Progressive Multiple Sclerosis with Theiler’s Murine Encephalomyelitis Virus Induced Demyelinating Disease», *Int J Mol Sci*, vol. 20, n. 4, pag. E989, feb. 2019, doi: 10.3390/ijms20040989.
- [174] M. Kipp *et al.*, «Experimental in vivo and in vitro models of multiple sclerosis: EAE and beyond», *Mult Scler Relat Disord*, vol. 1, n. 1, pagg. 15–28, gen. 2012, doi: 10.1016/j.msard.2011.09.002.
- [175] S. Bittner, A. M. Afzali, H. Wiendl, e S. G. Meuth, «Myelin oligodendrocyte glycoprotein (MOG35-55) induced experimental autoimmune encephalomyelitis (EAE) in C57BL/6 mice», *J Vis Exp*, n. 86, apr. 2014, doi: 10.3791/51275.
- [176] A. P. Robinson, C. T. Harp, A. Noronha, e S. D. Miller, «The experimental autoimmune encephalomyelitis (EAE) model of MS: utility for understanding disease pathophysiology and treatment», *Handb Clin Neurol*, vol. 122, pagg. 173–189, 2014, doi: 10.1016/B978-0-444-52001-2.00008-X.
- [177] A. G. Baxter, «The origin and application of experimental autoimmune encephalomyelitis», *Nat Rev Immunol*, vol. 7, n. 11, pagg. 904–912, nov. 2007, doi: 10.1038/nri2190.
- [178] C. Laaker, M. Hsu, Z. Fabry, S. D. Miller, e W. J. Karpus, «Experimental Autoimmune Encephalomyelitis in the Mouse», *Curr Protoc*, vol. 1, n. 12, pag. e300, dic. 2021, doi: 10.1002/cpz1.300.
- [179] C. S. Constantinescu, N. Farooqi, K. O’Brien, e B. Gran, «Experimental autoimmune encephalomyelitis (EAE) as a model for multiple sclerosis (MS)», *Br J Pharmacol*, vol. 164, n. 4, pagg. 1079–1106, ott. 2011, doi: 10.1111/j.1476-5381.2011.01302.x.
- [180] M. Kipp, S. Nyamoya, T. Hochstrasser, e S. Amor, «Multiple sclerosis animal models: a clinical and histopathological perspective», *Brain Pathol*, vol. 27, n. 2, pagg. 123–137, mar. 2017, doi: 10.1111/bpa.12454.

- [181] M. Schroeter, G. Stoll, R. Weissert, H.-P. Hartung, H. Lassmann, e S. Jander, «CD8+ phagocyte recruitment in rat experimental autoimmune encephalomyelitis: association with inflammatory tissue destruction», *Am J Pathol*, vol. 163, n. 4, pagg. 1517–1524, ott. 2003, doi: 10.1016/S0002-9440(10)63508-0.
- [182] M. Bauer *et al.*, «Beta1 integrins differentially control extravasation of inflammatory cell subsets into the CNS during autoimmunity», *Proc Natl Acad Sci U S A*, vol. 106, n. 6, pagg. 1920–1925, feb. 2009, doi: 10.1073/pnas.0808909106.
- [183] M. Scheld *et al.*, «Neurodegeneration Triggers Peripheral Immune Cell Recruitment into the Forebrain», *J Neurosci*, vol. 36, n. 4, pagg. 1410–1415, gen. 2016, doi: 10.1523/JNEUROSCI.2456-15.2016.
- [184] V. K. Tuohy, Z. Lu, R. A. Sobel, R. A. Laursen, e M. B. Lees, «Identification of an encephalitogenic determinant of myelin proteolipid protein for SJL mice», *J Immunol*, vol. 142, n. 5, pagg. 1523–1527, mar. 1989.
- [185] E. Mix, H. Meyer-Rienecker, H.-P. Hartung, e U. K. Zettl, «Animal models of multiple sclerosis--potentials and limitations», *Prog Neurobiol*, vol. 92, n. 3, pagg. 386–404, nov. 2010, doi: 10.1016/j.pneurobio.2010.06.005.
- [186] L. Steinman e S. S. Zamvil, «How to successfully apply animal studies in experimental allergic encephalomyelitis to research on multiple sclerosis», *Ann Neurol*, vol. 60, n. 1, pagg. 12–21, lug. 2006, doi: 10.1002/ana.20913.
- [187] D. J. Daugherty, V. Selvaraj, O. V. Chechneva, X.-B. Liu, D. E. Pleasure, e W. Deng, «A TSPO ligand is protective in a mouse model of multiple sclerosis», *EMBO Mol Med*, vol. 5, n. 6, pagg. 891–903, giu. 2013, doi: 10.1002/emmm.201202124.
- [188] S. Moore *et al.*, «Restoration of axon conduction and motor deficits by therapeutic treatment with glatiramer acetate», *J Neurosci Res*, vol. 92, n. 12, pagg. 1621–1636, dic. 2014, doi: 10.1002/jnr.23440.
- [189] C. Goldschmidt e M. P. McGinley, «Advances in the Treatment of Multiple Sclerosis», *Neurol Clin*, vol. 39, n. 1, pagg. 21–33, feb. 2021, doi: 10.1016/j.ncl.2020.09.002.
- [190] A. Gajofatto e M. D. Benedetti, «Treatment strategies for multiple sclerosis: When to start, when to change, when to stop?», *World J Clin Cases*, vol. 3, n. 7, pagg. 545–555, lug. 2015, doi: 10.12998/wjcc.v3.i7.545.
- [191] N. Grigoriadis, M. Linnebank, N. Alexandri, S. Muehl, e G. F. L. Hofbauer, «Considerations on long-term immuno-intervention in the treatment of multiple sclerosis: an expert opinion», *Expert*

- Opin Pharmacother*, vol. 17, n. 15, pagg. 2085–2095, ott. 2016, doi: 10.1080/14656566.2016.1232712.
- [192] I. Smets *et al.*, «Corticosteroids in the management of acute multiple sclerosis exacerbations», *Acta Neurol Belg*, vol. 117, n. 3, pagg. 623–633, set. 2017, doi: 10.1007/s13760-017-0772-0.
- [193] P. Küry, D. Kremer, e P. Göttle, «Drug repurposing for neuroregeneration in multiple sclerosis», *Neural Regen Res*, vol. 13, n. 8, pagg. 1366–1367, ago. 2018, doi: 10.4103/1673-5374.235242.
- [194] M. M. Bakhuraysah, C. Siatskas, e S. Petratos, «Hematopoietic stem cell transplantation for multiple sclerosis: is it a clinical reality?», *Stem Cell Res Ther*, vol. 7, pag. 12, gen. 2016, doi: 10.1186/s13287-015-0272-1.
- [195] A. Dulamea, «Mesenchymal stem cells in multiple sclerosis - translation to clinical trials», *J Med Life*, vol. 8, n. 1, pagg. 24–27, mar. 2015.
- [196] B. Genc, H. R. Bozan, S. Genc, e K. Genc, «Stem Cell Therapy for Multiple Sclerosis», *Adv Exp Med Biol*, vol. 1084, pagg. 145–174, 2019, doi: 10.1007/5584\_2018\_247.
- [197] S. Barati, F. Tahmasebi, e F. Faghihi, «Effects of mesenchymal stem cells transplantation on multiple sclerosis patients», *Neuropeptides*, vol. 84, pag. 102095, dic. 2020, doi: 10.1016/j.npep.2020.102095.
- [198] L. Peruzzotti-Jametti *et al.*, «Macrophage-Derived Extracellular Succinate Licenses Neural Stem Cells to Suppress Chronic Neuroinflammation», *Cell Stem Cell*, vol. 22, n. 3, pagg. 355-368.e13, mar. 2018, doi: 10.1016/j.stem.2018.01.020.
- [199] C. Krienke *et al.*, «A noninflammatory mRNA vaccine for treatment of experimental autoimmune encephalomyelitis», *Science*, vol. 371, n. 6525, pagg. 145–153, gen. 2021, doi: 10.1126/science.aay3638.
- [200] V. Papadopoulos, «Peripheral-type benzodiazepine/diazepam binding inhibitor receptor: biological role in steroidogenic cell function», *Endocr Rev*, vol. 14, n. 2, pagg. 222–240, apr. 1993, doi: 10.1210/edrv-14-2-222.
- [201] V. Papadopoulos *et al.*, «Translocator protein (18kDa): new nomenclature for the peripheral-type benzodiazepine receptor based on its structure and molecular function», *Trends Pharmacol Sci*, vol. 27, n. 8, pagg. 402–409, ago. 2006, doi: 10.1016/j.tips.2006.06.005.
- [202] L. Veenman e M. Gavish, «The peripheral-type benzodiazepine receptor and the cardiovascular system. Implications for drug development», *Pharmacol Ther*, vol. 110, n. 3, pagg. 503–524, giu. 2006, doi: 10.1016/j.pharmthera.2005.09.007.

- [203] S. Taliani, F. Da Settimo, E. Da Pozzo, B. Chelli, e C. Martini, «Translocator protein ligands as promising therapeutic tools for anxiety disorders», *Curr Med Chem*, vol. 16, n. 26, pagg. 3359–3380, 2009, doi: 10.2174/092986709789057653.
- [204] E. Barresi *et al.*, «An update into the medicinal chemistry of translocator protein (TSPO) ligands», *European Journal of Medicinal Chemistry*, vol. 209, pag. 112924, gen. 2021, doi: 10.1016/j.ejmech.2020.112924.
- [205] A. Batarseh e V. Papadopoulos, «Regulation of translocator protein 18 kDa (TSPO) expression in health and disease states», *Mol Cell Endocrinol*, vol. 327, n. 1–2, pagg. 1–12, ott. 2010, doi: 10.1016/j.mce.2010.06.013.
- [206] E. Nutma *et al.*, «Cellular sources of TSPO expression in healthy and diseased brain», *Eur J Nucl Med Mol Imaging*, vol. 49, n. 1, pagg. 146–163, dic. 2021, doi: 10.1007/s00259-020-05166-2.
- [207] E. L. Werry *et al.*, «Recent Developments in TSPO PET Imaging as A Biomarker of Neuroinflammation in Neurodegenerative Disorders», *Int J Mol Sci*, vol. 20, n. 13, pag. E3161, giu. 2019, doi: 10.3390/ijms20133161.
- [208] B. Costa, E. Da Pozzo, e C. Martini, «18-kDa translocator protein association complexes in the brain: From structure to function», *Biochem Pharmacol*, vol. 177, pag. 114015, lug. 2020, doi: 10.1016/j.bcp.2020.114015.
- [209] J.-J. Lacapere, L. Duma, S. Finet, M. Kassiou, e V. Papadopoulos, «Insight into the Structural Features of TSPO: Implications for Drug Development», *Trends Pharmacol Sci*, vol. 41, n. 2, pagg. 110–122, feb. 2020, doi: 10.1016/j.tips.2019.11.005.
- [210] L. Jaremko, M. Jaremko, K. Giller, S. Becker, e M. Zweckstetter, «Structure of the mitochondrial translocator protein in complex with a diagnostic ligand», *Science*, vol. 343, n. 6177, pagg. 1363–1366, mar. 2014, doi: 10.1126/science.1248725.
- [211] M. Jaremko, Ł. Jaremko, G. Jaipuria, S. Becker, e M. Zweckstetter, «Structure of the mammalian TSPO/PBR protein», *Biochem Soc Trans*, vol. 43, n. 4, pagg. 566–571, ago. 2015, doi: 10.1042/BST20150029.
- [212] J. Fan e V. Papadopoulos, «Evolutionary origin of the mitochondrial cholesterol transport machinery reveals a universal mechanism of steroid hormone biosynthesis in animals», *PLoS One*, vol. 8, n. 10, pag. e76701, 2013, doi: 10.1371/journal.pone.0076701.
- [213] J. Y. Chung, H. Chen, A. Midzak, A. L. Burnett, V. Papadopoulos, e B. R. Zirkin, «Drug ligand-induced activation of translocator protein (TSPO) stimulates steroid production by aged brown

- Norway rat Leydig cells», *Endocrinology*, vol. 154, n. 6, pagg. 2156–2165, giu. 2013, doi: 10.1210/en.2012-2226.
- [214] V. Papadopoulos, L. Lecanu, R. C. Brown, Z. Han, e Z.-X. Yao, «Peripheral-type benzodiazepine receptor in neurosteroid biosynthesis, neuropathology and neurological disorders», *Neuroscience*, vol. 138, n. 3, pagg. 749–756, 2006, doi: 10.1016/j.neuroscience.2005.05.063.
- [215] J. J. Lacapère e V. Papadopoulos, «Peripheral-type benzodiazepine receptor: structure and function of a cholesterol-binding protein in steroid and bile acid biosynthesis», *Steroids*, vol. 68, n. 7–8, pagg. 569–585, set. 2003, doi: 10.1016/s0039-128x(03)00101-6.
- [216] H. Li e V. Papadopoulos, «Peripheral-type benzodiazepine receptor function in cholesterol transport. Identification of a putative cholesterol recognition/interaction amino acid sequence and consensus pattern», *Endocrinology*, vol. 139, n. 12, pagg. 4991–4997, dic. 1998, doi: 10.1210/endo.139.12.6390.
- [217] N. Jamin *et al.*, «Characterization of the cholesterol recognition amino acid consensus sequence of the peripheral-type benzodiazepine receptor», *Mol Endocrinol*, vol. 19, n. 3, pagg. 588–594, mar. 2005, doi: 10.1210/me.2004-0308.
- [218] B. Costa *et al.*, «The spontaneous Ala147Thr amino acid substitution within the translocator protein influences pregnenolone production in lymphomonocytes of healthy individuals», *Endocrinology*, vol. 150, n. 12, pagg. 5438–5445, dic. 2009, doi: 10.1210/en.2009-0752.
- [219] M. B. Rone, J. Fan, e V. Papadopoulos, «Cholesterol transport in steroid biosynthesis: role of protein-protein interactions and implications in disease states», *Biochim Biophys Acta*, vol. 1791, n. 7, pagg. 646–658, lug. 2009, doi: 10.1016/j.bbali.2009.03.001.
- [220] E. Romeo *et al.*, «Stimulation of brain steroidogenesis by 2-aryl-indole-3-acetamide derivatives acting at the mitochondrial diazepam-binding inhibitor receptor complex», *J Pharmacol Exp Ther*, vol. 267, n. 1, pagg. 462–471, ott. 1993.
- [221] L. Wolf *et al.*, «Enhancing neurosteroid synthesis--relationship to the pharmacology of translocator protein (18 kDa) (TSPO) ligands and benzodiazepines», *Pharmacopsychiatry*, vol. 48, n. 2, pagg. 72–77, mar. 2015, doi: 10.1055/s-0034-1398507.
- [222] M. Verleye *et al.*, «The anxiolytic etifoxine activates the peripheral benzodiazepine receptor and increases the neurosteroid levels in rat brain», *Pharmacol Biochem Behav*, vol. 82, n. 4, pagg. 712–720, dic. 2005, doi: 10.1016/j.pbb.2005.11.013.
- [223] D. Bitran, M. Foley, D. Audette, N. Leslie, e C. A. Frye, «Activation of peripheral mitochondrial benzodiazepine receptors in the hippocampus stimulates allopregnanolone synthesis

- and produces anxiolytic-like effects in the rat», *Psychopharmacology (Berl)*, vol. 151, n. 1, pagg. 64–71, lug. 2000, doi: 10.1007/s002130000471.
- [224] B. Costa *et al.*, «TSPO ligand residence time: a new parameter to predict compound neurosteroidogenic efficacy», *Sci Rep*, vol. 6, pag. 18164, gen. 2016, doi: 10.1038/srep18164.
- [225] B. Costa, C. Cavallini, E. Da Pozzo, S. Taliani, F. Da Settimo, e C. Martini, «The Anxiolytic Etifoxine Binds to TSPO Ro5-4864 Binding Site with Long Residence Time Showing a High Neurosteroidogenic Activity», *ACS Chem Neurosci*, vol. 8, n. 7, pagg. 1448–1454, lug. 2017, doi: 10.1021/acschemneuro.7b00027.
- [226] E. Da Pozzo *et al.*, «TSPO PIGA Ligands Promote Neurosteroidogenesis and Human Astrocyte Well-Being», *Int J Mol Sci*, vol. 17, n. 7, pag. E1028, giu. 2016, doi: 10.3390/ijms17071028.
- [227] A. Midzak e V. Papadopoulos, «Adrenal Mitochondria and Steroidogenesis: From Individual Proteins to Functional Protein Assemblies», *Front Endocrinol (Lausanne)*, vol. 7, pag. 106, 2016, doi: 10.3389/fendo.2016.00106.
- [228] C. Betlazar, R. J. Middleton, R. Banati, e G.-J. Liu, «The Translocator Protein (TSPO) in Mitochondrial Bioenergetics and Immune Processes», *Cells*, vol. 9, n. 2, pag. E512, feb. 2020, doi: 10.3390/cells9020512.
- [229] C. Tremolanti *et al.*, «Translocator Protein 18-kDa: a promising target to treat neuroinflammation-related degenerative diseases», *Curr Med Chem*, apr. 2022, doi: 10.2174/0929867329666220415120820.
- [230] A. G. Mensah-Nyagan, J. L. Do-Rego, D. Beaujean, V. Luu-The, G. Pelletier, e H. Vaudry, «Neurosteroids: expression of steroidogenic enzymes and regulation of steroid biosynthesis in the central nervous system», *Pharmacol Rev*, vol. 51, n. 1, pagg. 63–81, mar. 1999.
- [231] G. C. Panzica *et al.*, «Milestones on Steroids and the Nervous System: 10 years of basic and translational research», *J Neuroendocrinol*, vol. 24, n. 1, pagg. 1–15, gen. 2012, doi: 10.1111/j.1365-2826.2011.02265.x.
- [232] A. M. Hosie, M. E. Wilkins, H. M. A. da Silva, e T. G. Smart, «Endogenous neurosteroids regulate GABAA receptors through two discrete transmembrane sites», *Nature*, vol. 444, n. 7118, pagg. 486–489, nov. 2006, doi: 10.1038/nature05324.
- [233] L. N. Tu *et al.*, «Peripheral benzodiazepine receptor/translocator protein global knock-out mice are viable with no effects on steroid hormone biosynthesis», *J Biol Chem*, vol. 289, n. 40, pagg. 27444–27454, ott. 2014, doi: 10.1074/jbc.M114.578286.

- [234] V. Selvaraj, L. N. Tu, e D. M. Stocco, «Crucial Role Reported for TSPO in Viability and Steroidogenesis is a Misconception. Commentary: Conditional Steroidogenic Cell-Targeted Deletion of TSPO Unveils a Crucial Role in Viability and Hormone-Dependent Steroid Formation», *Front Endocrinol (Lausanne)*, vol. 7, pag. 91, 2016, doi: 10.3389/fendo.2016.00091.
- [235] J. Fan, E. Campioli, A. Midzak, M. Culty, e V. Papadopoulos, «Conditional steroidogenic cell-targeted deletion of TSPO unveils a crucial role in viability and hormone-dependent steroid formation», *Proc Natl Acad Sci U S A*, vol. 112, n. 23, pagg. 7261–7266, giu. 2015, doi: 10.1073/pnas.1502670112.
- [236] R. B. Banati *et al.*, «Positron emission tomography and functional characterization of a complete PBR/TSPO knockout», *Nat Commun*, vol. 5, pag. 5452, nov. 2014, doi: 10.1038/ncomms6452.
- [237] K. Morohaku, S. H. Pelton, D. J. Daugherty, W. R. Butler, W. Deng, e V. Selvaraj, «Translocator protein/peripheral benzodiazepine receptor is not required for steroid hormone biosynthesis», *Endocrinology*, vol. 155, n. 1, pagg. 89–97, gen. 2014, doi: 10.1210/en.2013-1556.
- [238] J. Fan, E. Campioli, C. Sottas, B. Zirkin, e V. Papadopoulos, «Amhr2-Cre-Mediated Global Tspo Knockout», *J Endocr Soc*, vol. 4, n. 2, pag. bvaa001, feb. 2020, doi: 10.1210/jendso/bvaa001.
- [239] H. Wang *et al.*, «Global Deletion of TSPO Does Not Affect the Viability and Gene Expression Profile», *PLoS One*, vol. 11, n. 12, pag. e0167307, 2016, doi: 10.1371/journal.pone.0167307.
- [240] R. Rupprecht *et al.*, «Translocator protein (18 kDa) (TSPO) as a therapeutic target for neurological and psychiatric disorders», *Nat Rev Drug Discov*, vol. 9, n. 12, pagg. 971–988, dic. 2010, doi: 10.1038/nrd3295.
- [241] F. Bonsack e S. Sukumari-Ramesh, «TSPO: An Evolutionarily Conserved Protein with Elusive Functions», *Int J Mol Sci*, vol. 19, n. 6, pag. E1694, giu. 2018, doi: 10.3390/ijms19061694.
- [242] V. Papadopoulos, J. Fan, e B. Zirkin, «Translocator protein (18 kDa): an update on its function in steroidogenesis», *J Neuroendocrinol*, vol. 30, n. 2, feb. 2018, doi: 10.1111/jne.12500.
- [243] M. W. McEnery, A. M. Snowman, R. R. Trifiletti, e S. H. Snyder, «Isolation of the mitochondrial benzodiazepine receptor: association with the voltage-dependent anion channel and the adenine nucleotide carrier», *Proc Natl Acad Sci U S A*, vol. 89, n. 8, pagg. 3170–3174, apr. 1992, doi: 10.1073/pnas.89.8.3170.
- [244] M. Carraro, V. Checchetto, I. Szabó, e P. Bernardi, «F-ATP synthase and the permeability transition pore: fewer doubts, more certainties», *FEBS Lett*, vol. 593, n. 13, pagg. 1542–1553, lug. 2019, doi: 10.1002/1873-3468.13485.

- [245] L. Veenman, Y. Shandalov, e M. Gavish, «VDAC activation by the 18 kDa translocator protein (TSPO), implications for apoptosis», *J Bioenerg Biomembr*, vol. 40, n. 3, pagg. 199–205, giu. 2008, doi: 10.1007/s10863-008-9142-1.
- [246] L. Veenman, V. Papadopoulos, e M. Gavish, «Channel-like functions of the 18-kDa translocator protein (TSPO): regulation of apoptosis and steroidogenesis as part of the host-defense response», *Curr Pharm Des*, vol. 13, n. 23, pagg. 2385–2405, 2007, doi: 10.2174/138161207781368710.
- [247] P. Carayon *et al.*, «Involvement of peripheral benzodiazepine receptors in the protection of hematopoietic cells against oxygen radical damage», *Blood*, vol. 87, n. 8, pagg. 3170–3178, apr. 1996.
- [248] A. Grimm *et al.*, «Mitochondria modulatory effects of new TSPO ligands in a cellular model of tauopathies», *J Neuroendocrinol*, vol. 32, n. 1, pag. e12796, gen. 2020, doi: 10.1111/jne.12796.
- [249] E. Baez, G. P. Guio-Vega, V. Echeverria, D. A. Sandoval-Rueda, e G. E. Barreto, «4'-Chlorodiazepam Protects Mitochondria in T98G Astrocyte Cell Line from Glucose Deprivation», *Neurotox Res*, vol. 32, n. 2, pagg. 163–171, ago. 2017, doi: 10.1007/s12640-017-9733-x.
- [250] L. N. Tu, A. H. Zhao, M. Hussein, D. M. Stocco, e V. Selvaraj, «Translocator Protein (TSPO) Affects Mitochondrial Fatty Acid Oxidation in Steroidogenic Cells», *Endocrinology*, vol. 157, n. 3, pagg. 1110–1121, mar. 2016, doi: 10.1210/en.2015-1795.
- [251] M. Wang *et al.*, «Macroglia-microglia interactions via TSPO signaling regulates microglial activation in the mouse retina», *J Neurosci*, vol. 34, n. 10, pagg. 3793–3806, mar. 2014, doi: 10.1523/JNEUROSCI.3153-13.2014.
- [252] V. M. Milenkovic *et al.*, «CRISPR-Cas9 Mediated TSPO Gene Knockout alters Respiration and Cellular Metabolism in Human Primary Microglia Cells», *Int J Mol Sci*, vol. 20, n. 13, pag. E3359, lug. 2019, doi: 10.3390/ijms20133359.
- [253] Y. Fu *et al.*, «TSPO deficiency induces mitochondrial dysfunction, leading to hypoxia, angiogenesis, and a growth-promoting metabolic shift toward glycolysis in glioblastoma», *Neuro Oncol*, vol. 22, n. 2, pagg. 240–252, feb. 2020, doi: 10.1093/neuonc/noz183.
- [254] L. Veenman, A. Vainshtein, e M. Gavish, «TSPO as a target for treatments of diseases, including neuropathological disorders», *Cell Death Dis*, vol. 6, pag. e1911, ott. 2015, doi: 10.1038/cddis.2015.294.
- [255] A. Vainshtein *et al.*, «Quinazoline-based tricyclic compounds that regulate programmed cell death, induce neuronal differentiation, and are curative in animal models for excitotoxicity and

hereditary brain disease», *Cell Death Discov*, vol. 1, pag. 15027, 2015, doi: 10.1038/cddiscovery.2015.27.

[256] S. Mukherjee e S. K. Das, «Translocator protein (TSPO) in breast cancer», *Curr Mol Med*, vol. 12, n. 4, pagg. 443–457, mag. 2012.

[257] N. Yasin *et al.*, «Classical and Novel TSPO Ligands for the Mitochondrial TSPO Can Modulate Nuclear Gene Expression: Implications for Mitochondrial Retrograde Signaling», *Int J Mol Sci*, vol. 18, n. 4, pag. E786, apr. 2017, doi: 10.3390/ijms18040786.

[258] C. Betlazar, M. Harrison-Brown, R. J. Middleton, R. Banati, e G.-J. Liu, «Cellular Sources and Regional Variations in the Expression of the Neuroinflammatory Marker Translocator Protein (TSPO) in the Normal Brain», *Int J Mol Sci*, vol. 19, n. 9, pag. E2707, set. 2018, doi: 10.3390/ijms19092707.

[259] B. Varga *et al.*, «Translocator protein (TSPO 18kDa) is expressed by neural stem and neuronal precursor cells», *Neurosci Lett*, vol. 462, n. 3, pagg. 257–262, ott. 2009, doi: 10.1016/j.neulet.2009.06.051.

[260] K. Magalon *et al.*, «Olesoxime accelerates myelination and promotes repair in models of demyelination», *Ann Neurol*, vol. 71, n. 2, pagg. 213–226, feb. 2012, doi: 10.1002/ana.22593.

[261] B. D. Arbo, F. Benetti, L. M. Garcia-Segura, e M. F. Ribeiro, «Therapeutic actions of translocator protein (18 kDa) ligands in experimental models of psychiatric disorders and neurodegenerative diseases», *J Steroid Biochem Mol Biol*, vol. 154, pagg. 68–74, nov. 2015, doi: 10.1016/j.jsbmb.2015.07.007.

[262] D. G. Walker e L.-F. Lue, «Immune phenotypes of microglia in human neurodegenerative disease: challenges to detecting microglial polarization in human brains», *Alzheimers Res Ther*, vol. 7, n. 1, pag. 56, ago. 2015, doi: 10.1186/s13195-015-0139-9.

[263] K.-R. Bae, H.-J. Shim, D. Balu, S. R. Kim, e S.-W. Yu, «Translocator protein 18 kDa negatively regulates inflammation in microglia», *J Neuroimmune Pharmacol*, vol. 9, n. 3, pagg. 424–437, giu. 2014, doi: 10.1007/s11481-014-9540-6.

[264] H. Feng *et al.*, «TSPO Ligands PK11195 and Midazolam Reduce NLRP3 Inflammasome Activation and Proinflammatory Cytokine Release in BV-2 Cells», *Front Cell Neurosci*, vol. 14, pag. 544431, 2020, doi: 10.3389/fncel.2020.544431.

[265] M. Gavish e L. Veenman, «Regulation of Mitochondrial, Cellular, and Organismal Functions by TSPO», *Adv Pharmacol*, vol. 82, pagg. 103–136, 2018, doi: 10.1016/bs.apha.2017.09.004.

- [266] S. Bader *et al.*, «Differential effects of TSPO ligands on mitochondrial function in mouse microglia cells», *Psychoneuroendocrinology*, vol. 106, pagg. 65–76, ago. 2019, doi: 10.1016/j.psyneuen.2019.03.029.
- [267] M. Karlstetter *et al.*, «Translocator protein (18 kDa) (TSPO) is expressed in reactive retinal microglia and modulates microglial inflammation and phagocytosis», *J Neuroinflammation*, vol. 11, pag. 3, gen. 2014, doi: 10.1186/1742-2094-11-3.
- [268] G. Leva *et al.*, «The translocator protein ligand XBD173 improves clinical symptoms and neuropathological markers in the SJL/J mouse model of multiple sclerosis», *Biochim Biophys Acta Mol Basis Dis*, vol. 1863, n. 12, pagg. 3016–3027, dic. 2017, doi: 10.1016/j.bbadis.2017.09.007.
- [269] B. Ravikumar *et al.*, «Differential efficacy of the TSPO ligands etifoxine and XBD-173 in two rodent models of Multiple Sclerosis», *Neuropharmacology*, vol. 108, pagg. 229–237, set. 2016, doi: 10.1016/j.neuropharm.2016.03.053.
- [270] F. Noorbakhsh *et al.*, «Impaired neurosteroid synthesis in multiple sclerosis», *Brain*, vol. 134, n. Pt 9, pagg. 2703–2721, set. 2011, doi: 10.1093/brain/awr200.
- [271] S. Luchetti, I. Huitinga, e D. F. Swaab, «Neurosteroid and GABA-A receptor alterations in Alzheimer's disease, Parkinson's disease and multiple sclerosis», *Neuroscience*, vol. 191, pagg. 6–21, set. 2011, doi: 10.1016/j.neuroscience.2011.04.010.
- [272] S. Giatti *et al.*, «Neuroprotective effects of progesterone in chronic experimental autoimmune encephalomyelitis», *J Neuroendocrinol*, vol. 24, n. 6, pagg. 851–861, giu. 2012, doi: 10.1111/j.1365-2826.2012.02284.x.
- [273] A. F. De Nicola *et al.*, «Neurosteroidogenesis and progesterone anti-inflammatory/neuroprotective effects», *J Neuroendocrinol*, vol. 30, n. 2, feb. 2018, doi: 10.1111/jne.12502.
- [274] F. Noorbakhsh, G. B. Baker, e C. Power, «Allopregnanolone and neuroinflammation: a focus on multiple sclerosis», *Front Cell Neurosci*, vol. 8, pag. 134, 2014, doi: 10.3389/fncel.2014.00134.
- [275] E. Nutma *et al.*, «A quantitative neuropathological assessment of translocator protein expression in multiple sclerosis», *Brain*, vol. 142, n. 11, pagg. 3440–3455, nov. 2019, doi: 10.1093/brain/awz287.
- [276] B. Zinnhardt *et al.*, «Molecular Imaging of Immune Cell Dynamics During De- and Remyelination in the Cuprizone Model of Multiple Sclerosis by [18F]DPA-714 PET and MRI», *Theranostics*, vol. 9, n. 6, pagg. 1523–1537, 2019, doi: 10.7150/thno.32461.

- [277] N. Nguyen *et al.*, «Efficacy of etifoxine compared to lorazepam monotherapy in the treatment of patients with adjustment disorders with anxiety: a double-blind controlled study in general practice», *Hum Psychopharmacol*, vol. 21, n. 3, pagg. 139–149, apr. 2006, doi: 10.1002/hup.757.
- [278] D. J. Daugherty, O. Chechneva, F. Mayrhofer, e W. Deng, «The hGFAP-driven conditional TSPO knockout is protective in a mouse model of multiple sclerosis», *Sci Rep*, vol. 6, pag. 22556, mar. 2016, doi: 10.1038/srep22556.
- [279] M. Haeussler *et al.*, «Evaluation of off-target and on-target scoring algorithms and integration into the guide RNA selection tool CRISPOR», *Genome Biol*, vol. 17, n. 1, pag. 148, lug. 2016, doi: 10.1186/s13059-016-1012-2.
- [280] C. T. Rueden *et al.*, «ImageJ2: ImageJ for the next generation of scientific image data», *BMC Bioinformatics*, vol. 18, n. 1, pag. 529, nov. 2017, doi: 10.1186/s12859-017-1934-z.
- [281] L. Germelli *et al.*, «De novo Neurosteroidogenesis in Human Microglia: Involvement of the 18 kDa Translocator Protein», *Int J Mol Sci*, vol. 22, n. 6, pag. 3115, mar. 2021, doi: 10.3390/ijms22063115.
- [282] J.-P. Concordet e M. Haeussler, «CRISPOR: intuitive guide selection for CRISPR/Cas9 genome editing experiments and screens», *Nucleic Acids Research*, vol. 46, n. W1, pagg. W242–W245, lug. 2018, doi: 10.1093/nar/gky354.
- [283] J. L. Gori, P. D. Hsu, M. L. Maeder, S. Shen, G. G. Welstead, e D. Bumcrot, «Delivery and Specificity of CRISPR-Cas9 Genome Editing Technologies for Human Gene Therapy», *Hum Gene Ther*, vol. 26, n. 7, pagg. 443–451, lug. 2015, doi: 10.1089/hum.2015.074.
- [284] A. V. Anzalone *et al.*, «Search-and-replace genome editing without double-strand breaks or donor DNA», *Nature*, vol. 576, n. 7785, pagg. 149–157, dic. 2019, doi: 10.1038/s41586-019-1711-4.
- [285] J. Scholefield e P. T. Harrison, «Prime editing - an update on the field», *Gene Ther*, vol. 28, n. 7–8, pagg. 396–401, ago. 2021, doi: 10.1038/s41434-021-00263-9.
- [286] Y. Garcia-Mesa *et al.*, «Immortalization of primary microglia: a new platform to study HIV regulation in the central nervous system», *J Neurovirol*, vol. 23, n. 1, pagg. 47–66, feb. 2017, doi: 10.1007/s13365-016-0499-3.
- [287] E. A. Bordt e B. M. Polster, «NADPH oxidase- and mitochondria-derived reactive oxygen species in proinflammatory microglial activation: a bipartisan affair?», *Free Radical Biology and Medicine*, vol. 76, pagg. 34–46, nov. 2014, doi: 10.1016/j.freeradbiomed.2014.07.033.

- [288] E. Da Pozzo *et al.*, «Microglial Pro-Inflammatory and Anti-Inflammatory Phenotypes Are Modulated by Translocator Protein Activation», *Int J Mol Sci*, vol. 20, n. 18, pag. E4467, set. 2019, doi: 10.3390/ijms20184467.
- [289] N. C. Derecki *et al.*, «Regulation of learning and memory by meningeal immunity: a key role for IL-4», *Journal of Experimental Medicine*, vol. 207, n. 5, pagg. 1067–1080, mag. 2010, doi: 10.1084/jem.20091419.
- [290] X. Messeguer, R. Escudero, D. Farré, O. Núñez, J. Martínez, e M. M. Albà, «PROMO: detection of known transcription regulatory elements using species-tailored searches», *Bioinformatics*, vol. 18, n. 2, pagg. 333–334, feb. 2002, doi: 10.1093/bioinformatics/18.2.333.
- [291] R. Crinelli, A. Antonelli, M. Bianchi, L. Gentilini, S. Scaramucci, e M. Magnani, «Selective Inhibition of NF- $\kappa$ B Activation and TNF- $\alpha$  Production in Macrophages by Red Blood Cell-Mediated Delivery of Dexamethasone», *Blood Cells, Molecules, and Diseases*, vol. 26, n. 3, pagg. 211–222, giu. 2000, doi: 10.1006/bcmd.2000.0298.
- [292] Y. Tang e W. Le, «Differential Roles of M1 and M2 Microglia in Neurodegenerative Diseases», *Mol Neurobiol*, vol. 53, n. 2, pagg. 1181–1194, mar. 2016, doi: 10.1007/s12035-014-9070-5.
- [293] R. Scholz *et al.*, «Targeting translocator protein (18 kDa) (TSPO) dampens pro-inflammatory microglia reactivity in the retina and protects from degeneration», *J Neuroinflammation*, vol. 12, n. 1, pag. 201, dic. 2015, doi: 10.1186/s12974-015-0422-5.
- [294] A. M. Smith e M. Dragunow, «The human side of microglia», *Trends in Neurosciences*, vol. 37, n. 3, pagg. 125–135, mar. 2014, doi: 10.1016/j.tins.2013.12.001.
- [295] R. L. Davis, D. J. Buck, K. McCracken, G. W. Cox, e S. Das, «Interleukin-1 $\beta$ -induced inflammatory signaling in C20 human microglial cells», *NN*, vol. 2018, dic. 2018, doi: 10.20517/2347-8659.2018.60.
- [296] D. K. Kaushik, M. C. Thounaojam, K. L. Kumawat, M. Gupta, e A. Basu, «Interleukin-1 $\beta$  orchestrates underlying inflammatory responses in microglia via Krüppel-like factor 4», *J. Neurochem.*, vol. 127, n. 2, pagg. 233–244, ott. 2013, doi: 10.1111/jnc.12382.
- [297] D. Vergara *et al.*, «Distinct Protein Expression Networks are Activated in Microglia Cells after Stimulation with IFN- $\gamma$  and IL-4», *Cells*, vol. 8, n. 6, pag. 580, giu. 2019, doi: 10.3390/cells8060580.
- [298] C. Kim *et al.*, « $\beta$ 1-integrin-dependent migration of microglia in response to neuron-released  $\alpha$ -synuclein», *Exp Mol Med*, vol. 46, n. 4, pagg. e91–e91, apr. 2014, doi: 10.1038/emm.2014.6.

- [299] Y. Liu, A. Beyer, e R. Aebersold, «On the Dependency of Cellular Protein Levels on mRNA Abundance», *Cell*, vol. 165, n. 3, pagg. 535–550, apr. 2016, doi: 10.1016/j.cell.2016.03.014.
- [300] A. Hamon, A. Morel, B. Hue, M. Verleye, e J.-M. Gillardin, «The modulatory effects of the anxiolytic etifoxine on GABAA receptors are mediated by the  $\beta$  subunit», *Neuropharmacology*, vol. 45, n. 3, pagg. 293–303, set. 2003, doi: 10.1016/S0028-3908(03)00187-4.
- [301] J. Choi, M. Ifuku, M. Noda, e T. R. Guilarte, «Translocator protein (18 kDa)/peripheral benzodiazepine receptor specific ligands induce microglia functions consistent with an activated state», *Glia*, vol. 59, n. 2, pagg. 219–230, feb. 2011, doi: 10.1002/glia.21091.
- [302] C. Yilmaz *et al.*, «Neurosteroids as regulators of neuroinflammation», *Frontiers in Neuroendocrinology*, vol. 55, pag. 100788, ott. 2019, doi: 10.1016/j.yfrne.2019.100788.
- [303] S. Giatti, M. Boraso, R. C. Melcangi, e B. Viviani, «Neuroactive steroids, their metabolites, and neuroinflammation», *Journal of Molecular Endocrinology*, vol. 49, n. 3, pagg. R125–R134, dic. 2012, doi: 10.1530/JME-12-0127.
- [304] H. Liu, R. K. Leak, e X. Hu, «Neurotransmitter receptors on microglia», *Stroke Vasc Neurol*, vol. 1, n. 2, pagg. 52–58, giu. 2016, doi: 10.1136/svn-2016-000012.
- [305] M. Lee, C. Schwab, e P. L. Mcgeer, «Astrocytes are GABAergic cells that modulate microglial activity», *Glia*, vol. 59, n. 1, pagg. 152–165, gen. 2011, doi: 10.1002/glia.21087.
- [306] L. de V. K. Kupa, C. C. Drewes, E. D. Barioni, C. L. Neves, S. C. Sampaio, e S. H. P. Farsky, «Role of Translocator 18 KDa Ligands in the Activation of Leukotriene B4 Activated G-Protein Coupled Receptor and Toll Like Receptor-4 Pathways in Neutrophils», *Front. Pharmacol.*, vol. 8, pag. 766, ott. 2017, doi: 10.3389/fphar.2017.00766.
- [307] S. Monga, R. Nagler, R. Amara, A. Weizman, e M. Gavish, «Inhibitory Effects of the Two Novel TSPO Ligands 2-Cl-MGV-1 and MGV-1 on LPS-induced Microglial Activation», *Cells*, vol. 8, n. 5, pag. 486, mag. 2019, doi: 10.3390/cells8050486.
- [308] K. Rashid, M. Verhoyen, M. Taiwo, e T. Langmann, «Translocator protein (18 kDa) (TSPO) ligands activate Nrf2 signaling and attenuate inflammatory responses and oxidative stress in human retinal pigment epithelial cells», *Biochemical and Biophysical Research Communications*, vol. 528, n. 2, pagg. 261–268, lug. 2020, doi: 10.1016/j.bbrc.2020.05.114.
- [309] J. Gatliff *et al.*, «A role for TSPO in mitochondrial Ca<sup>2+</sup> homeostasis and redox stress signaling», *Cell Death Dis*, vol. 8, n. 6, pagg. e2896–e2896, giu. 2017, doi: 10.1038/cddis.2017.186.
- [310] S. Zeno, L. Veenman, Y. Katz, J. Bode, M. Gavish, e M. Zaaroor, «The 18 kDa Mitochondrial Translocator Protein (TSPO) Prevents Accumulation of Protoporphyrin IX. Involvement of Reactive

Oxygen Species (ROS)», *Current Molecular Medicine*, vol. 12, n. 4, pagg. 494–501, mag. 2012, doi: 10.2174/156652412800163424.

[311] M. K. Loth *et al.*, «A Novel Interaction of Translocator Protein 18 kDa (TSPO) with NADPH Oxidase in Microglia», *Mol Neurobiol*, vol. 57, n. 11, pagg. 4467–4487, nov. 2020, doi: 10.1007/s12035-020-02042-w.

[312] L. Beckers *et al.*, «Increased Expression of Translocator Protein (TSPO) Marks Pro-inflammatory Microglia but Does Not Predict Neurodegeneration», *Mol Imaging Biol*, vol. 20, n. 1, pagg. 94–102, feb. 2018, doi: 10.1007/s11307-017-1099-1.

[313] B. B. Tournier, S. Tsartsalis, K. Ceyzériat, V. Garibotto, e P. Millet, «In Vivo TSPO Signal and Neuroinflammation in Alzheimer’s Disease», *Cells*, vol. 9, n. 9, pag. 1941, ago. 2020, doi: 10.3390/cells9091941.

[314] R. J. Middleton, W. W.-Y. Kam, G.-J. Liu, e R. B. Banati, «Epigenetic Silencing of the Human 18 kDa Translocator Protein in a T Cell Leukemia Cell Line», *DNA and Cell Biology*, vol. 36, n. 2, pagg. 103–108, feb. 2017, doi: 10.1089/dna.2016.3385.

[315] C. Tremolanti *et al.*, «Translocator Protein Ligand PIGA1138 Reduces Disease Symptoms and Severity in Experimental Autoimmune Encephalomyelitis Model of Primary Progressive Multiple Sclerosis», *Mol Neurobiol*, gen. 2022, doi: 10.1007/s12035-022-02737-2.

[316] M.-T. Weil *et al.*, «Loss of Myelin Basic Protein Function Triggers Myelin Breakdown in Models of Demyelinating Diseases», *Cell Rep*, vol. 16, n. 2, pagg. 314–322, lug. 2016, doi: 10.1016/j.celrep.2016.06.008.

[317] E. C. Tallantyre *et al.*, «Greater loss of axons in primary progressive multiple sclerosis plaques compared to secondary progressive disease», *Brain*, vol. 132, n. Pt 5, pagg. 1190–1199, mag. 2009, doi: 10.1093/brain/awp106.

[318] H. Wang *et al.*, «Neurofilament proteins in axonal regeneration and neurodegenerative diseases», *Neural Regen Res*, vol. 7, n. 8, pagg. 620–626, mar. 2012, doi: 10.3969/j.issn.1673-5374.2012.08.010.

[319] A. Wilkins, «Cerebellar Dysfunction in Multiple Sclerosis», *Front Neurol*, vol. 8, pag. 312, 2017, doi: 10.3389/fneur.2017.00312.

[320] A. Kutzelnigg *et al.*, «Cortical demyelination and diffuse white matter injury in multiple sclerosis», *Brain*, vol. 128, n. Pt 11, pagg. 2705–2712, nov. 2005, doi: 10.1093/brain/awh641.

- [321] H. Nyland, S. Mörk, e R. Matre, «In-situ characterization of mononuclear cell infiltrates in lesions of multiple sclerosis», *Neuropathol Appl Neurobiol*, vol. 8, n. 5, pagg. 403–411, ott. 1982, doi: 10.1111/j.1365-2990.1982.tb00308.x.
- [322] A. J. Kwilasz, P. M. Grace, P. Serbedzija, S. F. Maier, e L. R. Watkins, «The therapeutic potential of interleukin-10 in neuroimmune diseases», *Neuropharmacology*, vol. 96, n. Pt A, pagg. 55–69, set. 2015, doi: 10.1016/j.neuropharm.2014.10.020.
- [323] B. Costa *et al.*, «Residence Time, a New parameter to Predict Neurosteroidogenic Efficacy of Translocator Protein (TSPO) Ligands: the Case Study of N,N-Dialkyl-2-arylindol-3-ylglyoxylamides», *ChemMedChem*, vol. 12, n. 16, pagg. 1275–1278, ago. 2017, doi: 10.1002/cmde.201700220.
- [324] R. C. Melcangi e G. C. Panzica, «Allopregnanolone: state of the art», *Prog Neurobiol*, vol. 113, pagg. 1–5, feb. 2014, doi: 10.1016/j.pneurobio.2013.09.005.
- [325] P. N. Hoffman, D. W. Cleveland, J. W. Griffin, P. W. Landes, N. J. Cowan, e D. L. Price, «Neurofilament gene expression: a major determinant of axonal caliber», *Proc Natl Acad Sci U S A*, vol. 84, n. 10, pagg. 3472–3476, mag. 1987, doi: 10.1073/pnas.84.10.3472.
- [326] M. A. Lopes Pinheiro *et al.*, «Immune cell trafficking across the barriers of the central nervous system in multiple sclerosis and stroke», *Biochim Biophys Acta*, vol. 1862, n. 3, pagg. 461–471, mar. 2016, doi: 10.1016/j.bbadis.2015.10.018.
- [327] E. Bettelli, M. P. Das, E. D. Howard, H. L. Weiner, R. A. Sobel, e V. K. Kuchroo, «IL-10 is critical in the regulation of autoimmune encephalomyelitis as demonstrated by studies of IL-10- and IL-4-deficient and transgenic mice», *J Immunol*, vol. 161, n. 7, pagg. 3299–3306, ott. 1998.
- [328] B. Costa *et al.*, «Anxiolytic properties of a 2-phenylindolglyoxylamide TSPO ligand: Stimulation of in vitro neurosteroid production affecting GABAA receptor activity», *Psychoneuroendocrinology*, vol. 36, n. 4, pagg. 463–472, mag. 2011, doi: 10.1016/j.psyneuen.2010.07.021.
- [329] L. Meyer, C. Venard, V. Schaeffer, C. Patte-Mensah, e A. G. Mensah-Nyagan, «The biological activity of 3alpha-hydroxysteroid oxido-reductase in the spinal cord regulates thermal and mechanical pain thresholds after sciatic nerve injury», *Neurobiol Dis*, vol. 30, n. 1, pagg. 30–41, apr. 2008, doi: 10.1016/j.nbd.2007.12.001.
- [330] A. M. Ghoumari *et al.*, «Progesterone and its metabolites increase myelin basic protein expression in organotypic slice cultures of rat cerebellum», *J Neurochem*, vol. 86, n. 4, pagg. 848–859, ago. 2003, doi: 10.1046/j.1471-4159.2003.01881.x.

- [331] Y. Gilgun-Sherki, E. Melamed, e D. Offen, «The role of oxidative stress in the pathogenesis of multiple sclerosis: the need for effective antioxidant therapy», *J Neurol*, vol. 251, n. 3, pagg. 261–268, mar. 2004, doi: 10.1007/s00415-004-0348-9.
- [332] I. Lejri *et al.*, «TSPO Ligands Boost Mitochondrial Function and Pregnenolone Synthesis», *J Alzheimers Dis*, vol. 72, n. 4, pagg. 1045–1058, 2019, doi: 10.3233/JAD-190127.
- [333] P. Garrido-Pascual, A. Alonso-Varona, B. Castro, M. Burón, e T. Palomares, «Hydrogen Peroxide-Preconditioned Human Adipose-Derived Stem Cells Enhance the Recovery of Oligodendrocyte-Like Cells after Oxidative Stress-Induced Damage», *Int J Mol Sci*, vol. 21, n. 24, pag. E9513, dic. 2020, doi: 10.3390/ijms21249513.
- [334] G. Saher *et al.*, «High cholesterol level is essential for myelin membrane growth», *Nat Neurosci*, vol. 8, n. 4, pagg. 468–475, apr. 2005, doi: 10.1038/nn1426.
- [335] G. R. Post e G. Dawson, «Characterization of a cell line derived from a human oligodendroglioma», *Mol Chem Neuropathol*, vol. 16, n. 3, pagg. 303–317, giu. 1992, doi: 10.1007/BF03159976.
- [336] M. Buntinx *et al.*, «Characterization of three human oligodendroglial cell lines as a model to study oligodendrocyte injury: morphology and oligodendrocyte-specific gene expression», *J Neurocytol*, vol. 32, n. 1, pagg. 25–38, gen. 2003, doi: 10.1023/a:1027324230923.
- [337] G. H. De Vries e A. I. Boullerne, «Glial cell lines: an overview», *Neurochem Res*, vol. 35, n. 12, pagg. 1978–2000, dic. 2010, doi: 10.1007/s11064-010-0318-9.
- [338] K. M. A. De Kleijn, W. A. Zuure, J. Peijnenborg, J. M. Heuvelmans, e G. J. M. Martens, «Reappraisal of Human HOG and MO3.13 Cell Lines as a Model to Study Oligodendrocyte Functioning», *Cells*, vol. 8, n. 9, pag. E1096, set. 2019, doi: 10.3390/cells8091096.
- [339] H. A. Salhanick, «Basic studies on aminoglutethimide», *Basic studies on aminoglutethimide*, vol. 42, n. Issue 8, pagg. 3315s–3321s, 1982.